



# THESE

En vue de l'obtention du

## DOCTORAT DE L'UNIVERSITÉ DE TOULOUSE

Délivré par *l'Université Toulouse III - Paul Sabatier*  
Discipline ou spécialité : *Chimie macromoléculaire et supramoléculaire*

---

Présentée et soutenue par *Roland RAMSCH*  
Le *22 janvier 2010*

Titre : *Catanionic Surfactants in Polar Cohesive Solvents*  
-  
*Impact of Solvent Physical Parameters on their Aggregation Behavior*

---

### JURY

*Werner Kunz, Professeur à l'Université de Regensburg, Allemagne, Rapporteur*  
*Chantal Larpent, Professeur à l'Université de Versailles, France, Rapporteur*  
*Jean-Pierre Launay, Professeur à l'Université de Toulouse, Examineur*  
*Isabelle Rico-Lattes, Directeur de recherche, Directeur de thèse*  
*Stéphanie Cassel, Maître de Conférence à l'Université de Toulouse, Membre invité*

---

Ecole doctorale : *Science de la matière*  
Unité de recherche : *IMRCP*  
Directeur(s) de Thèse : *Isabelle Rico-Lattes*  
Rapporteurs : *C. Larpent et W. Kunz*



# Avant-propos



# Remerciements

Ces travaux de recherche ont été réalisés au laboratoire des Interaction Moléculaires et Réactivité Chimique et Photochimique dirigé successivement par Isabelle Rico-Lattes et Monique Mauzac. Je leur sais gré de m'avoir accueilli pour ces trois années de thèse.

Je souhaite remercier tout spécialement Isabelle Rico-Lattes, ma directrice de thèse, de m'avoir intégré dans son groupe. J'ai beaucoup apprécié son énergie, ses qualités scientifiques, ainsi que son humour dont j'ai eu le plaisir de profiter régulièrement dans son bureau.

Je voudrais également remercier Madame Chantale Larpent, Professeur à l'Université de Versailles et Monsieur Werner Kunz, Professeur à l'Université de Regensburg, pour l'attention qu'ils ont su porter à mes travaux en tant que rapporteurs. Je remercie également Monsieur Jean-Pierre Launay, Professeur à l'Université de Toulouse, d'avoir présidé ce jury.

Je tiens à exprimer ma reconnaissance à Stéphanie Cassel, qui m'a encadré au quotidien, pour le temps qu'elle m'a accordé, ainsi que pour l'aide et les excellents conseils qu'elle a pu m'apporter tout au long de ces travaux.

De même, je remercie émile Perez pour les conseils, l'imagination et les idées qu'il a partagés avec moi.

Je tiens à remercier le service de spectroscopie infra-rouge – particulièrement Corinne Routaboul – le service de résonance magnétique nucléaire, le service de mi-

---

croscopie électronique à transmission, le service de spectrométrie de masse – et personnellement Jean-Christophe Garrigues – ainsi que le service de microanalyse (LCC).

Je remercie également toutes les personnes qui ont participé à ces recherches pour leur disponibilité, leurs conseils et le travail qu'ils y ont consacré : Fernanda, Richard, Yann, Arielle, Florence, Fabienne, Charles-Louis...

Je suis profondément reconnaissant envers les membres du laboratoire que j'ai eu la chance de connaître ; ils m'ont facilité la vie quotidienne et rendu le travail agréable et enrichissant : Menana, Ariane, Pauline, Alex, Waël, Lacra, Javier, Florence, Sheila, Cécile, Elodie, Denis, Roberto, Hugo, Philippe, Plamen, Elisabeth, Romain, Cristina....

Enfin, je tiens à remercier mes amis et ma famille qui m'ont apporté tout le soutien dont j'ai eu besoin pour achever ces travaux.

# Abbreviations

APG	Alkylpolyglycosides
ATR-IR	Attenuated total reflectance-infrared
<i>CAC</i>	Critical aggregation concentration
CED	Cohesive-energy density
CI	Chemical ionization
<i>CMC</i>	Critical micelles concentration
$C_m^+/C_n^-$	Alkylammonium alkanoate
CPBr	Cetylpyridinium bromide (Hexadecylammonium bromide)
CTAB	Cetyltrimethylammonium bromide (Hexadecyltrimethylammonium bromide)
CTAOH	Cetyltrimethylammonium hydroxide (Hexadecyltrimethylammonium hydroxide)
CxC14	Cyclohexylammonium tetradecanoate
DLS	Dynamic quasi-elastic light scattering
DMF	<i>N,N</i> -dimethylformamide
DMSO	Dimethylsulfoxide
DNA	Deoxyribonucleic acid
DOPC	Dioleoylphosphatidylcholine
DOSY	Diffusion ordered spectroscopy
DTAB	Dodecyltrimethylammonium bromide
ESI	Electrospray ionization
FA	Formamide
FT-IR	Fourier-transform infrared spectroscopy
G-Hyd <sub><i>m</i></sub>	<i>N</i> -alkylamino-1-deoxy-D-glucitol
G-Hyd <sub>8</sub>	<i>N</i> -octylamino-1-deoxy-D-glucitol
G-Hyd <sub>12</sub>	<i>N</i> -dodecylamino-1-deoxy-D-glucitol
G-Hyd <sub>16</sub>	<i>N</i> -hexadecylamino-1-deoxy-D-glucitol
$G-Hyd_m^+/C_n^-$	<i>N</i> -alkylammonium-1-deoxy-D-glucitol alkanoate
Glyc	Glycerol
h	Planck's constant ( $6.626 \cdot 10^{-34}$ Js)
HRMS	High resolution mass spectrometry
L-Hyd	<i>N</i> -alkylamino-1-deoxy-D-lactitol
L-Hyd <sub>12</sub>	<i>N</i> -dodecylamino-1-deoxy-D-lactitol
L-Hyd <sub>16</sub>	<i>N</i> -hexadecylamino-1-deoxy-D-lactitol

---

$N_A$	Aggregation number
NbC12	Norbornene methyleneammonium dodecanoate
NbC14	Norbornene methyleneammonium tetradecanoate
NbC16	Norbornene methyleneammonium hexadecanoate
NbNH <sub>2</sub>	Norbornene methyleneamine (Bicyclo[2,2,1]hept-5-ene-2-methyleneamine)
NMF	<i>N</i> -methylformamide
NMR	Nuclear magnetic resonance
NMS	<i>N</i> -methylsydnone
$p$	Packing parameter
PDA	12-(1-pyrenyl)dodecanoic acid
PEO	Alkyl poly(ethylene oxide) C <sub><i>i</i></sub> E <sub><i>j</i></sub>
SAXS/WAXS	Small and wide angle X-ray scattering
SDS	Sodium dodecylsulfate
TEM	Transmission electron microscopy
$T_K$	Krafft temperature
Tricat	Tricatenar catanionic surfactant composed of L-Hyd and a phosphinic acid having two alkyl chains
TTAB	Tetradecyltrimethylammonium bromide
$V_m$	Molar volume
XRD	X-ray diffraction
$\Delta G$	Change in free energy
$\Delta H$	Change in enthalpy
$\Delta S$	Change in entropy
$\varepsilon$	Dielectric constant
$\varepsilon_{id}/\varepsilon_0$	Ideal dielectric constant of solvent mixtures
$\varepsilon_m/\varepsilon_0$	Measured real dielectric constant of solvent mixtures
$\gamma$	Surface tension
$\mu$	Dipole moment
$\nu$	Wave number
$\Pi$	Internal Pressure



# List of Synthesized Products

<b>3a</b>	$C_8^+/C_8^-$	Octylammonium octanoate
<b>3b</b>	$C_8^+/C_{12}^-$	Octylammonium dodecanoate
<b>3c</b>	$C_{12}^+/C_8^-$	Dodecylammonium octanoate
<b>3d</b>	$C_{12}^+/C_{12}^-$	Dodecylammonium dodecanoate
<b>3e</b>	$C_8^+/C_{16}^-$	Octylammonium hexadecanoate
<b>3f</b>	$C_{16}^+/C_8^-$	Hexadecylammonium octanoate
<b>3g</b>	$C_{16}^+/C_{16}^-$	Hexadecylammonium hexadecanoate
<b>4a</b>	G-Hyd <sub>8</sub>	<i>N</i> -octylamino-1-deoxy-D-glucitol
<b>4b</b>	G-Hyd <sub>12</sub>	<i>N</i> -dodecylamino-1-deoxy-D-glucitol
<b>4c</b>	G-Hyd <sub>16</sub>	<i>N</i> -hexadecylamino-1-deoxy-D-glucitol
<b>5a</b>	$G\text{-Hyd}_8^+/C_{12}^-$	<i>N</i> -octylammonium-1-deoxy-D-glucitol dodecanoate
<b>5b</b>	$G\text{-Hyd}_{12}^+/C_8^-$	<i>N</i> -dodecylammonium-1-deoxy-D-glucitol octanoate
<b>5c</b>	$G\text{-Hyd}_8^+/C_{16}^-$	<i>N</i> -octylammonium-1-deoxy-D-glucitol hexadecanoate
<b>5d</b>	$G\text{-Hyd}_{16}^+/C_8^-$	<i>N</i> -hexadecylammonium-1-deoxy-D-glucitol octanoate
<b>5e</b>	$G\text{-Hyd}_{16}^+/C_{12}^-$	<i>N</i> -hexadecylammonium-1-deoxy-D-glucitol dodecanoate
<b>5f</b>	$G\text{-Hyd}_{12}^+/C_{16}^-$	<i>N</i> -dodecylammonium-1-deoxy-D-glucitol hexadecanoate
<b>5g</b>	$G\text{-Hyd}_{12}^+/C_{18}^-$	<i>N</i> -dodecylammonium-1-deoxy-D-glucitol octadecanoate
<b>6</b>	NbNH <sub>2</sub>	Norbornene methyleneamine (Bicyclo[2,2,1]hept-5-ene-2-methyleneamine)
<b>7</b>	NbC14	Norbornene methyleneammonium tetradecanoate

---

# Contents

<b>I</b>	<b>General Introduction</b>	<b>1</b>
<b>II</b>	<b>Fundamentals</b>	<b>9</b>
<b>1</b>	<b>Surfactants in Aqueous Solution</b>	<b>11</b>
1.1	Binary Water-Surfactant Solutions . . . . .	11
1.2	Emulsions and Microemulsions . . . . .	16
1.3	Catanionic Surfactants in Aqueous Solution . . . . .	18
1.4	Surfactants with Large Organic Counterions . . . . .	25
1.4.1	General Information . . . . .	25
1.4.2	Concentration-Dependent Micelle-Vesicle Transition . . . . .	28
<b>2</b>	<b>Surfactants in Non-Aqueous Solution</b>	<b>31</b>
2.1	Introduction to Polar Non-Aqueous Solvents . . . . .	31
2.2	Surfactants in Non-Aqueous Solution . . . . .	39
2.2.1	General Information . . . . .	39
2.2.2	Thermodynamics of Micelle Formation in Non-Aqueous Solution	42
2.2.3	<i>N</i> -Methylsydnone – Insights on Headgroup-Solvent Interactions	49
2.2.4	Micellar Phase in Non-Aqueous Solution . . . . .	52
2.2.5	Hexagonal and Lamellar Phases in Non-Aqueous Solution . . . . .	55
2.2.6	Vesicle Formation in Non-Aqueous Solution . . . . .	57
2.2.7	Microemulsions in Non-Aqueous Solution . . . . .	58
2.3	Catanionic Surfactants and Surfactants with Large Organic Counterions in Non-Aqueous Solution . . . . .	60
<b>III</b>	<b>Results and Discussion</b>	<b>63</b>
<b>1</b>	<b>Conception of the Problem</b>	<b>65</b>
<b>2</b>	<b>Synthesis and Characterization of Catanionic Systems</b>	<b>69</b>
2.1	Model Systems of the Alkylammonium Alkanoate Type . . . . .	69
2.2	Sugar-Based Systems of the G-Hyd <sub><i>m</i></sub> <sup>+</sup> /C <sub><i>n</i></sub> <sup>-</sup> Type . . . . .	71

---

2.3	Characterization of the Catanionic Systems . . . . .	74
<b>3</b>	<b>Catanionic Surfactants in Non-Aqueous Solutions</b>	<b>79</b>
3.1	General Physico-Chemical Studies . . . . .	79
3.1.1	Krafft Temperature $T_K$ . . . . .	79
3.1.2	Critical Aggregation Concentration $CAC$ . . . . .	84
3.1.3	Influence of Chain Length and Chain Symmetry . . . . .	91
3.2	Characterization of the Aggregates Formed by the Catanionic Systems	94
3.3	Impact of the Solvent Dielectric Constant . . . . .	96
3.4	Impact of Ion-Ion Interactions Between the Oppositely Charged Surfactants . . . . .	109
3.5	Salt Effect on the Aggregation Behavior of Catanionic Surfactants . . .	122
3.6	Influence of Sample Preparation . . . . .	123
3.7	Conclusion . . . . .	127
<b>4</b>	<b>Surfactants Based upon Large Counterions</b>	<b>129</b>
4.1	General Information . . . . .	129
4.2	Physico-Chemical Studies on NbC14 in Water and in Formamide . . . .	133
4.3	Insights on Headgroup-Headgroup Interactions . . . . .	140
4.4	Conclusion . . . . .	145
<b>IV</b>	<b>General Conclusion and Perspectives</b>	<b>147</b>
<b>V</b>	<b>Experimental Part</b>	<b>157</b>
<b>1</b>	<b>Commercial Reagents</b>	<b>159</b>
1.1	Reagents . . . . .	160
1.2	Solvents . . . . .	161
<b>2</b>	<b>Characterization and Physico-Chemical Techniques</b>	<b>163</b>
2.1	NMR – Nuclear Magnetic Resonance Spectroscopy . . . . .	163
2.2	FT-IR – Fourier-Transform Infrared Spectroscopy . . . . .	164
2.3	HRMS – High Resolution Mass Spectrometry . . . . .	165
2.4	Elementary Analysis . . . . .	165
2.5	Krafft Temperature $T_K$ . . . . .	165
2.6	Surface Tension Measurements . . . . .	166
2.7	DLS – Dynamic Light Scattering . . . . .	168
2.8	TEM – Transmission Electron Microscopy . . . . .	170
2.9	Optical Microscopy . . . . .	170
2.10	Calculation of Partition coefficient $\log p$ . . . . .	171

---

<b>3</b>	<b>Syntheses of the Catanionic Surfactants</b>	<b>173</b>
3.1	Model Systems of the Alkylammonium Alkanoate Type . . . . .	173
3.2	Synthesis of <i>N</i> -amino-1-deoxy-D-glucitol G-Hyd <sub><i>m</i></sub> . . . . .	180
3.3	Synthesis of Catanionic Associations of the G-Hyd <sub><i>m</i></sub> <sup>+</sup> /C <sub><i>n</i></sub> <sup>-</sup> Type . . . . .	183
3.4	Synthesis of Bicyclo[2,2,1]hept-5-ene-2-methyleneamine (NbNH <sub>2</sub> ) . . . . .	191
3.5	Preparation of the Ion Pair NbC14 – Norbornene Methyleneammonium Tetradecanoate . . . . .	192
3.6	Ion Pair CxC14 – Cyclohexylammonium Tetradecanoate . . . . .	194
<b>4</b>	<b>Additional Experiments</b>	<b>195</b>
4.1	Influence of Sample Preparation . . . . .	195
4.1.1	Preparation of the Catanionic Associations . . . . .	195
4.1.2	Influence of the Solvent . . . . .	196
4.2	Salt Effect . . . . .	198
	<b>Bibliography</b>	<b>201</b>
	<b>List of Tables</b>	<b>213</b>
	<b>List of Figures</b>	<b>216</b>
	<b>Résumé</b>	<b>225</b>



# Part I

## General Introduction





Self-aggregation phenomena of amphiphilic molecules can be observed in nature as well as in daily human life. Amphiphilic molecules participate on a various number of biological mechanisms, and membranes of living cells are mainly composed of molecules having amphiphilic character. Surfactants have become a very important substance family, demonstrated by their widespread applications in all fields of chemical, pharmaceutical and agricultural industries. They are used in detergents, shampoos, glues, dyes, food and pharmaceutical preparations. Their attractiveness lies in their amphiphilic nature, i.e. they possess a hydrophilic part, also called polar headgroup on the one side, and a lipophilic part on the other side. The latter one is most of the time a long hydrogenated or perfluorinated alkyl chain and is therefore called hydrophobic tail. This chain contains generally at least eight carbon atoms.<sup>1</sup> A schematic representation is given in fig. 1.

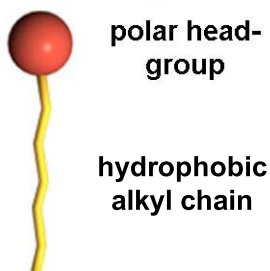


Figure 1: Schematic representation of a monocatener surfactant.

This amphiphilic structure confers it two important features. Firstly, the positioning at water-air or water-oil interfaces (fig. 2), which manifests itself in the decrease of the interfacial tension along with the increase of the surfactant concentration and, secondly, the ability to form molecular aggregates like micelles, vesicles or liquid crystals.

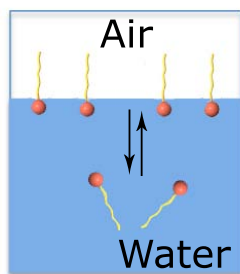


Figure 2: Positioning of surfactant molecules at the water-air interface.

There are several types of surfactants distinguished by the nature of the headgroup. We can differentiate between non-ionic surfactants without any headgroup charges (e.g. PEO = alkyl poly(ethylene oxide), APG = alkylpolyglycosides) and ionic surfactants (cationic, anionic) with positively or negatively charged headgroups. Surfactants with two opposite charges are called zwitterionic. Amphiphilic polymers are also known to have similar aggregation behavior as classic surfactants. The different kinds of headgroups provide widespread possibilities of structures and therefore applications. For example, anionic surfactants are often used as detergents, cationic or zwitterionic ones are used in hair conditioners or fabric softeners.

In addition, surfactants can be separated according to the number of hydrophobic alkyl chains into mono-, bi- or polycatenar species. Catanionic surfactants, which are associations of oppositely charged surfactants, can therefore be seen as a particular case of polycatenar surfactants. Aqueous solutions of catanionic surfactants have already been widely studied in our laboratory. They are globally neutral and possess aggregation properties comparable to bicatenar surfactants, which are known to spontaneously form vesicles in water. Vesicles are spherical objects composed of bilayers. They could be used for drug delivery in pharmaceutical and cosmetic applications. In our laboratory, industrial applications using sugar-based catanionic surfactants are under development. Catanionic surfactants have been extensively studied in aqueous

systems, but only few studies on catanionic associations in non-aqueous solvents can be found in the literature. Thus, we wanted to rationalize the behavior of catanionic surfactants in non-aqueous solvents in this work.

In the first place (Part II: Fundamentals), we will introduce the properties of surfactants in aqueous solution, since this is the most appropriate and therefore widespread solvent for surfactant aggregation. We will describe the different types of aggregates which can form in water, then we will present the properties and the advantages of catanionic associations. In addition, we will explain why surfactants have usually been studied in water, and what makes this solvent the best for aggregation phenomena. These conditions can be described with physical solvent parameters, among which the cohesive-energy density (CED) seems to be the most important one. Non-aqueous solvents such as formamide, glycerol, hydrazine or ethylammonium nitrate possess physico-chemical parameters close to those of water, and should therefore allow self-aggregation of surfactants. We therefore chose formamide and glycerol for our studies. In order to get a better understanding of the aggregation behavior of surfactants in non-aqueous solutions, we will give an introduction to the already known behavior of ionic and nonionic surfactants in non-aqueous solvents. Some of these studies on surfactants in formamide and in glycerol have been done in our laboratory, and these experiences were helpful in our research on the aggregation behavior of catanionic surfactants in non-aqueous solvents.

In the second place (Part III: Results and Discussion), we will describe three different catanionic systems. A first type will be catanionic associations of fatty amines and acids (alkylammonium alkanoate), then we will discuss sugar-based catanionic surfactants between an aminated glucose and a fatty acid (*N*-alkylammonium-1-deoxy-D-glucitol alkanoates) and finally, we will present catanionic associations between a fatty acid and a large organic counterion bearing an amine function (norbornene

## General Introduction

---

methyleneammonium tetradecanoate and cyclohexylammonium tetradecanoate). At first, we will present the syntheses of the alkylammonium alkanoates and the *N*-alkylammonium-1-deoxy-D-glucitol alkanoates type surfactant. Then, we will discuss the results on the alkylammonium alkanoates. These systems were easily prepared with commercially available starting products. We will discuss general parameters such as the Krafft temperatures  $T_K$  and the critical aggregation concentrations  $CAC$ . The influence of chain lengths and chain length symmetry of the hydrophobic part of the surfactant on the  $T_K$  and the  $CAC$  will be elucidated. In addition, we will present another cationic surfactant type based upon glucose (*N*-alkylammonium-1-deoxy-D-glucitol alkanoate) that was synthesized in our laboratory. It has been previously shown in our laboratory that similar lactose-based surfactants formed spontaneously vesicles in water. For solubility reasons, we synthesized glucose-based cationic associations, all displaying the same headgroup, but with various numbers of carbon atoms in the lipophilic part of the surfactant. The sugar-based headgroup confers the surfactant the required solubility in water, in formamide and in glycerol, as well as in mixtures of these solvents. This allowed us to study comparatively the behavior of cationic surfactants in aqueous and non-aqueous solutions. Thanks to this comparative work, we were able to explain the impact of several physical solvent parameters leading to differences in the aggregation behavior of these surfactants between aqueous and non-aqueous solution. Finally, a third type of cationic associations based upon ionic surfactants with large organic counterions will be discussed. This type of cationic assemblies exhibits interesting properties that are similar to cationic surfactants. Norbornene methyleneammonium tetradecanoate (NbC14) and cyclohexylammonium tetradecanoate (Cx14) have already been studied in water in our laboratory. These systems spontaneously formed vesicles in water. Moreover, the norbornene residue of NbC14 possesses a double bond, which can be polymerized. The polymerization of

vesicles formed in water can increase the stabilization of these aggregates. We studied both systems in water and in formamide in order to compare the results with what we have obtained on the previously discussed cationic surfactants. The importance of hydrophobic interactions in non-aqueous solvents will be discussed.



## Part II

# Fundamentals





# 1

## Surfactants in Aqueous Solution

### 1.1 Binary Water-Surfactant Solutions

One of the most important characteristics of surfactants is their ability to form molecular aggregates in solution. The formation of aggregates takes place above a certain concentration called critical aggregation concentration (*CAC*). Below this concentration, in dilute binary surfactant/water solutions, the amphiphilic molecules come in the form of monomers in water. The monomers tend to place themselves at the water-air interface. Increasing the concentration also increases the unfavorable hydrophobic

## Fundamentals

---

interactions between the lipophilic chains and water and therefore increases the total energy of the system. In order to lower this energy, amphiphilic molecules form aggregates, pointing the hydrophobic chains towards the middle of the aggregate. This conformation diminishes the water-hydrophobic chain interactions to a minimum, and the positive interactions between polar headgroups and water are favored. Another energetic parameter are the positive interactions between the hydrophobic chains (van der Waals interactions) on the one hand, and the repulsive interactions between the polar headgroups on the other hand. Counting all together, the formation of the aggregates is given by the equilibrium between the above mentioned forces and interactions. The total energy of the system is then the sum of the interaction energies between the surfactants on the one hand and between the surfactants and the solvent on the other hand. The latter one is also called solvophobic and is one of the main driving forces in the self-aggregation phenomenon. Thermodynamic calculations showed that the solvophobic effect is accompanied by a large gain of entropy. The change of entropy is mainly due to the removal of water from around the alkyl chains.

Above the critical aggregation concentration, different concentration-dependent (lyotropic) phases can be observed in a typical binary water/surfactant solution. The mesophases formed can usually be observed in a certain sequence:

Isotropic micellar phase ( $I_\alpha$ )  $\Leftrightarrow$  hexagonal phase ( $H_\alpha$ )  $\Leftrightarrow$  cubic phase ( $Q$ )  $\Leftrightarrow$   
lamellar phase ( $L_\alpha$ )

The simplest phase is composed of micelles (see fig. 1.1 (A)). This isotropic phase ( $I_\alpha$ ) is characterized by micelles that contain at least 10-20 monomers.<sup>1</sup> The number of monomers per micelle is called the aggregation number  $N_A$ . A typical micelle can contain up to 50 or more surfactant molecules and its size ranges from one to several nanometers.<sup>2</sup> Micelles can be observed by X-ray scattering experiments

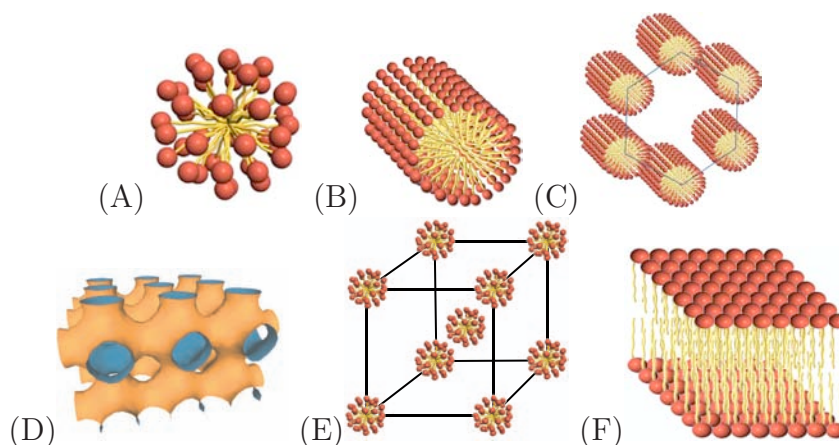


Figure 1.1: Micelle (A), cylindrical micelle (B), hexagonal phase  $H_\alpha$  (C), cubic phase I (D), cubic phase II (E), bilayer (lamellar phase  $L_\alpha$ ) (F).

(SAXS/WAXS). With increasing surfactant concentration in the aqueous solution, a two-dimensional hexagonal phase ( $H_\alpha$ ) forms. This type of aggregate can be described as micelles that expand in one direction to form rod-like micelles. These elongated micelles organize themselves on a hexagonal lattice. This anisotropic phase can be visualized using optical microscopy with cross polarizing filters. Moreover, this kind of phase can be studied more accurately by X-ray diffraction exhibiting a typical diffractogram. While still increasing surfactant concentration, a cubic phase can be observed. Cubic phases are isotropic and cannot be observed by optical microscopy. They are often formed by bicontinuous phases, where the solvent and the surfactant are placed on a cubic lattice (see fig. 1.1). At even higher concentration, the amphiphilic molecules assemble themselves to lamellar phases, called  $L_\alpha$ . When the concentration of surfactants is still increased, reverse structures can occur, that is to say with the polar headgroups gathered in the middle of the aggregates and the hydrophobic chains pointed towards the outside of the objects. Reverse structures can also be obtained in organic solvents like chloroform.

## Fundamentals

---

These concentration-dependent phases or lyotropic phases change with the concentration of the surfactant in the binary solution. It was also shown that surfactants form different phases depending on the temperature. In this case, the phases are formed at a fixed surfactant concentration while changing the temperature. This kind of phases are called thermotropic phases.

The geometry of a surfactant can allow to predict the aggregate type that will form. In 1976, Israelachvili et *al.* brought into relation the geometrical form of the monomer and the resulting aggregate formed.<sup>3</sup> A packing parameter  $p$  was introduced, which can allow to predict the type of aggregate in dilute aqueous solutions, and is defined as:

$$p = \frac{v}{a_0 \cdot l_c} \quad (1.1)$$

Where  $v$  and  $l_c$  are respectively the volume and the length of the hydrophobic part and  $a_0$  is the effective surface area of the polar headgroup. The parameters  $v$  and  $l_c$  can be approximatively calculated by the following equations:

$$v = 0.0274 + 0.0269 \cdot n_C \text{ [in } nm^3\text{]} \quad (1.2)$$

$$l = 0.15 + 0.127 \cdot n_C \text{ [in } nm\text{]} \quad (1.3)$$

where  $n_C$  is the total number of carbon atoms in the lipophilic part.

The parameter  $a_0$  is the effective surface area of the polar headgroup and has to be estimated. It is the crucial point of this geometrical approach. Whereas it is quite straightforward in the case of non-ionic surfactants, the effective surface area of ionic surfactants depends on the concentration of electrolytes and surfactants in the

solution. The effective surface area can change with the addition of salts and therefore the packing parameter can change as well. As a consequence, the type of aggregate can change with the concentration of salts added.

The relationship between the packing parameter and the aggregate formed is listed in fig. 1.2.



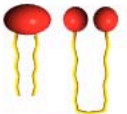


Surfactant type	Packing parameter	Geometric shape	Aggregation type
Monocatenar surfactant with large polar head group	$p < 1/2$		Direct micelles
Nonionic monocatenar surfactant	$p \approx 1/2$		Globular micelles Hexagonal phase I
Bolaform surfactant or bicatenar surfactant with large head group	$1/2 < p < 1$		Flexible lamellar phase = vesicles
Bicatenar surfactant	$p \approx 1$		Cubic phase $Q_{II}$ Lamellar phase
Bicatenar surfactant with small head group	$p > 1$		Reverse micelles Hexagonal phase II

Figure 1.2: Aggregation type according to the packing parameter  $p$ .

### 1.2 Emulsions and Microemulsions

Beside binary surfactant-water solutions, ternary and quaternary systems can also be formed. These systems are usually composed of two immiscible fluids (water and oil), surfactants and cosurfactants. Dispersions of water and oil stabilized by small quantities of surfactants are called emulsions. There are two typical types of emulsions:

1. Oil in water emulsion (O/W). Small oil droplets dispersed in a continuous water phase.
2. Water in oil emulsion (W/O). Small water droplets dispersed in a continuous oil phase.

These types of emulsions are not thermodynamically stable and tend to separate to an oil-rich phase and a water-rich phase. Microemulsions are thermodynamically stable systems, which are characterized by high surfactant contents. Microemulsions are transparent dispersions of water and oil and are formed by admixing amphiphilic molecules. A typical system contains four constituents: water, oil (hydrocarbon, fluorocarbon), surfactant (ionic, zwitterionic or non ionic amphiphiles) and cosurfactant (short chain alcohols, amines or oximes).<sup>4-7</sup> Four-component systems usually possess complex phase diagrams (see fig. 1.3), but single phase domains can be found for microemulsions. It has to be noted that ternary *n*-hexane, water and propan-2-ol mixtures were studied and exhibited microemulsion properties.<sup>8</sup> Because of the absence of a surfactant, these systems are called “detergentless microemulsions”.

Ternary mixtures without the help of cosurfactant are also known.<sup>9</sup> But the majority of microemulsions are composed of four components. In addition to the W/O and O/W microemulsions, bicontinuous phases can be found, in which the two pseudo-phases form “sponge” phases. The different types of microemulsions are represented

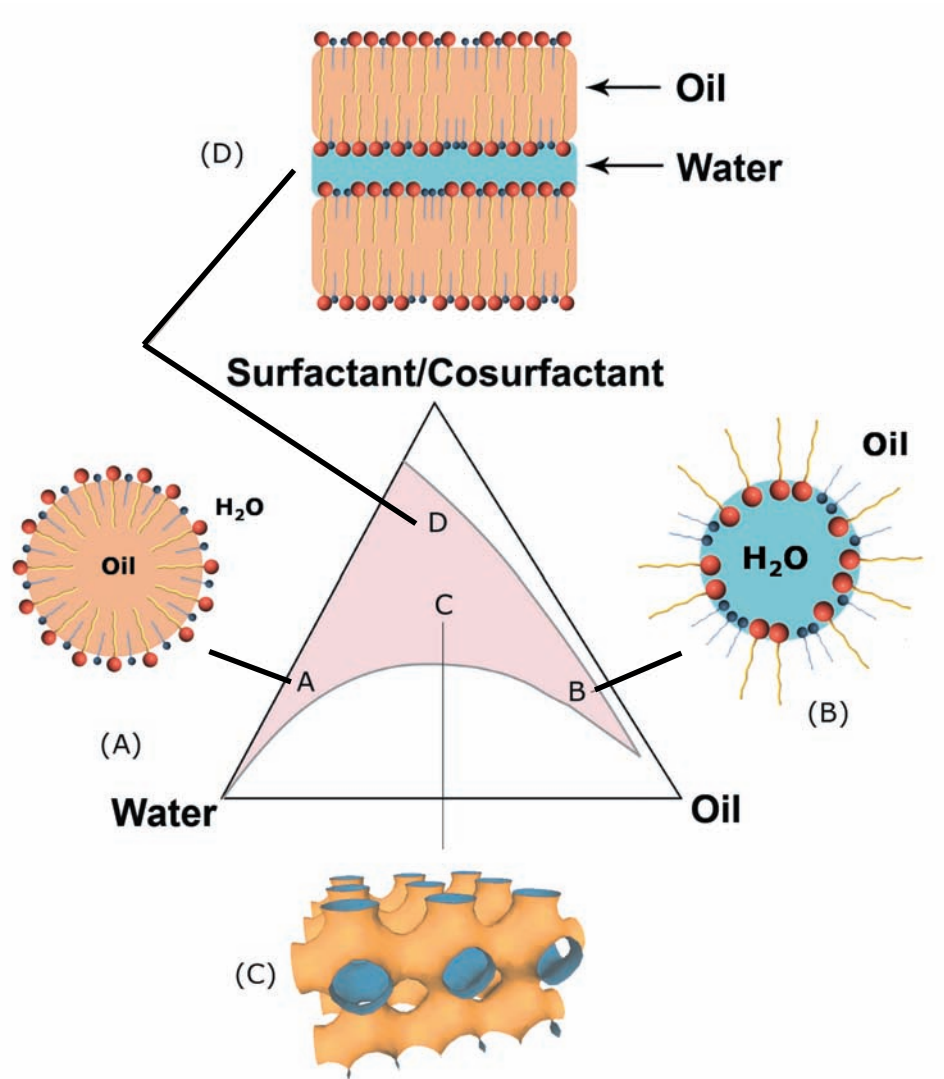


Figure 1.3: Typical phase diagram of a four-component system. (O/W) microemulsion (A), (W/O) microemulsion (B), bicontinuous microemulsion (C), lamellar phase (D).

## Fundamentals

---

by the schemes in fig. 1.3. Thermodynamically, microemulsions can be described in two ways depending on the thermodynamic or kinetic stability:

1. “A system of water, oil, and amphiphile(s) which is a single optically isotropic and thermodynamically stable liquid solution”.<sup>10</sup>
2. Fribergs’s definition, which considers that the thermodynamic stability appears to be an exception. Therefore a modification requiring spontaneous formation has been proposed.<sup>11</sup>

Aqueous microemulsions are of great interest, since a number of applications are known. In recent years, they have been used to increase oil recovery efficiency in oil fields.<sup>12,13</sup> Since non-negligible quantities of oil stay in the porous rocks around the oil reservoirs, large volumes of microemulsions are pumped into these areas in order to solubilize the crude oil. The microemulsion is recovered and a chemical process separates the oil from the microemulsion. There is a series of other applications like shoe creams or the enhancement of chemical reaction performances.

### 1.3 Catanionic Surfactants in Aqueous Solution

Catanionic surfactants offer many application possibilities and have been intensively studied in water. But little work has been done on catanionic surfactants in non-aqueous polar solvents.<sup>14-16</sup> In the following section, catanionic surfactants and their behavior in water will be described. Catanionic surfactants are entities obtained by the mixture of cationic and anionic surfactants. They are globally neutral, which confers them aggregation properties comparable to bicationic surfactants. Schematic representations of a catanionic association and a bicationic surfactant are given in fig. 1.4. Catanionic surfactants exhibit some special features that make them easy to handle.



One of these advantages lies in the packing parameters of cationic surfactants that are normally between 0.5 and 1. Estimating this geometry, certain cationic surfactants tend to form vesicles,<sup>17–19</sup> cone structures,<sup>20,21</sup> nanodiscs<sup>22</sup> or icosahedra.<sup>23,24</sup> But also tubule and helix structures have been found with a fluorescent sugar-based cationic system.<sup>17</sup> It has to be noted that these objects are only formed in a certain range of surfactant ratio and concentration, that is to say between concentrations over the *CAC* up to 5 weight percent of surfactant. Higher concentrations can lead to the formation of lyotropic liquid crystals.

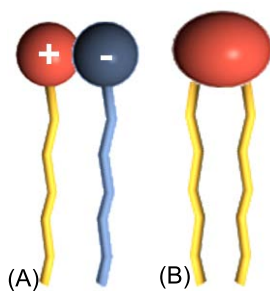


Figure 1.4: Schematic representations of cationic (A) and bicationic (B) surfactants.

An important advantage of cationic surfactants are the simple strategies of their syntheses. However, it has to be noted that two different types of cationic surfactants exist – residual salts containing cationic surfactants (cationic-anionic surfactant mixtures) and pure cationic surfactants, that is to say ion pairs without any residual salts. The first kind is the product of an ion-exchange reaction between two charged surfactants, such as alkylammonium chlorides and sodium alkanoates with production of sodium chloride that stays in the surfactant solution. It is not recommended to use this mixture of cationic surfactants and residual salts for pharmaceutical application. The salt-free cationic surfactants can be synthesized by four different methods described in the literature.<sup>22,23,25</sup>

## Fundamentals

---

- The extraction method<sup>25</sup> is based upon mixing two oppositely charged surfactants solubilized in water beforehand. An adequate organic solvent is added to extract the catanionic association formed whereas the residual salts stay in the aqueous phase.
- The precipitation method<sup>25</sup> can be carried out in three ways. The first possibility is the precipitation of the silver salt of an anionic surfactant (in association with potassium, sodium or lithium) in aqueous solution. The precipitate is purified, dissolved in a mixture of water and an organic solvent, and then a cationic surfactant with a halogen counterion (chloride or bromide) is added. The pure catanionic surfactant is obtained after filtration of the precipitated silver halogenide. The second possibility is based upon mixing two equimolar supersaturated aqueous solutions of two oppositely charged surfactants. The catanionic ion pair precipitates and can be filtered off whereas the residual salts stay in solution. The third possibility consists in the equimolar precipitation of catanionic surfactants by pouring together two saturated solutions of two oppositely charged surfactants in hexane or diethyl ether. The precipitate is equimolar and the excess product stays in solution.<sup>26,27</sup>
- The ion-exchange method<sup>25</sup> can be applied after conversion of the cationic surfactant into a hydroxide species like CTAOH (cetyltrimethylammonium hydroxide) and the anionic surfactant into the acidic form via an ion exchange resin. The two resulting solutions are mixed and the catanionic surfactant is obtained by an acid-base reaction.<sup>22-24</sup>
- Finally, a method introduced by our laboratory is based upon a simple acid-base reaction between an acid-functionalized surfactant and a *N*-alkyl glycoside.<sup>28,29</sup> Equimolar aqueous solutions of these two components are stirred, and after suf-

ficient time the solution is freeze-dried and the catanionic association is obtained in quantitative yield without any residual salts.

These preparation methods are of great interest since they are much easier to perform than the syntheses of covalently linked bicatenar surfactant that possess similar aggregation properties. Moreover, a large series of homologous surfactants can easily be prepared by replacing one of the components – anionic or cationic surfactants – with different chain lengths.

As already mentioned, an important advantage of catanionic surfactants is the capacity to spontaneously form vesicles in water.<sup>30,31</sup> Vesicle formation is of great interest for pharmaceutical applications. Fig. 1.5 is a schematic representation of a vesicle. The particular structure of vesicles allows a versatile transport of active principles. Hydrophilic drugs can be encapsulated in the aqueous cavity, whereas lipophilic drugs can be incorporated in the bilayer structure.

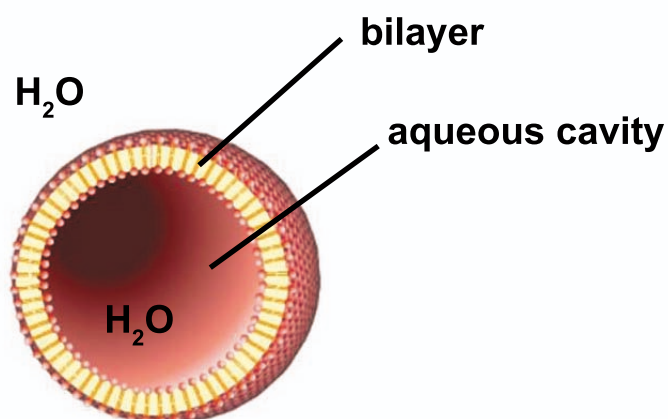


Figure 1.5: Schematic representation of a vesicle.

## Fundamentals

---

Nevertheless, it has to be noted that a large number of equimolar cationic associations tend to precipitate in water.<sup>31</sup> Effectively, the electrostatic interactions between the opposite charges lead to a smaller polar headgroup compared to the simple sum of the two effective headgroup surfaces. Therefore, the hydrophilicity of the system is reduced. The reduced solvation sphere leads to solubilization difficulties. For this reason, cationic vesicles are usually composed by an excess of positive or negative charges. However, Menger *et al.* could synthesize a water soluble cationic surfactant based upon a glycosidic amphiphile.<sup>32</sup>

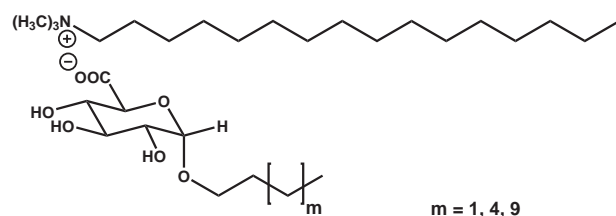


Figure 1.6: Structure of the first water soluble cationic surfactant at equimolarity.

In our laboratory, water soluble sugar-based cationic surfactants have been developed.<sup>28,29,33-35</sup> These surfactants are obtained by a reductive amination of unprotected lactose with a long chain amine. In a second step, the obtained *N*-alkylamino-1-deoxy-D-lactitol (L-Hyd<sub>12</sub> or L-Hyd<sub>16</sub>) reacts in an acid-base reaction with a fatty acid to the cationic assembly in water. Fig. 1.7 shows the structure of two types of water soluble cationic surfactants derived from lactitol-based surfactants, which were synthesized in our laboratory. The lactitol headgroups confer the cationic surfactants the hydrophilicity required to render them water soluble. This behavior shows the importance of the sugar headgroups. Moreover, lactitol-based surfactants are analogues of galactosylceramide (gal $\beta$ <sub>1</sub>cer), and therefore possess a considerable anti-HIV-1 activity.<sup>28,29,34,36</sup>

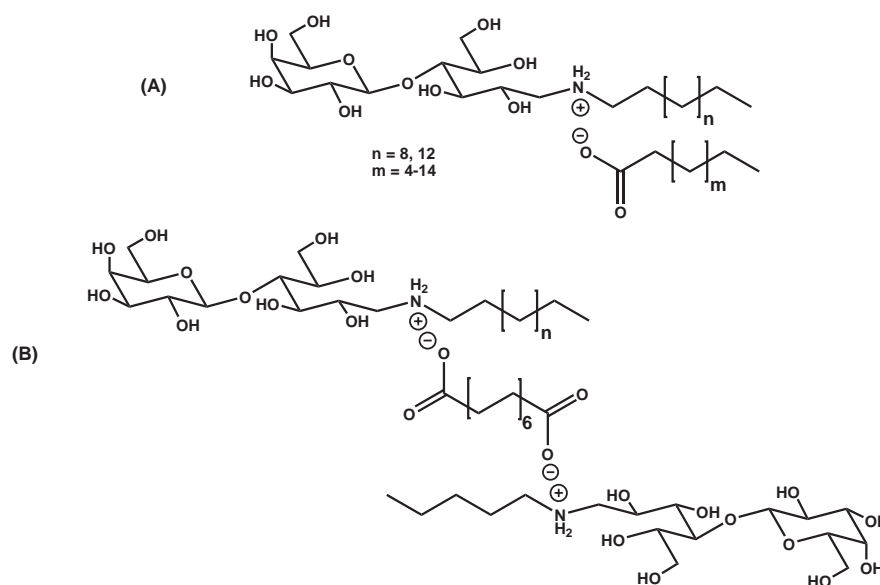


Figure 1.7: Catanionic systems synthesized in our laboratory with a bicatenar (A) and a gemini (B) structure.

Another recent approach of drug delivery has been envisaged by using a combination of sugar-based surfactants and ionizable drugs that could form a catanionic association.<sup>37,38</sup> In our laboratory, this concept led to an industrial application. An anti-inflammatory drug (indometacin) with an acid group was combined with the above mentioned L-Hyd<sub>12</sub> to a catanionic association (see fig. 1.8).

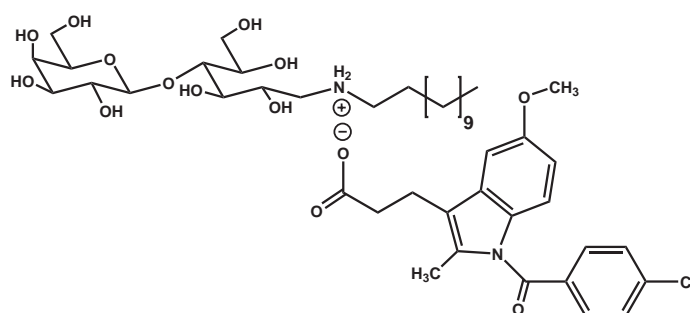


Figure 1.8: Structure of a catanionic surfactant resulting from the association of an anti-inflammatory drug (indometacin) with a sugar-derived surfactant.

## Fundamentals

---

This preparation was developed for a cutaneous application.<sup>39,40</sup> This cationic association spontaneously formed vesicles, which could increase the anti-inflammatory activity of the drug. In addition, the release of the drug through the skin could be controlled and prolonged. It was also shown that the drug was protected from harmful irradiation effects.<sup>39,40</sup>

Sugar-based tricatener (three-chain) cationic surfactants have been designed and synthesized in our laboratory in order to obtain more stable vesicles for drug vectorization. For this issue, the lactitol-based cationic surfactant was combined with a phosphinic acid bearing two alkyl chains (see fig. 1.9).

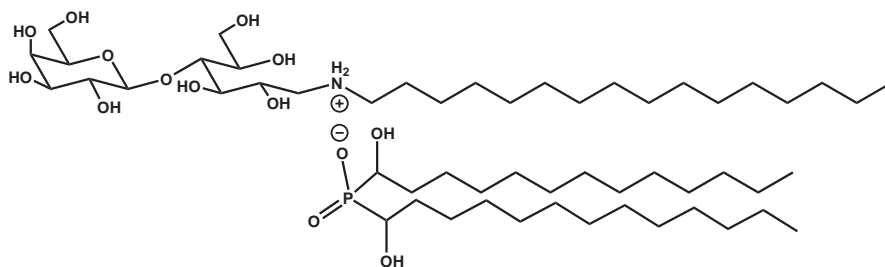


Figure 1.9: Tricatener cationic surfactant.

These cationic surfactants could be studied in pure water and in a phosphate buffer.<sup>41,42</sup> Vesicles formed spontaneously in both mediums. A hydrophilic probe (arbutin) could be entrapped in the vesicles up to 8 %, independent of the conditions of vesicle formation (in water or in buffer solution). This was one of the highest drug encapsulation efficiencies that have been obtained with equimolar cationic vesicles.<sup>43-45</sup> Moreover, drugs could be retained in the aqueous cavity of the vesicles for at least 30 h, which was one of the highest probe entrapment stabilities for cationic surfactants in equimolar ratio.

In summary, the simple preparation methods and the particular aggregation properties of cationic associations, namely the spontaneous formation of vesicles, are of great interest. They are promising candidates for pharmaceutical applications such as drug delivery.<sup>46</sup> The bilayer structure with an aqueous cavity allows incorporation of both hydrophobic and hydrophilic active principles.

## 1.4 Surfactants with Large Organic Counterions

### 1.4.1 General Information

A special group of surfactants, which are extensively studied in our laboratory, is composed of ionic surfactants with large organic counterions. Because of the large size of the counterions, they form an intermediate type between classic ionic surfactants and cationic surfactants. The large counterions can interact with the surfactant alkyl chain with the help of hydrophobic van der Waals interactions. In this case they can be compared to cationic surfactants. But in some cases, the interactions are not strong enough and the large organic counterions behave more like classic counterions.

Surfactants with large counterions are of great interest, because the counterion can “functionalize” the surfactant. For example, in our laboratory, polymerizable cationic surfactants are synthesized based upon norbornene ammonium or carboxylate counterions. This type of associations spontaneously forms vesicles in water. In addition, the double bond of the norbornene residue can be polymerized. This polymerization of in water formed vesicles could enhance their stabilization.<sup>47,48</sup> Another type of surfactants with large organic counterions and based upon caffeic acid was synthesized in our laboratory. In combination with fatty amines, the caffeic acid formed a cationic association that could spontaneously form vesicles in water. Caffeic acid displays antioxidant properties, that is to say it possesses a very low oxidation potential

## Fundamentals

---

and is oxidized very easily. Therefore it retards and even prevents oxidation of other molecules in a solution. These vesicles can be used for the preservation of lipophilic drugs, since these drugs are often light and heat sensitive and oxidize easily. Preparation with caffeic acid catanionic surfactant and DNA were studied in our laboratory, and it was shown that caffeic acid can protect DNA from photodegradation.<sup>49,50</sup>

However, ionic surfactants with large counterions exhibit some interesting behaviors depending on the nature of the organic counterion. The influence of organic counterion on ionic surfactants has already been shown by Underwood *et al.*<sup>51</sup> It was demonstrated that the position of the counterion plays a dominant role in the aggregation of surfactants.<sup>52-57</sup> In comparison to inorganic counterions, which are only localized on the outer solubilization layer of the aggregate, it was shown that the organic counterions can, depending on their hydrophobia, interact with the alkyl chains of the surfactant. Therefore, they can influence the aggregation process. Modification of the counterion/surfactant ratio or the counterion concentration can lead to phase transitions. For example, a spherical-cylindric micelle transition was observed in the SDS-*para*-toluidine hydrochloride system (see fig. 1.10) as the toluidine hydrochloride salt concentration was increased.<sup>58</sup>

Other transitions with organic counterions were observed when the counterion-surfactant ratio was changed. For the sodium naphthalene-2-sulfonate/tetradecylaminoxide hydrochloride (see fig. 1.10), an elongated micelle-unilamellar vesicle transition was reported when the counterion concentration was increased. For very high counterion concentration, a sedimentation of multilamellar vesicles occurred.<sup>59</sup>

In other cases, a micelle-vesicle transition was observed depending on the counterion concentration and on the solution pH. In the sodium dodecylbenzenesulfonate/histidine mixture (see fig. 1.10), a decrease of the pH value induced the micelle-vesicle transition.<sup>60</sup> More complex systems like cationic/anionic surfactant mixtures



of dodecyltrimethylammonium bromide and sodium dodecylsulfate (DTAB/SDS) with organic additives such as octylamine or octanol led to micelle-vesicle transitions. In these cases, the additives acted like cosurfactants.<sup>61</sup>

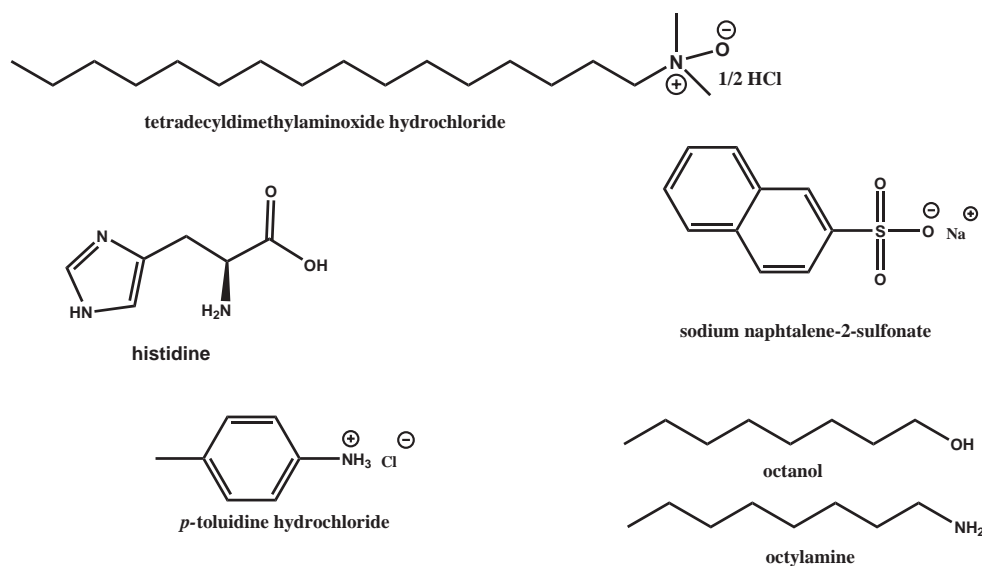


Figure 1.10: Counterions influencing the aggregation behavior.

Altogether, the hydrophobic interactions between organic counterions and ionic surfactants can influence the aggregation behavior of these associations. Moreover, concentration, charge and position of the counterion can lead to a transition from micelles to elongated micelles or even to the formation of vesicles.

### 1.4.2 Concentration-Dependent Micelle-Vesicle Transition

Recent research in our laboratory on surfactant systems with large organic counterions revealed a new concentration-dependent type of micelle-vesicle transition. Bordes *et al.* showed that the catanionic norbornene methyleneammonium tetradecanoate system (NbC14, see fig. 1.11) – composed by a long chain acid and a norbornene methyleneamine – underwent a transition from micelles to vesicles when increasing the concentration of the catanionic association.<sup>47,48</sup>

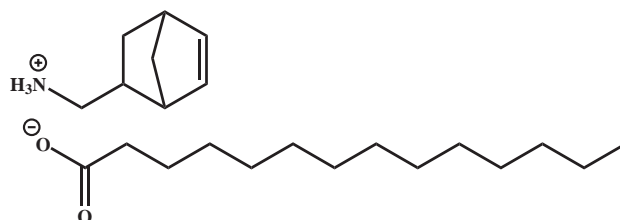


Figure 1.11: Norbornene methyleneammonium tetradecanoate NbC14.

They also observed this micelle-vesicle transition with NbC16 at 45 °C. Surface tension measurements of these surfactants were characterized by two plateaus. The first intermediate plateau indicated micelle formation and the second one the formation of vesicles (see fig. 1.12). The vesicles with diameters between 50 and 450 nm could be visualized on electron micrographs.

Bordes *et al.* demonstrated that the micelle-vesicle transition depended on two factors. A prerequisite for the transition was an optimal ratio of headgroup volume and surfactant chain length, that is to say a bulky counterion was needed to obtain this type of micelle-vesicle transition. They showed that cyclohexylamine, cyclohexylmethyleneamine and 3,3-dimethylbutylamine-derived catanionic surfactants also underwent this transition while increasing the concentration of the catanionic association. On the other hand, two long chain alkylammonium counterion systems (hexylammo-

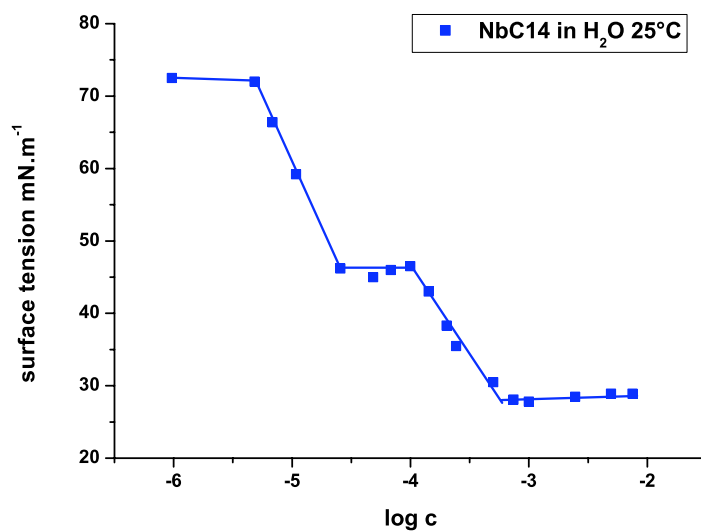


Figure 1.12: Surface tension measurements of NbC14 in H<sub>2</sub>O at 25 °C.

nium and octylammonium) did not exhibit any transition. The second factor which induced the micelle-vesicle transition, was the freedom of positioning. Fig. 1.13 shows a schematic representation of the micelle-vesicle transition in water.

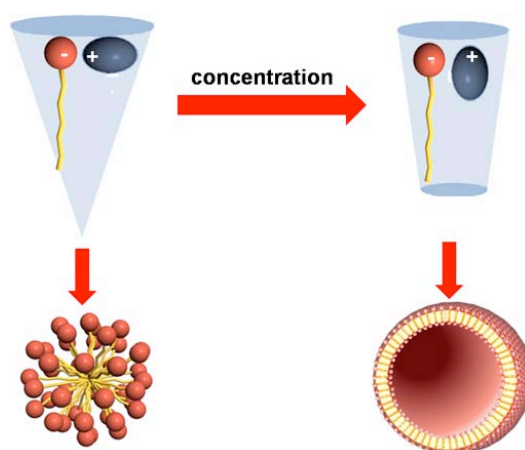


Figure 1.13: Schematic representation of the micelle-vesicle transition mechanism.

## Fundamentals

---

It was shown that the counterion was less associated to the ionic surfactant at low concentration and placed at the outer solvation sphere of the micelle. This conferred the surfactant a cone-like structure, which led, according to Israelachvili,<sup>3</sup> to the formation of micelles. In this case, the counterion behaved comparable to classic counterions. At higher concentrations, the solvophobic effect increased, and the counterion was placed side-by-side between the ionic surfactants in the inner more hydrophobic part of the aggregate. This conformation could be compared to a truncated cone-like geometry, which led to the formation of vesicles.

In summary, cationic associations composed of ionic surfactants with large counterions possess interesting properties. The type of aggregate can depend on the counterion concentration or the pH of the solution, but also, as it was demonstrated for NbC14, on the concentration of the cationic association. A concentration-dependent micelle-vesicle transition was observed for this system induced by two major factors. An optimal ratio of surfactant chain length and headgroup volume was required on the one hand, and a modification of the degree of hydrophobic interactions between the counterion and the ionic surfactant on the other hand led to a different positioning of the counterion with increasing concentration. Latter phenomenon manifested itself in a change of the packing parameter, which accompanied the phase transition.

# 2

## Surfactants in Non-Aqueous Solution

### **2.1 Introduction to Polar Non-Aqueous Solvents**

In general, surfactant aggregation is described in aqueous systems, because water offers the best conditions for aggregation phenomena. In order to understand which physical characteristics are important to allow self-aggregation, water will be described in detail in the following chapter. Water is known to be a highly polar solvent with a highly ordered structure. The organized nature of a solvent, mainly indicated by the cohesive-energy density, seems to be a very important parameter.<sup>62</sup>

## Fundamentals

---

The polar character also seems to play an important role, but the concept of polarity is hard to describe. A qualitative approach consists in analyzing the capacity of a solvent to dissolve charged or neutral, apolar or dipolar species. For example, a polar solvent such as water is able to dissolve dipolar or charged species such as salts.

But an accurate and quantitative description of polarity is difficult and still under discussion. Most often the distinction is made by an approach using the dielectric constant  $\epsilon_r$ , also called relative permittivity. Following Lowery and Richardson, solvents with a dielectric constant above 15 are polar solvents and those with dielectric constants below are non-polar ones.<sup>63</sup> This approach, deduced from idealized theories, is most often inadequate, since these theories view solvents as a non-structured isotropic continuum.<sup>64</sup> In reality, they are composed of individual solvent molecules with their own solvent/solvent interactions. In addition, these theories do not take into account specific solute/solvent interactions such as hydrogen-bonding and EPD/EPA (Electron Pair Donor/Electron Pair Acceptor) interactions, which often play a dominant role in solute/solvent interactions.<sup>64</sup>

Another parameter, often used to describe solvent polarity, is the dipole moment  $\mu$ . The dipole moment is a result of the asymmetry of the molecule geometry. This can be expressed by two opposite charges (zwitterion) or by the asymmetrical distribution of atoms with highly different electronegativities, e.g. water (see fig. 2.1).

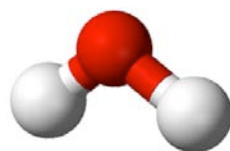


Figure 2.1: 3D model of a water molecule.

Solvent molecules having high permanent dipole moment can rearrange themselves to form highly ordered structures. Nevertheless, using the solvent dipole moment as the only parameter to measure solvent polarity is not adequate, since the charge distribution of a solvent molecule may not only be given by its dipole moment, but also by its quadrupole or higher multipole moments. The lack of simple theoretical expressions for calculating solvent effects and the inadequacy of defining solvent polarity in terms of single physical constants has stimulated attempts to introduce empirical scales of solvent polarity.<sup>65-69</sup> These scales work with well known reference systems and measure the polarity in relation to these systems. Therefore, these scales do not give absolute polarity values, but help to estimate a relative value to the reference systems. There are scales that use reaction rates (Grunwald Winstein mY scale<sup>65</sup>), spectral absorption (Kosowers Z scale<sup>66-68</sup>) or interactions with specific substances like Lewis acids or bases (donor number and donor acceptor scale<sup>69</sup>).

Beside the solvent polarity, the cohesive nature of solvents is a requirement for aggregation phenomena. This can be expressed by the surface tension (at the water-air interface), the internal pressure ( $\Pi$ ) or the cohesive-energy density (CED). The latter parameter is listed together with dipole moment and dielectric constant in table 2.1. Water is able to form hydrogen bonds, which participate to build up a network. This network is made up by a corner linked tetrahedral structure. One tetrahedron is built up by five water molecules, with four water molecules placed on the corner positions around a fifth molecule at the center position of the tetrahedron. A schematic representation is given in fig. 2.2. The highly ordered structure is expressed by a high cohesive-energy density (CED).

## Fundamentals

---

Solvent	CED	$\epsilon/\epsilon_r$	$\mu$
	Cohesive-energy density	Dielectric constant	Dipole moment
	mPa		D
Water	2294	78.5	1.6
Hydrazine	2100	51.7	1.86
Formamide (FA)	1568/1638	109	3.4
Glycerol (Glyc)	1570/1600	42.9	1.52
<i>N</i> -methylsydnone (NMS)	1340	144	7.3
Ethylammonium nitrate	1300	–	–
<i>N</i> -methylformamide (NMF)	992	182.4	3.8
Methanol	873.6/928	32.63	1.700
Dimethyl sulfoxide (DMSO)	708	48	3.96
<i>N,N</i> -dimethylformamide (DMF)	580.4	38.3/36.7	3.82
Carbon tetrachloride	306.9	2.238	0

Table 2.1: Physical parameters of common solvents at 25 °C.<sup>64,70–72</sup>

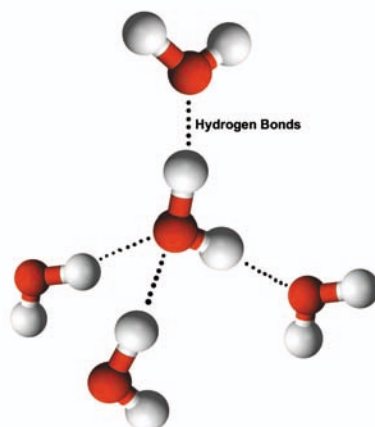


Figure 2.2: Representation of the 3D structure of liquid water.



The cohesive-energy density measures the total molecular cohesion per volume unit. It is also called cohesive-energy pressure (see eq. 2.1).

$$CED = \frac{\Delta U_v}{V_m} = \frac{\Delta H_v - R \cdot T}{V_m} \quad (2.1)$$

where  $V_m$  is the molar volume of the solvent,  $\Delta U_v$  and  $\Delta H_v$  are the energy and enthalpy (heat) of vaporization of the solvent to a non-interacting vapor, in which all intermolecular solvent-solvent interactions will be broken. Therefore, the CED represents the total strength of the intermolecular solvent structure. Hence, very high CED values indicate solvents of high polarity, whereas solvents with low polarity, such as perfluorhydrocarbons with weak interaction forces, are characterized by low CED values. Intermolecular hydrogen bonding, one of the interactions in highly ordered structures, increases the cohesive-energy density. Therefore, cohesive-energy density is a very important parameter to describe solvent polarity and cohesion. Thus, solvents with CED values close to that of water should allow surfactant aggregation.

Hildebrand et *al.*<sup>73</sup> described a relationship between CED and surface tension  $\gamma$ :

$$CED = \frac{\gamma}{V_m^{1/3}} \quad (2.2)$$

Lewis also explained that the attractive forces that induce cohesion are responsible for the surface tension.<sup>74</sup> This relationship was utilized by Gordon to measure the CED<sup>75</sup> of some polar solvents and even of melted salts. As we have seen, water offers physical parameters that allow surfactant aggregation. Namely, these are the high polarity, expressed by the high dipole moment and dielectric constant, and as well, the cohesive nature, which is a consequence of the structured nature of this solvent. In the frame of this work, we wanted to study the behavior of catanionic surfactants in non-aqueous polar solvents. The influence of some physical parameters should be

## Fundamentals

---

elucidated. In table 2.1, dipolar moment  $\mu$ , dielectric constant  $\epsilon_r$ , and cohesive-energy density CED of some common solvents are listed.

One can see that formamide, hydrazine and glycerol have parameters close to those of water. Especially, the values of the cohesive-energy density are elevated. However, the chemical stability of formamide and glycerol is higher than that of hydrazine. Moreover, the aggregation behavior of ionic and nonionic surfactants have been already studied in both formamide and glycerol in our laboratory. In addition, formamide can also be used as reaction medium, whereas glycerol is known to be used in pharmaceutical applications. Altogether, these solvents seem to be the best candidates to allow aggregate formation of cationic surfactants. In detail, formamide and water possess relatively high dielectric constants and dipole moments. In fig. 2.1 and 2.3, one can see that water and formamide exhibit a quite asymmetric structure and therefore their dielectric constants and dipole moments are higher than that of glycerol. Nevertheless, all three solvents are characterized by a highly ordered structure, which can be explained by the formation of hydrogen bonds in the liquid phase. All three molecules are built up by atoms with high electronegativities (O, N) in combination with H atoms that can form hydrogen bonds of the type O-H $\cdots$ O or N-H $\cdots$ O.

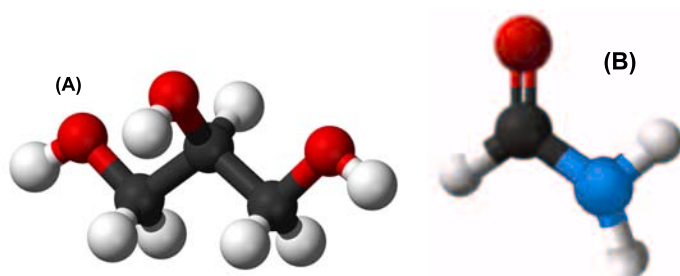


Figure 2.3: 3D models of glycerol (A) and formamide (B).

The structure of liquid glycerol was studied by Root *et al.* by molecular dynamics simulations.<sup>76</sup> They compared the crystalline structure of glycerol with those of stable (303.2 K) and supercooled (202.4 K) liquid glycerol. In the crystalline phase, a dimer is formed with two types of intermolecular hydrogen bonds. The dimer is visualized in fig. 2.4 (A). The authors were able to show that the molecules in the liquid network are bent differently than in the crystalline phase. In addition, they detected more hydrogen bonds than in the solid state, which they attributed to the formation of supplementary intramolecular hydrogen bonds in the liquid phase. An optimized structure of the liquid phase is given in fig 2.4 (B). This highly ordered structure is also reflected by an elevated value of the cohesive-energy density.

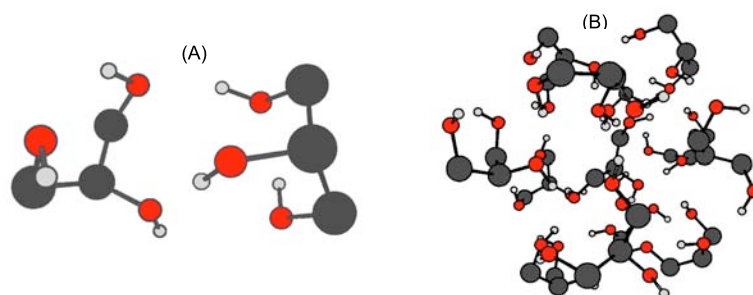


Figure 2.4: Structures of the glycerol dimer (A) and the condensed glycerol phase (B).

The structure of liquid formamide has been extensively studied by Ohtaki *et al.*<sup>77</sup> They studied different states of formamide using X-ray diffraction (XRD). In the crystalline and in the gas phase, all the atoms of the formamide molecule lay on a plane. Since this feature is true for the crystalline and the gas phase, one can also expect a planar structure for the liquid phase. Formamide crystals are made up by large ring structures that are formed by formamide cyclic dimers. This structure does not fit the condensed phase as it does not explain the high dielectric constant. However, X-ray diffraction measurements gave rise to the idea of the formation of two different

## Fundamentals

---

types of dimers in liquid formamide: a ring dimer and a linear dimer (see fig. 2.5). Ohtaki *et al.* showed by *ab initio* calculations that the ring dimer is the more stable one, but an open-chain structure with more than 16 molecules (8 chain dimers) seemed to possess higher stabilization energy in comparison to a ring dimer-based structure. Hence, a chain structure sporadically linked by ring dimers was the preferred model for liquid formamide. This model fits very well the X-ray and molecular dynamics data (see fig. 2.6).

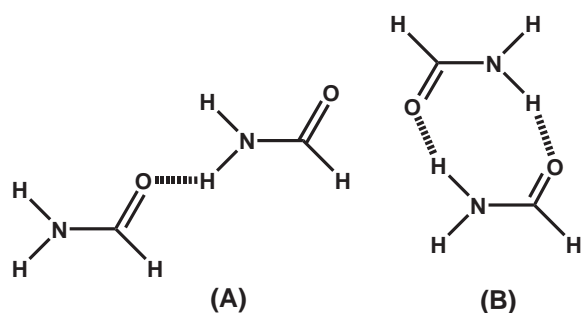


Figure 2.5: Possible arrangements of FA molecules in the liquid state. Linear dimer (A); ring structure (B).<sup>78</sup>

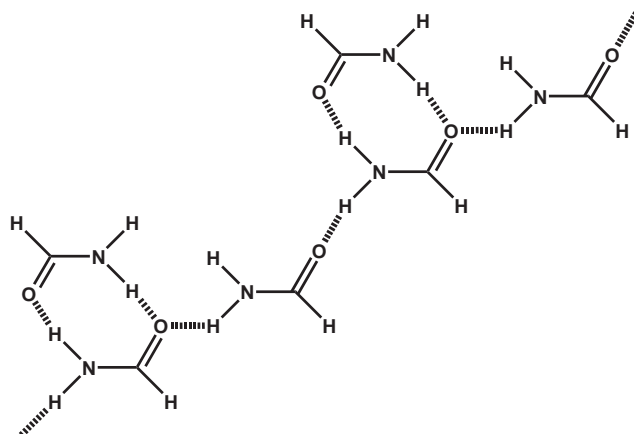


Figure 2.6: Proposed structure for liquid formamide.<sup>78</sup>

In summary, formamide and glycerol possess physical parameters close to those of water. A high dipole moment and a high dielectric constant combined to the possibility of H-bond formation favor highly ordered structures, which are expressed by elevated values of cohesive-energy density. Altogether, the physical characteristics presented make clear that formamide and glycerol are well adapted to be used as solvents in aggregation processes. Indeed, surfactant aggregation has already been observed in formamide and other polar solvents. The following chapter will give a bibliographical overview on the aggregation behavior of surfactants in formamide, glycerol and other polar and cohesive non-aqueous solvents.

## 2.2 Surfactants in Non-Aqueous Solution

### 2.2.1 General Information

Surfactant aggregation can be observed not only in aqueous solutions, but also in some non-aqueous solvents. Micelle formation has already been observed in apolar solvents, like chloroform, as well as in polar solvents, like formamide and glycerol.

In the first case, the main type of aggregates are reverse micelles, whose formation is due to dipole-dipole interactions between the polar headgroups of the surfactant molecules. In this case, the formation of micelles is possible even at very low concentrations and follows a step-by-step model.<sup>79</sup> Contrary to aqueous systems, where the micellization process is most of the time supposed to be a single step process with a precise *CMC*, the *CMC* of surfactants in apolar solvents is difficult to determine. In some cases, water traces favor the micellization in apolar solvents.<sup>79,80</sup>

In the second case, the formation of objects in a polar solvent requires a highly structured nature of this solvent. As we have seen, formamide and glycerol offer the closest physical characteristics to water. But in the literature, a wide series of

## Fundamentals

---

publications can be found, describing the aggregation process of amphiphilic molecules in hydrazine,<sup>81</sup> ethylammonium nitrate,<sup>82</sup> *N*-methylnone<sup>83</sup> or other low-melting salts.<sup>84–86</sup>

First experiments with formamide as non-aqueous solvent were performed in the early eighties by the group of Rico and Lattes.<sup>7</sup> They demonstrated that surfactants can principally form the same kind of mesophases in formamide as in water. But they also observed some differences between the aggregation behavior in formamide and in water.

One of these differences relates only to ionic surfactants in formamide. It was shown that Krafft temperatures  $T_K$  are higher in formamide than in water. For example, the Krafft temperature of CTAB (cetyltrimethylammonium bromide) in water is 26 °C, whereas it is 43 °C in formamide.<sup>87</sup> Qualitatively,  $T_K$  is defined as the intersection point between the solubility curve and the critical micelle concentration curve. The  $T_K$  is visualized in fig. 2.7.

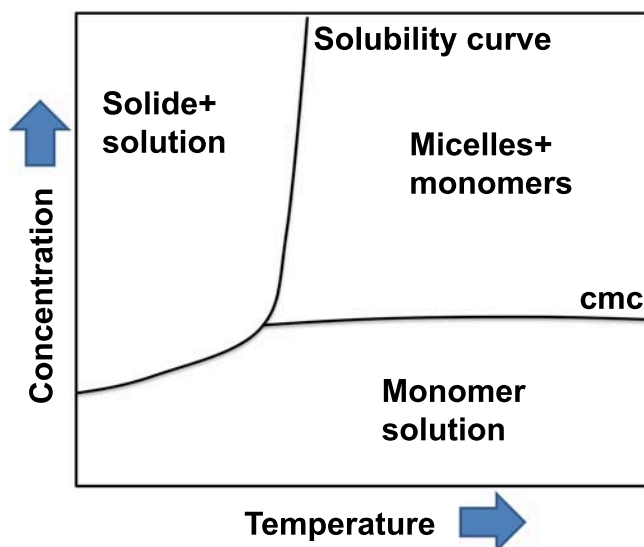


Figure 2.7: Schematic representation of a simple phase diagram indicating the  $T_K$ .

The differences in Krafft temperature  $T_K$  in formamide and water can be explained in terms of the medium structure. Firstly, the Krafft temperature  $T_K$  can also be defined as the melting temperature of solvated surfactants. Secondly, many investigations using NMR, IR, Raman spectroscopy, etc.<sup>88-92</sup> have demonstrated an almost totally ionic structure for formamide in the liquid state (see fig. 2.8). It can be viewed as a planar molecule with a substantial contribution from a resonance structure.

The C-N bond has a considerable double bond character<sup>93</sup> and the Arrhenius energy of activation for internal rotation was estimated at around 75-79 kJ.mol<sup>-1</sup>.<sup>93,94</sup>

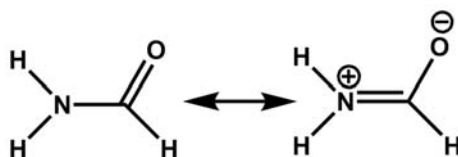


Figure 2.8: Mesomeric structure of liquid formamide.

It was shown that ion solvation by formamide involves the oxygen atom for cations and the nitrogen atom for anions, i.e. mainly electrostatic interactions are active in the solvation process.<sup>95</sup> The structures of liquid formamide and solvated salts in formamide can therefore be expected similar to the fused salt structures of compounds such as ethylammonium nitrate. It was shown that solvated surfactants in the low-melting salt ethylammonium nitrate possessed a much more rigid structure than their hydrated homologues.<sup>82</sup> In the non-aqueous system, the mixture of ethylammonium nitrate and surfactant can be seen as a type of mixed salt with electrostatic interactions. The structure of the hydrated surfactant, on the other hand, is only held together by dipole type interactions, producing a more fragile entity in comparison to the non-aqueous system. A similar explanation can be given for formamide, which is almost totally ionic in the liquid state. Solvated surfactants in formamide can therefore be compared

## Fundamentals

---

to mixed salts with higher melting points than their hydrated homologues. The Krafft temperature of ionic surfactants is therefore much higher in formamide than in water.

Another difference between aqueous and non-aqueous systems is the fact that the *CMCs* are higher in polar solvents than in water. At the origin of this behavior is the less cohesive nature of formamide and glycerol. As mentioned before, solvophobic interactions between the hydrophobic surfactant chains and the solvent is the main driving force for aggregation phenomena. As a consequence of the less cohesive nature, the solvophobic driving forces are reduced in favor of a higher solubility of the surfactant. Hence, the minimum concentration to obtain a sufficient repulsive effect between the tails and the solvent has to be higher in non-aqueous solvents than in water. This is true for ionic and nonionic surfactants in all organic polar solvents.<sup>96–98</sup> For example, studies on nonionic alkyl poly(ethylene oxide) surfactant  $C_iE_j$  showed that the *CMC* in formamide is about two orders of magnitude higher than in water.<sup>99</sup>

### 2.2.2 Thermodynamics of Micelle Formation in Non-Aqueous Solution

As we have seen, there are differences between the aggregation behavior of surfactants in water and in non-aqueous solvents. The high  $T_K$  in formamide could be explained by the ionic nature of liquid formamide. The differences in the *CACs* between aqueous and non-aqueous solvents can be qualitatively explained by the less cohesive nature of the non-aqueous solvents. Nevertheless, the main driving force of aggregate formation in water and in non-aqueous solutions is the solvophobic effect between the alkyl chains and the solvent. This solvophobic effect is accompanied by a gain in the free energy  $\Delta G$  and some modifications of the enthalpy  $\Delta H$  and the entropy  $\Delta S$ .

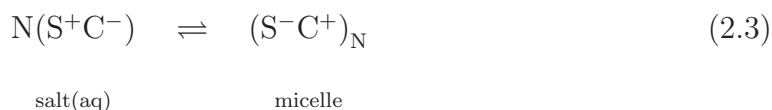
These parameters can be calculated or measured using two models, developed for aqueous systems.<sup>100,101</sup> Therefore, in a first step, we will introduce the thermodynamics



in aqueous systems. In a second step, the differences between thermodynamical values of the aqueous systems ( $\Delta G$ ,  $\Delta H$  and  $\Delta S$ ) will be compared to those of non-aqueous solvents.

Thermodynamical calculations for surfactant aggregation are generally based on two models – the equilibrium model (phase-separation model)<sup>100</sup> and the mass action model.<sup>101</sup> Both models were developed on aqueous solutions and are based upon an equilibrium between surfactant monomers in solution and a certain number of surfactant molecules in micelles. Both models start from the same basic equilibrium conditions between the monomer and the micelles. These models assume a single step mechanism for micelle formation. In other words, in the solution are present only monomers and micelles of a certain well-defined aggregation number  $N_A$ . These models do not work on micelle solutions with varying aggregation numbers.<sup>102,103</sup>

A typical ionic surfactant such as SDS can be viewed as a salt of the type  $S^-$  ( $S$  = surfactant) and  $C^+$  ( $C$  = counterion), where  $S$  is the dodecylsulfate part and  $C$  is the counterion ( $Na^+$ ). The chemical equilibrium is then given by<sup>104</sup>:



Then at equilibrium the chemical potentials of substances across the equilibrium sign are equal.

$$N \cdot \mu^{eq}(S^-; aq; \text{at } CMC) = \mu^{eq}\{(S^-C^+)_N; \text{micelle at the } CMC\} \tag{2.4}$$

Eq. 2.4 is the key thermodynamical condition for both above mentioned models. However, the further treatments of this equation differ depending on the model applied. Whereas the mass action model treats micelles and surfactant monomers as solutes in the aqueous solution, the phase equilibrium model views the micelles as a

## Fundamentals

---

separate phase in coexistence with the aqueous monomer solution. However, Blandamer et *al.* showed that the two systems gave similar results.<sup>104</sup> Nevertheless, the equilibrium model also takes into account the ion binding degree. In addition, this model has also been used for thermodynamical calculations on non-aqueous solutions in the literature.<sup>81,83</sup> Therefore this system will be described more precisely.

The model is based upon the assumption that solvated surfactants and micelles form two different phases, which are in equilibrium. One can compare it with the equilibrium between the gas phase and the liquid phase of a solvent. Solvent molecules will swap between phases (liquid  $\rightarrow$  gas) and (gas  $\rightarrow$  liquid) until an equilibrium is reached. A similar equilibrium is given for micelles in a dilute aqueous solution. Solvated monomers are in continuous exchange with micellized monomers. Hence, for a typical anionic surfactant (such as SDS) the equilibrium condition can be described as:



where for an anionic surfactant,  $C^+$ ,  $S^-$  and  $M^{p-}$  are the counterion, surfactant monomer and micelle, respectively. The parameter  $p$  corresponds to the aggregation number  $N_A$  and indicates the charge of the micelle without counterions. The corresponding equilibrium constant  $K$  is given by:

$$K = C_{M^{p-}} / \{(C_{C^+})^{n-p}(C_{S^-})^n\} \quad (2.6)$$

The equilibrium constant is related to the standard free energy of micelle formation per monomer unit by:

$$\frac{\Delta G}{nRT} = -\frac{1}{n} \ln C_{M^{p-}} + \ln C_{S^-} + \left(1 - \frac{p}{n}\right) \ln C_{C^+} \quad (2.7)$$

Typical micelles possess a high aggregation number ( $N_A = 50 - 100$ ). Hence, the  $C_{Mp-}$  term is small and insensitive to large errors in the estimated  $C_{Mp-}$ . In the absence of added salt, both  $C_{C+}$  and  $C_{S-}$  can be replaced by the  $CMC$  in the second and third terms in eq. 2.7, giving eq. 2.8:

$$\frac{\Delta G}{nRT} = (2 - \beta) \ln X_{CMC} \quad (2.8)$$

This is the reduced thermodynamic relationship between the standard free energy of micelle formation and the  $CMC$ , where  $\beta = p/n$  indicates the degree of dissociation of the counterions from the micelle.  $\beta = 1$  for completely ionized micelles, and  $\beta = 0$  for “neutral” micelles. Eq. 2.8 is useful to analyze the modification of the  $CMC$  with the variation of the chain length of a homologous series of surfactants.

A plot of the  $\ln X_{CMC}$  against the carbon number  $n_c$  of a homologous series can be described by:

$$\ln X_{CMC} = a_0 - a_1 n_c \quad (2.9)$$

where  $a_1$  and  $a_0$  are the contributions of the hydrophobic chains and of the polar headgroup, respectively.

One can combine eq. 2.8 and eq. 2.9 to get:

$$\frac{\partial \Delta G}{\partial n_c} = (2 - \beta) RT \left( \frac{\partial \ln X_{CMC}}{\partial n_c} \right) = (2 - \beta) RT a_1 \quad (2.10)$$

Eq. 2.10 is the free energy for the transfer of a methylene group from the bulk phase of the solvent into the micelles. In water, the free energy of micellization is negative and predominated by a large positive entropy change. The change of entropy in micelle formation is a composite result of two processes. In the first one, a large positive entropy change accompanies the removal of water from around the hydrocarbon chain.

## Fundamentals

---

	$\Delta G$ kcal.mol <sup>-1</sup>	$\Delta H$ kcal.mol <sup>-1</sup>	$\Delta S$ J.K <sup>-1</sup> .mol <sup>-1</sup>
H <sub>2</sub> O	-9.6	-6.1	11
Hydrazine	-7.8	-13.3	-18

Table 2.2: Free energy, free enthalpy and entropy of micellization in H<sub>2</sub>O and hydrazine.

In the second, a negative entropy change corresponds to the transfer of surfactants and counterions into the micelles. The enthalpy change in water is also the sum of two contributions of opposite sign. The removal of water is endothermic and the remaining transfer process is exothermic. Counting all together, the negative free energy of micellization is predominated by the positive entropy change in aqueous solutions. Eq. 2.8 and eq. 2.10 can be used to analyze the aggregation process in non-aqueous systems. It has to be said that these models are not perfectly correct in non-aqueous solvents, but some authors tried to get a better insight on aggregation mechanisms in non-aqueous solution. For example, Ramadan *et al.* compared the aggregation behavior of alkyl sulfates in water with that in hydrazine<sup>81</sup> using the phase-separation (equilibrium) model, as it was described above. They made a thermodynamical study on these systems mentioning hydrazine a “regular” water. They explained that these two solvents possess many almost identical parameters, but at low temperatures, they differ in just those parameters which reflect the unique behavior of water.

On the basis of eq. 2.8, Ramadan *et al.* calculated the free energies of the aqueous and the hydrazine systems. The values of standard free energy of micellization (of about -9.6 kcal.mol<sup>-1</sup> in water and -7.8 kcal.mol<sup>-1</sup> in hydrazine) are comparable, whereas the values for the free enthalpy (-6.1 and -13.3 kcal.mol<sup>-1</sup>, respectively) and entropy (11 and -18 J.K<sup>-1</sup>.mol<sup>-1</sup>, respectively) are very different. The fact that the free energies of micellization are comparable in water and in hydrazine indicates that these solvents possess a lipophobicity in the same order of magnitude.

On the other hand, the differences in the free enthalpies and the entropies are striking. In water, the favorable entropy gain leads to the formation of micelles, whereas in hydrazine, micelle formation seems to be a result of the favorable enthalpy change. As in the case of water, a homologous series of surfactants can be studied in non-aqueous solvents using eq. 2.10. This is the free energy for the transfer of a methylene group from the solvent into the micelles. The free energies of the methylene transfer in water and in hydrazine are practically the same, which confirms the above mentioned values of the free standard micellization energies. The lipophobicities of both solvents are similar.<sup>81</sup>

Similar studies were done on cetylpyridinium bromide in formamide and *N*-methylsydnone by Rico *et al.*<sup>83,105</sup> They could also demonstrate that the solvophobic interactions in formamide and *N*-methylsydnone are comparable to those in water. The differences in the behavior of aqueous and non-aqueous systems must be explained in terms of entropy and enthalpy changes. As mentioned previously, the entropy change of aqueous systems is positive and represents the driving force for self-aggregation, whereas the entropy changes in hydrazine is largely negative and reflects the association and ordering that accompanies the transfer of surfactant ions and counterions into the micellar structure. The formation of micelles in hydrazine appears to be entirely a result of the favorable enthalpy change ( $-13.3 \text{ kcal.mol}^{-1}$ ). Similar results have been obtained for formamide-based systems.

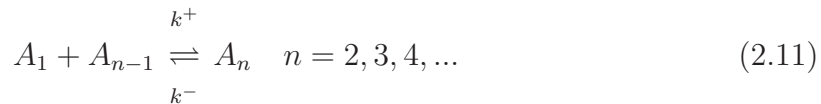
As a conclusion of this study, the aggregation process in non-aqueous solvents is not necessarily entropy driven as it is the case in water. The free energies of micellization are comparable in water, hydrazine, formamide and *N*-methylsydnone. This would indicate the same magnitude of lipophobicity of these solvents. The slightly higher values of  $\Delta G$  would not entirely explain the higher *CMCs* in non-aqueous solvents. Thus, other mechanisms, forces and interactions seem to play an important role.

## Fundamentals

---

Indeed, the different solvophobic interactions (van der Waals interactions between surfactant alkyl chains and solvent) and different solvent/polar headgroup interactions have an eminent influence on the aggregation behavior. This will be described in the next chapter (2.2.3).

In the above calculations, the equilibrium model was applied, assuming a single-step mechanism for micelle formation. But studies on the aggregation behavior of surfactants in non-aqueous solvents suggested that a multi-step equilibrium model is more likely in formamide. As a consequence, the results mentioned above are approximations that help to understand the rules of surfactant aggregation in formamide. However, Thomason *et al.*<sup>106</sup> studied nonionic alkyl poly(ethylene oxides) in formamide by ultrasonic relaxation. They observed a perturbation of the monomer/micellar equilibrium, which indicated a multi-step bimolecular aggregation process of the type (eq. 2.11):



In other words, this equation means that at least one step of the aggregation process is bimolecular and that in addition to micelles and monomers, intermediate aggregates were also present in the solution. The concentration of these intermediate aggregates was undetectably small, but was a necessary requirement for the above given scheme. Similar observations were done by Almgren *et al.*<sup>107</sup> and Belmajdoub *et al.*<sup>108</sup> They could detect a preorganization of the surfactant at low temperatures, that is to say at temperatures below the Krafft point  $T_K$ . Perche *et al.* showed by neutron scattering measurements on SDS in formamide that size and aggregation number increased over a wide concentration range.<sup>109</sup> This is contradictory to a pseudophase model and also indicates an existing multi-equilibria model for surfactant aggregation in formamide. As a consequence, the aggregation number can change with concentration and the

variance of distribution can achieve 80%. Therefore, polydispersity can be higher and the *CMC* is much more difficult to determine. A similar observation was made with reverse micelles in apolar solvents, where *CMCs* cannot be determined by surface tension measurements (see chapter 2.2.1).

### 2.2.3 *N*-Methylsydnone – Insights on Headgroup-Solvent Interactions

As mentioned above, headgroup-solvent interactions seem to play a key role in the aggregation process in non-aqueous solvents. An interesting case of non-aqueous polar solvent is *N*-methylsydnone (NMS), since this solvent points out the importance of headgroup-solvent interactions. It is a mesoionic solvent with a resonance structure (see fig. 2.9).

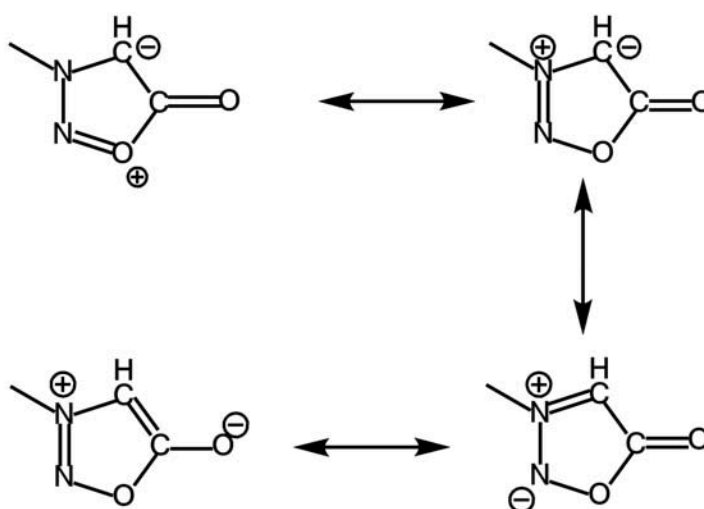


Figure 2.9: Mesomeric structure of *N*-methylsydnone.

An interesting fact is that *N*-methylsydnone is an aprotic solvent that cannot form hydrogen bonds. Therefore, the formation of a H-bond network like that of water, formamide or glycerol, is not possible. Nevertheless, *N*-methylsydnone possesses a

## Fundamentals

---

highly ordered structure, which is confirmed by an elevated value of the cohesive-energy density (1340 mPa, 25 °C). This can be explained by the asymmetric geometry of the molecule, which implies high values of dielectric constant  $\varepsilon/\varepsilon_0$  (144, 25 °C) and dipole moment  $\mu$  (7.3 D). The extremely high value of the permanent dipole moment allows NMS molecules to reorientate their dipole moment vectors in the same direction, which leads to a highly structured network. The parameters of *N*-methylsydnone are given in table 2.1 (page 34). Following these parameters, *N*-methylsydnone should allow aggregation of surfactants. Indeed, Auvray et al.<sup>110,111</sup> and Rico et al.<sup>83</sup> described the formation of micellar, liquid crystalline and lamellar phases by cetylpyridinium bromide (CPBr) in this aprotic solvent. These studies also demonstrated that the formation of H-bonds is not a prerequisite of aggregate formation. Optical micrographs showed the formation of ordered lamellar and hexagonal phases. They were able to prove this by X-ray scattering methods and X-ray diffraction measurements. CPBr undergoes a micelle-elongated micelle transition before the hexagonal phase is built. A similar transition behavior was observed for the CTAB/formamide system.<sup>112</sup>

However, optical micrographs of CTAB in *N*-methylsydnone did not show any evidence of hexagonal liquid crystalline phases. X-ray diffraction did not allow to detect any hexagonal phase. Nevertheless, micellar and lamellar phases could be observed. This study gave insight on the influence of headgroup-solvent interactions on the aggregation behavior in non-aqueous solvents. The reason why cetylpyridinium bromide does form liquid crystals and hexadecyltrimethylammonium bromide does not, lie in the different nature of the headgroups. One surfactant possesses a delocalized charge system in the pyridinium ring and the other surfactant possesses a localized charge on the single nitrogen atom of the ammonium group. While in water the hydrogen bonds between the polar head and water plays a dominant role, dipole-dipole interactions predominate in formamide and *N*-methylsydnone. This is due to the delocalized



structures of these solvents (see fig. 2.8 and 2.9). It was shown that the CPBr/*N*-methylsydnone system was characterized by more dipole-dipole interactions than the CTAB/*N*-methylsydnone system. In addition,  $\pi$ -stacking phenomena were not favored in the latter system. Further studies on zwitterionic and mesoionic surfactants were done in *N*-methylsydnone in comparison to formamide and water.<sup>83</sup> Homologous series of surfactants with a given headgroup were compared. As it was mentioned previously, a linear relationship between  $\ln X_{CMC}$  and the influence of headgroup and chain length can be described by the following equation:

$$\ln X_{CMC} = a_0 - a_1 n_c \quad (2.12)$$

where  $a_0$  is the contribution of the polar head to the micellization and  $a_1$  the increment per  $\text{CH}_2$  group, and  $n_c$  the total number of carbon atoms in the hydrophobic tail. One can plot  $\ln X_{CMC}$  against the number of carbon atoms in the alkyl chains. By calculating the slopes of eq. 2.12, it was demonstrated that the  $\text{CH}_2$  group increments  $a_1$  are the same in *N*-methylsydnone, formamide and water. In other words, the solvophobia of the alkyl chains are almost equal in these three solvents. Nevertheless, non-aqueous solvents are characterized by a less cohesive nature, which is also expressed by lower CED values. This deficit has to be compensated by other positive interactions, such as headgroup-solvent interactions. The headgroup parameters  $a_0$  of a given surfactant were different in these three solvents. In the case of CTAB, this was expressed by the formation of a hexagonal phase in water and formamide, but not in *N*-methylsydnone. Further studies on CPBr and CTAB systems in *N*-methylformamide (NMF) and *N,N*-dimethylformamide (DMF) confirmed this dependence on the headgroup-solvent interactions.<sup>111</sup> CPBr formed the same sequences of lyotropic phases in the protic solvents water, formamide, *N*-methylformamide (NMF). CTAB showed a different behavior in NMF, in which only the lamellar phase was ob-

## Fundamentals

---

served. In the aprotic solvent DMF, both surfactants showed only the formation of a lamellar phase. The behavior of CPBr in NMF seemed to be a limiting case, for which the headgroup type influenced significantly the aggregation behavior. The small CED value of NMF was balanced by the formation of dipole-dipole interactions between the pyridinium headgroup and the solvent. CTAB did not form a hexagonal liquid crystalline phase in NMF, which indicates less interactions of the localized charge of the ammonium headgroup with the solvent. Moreover, in the aprotic solvent DMF, the deficit in the CED could not be compensated by the dipole-dipole interactions of CPBr. As a conclusion, the aggregation behavior of surfactants in non-aqueous solvents depends strongly on the headgroup type. Aggregation phenomena in non-aqueous solvents therefore is the result of well chosen combinations of solvents and surfactants.

### 2.2.4 Micellar Phase in Non-Aqueous Solution

As we have seen, surfactants assemble themselves in aqueous solutions to aggregates. This phenomenon is driven by large gains of free energy  $\Delta G$  and entropy  $\Delta S$ . It was also mentioned previously that surfactants can form aggregates in non-aqueous solvents due to changes in  $\Delta G$  and  $\Delta S$  as well as favorable changes of the free enthalpy  $\Delta H$ . Principally, all mesophases found in water can also be found in non-aqueous solvents. One of the first micelle formation in a pure polar non-aqueous solvent was reported by Evans *et al.* in 1982.<sup>82</sup> They studied the *CMCs* of a series of cationic surfactants (alkyltrimethylammonium bromides and alkyipyridinium bromides) at 50 °C and of a non-ionic surfactant (Triton X-100) at 20 and 50 °C in ethylammonium nitrate, a low-melting anhydrous fused salt. Low-melting salts are also known as ionic liquids. Ionic liquids are organic compounds with a melting point below 100 °C. They are recently used as non-aqueous media, in which self-aggregation has been

demonstrated.<sup>113</sup> However, Evans et *al.* determined by surface tension measurements the *CMCs* of ionic and non-ionic surfactants in ethylammonium nitrate, which were about 5-10 times higher in the polar solvent than in water. Viscosity measurements gave indications about the micelle shape, since the shape of dispersed aggregates is directly related to the solution viscosity. They concluded from these measurements that the objects should possess spherical shape.

Later Ramadan et *al.*<sup>81</sup> studied hydrazine as a water substitute. Hydrazine possess a series of parameters close to those of water. They determined *CMC* higher in hydrazine than in water and a non-negligible contribution of the enthalpy  $\Delta H$  to the micelle formation.

The structure of micelles in formamide was then characterized by Rico and Lattes in the following years. A short review of the most important results about FA/surfactant systems is available.<sup>114</sup> In general, the aggregation number and the mean micelle diameter are smaller in formamide than in water, but they still possess a spherical shape at concentration values close to the *CMC*.<sup>109</sup> These two parameters are not concentration independent, that is to say that size and aggregation number can grow up with concentration.

Nuclear magnetic relaxation measurements<sup>115</sup> showed that the hydrocarbon tails are slightly more ordered than in the analogous water systems. This can be explained by the different polar nature ( $\epsilon_r$ ) of these solvents. The more polar environment of formamide can modify the conformational equilibrium, which leads to higher order parameter.

The same relaxation studies demonstrated a higher mobility of the alkyl chains around their long axes in formamide systems. Differences concerning the object-solvent interfaces are more important. The order parameter of hydrophobic-hydrophilic interfaces is much higher in water than in formamide, i.e. a less structured interface

## Fundamentals

---

and a higher lateral diffusion could be observed, which was explained by the larger bulkiness of formamide compared to water. But contrary to the chain mobility, the interface mobility is less influenced by the solvent, that is to say the surface is more rigid. It was also described that the effective headgroup surface per monomer is bigger in formamide than in water. A possible explanation is that formamide can penetrate deeper in the micelle solvation layer. This is reasonable, since the surfactants are more soluble in formamide than in water. Hence, the reduced solvophobic forces lead to a higher participation of formamide in the outer solvation layer.

Micelles of tetradecyltrimethylammonium bromide (TTAB) in water/glycerol mixtures were studied by Carnero Ruiz *et al.*<sup>116</sup> They found that micelle formation was not much affected by small quantities of glycerol up to 20 % (w/w). They explained the augmentation of the *CMC* values by an indirect effect of the mixing of these two solvents. Since the dielectric constant ( $\epsilon_r/\epsilon_0$ ) of glycerol is much smaller (42.9, 25 °C) than that of water (78.5, 25 °C), the medium properties were changed. Especially, the reduced dielectric constant of the solvent mixture had an important influence on the aggregation behavior of TTAB. In addition, they found that micelle size and number decreased with increasing glycerol content. At the same time, the surface area per headgroup increased, which was attributed to the higher participation of glycerol in the micelle solvation layer. This could also be observed for surfactant/FA systems.

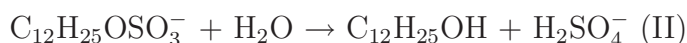
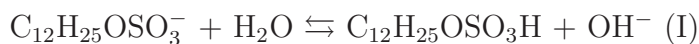
Other studies on CTAB in glycerol and SDS in formamide allowed to image micelles in non-aqueous solvents for the first time using cryo-TEM.<sup>117</sup> They observed spherical objects of CTAB in glycerol and SDS in formamide and compared them to the spherical objects formed in the corresponding aqueous solutions. They noted that the size of the spherical objects in polar solvents did not differ much from that in water. However, they could offer a first visual evidence of micelle formation in non-aqueous solution.

### 2.2.5 Hexagonal and Lamellar Phases in Non-Aqueous Solution

In addition to micellar phases, hexagonal and lamellar phases can be obtained in non-aqueous solvents. Hexagonal and lamellar phases are anisotropic and can be observed by optical microscopy under cross polarized light and by X-ray diffraction methods. Hexagonal phases are usually formed by rod-like micelles occupying a hexagonal lattice, whereas lamellar phases are built up by bilayers. Belmajdoub et al.<sup>108</sup> studied a CTAB/FA system. They were able to identify a hexagonal phase and a lamellar phase. The optical micrographs are similar to those of the analogous CTAB/H<sub>2</sub>O system. They observed a micelle/elongated micelle transition at concentrations above the *CMC* before a hexagonal liquid crystalline phase was formed. The same kind of transition was observed for the CPBr/*N*-methylsydnone and SDS/water systems. SDS forms liquid crystalline structures in formamide.<sup>118</sup> The binary system exhibited the following sequence of mesophases with similar lattice parameters to the analogous water system:



In comparison to SDS in water, the sequence of mesophases is less complex. This is due to the fact that SDS is stable in formamide, whereas in water, SDS undergoes two degradation reactions:



## Fundamentals

---

Therefore, the SDS/water system exhibits a more complex phase diagram. However, the hexagonal lyotropic phase is characterized by typical phase defects under polarizing light. Fig. 2.10 shows these defects.

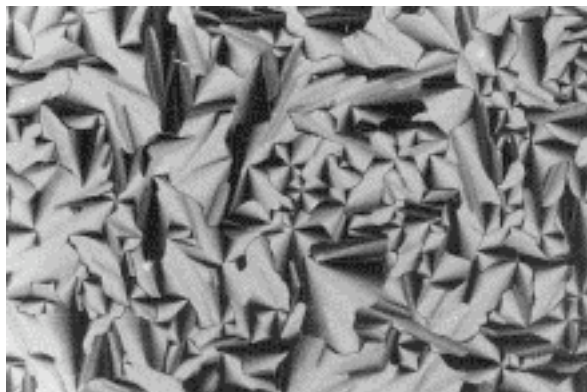


Figure 2.10: Optical micrograph under polarizing light: lyotropic hexagonal phase of SDS in FA.<sup>114</sup>

A similar study was done by Wörnheim *et al.*<sup>119</sup> They compared the phase diagrams of several alkyltrimethylammonium surfactants in water, formamide, glycerol and ethylene glycol. In water CTAB forms a typical sequence, that is to say a solution phase  $I_\alpha$ , a hexagonal liquid crystalline phase, a cubic phase Q and a lamellar phase  $L_\alpha$  with increasing surfactant concentration. The same sequence could be identified in formamide, in glycerol and in ethylene glycol. A general conclusion was that existence regions of lyotropic liquid crystals are smaller in polar solvents than those observed in water. At the same time, the isotropic solution domain increases using polar solvents instead of water. In other words, lyotropic hexagonal liquid crystalline phases are less readily formed in polar solvents than in water. Lamellar phases are quite often observed in non-aqueous solvents. Ionic surfactants like CPBr and CTAB formed lamellar phases in protic and aprotic solvents.<sup>83,111</sup> It was even shown that lamellar phases were formed in *N,N*-dimethylformamide (DMF).<sup>111</sup>

This is an interesting result, because DMF is an aprotic solvent, which cohesive-energy density is low in comparison to water. Therefore, it was not possible to observe micellization and formation of liquid crystals, but lamellar structures seemed to be formed more easily than other types of aggregate.

### 2.2.6 Vesicle Formation in Non-Aqueous Solution

The formation of lamellar phases is a requirement for vesicle formation, since vesicles are built up by flexible bilayers. Vesicles formed by dioleoylphosphatidylcholine (DOPC) in glycerol-water mixtures were observed by Johansson *et al.*<sup>120</sup> They were able to form vesicles by sonication of a diluted DOPC solution containing a lamellar phase. With increasing glycerol content up to 50 %, the size of the vesicles decreased continuously. A similar phenomenon was observed for the micelle size in non-aqueous solutions. After this decrease of the vesicle size, they could observe an increase of the aggregate size, when the water content was reduced to a value of 10 %. The mean diameter of the vesicles increased rapidly and was measured at about 90 nm. The authors mentioned a long-time stability (several months) for vesicles in a 91:9 glycerol-water mixture.

Meliani *et al.* studied cationic bicationic surfactants of the type dialkyldimethylammonium bromide.<sup>121</sup> The formation of multilamellar vesicles in formamide with diameters of 100-500 nm was reported. Higher concentrations and longer sonication times were necessary to obtain vesicles in formamide compared to the analogous aqueous systems. The layer thickness was evaluated at 2 nm, which is “slightly” smaller than in water (4 nm). The polydispersity of the vesicles was large and the vesicles grew rapidly. Phase transition temperature  $T_c$  of the dodecylalkyldimethylammonium bromide/formamide system was determined by a probe reaction (decarboxylation of

## Fundamentals

---

6-nitrobenzisoazole). The measured temperatures are much higher (about 40 °C) in the formamide systems than in comparable aqueous systems (about 28 °C).

In further studies, lecithin (Lipoid 80) surfactants in formamide gave rise to the formation of liposomes with stabilities lasting for more than 2 weeks.<sup>122</sup> It is interesting to note that the size of the liposomes was found larger than in water. But electron micrographs showed that the bilayer thickness were about 4 nm in formamide systems and 7 to 10 nm in aqueous systems. Taking all together, the observations made for vesicle/formamide systems are in line with those made for classic monocatenar surfactants. The structural parameters were smaller in formamide systems than in the corresponding aqueous systems. This fact can be attributed to the less ordered structure of formamide. Nevertheless, it was shown undoubtedly that vesicle formation was possible in formamide and in glycerol.

### 2.2.7 Microemulsions in Non-Aqueous Solution

As we have seen, aggregate formation is possible in cohesive non-aqueous solvents. Binary surfactant/FA systems can form similar phases to the ones observed in aqueous systems. Therefore, it is not surprising that the formation of waterless microemulsions is also possible with formamide,<sup>4,62,112</sup> glycerol,<sup>123,124</sup> and ethylene glycol<sup>11</sup> as polar continuous phase instead of water. Lattes and co-workers<sup>4,6,7,62,112,125-127</sup> studied formamide-based systems. It was found that O/FA and FA/O microemulsions can be formed as well as bicontinuous phases. SAXS measurements on a formamide-octane microemulsion gave an insight on the microstructure of the microemulsion. They did not detect any spherical droplets or cell like objects that aqueous microemulsions display. These studies gave evidence of the formation of formamide-rich particles, and more precisely formamide filaments.<sup>112</sup> These studies with formamide microemulsions showed that chemical reactions such as (photo-)amidation of olefins<sup>4,5,127</sup> or the



Wacker process<sup>126</sup> can be performed with higher yields and higher reaction rates than in the analogous heterogeneous classic aqueous systems. Non-aqueous microemulsions, namely those with formamide, were recently used for the synthesis of nanoparticles and nanocrystals. Hsiao et al. obtained nanoporous polymeric crystals with the help of microemulsions.<sup>128</sup> The reversed microemulsion was formed by formamide droplets dispersed in an acrylate monomer phase. After polymerization of the acrylate phase, formamide was evaporated and a well defined nanoporous structure was obtained. The use of formamide was explained by the formation of well dispersed formamide droplets in this kind of microemulsions.<sup>128</sup> Formamide microemulsions with the help of non-ionic surfactants were described by Schubert et al.<sup>99,129</sup> The amphiphiles used were a series of alkyl poly(ethylene oxides) ( $C_iE_j$ ). They compared the aqueous systems with the analogous formamide systems. As already mentioned above, surfactants get less effective in non-aqueous solvents due to a higher solubility and a reduced surface activity. As a consequence, ternary formamide-surfactant-oil microemulsions are characterized by higher surfactant concentrations than the analogous aqueous systems, when the same surfactant is used. However, the authors described a similar behavior of formamide microemulsions, if the hydrophobic chain length of the surfactant is about 4 C-atoms longer than in the aqueous system. In addition, they were able to identify bicontinuous structures similar to the ones that can be found in the aqueous microemulsions. Further studies were done on the influence of the amphiphilicity.<sup>99,129</sup> They augmented simultaneously the number of glycol ether groups of the polar head and the carbon number of the alkyl chain. With increasing amphiphilicity, the existing regions of microemulsions increased, too. In addition, the authors showed that the  $C_iE_j$ /FA microemulsions reacted in the same way to inorganic salt additions as the corresponding aqueous systems. The addition of lyotropic salts, such as NaCl, dropped

the cloud-point of the nonionic surfactant, whereas hydrotropic salts like NaSCN rose the cloud-point.

As a conclusion, microemulsions can be obtained using formamide or glycerol instead of water. Moreover, they can be used to improve chemical reactions such as (photo-)amidations of olefins. Nevertheless, the microstructure of non-aqueous microemulsions is not similar to that of analogous aqueous systems.

### 2.3 Catanionic Surfactants and Surfactants with Large Organic Counterions in Non-Aqueous Solution

As we have seen, surfactants – ionic and non-ionic ones – have been extensively studied in non-aqueous solvents. But little work has been done so far on catanionic surfactants in non-aqueous solvents. The aim of this study was then to rationalize the influence of polar non-aqueous solvents on the aggregation behavior of catanionic associations. Therefore, we give here an overview about the work already done on catanionic surfactants in non-aqueous solvents, especially formamide. Friberg *et al.* were one of the groups that worked on catanionic associations in non-aqueous solvents. They worked on ternary phase diagrams of the system octylamine, octanoic acid and formamide.<sup>14</sup> The system underwent an acid-base reaction in formamide and formed a kind of catanionic entity. The equilibration times were long and the final phase diagram was obtained after 3 weeks (see. fig. 2.11). They were able to obtain a liquid isotropic phase ( $I_\alpha$ ), which was in equilibrium with the crystalline salt formed at equimolar ratio of octanoic acid and octylamine (A). An equimolar ratio of amine and acid led to precipitation. They compared the formamide system to the water-octylamine-octanoic acid system and reported that the non-aqueous system did not

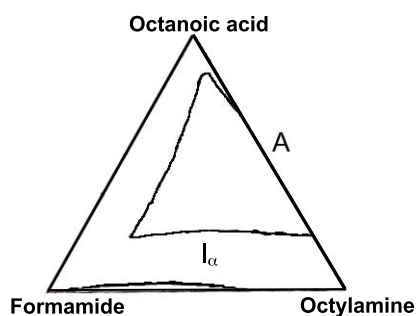


Figure 2.11: Phase diagram of formamide, octylamine and octanoic acid.  $I_{\alpha}$ : liquid isotropic phase; A: crystalline salt formed by octanoic acid and octylamine at equimolar ratio.

form any liquid crystalline phases, whereas the aqueous system did. In any case, they could not find any evidence for micelle or vesicle formation.

Further studies on aqueous mixed cationic-anionic systems of the type alkylammonium alkanoate (comprising NaBr residual salts) were done by the research group of Huang *et al.*<sup>15,16</sup> They investigated the influence of polar solvents on the stability of catanionic vesicles preformed in water. Whereas a small amount of formamide destroyed these vesicles, it was shown that the vesicles were stable in ethanol-water and DMSO-water mixtures. They explained this effect by the medium dielectric constant, which has an influence on the electrostatic interactions of the polar headgroups and therefore on the geometric shape of the catanionic surfactant. While ethanol and DMSO possess dielectric constants lower than water, they can improve electrostatic interactions. Formamide, having a much larger dielectric constant reduces headgroup interactions and can dissociate the catanionic association. Hence, the formation of vesicles was not possible anymore. However, the studies of Friberg *et al.* did not imply a beforehand prepared catanionic association. The reaction was performed directly in formamide. Huang *et al.* studied catanionic systems with residual salts. But catanionic surfactants without residual salts have not yet been studied in non-aqueous solutions. We wanted therefore to study the behavior of residual-salt free

## Fundamentals

---

catanionic surfactants in formamide and other non-aqueous polar solvents. Moreover, a special type of catanionic associations – ionic surfactants with large organic counterions – was developed in our laboratory. In some extent, these surfactants show properties similar to those of catanionic surfactants. In our laboratory, a new kind of norbornene methyleneammonium alkanoate was synthesized and a concentration dependent micelle-vesicle transition was reported. As it was explained, geometry and headgroup-counterion interactions play a dominant role in the aggregation process. These ionic surfactants with large counterions have not yet been studied in polar non-aqueous solvents. For that reason, it would be of great interest to study the aggregation process of these organic counterion surfactants in non-aqueous solvents, in which the solute-solvent interactions are very important.

## Part III

# Results and Discussion



# 1

## Conception of the Problem

In this work, we wanted to rationalize the aggregation behavior of cationic surfactants in non-aqueous solutions. For this issue we started to study simple model systems based upon fatty acids and amines. These commercially available products form simple straightforward cationic systems (alkylammonium alkanoates), on which we could test the general behavior of cationic surfactants. In particular, we were interested in the following question: do cationic surfactants show a different behavior in non-aqueous polar solvents in comparison to water, and to what extent? In addition, we tested the influence of chain lengths and chain symmetry. These results would

## Results and Discussion

---

be of great interest to understand the general behavior of cationic surfactants in formamide.

Nevertheless, the simple model systems were not enough soluble in water. A comparative study of the aggregation behavior of cationic systems in aqueous and non-aqueous solvents requires a cationic system which is well soluble in water, in formamide and in glycerol, as well as in the mixtures of these solvents. In order to increase the solubility in non-aqueous solvents, we synthesized glucose-based surfactants. It was shown that this type of cationic associations was reasonable soluble in water, in glycerol and in formamide, as well as in the mixtures of these solvents. The glucose-based surfactants, hence called G-Hyd<sub>m</sub>, were prepared with various chain lengths in the lipophilic part. In a second step, the cationic associations were formed with fatty acids of varying chain lengths by a simple acid-base reaction in water. The aggregate types of these cationic surfactants in formamide and in other non-aqueous solvents were compared to those in aqueous systems.

We have seen that a high value of cohesive-energy density of the solvent was a predominant requirement for self-aggregation. Nevertheless, previous studies indicated that additional parameters can influence the type of aggregates in non-aqueous cationic systems. For example, Huang *et al.*<sup>15,16</sup> have already reported that the addition of formamide to cationic aqueous solutions had eminent consequences on the aggregate type. Beforehand formed vesicles in water were destroyed after addition of formamide. They mentioned the influence of the dielectric constant on the ion pair integrity. It has to be remembered that cationic surfactants are composed of an ion pair formed by two oppositely charged surfactants. They can be compared to organic salts with amphiphilic character. The aim of this work was then to rationalize the aggregation behavior of cationic surfactant in non-aqueous solvents and to determine the influence of physical solvent parameters such as the dielectric constant.



## Results and Discussion

---

Moreover, cationic surfactants with a various number of carbon atoms in the hydrophobic part were tested in order to elucidate the influence of the solvophobic effect on the aggregation behavior. Finally, cationic associations with large counterions were synthesized and the results were compared to what have been obtained with the sugar-based systems. In this way, the influence of the headgroup could be studied.



# 2

## Synthesis and Characterization of Catanionic Systems

### 2.1 Model Systems of the Alkylammonium Alkanoate Type

In a first step, we wanted to study the general behavior of cationic surfactants in formamide. Therefore, we synthesized straightforward model systems (**3a-g**) of the alkylammonium alkanoate type ( $C_m^+/C_n^-$ ) with various chain lengths in the cationic

## Results and Discussion

---

and the anionic part. The systems were based upon fatty acids and amines, which were commercially available. The model systems were synthesized by a simple acid-base reaction in diethyl ether followed by a co-precipitation of the cationic system in equimolar ratio (see fig. 2.1).<sup>26,27</sup>

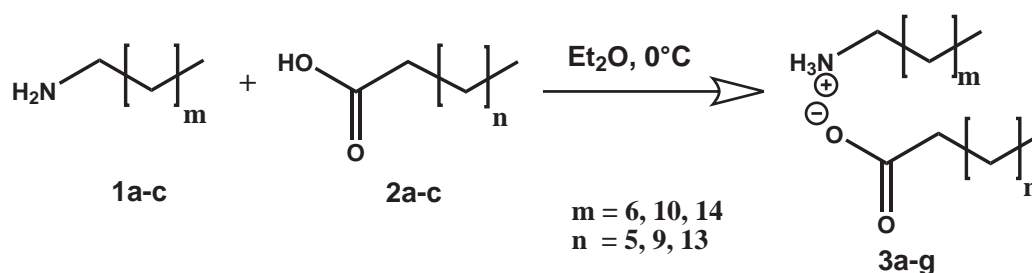


Figure 2.1: Synthesis of simple model systems  $C_m^+/C_n^-$ .

To perform the reaction, both acids and amines were separately dissolved in diethyl ether. The solutions were cooled down to 0 °C and poured together under stirring. The alkylammonium alkanoates precipitated as white crystalline powders, with reaction yields ranging between 80 and 90 %. This reaction allowed us to obtain in a simple way equimolar associations of cationic and anionic surfactants without residual salts. Various chain lengths of 8, 12 and 16 carbon atoms in both amine and acid moiety allowed us to synthesize 7 different systems (see table 2.1). As it was explained previously, Krafft temperature and *CAC* are higher in formamide than in aqueous solution. It is important to study the behavior of cationic surfactants in formamide with respect to these parameters. The simple easily prepared model systems were adequate to study the general behavior of cationic surfactants.

Compound	Yield	Number of C-atoms
<b>3a</b>	C <sub>8</sub> <sup>+</sup> /C <sub>8</sub> <sup>-</sup> 90 %	16
<b>3b</b>	C <sub>8</sub> <sup>+</sup> /C <sub>12</sub> <sup>-</sup> 92 %	20
<b>3c</b>	C <sub>12</sub> <sup>+</sup> /C <sub>8</sub> <sup>-</sup> 91 %	20
<b>3d</b>	C <sub>12</sub> <sup>+</sup> /C <sub>12</sub> <sup>-</sup> 79 %	24
<b>3e</b>	C <sub>8</sub> <sup>+</sup> /C <sub>16</sub> <sup>-</sup> 89 %	24
<b>3f</b>	C <sub>16</sub> <sup>+</sup> /C <sub>8</sub> <sup>-</sup> 84 %	24
<b>3g</b>	C <sub>16</sub> <sup>+</sup> /C <sub>16</sub> <sup>-</sup> 89 %	32

Table 2.1: Model systems **3a-g**.

## 2.2 Sugar-Based Systems of the G-Hyd<sub>m</sub><sup>+</sup>/C<sub>n</sub><sup>-</sup> Type

Nevertheless, the simple systems were not soluble in water at equimolar ratio. This is a well known behavior of catanionic surfactants and can be explained by the fact that the effective headgroup area of a catanionic association is smaller than the simple sum of the headgroup areas of the two ionic surfactant. The reduced solvation sphere decreases the water solubility and catanionic surfactants tend to precipitate at equimolar ratio.<sup>31,130</sup> Since we wanted to compare the behavior of catanionic surfactants in formamide with that in water, a catanionic system with a reasonably high solubility in water, in formamide and in glycerol was required. Previous studies on catanionic surfactant showed that sugar-based catanionic surfactants are water soluble at equimolar ratio.<sup>32</sup> In our laboratory, some lactose-based catanionic systems were synthesized (L-Hyd<sub>12</sub> and L-Hyd<sub>16</sub>), and were well water soluble. Moreover, these systems spontaneously formed vesicles in water, and as previously mentioned, pharmaceutical applications are under development.<sup>35,39,40,46</sup> We started to test these systems in formamide, but their solubility was not sufficient to perform comparative studies in water and in formamide. This could be explained by the fact that these systems

## Results and Discussion

are very hydrophilic. The lactitol-based surfactants, developed for aqueous systems, possess a too hydrophilic nature to be sufficiently soluble in formamide, which is characterized by a less cohesive nature than water. The hydrophilicity can be decreased by reducing the number of hydroxyl groups. Glucose-based cationic surfactants are less hydrophilic and may be more soluble in formamide than the L-Hyd<sub>x</sub> type surfactant. Therefore, we synthesized a system similar to the above mentioned cationic lactitol systems but based upon glucose. The sugar-based amine, *N*-alkylamino-1-deoxy-D-glucitol (compound **4a-c**), was synthesized in our laboratory<sup>131</sup> (see fig. 2.2).

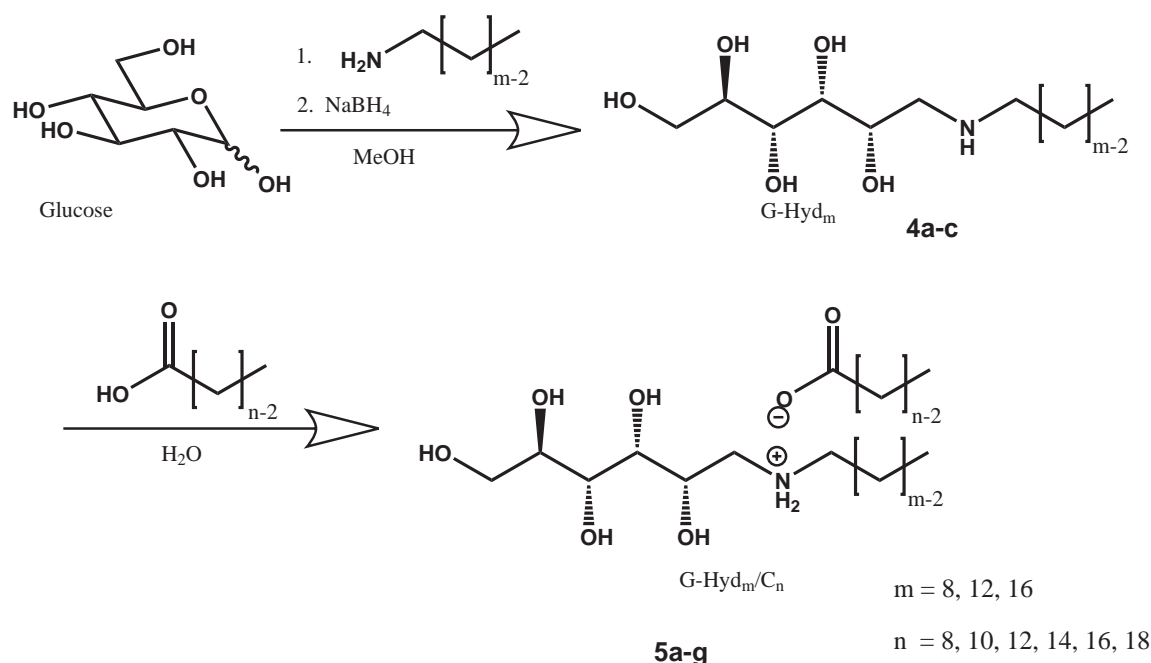


Figure 2.2: Reaction scheme for compounds of the type G-Hyd<sub>m</sub><sup>+</sup>/C<sub>n</sub><sup>-</sup>.

Non-protected glucose was reacted with a fatty amine to give an imine, which was reduced by sodium borohydride (NaBH<sub>4</sub>). After addition of concentrated hydrochloric acid, a white powder precipitated. A bit of the solvent was evaporated in order to eliminate the highly volatile methyl borates. The powder was filtered off and washed. The final product was obtained by stirring the crude product with a slight excess

of sodium hydroxide in methanol. The free amine was filtered off and washed with ice-cold water and ethanol.

	Compound	Yield	Number of C-atoms
<b>4a</b>	G-Hyd <sub>8</sub>	40 %	8
<b>4b</b>	G-Hyd <sub>12</sub>	50 %	12
<b>4c</b>	G-Hyd <sub>16</sub>	50 %	16
<b>5a</b>	G-Hyd <sub>8</sub> <sup>+</sup> /C <sub>12</sub> <sup>-</sup>	quant.	20
<b>5b</b>	G-Hyd <sub>12</sub> <sup>+</sup> /C <sub>8</sub> <sup>-</sup>	quant.	20
<b>5c</b>	G-Hyd <sub>8</sub> <sup>+</sup> /C <sub>16</sub> <sup>-</sup>	quant.	24
<b>5d</b>	G-Hyd <sub>16</sub> <sup>+</sup> /C <sub>8</sub> <sup>-</sup>	quant.	24
<b>5e</b>	G-Hyd <sub>16</sub> <sup>+</sup> /C <sub>12</sub> <sup>-</sup>	quant.	28
<b>5f</b>	G-Hyd <sub>12</sub> <sup>+</sup> /C <sub>16</sub> <sup>-</sup>	quant.	28
<b>5g</b>	G-Hyd <sub>12</sub> <sup>+</sup> /C <sub>18</sub> <sup>-</sup>	quant.	30

Table 2.2: Sugar-based surfactants **4a-c** and catanionic systems **5a-g**

Three *N*-alkylamino-1-deoxy-D-glucitols were synthesized with 8, 12 or 16 carbon atoms in the alkyl chain. The reaction yields depended on the chain length in the lipophilic part. In the case of G-Hyd<sub>8</sub>, 40 % of the theoretical yield was obtained, whereas the systems G-Hyd<sub>12</sub> and G-Hyd<sub>16</sub> were synthesized with 50-60 % yield. The lower yield in the case of the short chain amine can be explained by the higher solubility in water and methanol. The catanionic association was then obtained by an acid-base reaction between the glucose-based surfactant G-Hyd<sub>*m*</sub> and simple fatty acids in water. The final product, a colorless powder, was obtained in quantitative yield after freeze-drying. Being a simple reaction, a wide series of *N*-alkylammonium-1-deoxy-D-glucitol alkanoates (G-Hyd<sub>*m*</sub><sup>+</sup>/C<sub>*n*</sub><sup>-</sup>) could be prepared in order to study their aggregation behavior in relation to the number of carbon atoms in the hydrophobic part. These catanionic systems were enough soluble in water and in formamide to perform comparative studies. The solubility depends on the number of carbon atoms in the hydrophilic part. G-Hyd<sub>8</sub><sup>+</sup>/C<sub>12</sub><sup>-</sup> for example was soluble up to 5.10<sup>-1</sup> mol.L<sup>-1</sup>

## Results and Discussion

---

in water (25 °C), whereas G-Hyd<sub>16</sub><sup>+</sup>/C<sub>12</sub><sup>-</sup> was soluble up to 1.10<sup>-3</sup> mol.L<sup>-1</sup> in water (25 °C). Moreover, the systems were also soluble in formamide and glycerol in sufficient quantities (up to 5.10<sup>-1</sup> mol.L<sup>-1</sup>) to perform physico-chemical studies and to compare the aggregation behavior of catanionic systems in non-aqueous solutions and in water.

### 2.3 Characterization of the Catanionic Systems

In order to study the behavior of catanionic systems in polar solvents, we characterized the systems prior to any physico-chemical study. On the one hand, we had to check the formation of the catanionic association (and its purity) and on the other hand, we had to prove that we obtained an equimolar ratio between anionic and cationic moieties in the association. The formation of the ion pair can be demonstrated by three different methods. NMR and IR techniques allow to follow the reaction and give information about the completeness of the reaction. In addition, mass spectrometry can show the existence of the ion pair as a full-fledged entity. The equimolarity between anionic and cationic parts can be proved by elemental analysis.

The formation of the catanionic association can be proved indirectly by NMR spectroscopy. Our catanionic systems are synthesized by an acid-base reaction between a fatty acid and an amine. Acid-base reactions are usually reactions with an equilibrium, i. e. the starting products do not necessarily react completely to the catanionic association. The reaction is performed with equimolar quantities of acid and base, so that after a complete reaction the initial acid should have reacted to the corresponding carboxylate group. The chemical shifts of the carboxylic and the carboxylate groups are significantly different, and residual unreacted acid can be observed by NMR spectroscopy. Therefore, the spectra of a pure catanionic association should not exhibit any signal for the carboxylic acid. The signal for the carbon atom in the carboxylic groups is expected to be around 170-176 ppm, whereas the signal of the carboxylate



group can be observed around 180-185 ppm. It has to be noted that the chemical shift of the  $\alpha$  proton of the ammonium species can be used as well as proof for the formation of the cationic association. Fig. 2.3 shows the  $^{13}\text{C}$  NMR spectra of hexadecanoic acid and G-Hyd $_8^+$ /C $_{16}^-$ . In the case of the hexadecanoic acid, we observed a single peak at 176.4 ppm. In the case of the cationic association, a single peak at 181.1 was measured. The spectrum of the cationic association did not exhibit a peak between 170 and 176 ppm, which indicated that the product was free of residual carboxylic acid. Thus, the reaction was performed completely and the formation of the ion pair was ensured.

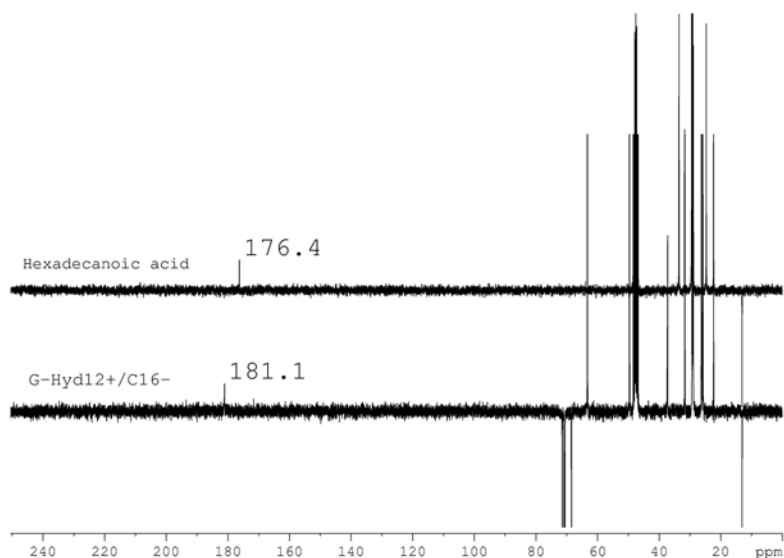


Figure 2.3:  $^{13}\text{C}$  NMR spectra of the hexadecanoic acid **2c** and the cationic surfactant **5f** (G-Hyd $_{12}^+$ /C $_{16}^-$ ) in  $\text{CD}_3\text{OD}$ .

The formation of the cationic association can also be proved by infrared spectroscopy. In this case, we can also compare the spectra of the initial reagent with that of the synthesized product. The signals of carboxylic acids and of their corresponding carboxylate groups are quite different. The peak of carboxylic acids can be

## Results and Discussion

---

found around  $1650\text{-}1750\text{ cm}^{-1}$ , whereas the carboxylate group can be identified around  $1500\text{-}1600\text{ cm}^{-1}$ . The catanionic association should be free of residual carboxylic acid. Thus, we expected to obtain a IR spectrum without the characteristic peak for the acid around  $1650\text{-}1750\text{ cm}^{-1}$ . In fig. 2.4, the differences are exemplary given for the catanionic  $\text{G-Hyd}_{12}^+/\text{C}_{16}^-$  system and the initial carboxylic acid (hexadecanoic acid). The peak of the carboxylic group of the hexadecanoic acid was identified at  $1702\text{ cm}^{-1}$ , whereas the  $\text{G-Hyd}_{12}^+/\text{C}_{16}^-$  system exhibited a sharp peak at  $1577\text{ cm}^{-1}$ . The latter system was not characterized by a peak for the carboxylic acid, which indicated that the product did not contain any residual carboxylic acid. Thus, the formation of the ion pair was assumed.

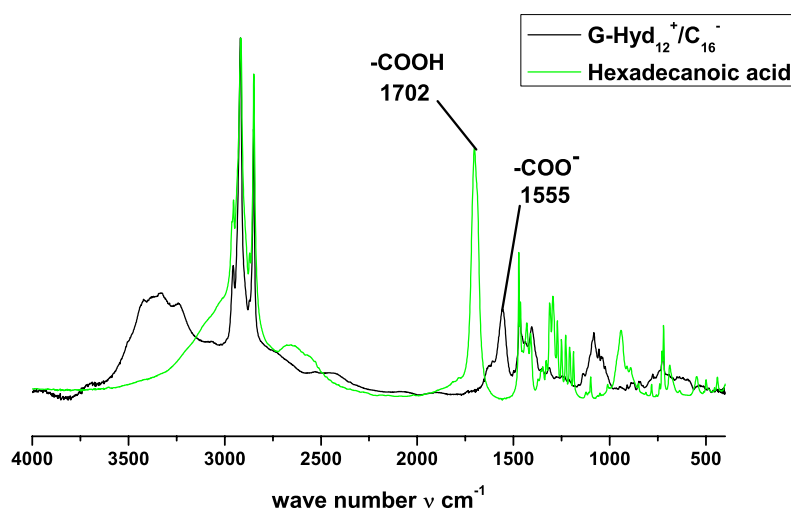


Figure 2.4: FT-IR spectra of the hexadecanoic acid **2c** and the catanionic surfactant **5f** ( $\text{G-Hyd}_{12}^+/\text{C}_{16}^-$ ).

Another possibility to prove the formation of the catanionic association is mass spectrometry. With this method, the formation of the catanionic association can be observed directly. Mass spectrometry generally consists in the separation of charged molecules in an electromagnetic field, depending on the ratio between mass and charge

( $m/z$ ). In our laboratory, a method was developed to visualize the catanionic entity by mass spectrometry. An aqueous solution of the catanionic association was mixed with a NaI solution to yield a positively charged sodium adduct ( $[M+Na]^+$ ). The sample was introduced by electrospray ionization since this method ionizes the molecules at atmospheric pressure and room temperature. These are mild conditions that do not destroy the catanionic entity. In this mode, mass spectrometry can be performed in positive or negative mode, that is to say anions or cations can be detected.

Fig. 2.5 shows the mass spectrum of  $C_8^+/C_8^-$ . The exact mass of the  $C_8^+/C_8^-Na^+$  adduct was found at  $296.2943 \text{ g.mol}^{-1}$ . This was compared to the calculated mass of  $296.2565 \text{ g.mol}^{-1}$  for the surfactant/ $Na^+$  adduct (see fig. 2.5). The error of less than  $40 \text{ mg.mol}^{-1}$  proved the formation of the catanionic association.

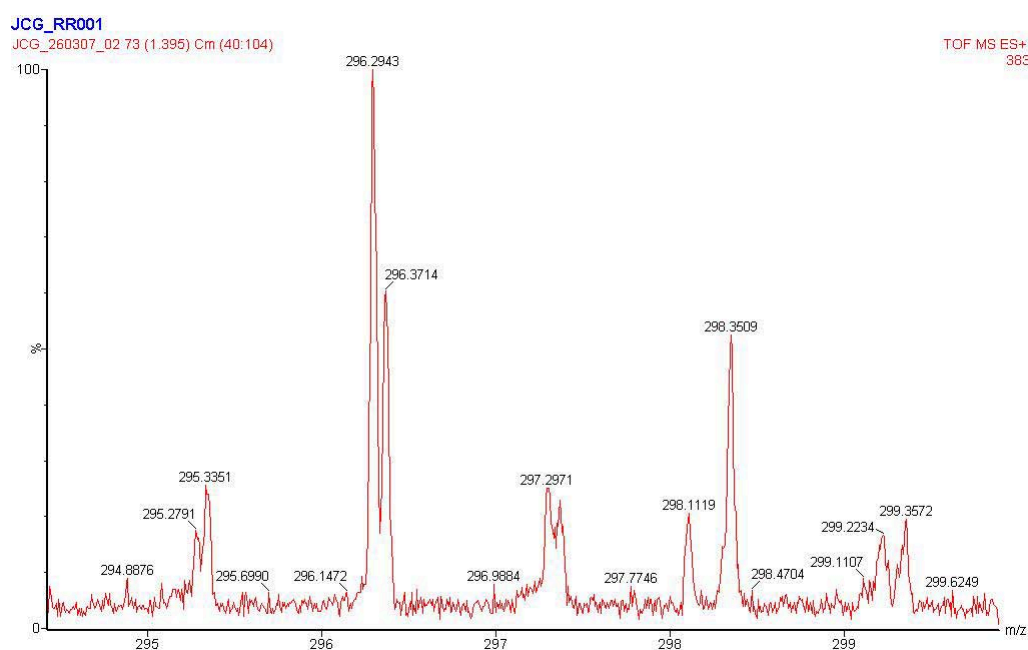


Figure 2.5: Mass spectrum of compound **3a** ( $C_8^+/C_8^-$ ).

## Results and Discussion

---

As we have seen, NMR, IR spectroscopy and mass spectrometry can prove the formation of the ion pair. But spectroscopic methods cannot estimate the ratio of the anionic and cationic part in the association. This can be proved by elemental analysis. Elemental analysis estimates the percentage of the elements, which are present in the compound. Our catanionic surfactants are composed of carbon, hydrogen, nitrogen and oxygen. The catanionic surfactants are formed by an anionic part and a cationic part. The anionic part is in our case a fatty acid that contains carbon, hydrogen and oxygen. The cationic part, on the other hand, is a surfactant with an ammonium group and is therefore composed of carbon, hydrogen, oxygen (only in the sugar-based surfactants) and one nitrogen atom. We can use the fact that the catanionic association possesses only one nitrogen atom in the cationic part. A deficit of nitrogen implies therefore a deficit of the cationic part and an excess of nitrogen shows an excess of the cationic part. For example, the elemental analysis of compound **3a** (octylammonium octanoate,  $C_{16}H_{35}NO_2$ ) gave 70.44 % for C (70.22 calc.), 13.15 % for H (12.90 calc.) and 5.02 % for N (5.12 calc.). 5.02 % corresponded to 98 % of the theoretical content of nitrogen. Taking into account the results of the spectroscopic methods and the purities of the initial products (98.0 to 99.0 %, see experimental part), 98 % gives a reasonable indication of the equimolarity of the anionic and cationic moieties in the catanionic association. This is an efficient way to verify the equimolar ratio of anionic and cationic surfactant in the catanionic association.

# 3

## Catanionic Surfactants in Non-Aqueous Solutions

### **3.1 General Physico-Chemical Studies**

#### **3.1.1 Krafft Temperature $T_K$**

Temperature is a very important parameter for self-aggregation phenomena. The influence of temperature on the behavior of surfactants can lead from modifications of the aggregate type to complete loss of solubility. The Krafft point  $T_K$  has already been

## Results and Discussion

---

introduced in chapter 2.2.1 of the fundamental part. In order to perform physico-chemical studies on ionic surfactants, one has to check if the system possesses a Krafft temperature, and to determine its value, since only above this temperature objects will be formed. In addition, the Krafft temperatures of surfactants in formamide systems are very important from the experimental point of view. As described in chapter 2.2.1, the Krafft points of ionic surfactants are higher in formamide than in water. This was explained by the ionic nature of liquid formamide. In formamide, the solvated surfactants are considered as mixed salts, which are characterized by higher melting points than their hydrated homologues. However, catanionic surfactants are globally neutral entities but they are still composed of two ionic surfactants, which let us expect that the systems are characterized by Krafft temperatures. We therefore studied our catanionic surfactants in pure formamide, in H<sub>2</sub>O/FA mixtures and in water (in the case of the water soluble glucose-based surfactants). The Krafft points were approximately determined using a visual method. We used the fact that the solubility curve of surfactants increases exponentially above the Krafft point due to aggregate formation. Two highly concentrated solutions should therefore possess almost equal solubilization temperature, which was taken as Krafft points.

We expected to find higher Krafft temperatures in formamide than in water. We observed that our model systems were characterized by high Krafft temperatures. For example, C<sub>8</sub><sup>+</sup>C<sub>12</sub><sup>-</sup> possesses a  $T_K$  of about 50 °C. In table 3.1, are listed the  $T_K$  of all studied systems. It has to be noted that the  $T_K$  of the model systems in water could not be determined due to solubility problems. Hence, a comparative study in aqueous and non-aqueous solution was not possible and the  $T_K$  of the model systems (**3b-g**) in H<sub>2</sub>O/FA were not measured. It was also observed that these systems were not soluble in H<sub>2</sub>O/glycerol mixtures. Moreover, the sugar-based surfactants **5e-5g** were not soluble in H<sub>2</sub>O/FA mixtures. This phenomenon is not totally understood, but it

can be imagined that the solvent mixtures are less organized than the pure solvents. A less organized structure leads to a loss of the cohesion, which may reduce the crystal solubilization capacity.

Compound	Number of C-atoms	H <sub>2</sub> O	H <sub>2</sub> O/FA (v/v)			FA	H <sub>2</sub> O/Glycerol 50:50 (v/v)	
			70:30	50:50	30:70			
<b>3a</b>	C <sub>8</sub> <sup>+</sup> C <sub>8</sub> <sup>-</sup>	16	n. s.	<25	< 25	< 25	25	n. s.
<b>3b</b>	C <sub>8</sub> <sup>+</sup> C <sub>12</sub> <sup>-</sup>	20	n. s.	n. s.	n. d.	n. d.	50	n. s.
<b>3c</b>	C <sub>12</sub> <sup>+</sup> C <sub>8</sub> <sup>-</sup>	20	n. s.	n. s.	n. d.	n. d.	52	n. s.
<b>3d</b>	C <sub>12</sub> <sup>+</sup> C <sub>12</sub> <sup>-</sup>	24	n. s.	n. s.	n. d.	n. d.	41-43	n. s.
<b>3e</b>	C <sub>8</sub> <sup>+</sup> C <sub>16</sub> <sup>-</sup>	24	n. s.	n. d.	n. d.	n. d.	61-63	n. s.
<b>3f</b>	C <sub>16</sub> <sup>+</sup> C <sub>8</sub> <sup>-</sup>	24	n. s.	n. d.	n. d.	n. d.	63-64	n. s.
<b>5a</b>	G-Hyd <sub>8</sub> <sup>+</sup> /C <sub>12</sub> <sup>-</sup>	20	<25	28	33	36	40	33
<b>5b</b>	G-Hyd <sub>12</sub> <sup>+</sup> /C <sub>8</sub> <sup>-</sup>	20	<25	30	34	38	44	35
<b>5c</b>	G-Hyd <sub>8</sub> <sup>+</sup> /C <sub>16</sub> <sup>-</sup>	24	30	35	38	42	45	36
<b>5d</b>	G-Hyd <sub>16</sub> <sup>+</sup> /C <sub>8</sub> <sup>-</sup>	24	32	36	39	44	47	34
<b>5e</b>	G-Hyd <sub>16</sub> <sup>+</sup> /C <sub>12</sub> <sup>-</sup>	28	45	n. s.	n. s.	n. s.	56	51
<b>5f</b>	G-Hyd <sub>12</sub> <sup>+</sup> /C <sub>16</sub> <sup>-</sup>	28	47	n. s.	n. s.	n. s.	58	49
<b>5g</b>	G-Hyd <sub>12</sub> <sup>+</sup> /C <sub>18</sub> <sup>-</sup>	30	47	n. s.	n. s.	n. s.	66	60

n. s. - not soluble

n. d. - not determined

Table 3.1: Krafft temperatures  $T_K$  (°C) of different catanionic surfactants in polar solvents.

One can see in tab. 3.1 that the Krafft temperatures of the catanionic surfactants were not only higher in formamide than in water, but also, that the Krafft temperatures increased with the number of carbon atoms in the hydrophobic chains. For example, C<sub>8</sub><sup>+</sup>C<sub>8</sub><sup>-</sup>, which possesses 16 C-atoms, was characterized by a  $T_K$  of about 25 °C. The Krafft temperature of C<sub>8</sub><sup>+</sup>C<sub>16</sub><sup>-</sup>, possessing 24 C-atoms, was measured at 61 °C. This is a behavior that has already been observed for ionic surfactants in both formamide and aqueous solutions.

## Results and Discussion

---

It is interesting to note that the  $T_K$  of the  $C_{16}^+C_8^-$  and  $C_8^+C_{16}^-$  systems in formamide were comparable, whereas the  $C_{12}^+C_{12}^-$  system possesses a much lower  $T_K$  in formamide (45 °C). The three systems have the same total number of carbon atoms (24) and the same polar headgroup. But the latter system had two equal chains of 12 carbon atoms each. Both other systems are asymmetric and composed by an 8 and a 16 carbon atoms chain. The asymmetry of the chain lengths therefore seems to have an influence on the Krafft temperature of catanionic surfactants. It has already been described by Viseu *et al.* that catanionic surfactants with asymmetric chains behaved differently than their homologues having two identical chains.<sup>132</sup>

However, this behavior has not yet been entirely studied. The Krafft temperature, as explained previously, is a phenomenon linked to solvation phenomena of the solid. Vlachy *et al.* mentioned that the Krafft temperature depends on the packing of the solid state, which can increase the solubility temperature and the Krafft temperature.<sup>133</sup> Our catanionic surfactants of the  $C_m^+/C_n^-$  type are synthesized through co-precipitation in diethyl ether. Different crystallization of the catanionic surfactants may explain the differences in Krafft temperatures. We therefore studied the solid state of the  $C_{16}^+C_8^-$ ,  $C_8^+C_{16}^-$  and  $C_{12}^+C_{12}^-$  systems by X-ray diffraction. The X-ray diffraction patterns showed that the three surfactant systems crystallized in different ways. The slight differences between the  $C_{16}^+C_8^-$  and  $C_8^+C_{16}^-$  systems might also explain the slight differences in Krafft temperatures (61-63 and 63-64 °C). Effectively, Tomašić *et al.* studied the solid state of symmetric and asymmetric catanionic surfactants by X-ray diffraction. They reported that, in general, symmetric systems crystallized in crystal groups (lamellar) more densely packed than asymmetric ones.<sup>134</sup> Symmetric systems with alkyl chains therefore possessed higher crystal energies than those with asymmetric chains. Hence, higher Krafft temperatures for symmetric catanionic systems should be expected.



Nevertheless, we have obtained higher Krafft temperatures of asymmetric catanionic assemblies. Tomašić *et al.* also mentioned that in cases with strongly asymmetric chain distributions (e.g.  $C_{16}^+C_8^-$ ) an interdigitation effect<sup>134</sup> can occur, which stabilizes the bilayer structure. Our preliminary XRD results indicated that the lattice length (3 nm) of the  $C_{12}^+C_{12}^-$  system corresponded to twice the approximately calculated molecule lengths. Thus, a typical bilayer structure can be assumed. On the other hand, the lattice lengths (3 nm) of the asymmetric systems corresponded to one and a half of the molecule lengths of the longer surfactant. This would indicate an interdigitation of the differently long alkyl chains. This formation would stabilize the solid phase and might shift the Krafft temperature to higher values in comparison to the symmetric system. Nevertheless, further studies should be performed by X-ray diffraction on monocrystals, which would give more accurate information of the crystal groups.

In the case of the sugar-based catanionic systems ( $G\text{-Hyd}_m^+/C_n^-$ ), we also determined higher  $T_K$  in formamide than in water. For example, the  $G\text{-Hyd}_8^+/C_{12}^-$  system has a Krafft temperature below 25 °C in water, the  $T_K$  of the same system in formamide was measured at 40 °C. We confirmed that the Krafft temperature increases with increasing chain lengths (see table 3.1). In the case of compounds **5e-5g**, the surfactants were only soluble in pure water, in pure formamide and in a 50:50 H<sub>2</sub>O/glycerol mixture. In H<sub>2</sub>O/FA mixtures we observed a critical decrease of solubility. We have not yet been able to explain this behavior completely. These surfactants are characterized by longer chains. Hence, the hydrophobic interactions between the surfactants are increased as well as the crystal stability. As mentioned before, the solubility temperature, and thus the Krafft point, depends on the packing of the solid surfactant.<sup>133</sup> The fact that solvent mixtures are less ordered than the pure solvents may explain the decrease of solubility. Solvent mixtures possess a less cohesive nature than the

## Results and Discussion

---

pure solvents. In addition, the Krafft temperatures are higher in formamide than in water. The high Krafft points compelled us to work at high temperatures, which also decreases the solvent cohesion. Both effects can decrease the solvent cohesion and decreases the dissolution capacity of the solvent mixtures as well. The surfactant solubility can be significantly decreased.

As conclusion, we observed higher Krafft temperatures of catanionic surfactants in formamide than in water. This was an expected behavior, since it has already been reported for ionic surfactants in formamide. The determination of the Krafft temperatures was important in order to perform physico-chemical studies, like surface tension measurements and dynamic light scattering that have to be performed above the  $T_K$ .

### 3.1.2 Critical Aggregation Concentration *CAC*

In order to study the aggregation behavior of catanionic surfactants in polar non-aqueous solvents, we determined the critical aggregation concentration (*CAC*). As explained previously, aggregates are formed only above this concentration. Different methods to determine the *CAC* are known. These methods usually consist in the fact that a measurable parameter change significantly above the *CAC*. The most common methods are based upon the measurement of the surface tension. It was shown that the surface tension decreases with increasing surfactant concentration, whereas the surface tension does not decrease anymore above the *CAC* while increasing surfactant concentration. This break in the surface tension evolution is taken as *CAC*.

These methods use well defined geometries (Wilhelmy plate, DeNouy) that form a film between the solution and the geometry. The formed films are more or less strong, depending on the surface tension. The stronger the surface tension is, the stronger is

the film. The mass of the formed film is measured by a microbalance. The surface tension can be calculated with the measured mass of the film.

The evolution of the surface tension can also be determined by the pendant drop shape analysis, which uses the fact that the shape of a droplet depends on the surface tension. A solution flows slowly through a vertical capillary. At the bottom of the capillary with a well defined diameter, the solution forms droplets. The more elevated the surface tension, the more spherical the droplet. A digital camera takes photos of the droplet and a software calculates the surface tension according to the shape of the droplet. It was shown that the *CAC* of sugar-based cationic surfactants cannot be measured by this method, because this type of surfactants adsorbed strongly on the capillary and influenced the measurements.

There are additional methods to determine the *CAC* using parameters such as conductivity or fluorescence. The conductometric method consists in measuring the evolution of the conductivity in the presence of charged surfactants with increasing surfactant concentration. However, Almgren *et al.* showed for ionic surfactants that a break in the conductivity does not necessarily indicate the formation of aggregates in formamide.<sup>135</sup> In the case of cationic surfactants, our conductometric studies did not lead to reproducible results. This can be explained by the fact that cationic surfactants possess a particular structure. Effectively, cationic surfactants are ion pairs of oppositely charged ionic surfactants, but they are considered as globally neutral entities, which are more or less associated. Therefore, our measurements were not reproducible. Finally, the *CAC* can be determined by fluorescence spectroscopy, measuring the modification of the fluorescence of pyrene above the *CAC*.<sup>136</sup>

For our experiments, we chose the Wilhelmy plate methods, and determined the *CAC* by measuring independently prepared samples having different concentrations. Fig. 3.1 is a schematic representation of surface tension measurements. At low concen-

## Results and Discussion

---

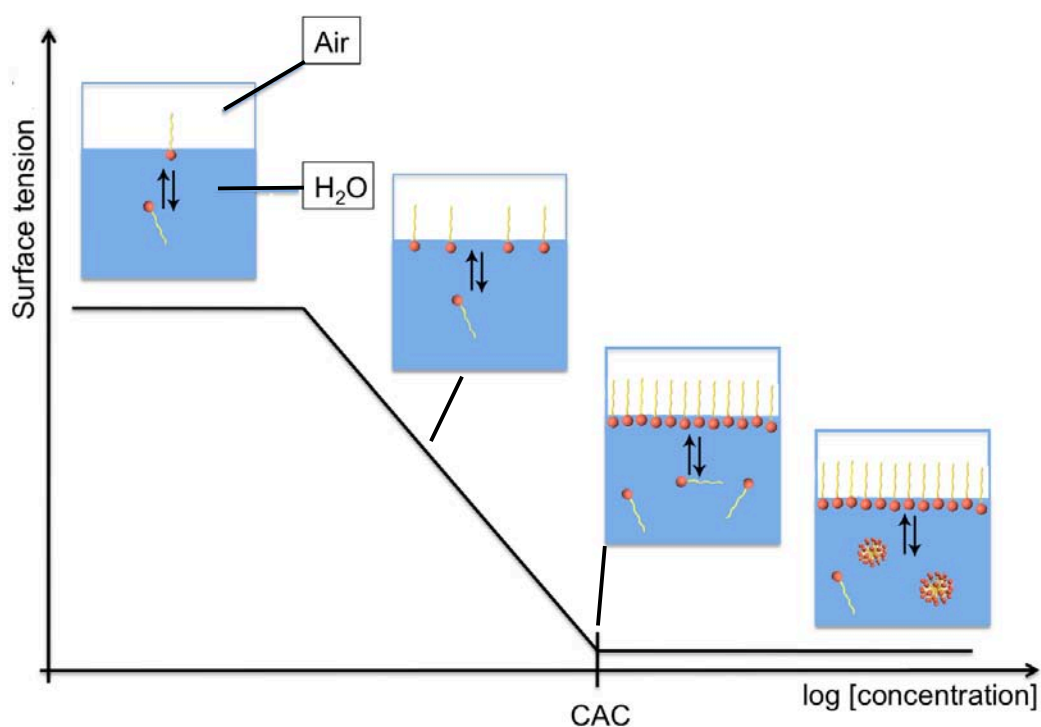


Figure 3.1: Evolution of the surface tension as a function of the surfactant concentration.

trations, surfactants gather themselves at the hydrophilic-hydrophobic interface due to their amphiphilic nature. The hydrophobic alkyl chains avoid the unfavorable water contact, whereas the polar headgroups try to be solvated. With increasing concentration, the local concentration at this interface increases as well. This accumulation of surfactant molecules at the interface is accompanied by a decrease in the surface tension. Moreover, surfactant molecules at the surface are in an equilibrium with the solvated ones in the bulk phase. At a certain concentration, called *CAC*, the surfactant molecules start to form objects (micelles, vesicles, etc) in order to minimize the increased free energy of the system. In this way, the contact between the hydrophobic alkyl chains and water can be reduced to a minimum. This process is driven by the solvophobic interaction between the hydrophobic chains and the polar and cohesive

solvent. Above this concentration, the surface tension of the interface does not change even when increasing the surfactant concentration.

It was explained previously that we expected to find higher *CACs* in polar non-aqueous solvents than in water, since these solvents exhibited a less cohesive nature. Solvophobic interactions between hydrophobic chains of the surfactant and the solvent are reduced, and therefore higher surfactant concentrations should be necessary to obtain self-aggregation phenomena.<sup>62,99,108,112,116,125,129</sup> This is true for ionic and non-ionic surfactants. In order to estimate the influence of the solvent on the aggregation behavior and more precisely on the *CAC*, we studied catanionic model systems ( $C_m^+C_n^-$ ) and glucose-based systems ( $G\text{-Hyd}_m^+/C_n^-$ ) in different solvents and solvent mixtures. Fig. 3.2 and fig. 3.3 show the *CACs* of compounds **3a** ( $C_8^+C_8^-$ ) and **5a** ( $G\text{-Hyd}_8^+/C_{12}^-$ ) in water, in  $H_2O/FA$  mixtures and in pure formamide. For a better visibility of the results, the surface tension curves were artificially spaced out. As indicated in the legend of the figures, the curves were shifted upwards with the indicated value (e.g.  $+4 \text{ mN}\cdot\text{m}^{-1}$ ). The plotted values are not the absolute measured values of the surface tensions. The values of the measured *CACs* are listed in table 3.2.

## Results and Discussion

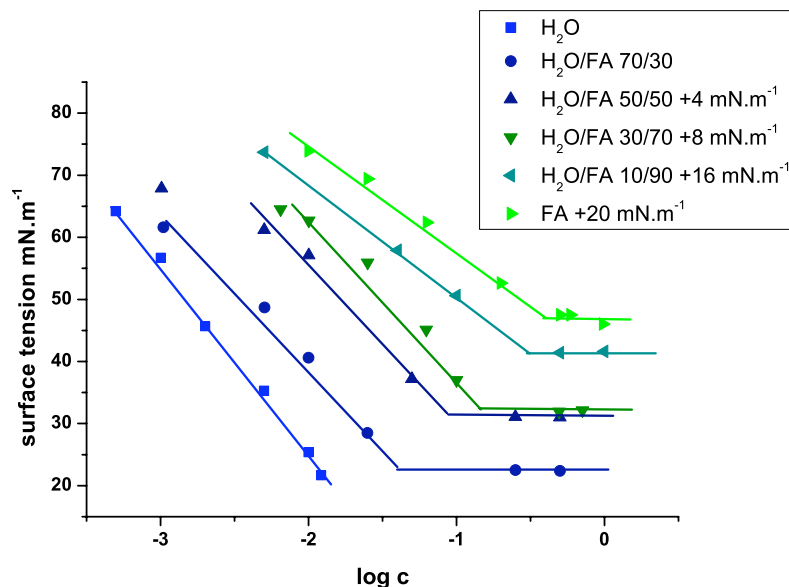


Figure 3.2: Surface tension measurements of compound **3a** at 25 °C in different H<sub>2</sub>O/FA mixtures.

In the case of  $C_8^+C_8^-$ , the  $CAC$  in pure water could not be determined because this system was not enough soluble in water at equimolar ratios.<sup>130</sup> However, as expected, with increasing formamide content, the  $CAC$  also increases, almost linearly, as can be seen in fig. 3.4. On the other hand, the surface tension evolution of  $G-Hyd_8^+/C_{12}^-$  was not linear. At low formamide ratio, the  $CAC$  did not increase much. Over 50 % formamide, the  $CACs$  increased more significantly, indicating a great influence of formamide on the aggregation behavior of  $G-Hyd_8^+/C_{12}^-$ . The  $CACs$  of the sugar-based systems in formamide differed almost by two orders of magnitudes compared to water. Schubert et al. already described this for ethylene glycol derived surfactants in formamide.<sup>99</sup>

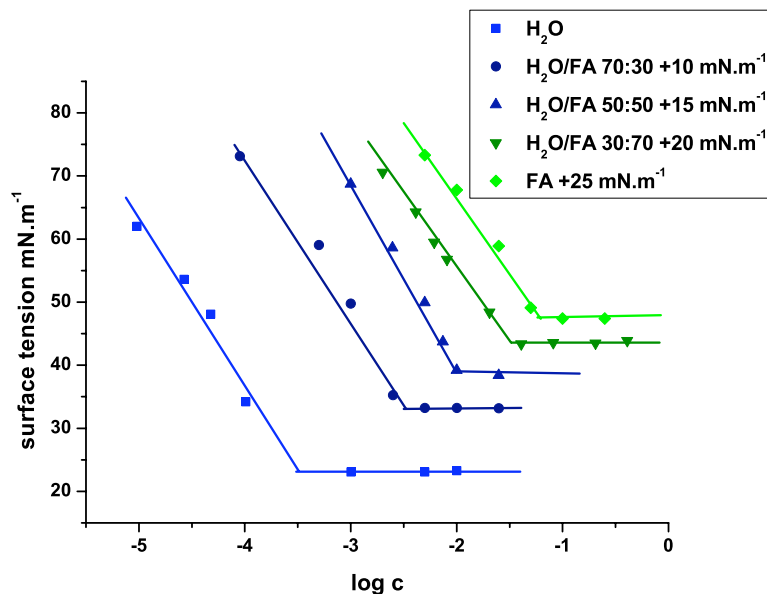


Figure 3.3: Surface tension measurements of compound **5a** at 45 °C in different H<sub>2</sub>O/FA mixtures.

System	H <sub>2</sub> O	H <sub>2</sub> O/FA (v/v)				FA
		70:30	50:50	30:70	10:90	
<b>3a</b> C <sub>8</sub> <sup>+</sup> C <sub>8</sub> <sup>-</sup>	–*	3.9.10 <sup>-2</sup>	7.9.10 <sup>-2</sup>	1.7.10 <sup>-1</sup>	3.2.10 <sup>-1</sup>	4.1.10 <sup>-1</sup>
<b>5a</b> G-Hyd <sub>8</sub> <sup>+</sup> /C <sub>12</sub> <sup>-</sup>	3.4.10 <sup>-4</sup>	2.9.10 <sup>-3</sup>	1.1.10 <sup>-2</sup>	5.0.10 <sup>-2</sup>	n. d.**	7.2.10 <sup>-2</sup>

\*Compound **3a** is not enough soluble in H<sub>2</sub>O

\*\* n. d. – not determined

Table 3.2: *CACs* (mol.L<sup>-1</sup>) of compounds **3a** (25 °C) and **5a** (45 °C) in H<sub>2</sub>O, in formamide and in H<sub>2</sub>O/FA mixtures.

It has to be noted that the modification of the solvent has a much less dramatic influence on the *CACs* of the simple model systems compared to what can be observed for the sugar-based surfactants. This different behavior may be explained by two different ways. The solvation behavior of the sugar headgroups and the ammonium carboxylate group is quite different in water and formamide. In the case of the sugar-based surfactants, water coordinates quite easily the sugar headgroups using H-bonds,

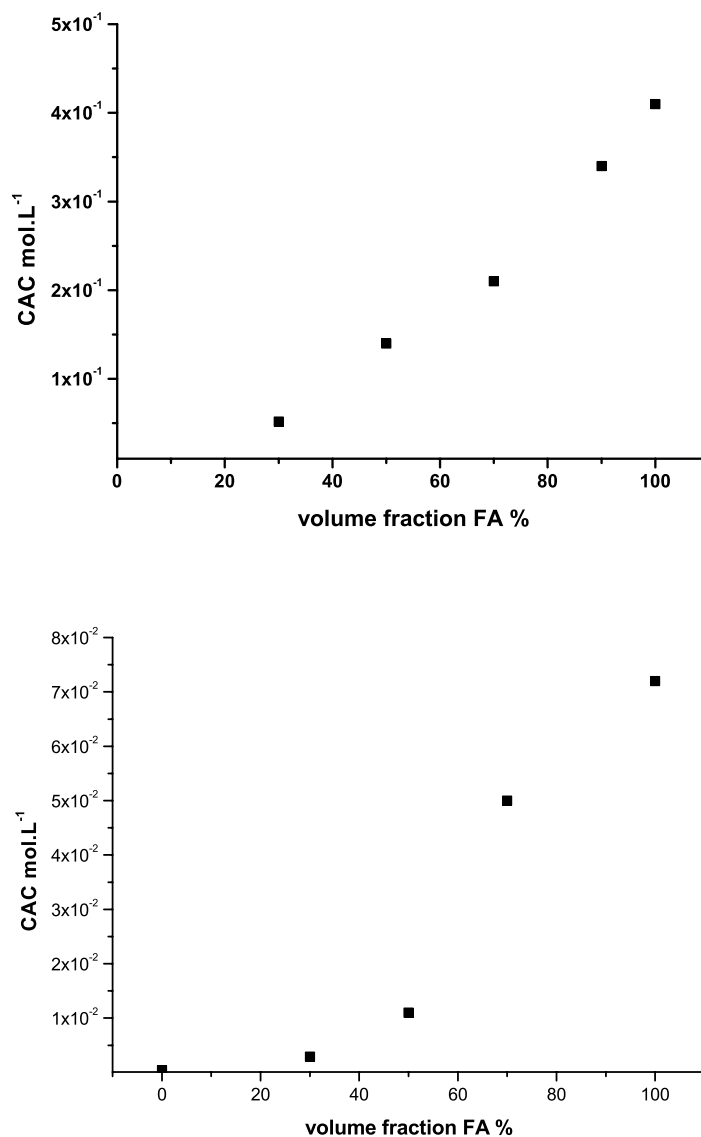


Figure 3.4: Evolution of the  $CAC$  as a function of the FA volume fraction for compounds **3a** (top, 25 °C) and **5a** (bottom, 45 °C).

whereas the more bulkier formamide coordinates less readily. In addition, the different behavior between the sugar-based surfactant and the simple model systems may be related to a different aggregation behavior. For this issue, the surfactant systems have to be studied by dynamic light scattering methods in order to determine the



aggregate type formed in formamide and H<sub>2</sub>O/FA mixtures. We will discuss this in chapters 3.2 and 3.3. However, it was shown as expected that catanionic surfactants behave similarly to ionic and nonionic surfactants, which was expressed, for example, by higher *CACs* in formamide than in water.

### 3.1.3 Influence of Chain Length and Chain Symmetry

It was shown that for all our surfactants the *CAC* increased with increasing formamide content. The *CACs* of catanionic systems in pure formamide were about two orders of magnitude higher than in water. The *CAC* of a homologous series of surfactants in pure water decreases with longer chain lengths. With increasing chain lengths, that is to say with increasing number of carbon atoms in the lipophilic tail, the solvophobic interactions between the alkyl chains and water increase as well. As a consequence, surfactants with longer chains tend to form aggregates at lower concentrations than those with shorter chains. In a more general way, the higher the total number of carbon atoms in the hydrophobic part of a surfactant, the lower the *CAC* of the system. In fig. 3.5 and fig. 3.6, we can see the surface tension measurements of the different model systems ( $C_m^+C_n^-$ ) and the glucose-based systems in pure formamide.

As expected, *CACs* decrease with increasing chain lengths. We could confirm this observation on our glucose-based systems, which were characterized by decreasing *CAC* values with increasing carbon atoms in the chains (see table 3.3). This behavior is in agreement with what has already been described in the literature for ionic and nonionic surfactants in formamide and other polar non-aqueous solvents.<sup>99,129</sup> It is interesting to note that the  $C_8^+C_{12}^-$  and  $C_{12}^+C_8^-$  systems as well as the  $C_8^+C_{16}^-$  and  $C_{16}^+C_8^-$  were characterized with *CACs* in the same order of magnitude, respectively. Moreover, the latter pair of catanionic associations ( $C_8^+C_{16}^-$  and  $C_{16}^+C_8^-$ ) possesses the same number of carbon atoms as the  $C_{12}^+C_{12}^-$  system. But the  $C_{12}^+C_{12}^-$  system was

## Results and Discussion

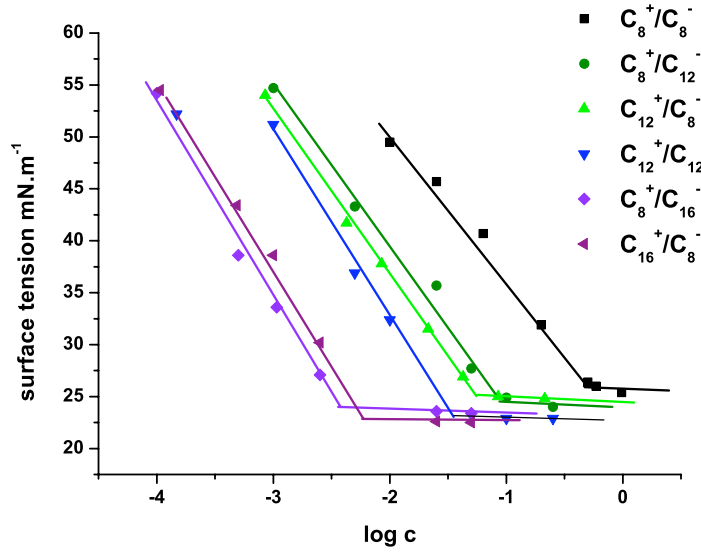


Figure 3.5: Surface tension measurements of the  $C_m^+C_n^-$  systems at 70 °C in pure FA.

characterized by a higher  $CAC$  ( $3.2 \cdot 10^{-2} \text{ mol.L}^{-1}$ ) in comparison to the asymmetric systems ( $4.0 \cdot 10^{-3} \text{ mol.L}^{-1}$  for  $C_8^+C_{16}^-$  and  $5.0 \cdot 10^{-3} \text{ mol.L}^{-1}$  for  $C_{16}^+C_8^-$ ). There is a difference of almost one order of magnitude between the symmetric and asymmetric systems. Lower  $CACs$  normally indicate that the system forms objects more readily. In our case, the asymmetric systems form objects at much lower concentrations than the symmetric system. A different behavior of these systems were also observed as the Krafft temperatures were determined. The asymmetric systems were characterized by higher Krafft temperatures than the symmetric one. The symmetry of the hydrophobic chains thus seems to have an influence on the aggregation behavior of the surfactants. A similar observation has been made for cationic surfactants in aqueous systems by Viseu et al.<sup>132</sup> They observed that the properties of monolayers formed by cationic systems in water are different depending on the use of symmetric or asymmetric cationic systems. In this special case, the collapse mechanisms of monolayers composed by surfactants with similar chain lengths were different to

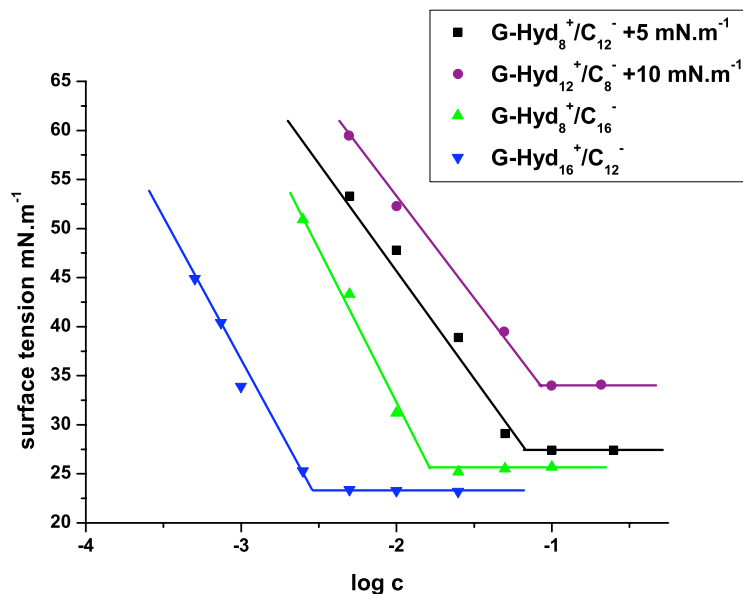


Figure 3.6: Surface tension measurements of the  $\text{G-Hyd}_m^+/\text{C}_n^-$  systems at 60 °C in pure FA.

those with asymmetric chains. These studies showed that asymmetric and symmetric cationic surfactants possessed different monolayer stability in water.

As a conclusion of our surface tension measurements, we confirmed two expected behaviors. Firstly, the  $CACs$  of cationic surfactants are higher in formamide than in water, which is due to the less cohesive nature of this solvent. This was already observed for ionic and nonionic surfactants in formamide.<sup>109,137,138</sup> Secondly, the  $CACs$  decrease with increasing chain lengths, which also was an expected result. In addition, the behavior of cationic surfactants depended also on the symmetry of the chains. Cationic surfactants with two identical alkyl chains did not behave in the same way as surfactants, having the same number of C-atoms, with two different alkyl chains. Asymmetric systems were characterized by lower  $CACs$ , which indicated that the objects are formed more readily.

	System	$CAC$ mol.L <sup>-1</sup>	Number of C-atoms
<b>3a</b>	C <sub>8</sub> <sup>+</sup> C <sub>8</sub> <sup>-</sup>	4.8.10 <sup>-1</sup>	16
<b>3b</b>	C <sub>8</sub> <sup>+</sup> C <sub>12</sub> <sup>-</sup>	6.5.10 <sup>-2</sup>	20
<b>3c</b>	C <sub>12</sub> <sup>+</sup> C <sub>8</sub> <sup>-</sup>	5.9.10 <sup>-2</sup>	20
<b>3d</b>	C <sub>12</sub> <sup>+</sup> C <sub>12</sub> <sup>-</sup>	3.2.10 <sup>-2</sup>	24
<b>3e</b>	C <sub>8</sub> <sup>+</sup> C <sub>16</sub> <sup>-</sup>	4.0.10 <sup>-3</sup>	24
<b>3f</b>	C <sub>16</sub> <sup>+</sup> C <sub>8</sub> <sup>-</sup>	5.0.10 <sup>-3</sup>	24
<b>5a</b>	G-Hyd <sub>8</sub> <sup>+</sup> /C <sub>12</sub> <sup>-</sup>	7.2.10 <sup>-2</sup>	20
<b>5b</b>	G-Hyd <sub>12</sub> <sup>+</sup> /C <sub>8</sub> <sup>-</sup>	8.0.10 <sup>-2</sup>	20
<b>5c</b>	G-Hyd <sub>8</sub> <sup>+</sup> /C <sub>16</sub> <sup>-</sup>	1.6.10 <sup>-2</sup>	24
<b>5e</b>	G-Hyd <sub>16</sub> <sup>+</sup> /C <sub>12</sub> <sup>-</sup>	2.5.10 <sup>-3</sup>	28

Table 3.3:  $CACs$  of the simple model systems (C<sub>*m*</sub><sup>+</sup>C<sub>*n*</sub><sup>-</sup>, 70 °C) and the sugar-based systems (G-Hyd<sub>*m*</sub><sup>+</sup>/C<sub>*n*</sub><sup>-</sup>, 60 °C) in pure formamide.

### 3.2 Characterization of the Aggregates Formed by the Catanionic Systems

As we have seen, the  $CACs$  of our catanionic surfactants were notably determined in pure formamide. The existence of a  $CAC$  usually indicates the formation of aggregates. Therefore we proceeded the study of the catanionic systems by dynamic quasi-elastic light scattering measurements (DLS) in order to determine the size of the aggregates formed in pure formamide. Solutions with concentrations over the  $CAC$  were prepared and studied at temperatures over the  $T_K$ . Since catanionic surfactants usually form vesicles in water, we expected the formation of vesicles in formamide, too. As we studied the simple systems in pure formamide, we could not record any signals. These solutions did not seem to scatter the incident light. There are two possible explanations. Firstly, these catanionic surfactants do not form any aggregates in pure formamide. This was inconsistent with the existence of the previously measured  $CACs$ . Hence, the absence of a scattered signal could also signify that the size of the objects was under the detection limit of the apparatus, that is to say smaller than

5 nm. This would be expected in the case of micelles, usually formed by monocatener surfactants with a packing parameter  $p$  below  $1/3$ .

The absence of vesicles in pure formamide intrigued us, since we expected this kind of objects. In order to elucidate the kind of objects formed in formamide, we studied the glucose-based cationic surfactant in pure formamide and in pure water. It was shown that  $\text{G-Hyd}_8^+/\text{C}_{12}^-$  does form vesicles in water. Electron micrographs show vesicles in water with diameters between 50 and 200 nm (see fig. 3.7). On the electron micrographs, one can see the formation of fibers. Effectively, at very high concentrations ( $10^{-1} \text{ mol.L}^{-1}$ ) compound **5a** formed a jelly-like phase in pure water. The fibers are formed during the dehydration process of the sample preparation. Similar cationic systems based upon glucose are known to form this kind of fibers.<sup>131,139</sup>

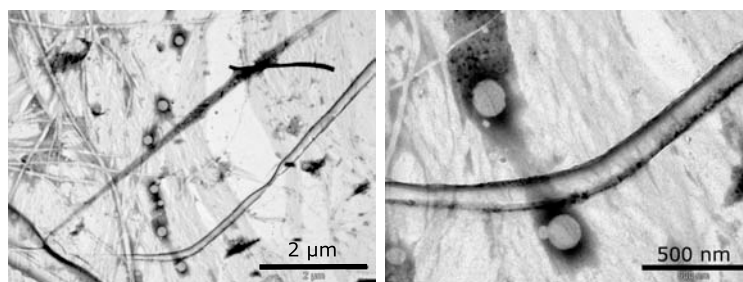


Figure 3.7: Electron micrographs of compound **5a** ( $\text{G-Hyd}_8^+/\text{C}_{12}^-$ ) in  $\text{H}_2\text{O}$  ( $1.10^{-3} \text{ mol.L}^{-1}$ ).

DLS measurements indicated the presence of vesicles with diameters between 90-180 nm. In addition, glass slides were prepared using the contact method. This method is a simple way to observe the different lyotropic mesophases formed by the surfactant. Under cross polarized light, anisotropic mesophases like lamellar or hexagonal phases show typical phase defects. In the case of a lamellar phase, one can usually observe Maltese crosses along with oily stripes. The possibility to form lamellar phases is a prerequisite for vesicle formation, since vesicles are composed of bilayers. Micrographs of  $\text{G-Hyd}_8^+/\text{C}_{12}^-$  in water showed the typical defects of a lamellar phase (see fig. 3.8).

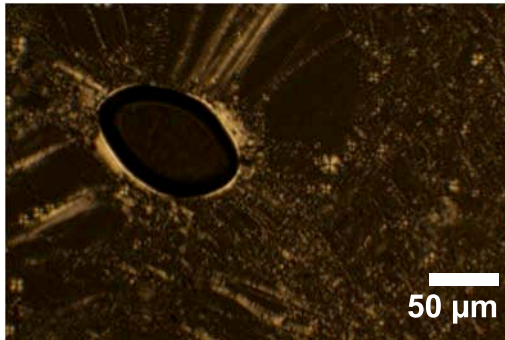


Figure 3.8: Micrograph of G-Hyd<sub>8</sub><sup>+</sup>/C<sub>12</sub><sup>-</sup> in H<sub>2</sub>O at 25 °C.

Our results demonstrated that G-Hyd<sub>8</sub><sup>+</sup>/C<sub>12</sub><sup>-</sup> formed vesicles in water. In pure formamide, G-Hyd<sub>8</sub><sup>+</sup>/C<sub>12</sub><sup>-</sup> did not show any evidence of vesicle formation by DLS measurements as we had already observed in the case of the simple model systems. We also studied the system by optical and electron microscopy. Neither gave any indication of vesicle formation. For G-Hyd<sub>8</sub><sup>+</sup>/C<sub>12</sub><sup>-</sup>, a *CAC* could be measured in pure formamide, but it did not correspond to the formation of vesicles. The absence of a DLS signal made us suspect the formation of micelles rather than vesicles.

### 3.3 Impact of the Solvent Dielectric Constant

The fact that G-Hyd<sub>8</sub><sup>+</sup>/C<sub>12</sub><sup>-</sup> did not form vesicles in formamide was surprising, since we expected the formation of this type of aggregates. In addition, G-Hyd<sub>8</sub><sup>+</sup>/C<sub>12</sub><sup>-</sup> did form vesicles in water. In order to understand why vesicles were formed in water, but not in formamide, we examined the physico-chemical parameters of these two solvents. Water and formamide are characterized by elevated values of the cohesive-energy density (2292 mPa and 1638 mPa, respectively) which indicates a highly ordered structure of the solvent. This feature should allow self-aggregation in these solvents as already described in the bibliographic part. Micellar, hexagonal and lamellar phases have been

reported for surfactant/FA solutions. Even vesicle formation by bicationic surfactants was reported in pure formamide.<sup>122,140</sup> Consequently, the cohesive-energy density value of formamide should be sufficient to allow the formation of vesicles. Hence, the non-formation of vesicles by catanionic surfactant systems in formamide must have another explanation. Formamide is also characterized by a higher dipole moment and dielectric constant than water. We then supposed that the dielectric constant might have an influence on the catanionic association integrity. We have to remember that catanionic associations are ion pairs of two oppositely charged surfactants. The solvent dielectric constant can be brought into relation with the electrostatic interactions of the polar headgroups. According to Coulomb's law, the electrostatic interactions decrease with increasing dielectric constants (see eq. 3.1).<sup>15,16</sup>

$$F = \frac{1}{4\pi\epsilon_0} \frac{q_1 q_2}{r^2} \quad (3.1)$$

where  $F$  is the magnitude of the electrostatic force of a charge  $q_1$  in the presence of a second charge  $q_2$ , and  $r$  is the distance between both charges. This is a rough approach, because Coulomb's law is only valid for spherical charges in neutral solvents. However, the interactions of the catanionic association are an essential requirement for vesicle formation, since they confer its integrity to the ion pair and therefore the resulting geometrical features of a truncated cone. If the surfactants are not associated and the distance between the polar headgroups is increased, a simple mixture of cationic and anionic surfactants is formed. Moreover, the geometry of the surfactant in solution is changed as well and micelles might be formed instead of vesicles. The scheme in fig. 3.9 visualize our hypothesis of the influence of the dielectric constant on the aggregation behavior of catanionic associations.

In order to check this hypothesis, compound **5a** (G-Hyd<sub>8</sub><sup>+</sup>/C<sub>12</sub><sup>-</sup>) was tested in H<sub>2</sub>O/FA and H<sub>2</sub>O/glycerol mixtures. Glycerol, having a dielectric constant (42.9,

## Results and Discussion

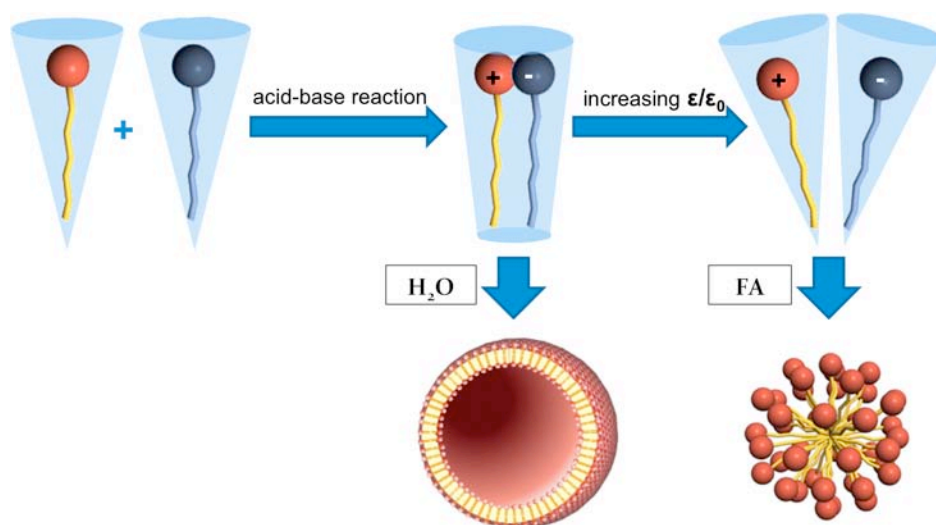


Figure 3.9: Model of the influence of the medium dielectric constant on the aggregation behavior of catanionic surfactants.

25 °C) lower than water, should allow vesicle formation according to our hypothesis. The solvent mixtures and their dielectric constants are listed in table 3.4 and 3.6. The dielectric constants ranged between 55 and 109. The solvent mixtures are given by volume fraction.

The first line of dielectric constants  $\epsilon_{id}$  is the calculated value, determined using the Moore<sup>141</sup> equation:

$$\epsilon_{12} = \Phi_1\epsilon_1 + \Phi_2\epsilon_2 \quad (3.2)$$

This is an equation for ideal liquids. Neither water nor formamide behave as ideal solvents. As a consequence, the measured values differ significantly from the calculated ones. Fig. 3.10 represents the dielectric constant of H<sub>2</sub>O/FA mixtures at 25 °C. The dashed line indicates the ideal behavior.



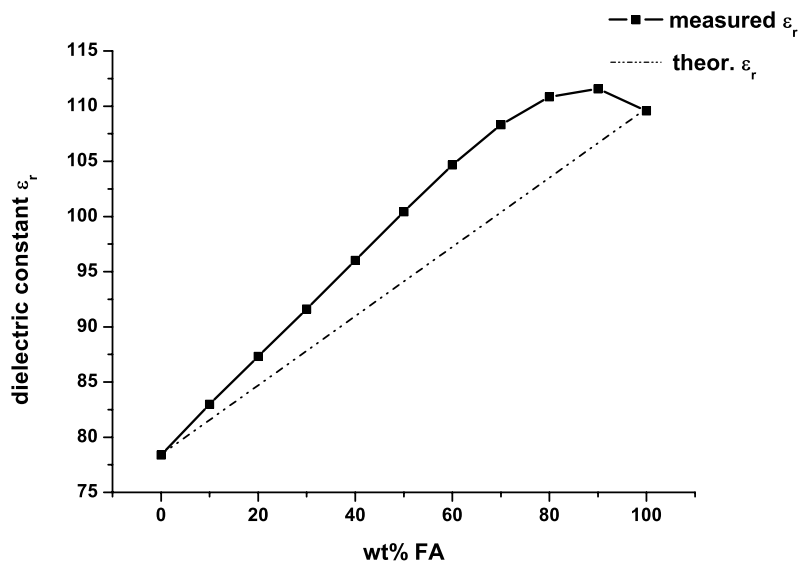


Figure 3.10: Evolution of the dielectric constant of H<sub>2</sub>O/FA mixtures at 25 °C.

The measured dielectric constants at 25 °C are given in the second line of table 3.4.<sup>142,143</sup> It has to be noted that the dielectric constant is temperature-dependent. The dielectric constant decreases with increasing temperature. Nevertheless, the G-Hyd<sub>8</sub><sup>+</sup>/C<sub>12</sub><sup>-</sup> system was tested at 45 °C in all solvent and solvent mixtures in order to compare the results.

Solvent	H <sub>2</sub> O	H <sub>2</sub> O/FA (v/v)			FA
		70:30	50:50	30:70	
$\epsilon_{id}/\epsilon_0$	78.4	87.8	94.0	100.2	109.6
$\epsilon_m/\epsilon_0$	78.4	92	102	108	109.6
object size* nm	90-180	100-150	150-200	NO SIGNAL	

\*DLS

Table 3.4: Dielectric constants of H<sub>2</sub>O/FA mixtures at 25 °C and objects obtained with G-Hyd<sub>8</sub><sup>+</sup>/C<sub>12</sub><sup>-</sup>.

## Results and Discussion

---

We were able to detect objects by DLS measurements in water and in H<sub>2</sub>O/FA mixtures up to a 50:50 ratio (v/v). The objects had diameters between 80 and 200 nm. This would correspond to the formation of vesicles. In H<sub>2</sub>O/FA mixtures with 70 % formamide and more, we could not detect any “big” objects. A 50:50 H<sub>2</sub>O/FA mixture corresponds to a dielectric constant of about 100 (25 °C) which was the maximum dielectric constant at which we could observe “big” objects formed by the G-Hyd<sub>8</sub><sup>+</sup>/C<sub>12</sub><sup>-</sup> system.

In order to ensure the formation of vesicles in H<sub>2</sub>O/FA mixtures, the system was studied by electron microscopy. Fig. 3.11 shows exemplary vesicle formation in a 70:30 H<sub>2</sub>O/FA mixture. The objects had diameters between 40-200 nm.

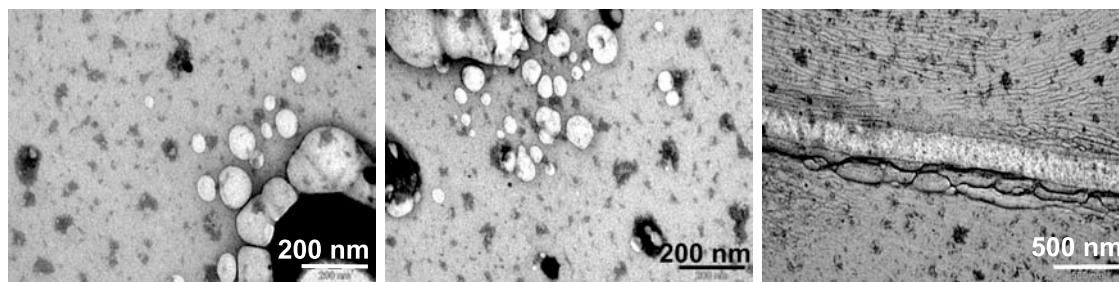


Figure 3.11: Electron micrographs of G-Hyd<sub>8</sub><sup>+</sup>/C<sub>12</sub><sup>-</sup> in a 70:30 H<sub>2</sub>O/FA mixture ( $1.10^{-2}$  mol.L<sup>-1</sup>).

The diameters are in the same order of magnitude as those determined by DLS measurements. On the micrographs, the objects seemed to coalesce with the neighboring objects. The polydispersity of the vesicles was high (40-60 %). We could already observe this by DLS measurements. It is interesting to note that the polydispersity decreased with increasing water content. The polydispersity of the G-Hyd<sub>8</sub><sup>+</sup>/C<sub>12</sub><sup>-</sup> system in water was about 20-30 %. The high polydispersity in H<sub>2</sub>O/FA mixtures was in agreement with former studies on ionic surfactants in formamide. In fact, it was explained that polydispersity is higher in formamide than in water due to the fact that

objects are formed in formamide through a multi-step mechanism.<sup>106</sup> In addition, former studies showed that aggregate size and aggregate number can increase with increasing surfactant concentration.<sup>109</sup> As a consequence, polydispersity is higher in formamide than in water.

From the experimental point of view, it has to be noted that to perform electron microscopy for formamide systems is quite difficult. Firstly, the systems usually possess higher Krafft temperatures than aqueous systems. Therefore, the grids had to be prepared at higher temperatures, which can damage the sodium phosphotungstate contrast agent. Reference grids were prepared with pure solvents or solvent mixtures without surfactants at temperatures above the Krafft temperature. We tested then to dunk the grids in warm contrast agent solutions. In this case, black points were visible on the electron micrographs. It was likely that the contrast agent aggregated/precipitated at high temperatures. Secondly, *CACs* are higher in formamide than in water due to the less cohesive nature of formamide. Therefore, the samples for electron microscopy had to be more concentrated. But highly concentrated solutions tend to precipitate on the edge of the grids. In addition, the concentrated sample films burst more easily under the electron beam than less concentrated ones. We tried to optimize the preparation of the grids. The solutions were heated over the  $T_K$  of the system before dunking the grids in them. After immersion in the contrast agent, the grids were dried at 25 to 30 °C. An additional problem was the fact that G-Hyd<sub>8</sub><sup>+</sup>/C<sub>12</sub><sup>-</sup> tended to form a gel phase in H<sub>2</sub>O/FA mixtures at room temperature. In some cases, the formation of fibers was observed on the electron micrographs. It seemed to be the result of vesicle fusion during the drying and cooling process. The vesicle fusion is visible in fig. 3.11. The formation of fibers by similar sugar-based cationic surfactants in water has already been reported by van Doren et al.<sup>131,139</sup>

## Results and Discussion

---

However, these experiments showed that G-Hyd<sub>8</sub><sup>+</sup>/C<sub>12</sub><sup>-</sup> does form vesicles in water and H<sub>2</sub>O/FA mixtures up to a 50:50 ratio. This strengthened our theory of the influence of the dielectric constant. In order to check that the dielectric constant, and not the low cohesive-energy density, was responsible for the non-formation of vesicles, we studied the system in a 50:50 H<sub>2</sub>O/glycerol and a 56:44 FA/glycerol mixtures.

*A priori*, the cohesive-energy densities of both solvent mixtures should be lower than that of water. Kinart et al.<sup>144</sup> worked on FA/glycerol mixtures and recorded densities, viscosities, molar volumes and relative permittivities of FA/glycerol mixtures. <sup>1</sup>H NMR experiments gave rise to the formation of two complexes of the type FA-glycerol and FA-glycerol-FA (see fig. 3.12). The authors supposed therefore that FA/glycerol mixtures possess an organized structure, which is a prerequisite for self-aggregation of surfactants. The exact structure of a 56:44 FA/glycerol mixture has not yet been determined.

Solvent	water	FA	Glycerol
CED mPa	2294	1568	1570

Table 3.5: Cohesive-energy densities of water, formamide and glycerol at 25 °C.

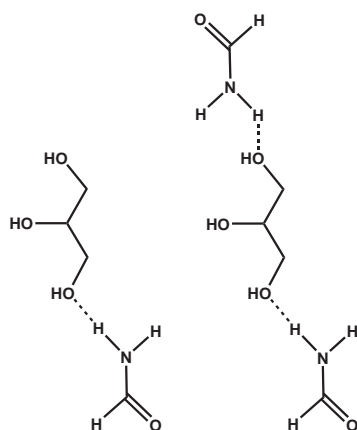


Figure 3.12: Proposed complexes for the structure of FA/glycerol mixtures.

Both solvent mixtures possess lower dielectric constants at 25 °C than water. The 56:44 FA/glycerol mixture has a dielectric constant of about 72, which is close to that of water. The theoretical and the measured dielectric constants of the solvent mixtures are given in table 3.6.<sup>144,145</sup>

Solvent	glycerol	H <sub>2</sub> O/glycerol (v/v)			FA/glycerol (v/v) 56:44	H <sub>2</sub> O	FA
		70:30	60:40	50:50			
$\epsilon_{id}/\epsilon_0$	42.9	53.6	57.1	60.7	78	78.4	109.6
$\epsilon_m/\epsilon_0$	42.9	55	58	64	72	78.4	109.6
object size* nm	too viscous	350	150	80-130	150-200	90-180	NO SIGNAL

\*DLS

Table 3.6: Dielectric constants of different polar solvent mixtures at 25 °C and objects obtained with compound **5a** at 45 °C.

The Krafft temperatures of compound **5a** in the H<sub>2</sub>O/glycerol and the FA/glycerol system were determined at 33 and 39 °C, respectively. In order to compare the results in the H<sub>2</sub>O/glycerol and the FA/glycerol mixtures with those obtained in the water and H<sub>2</sub>O/FA mixtures, we measured the *CAC* in both solvent mixtures at 45 °C (see. fig. 3.13).

## Results and Discussion

---

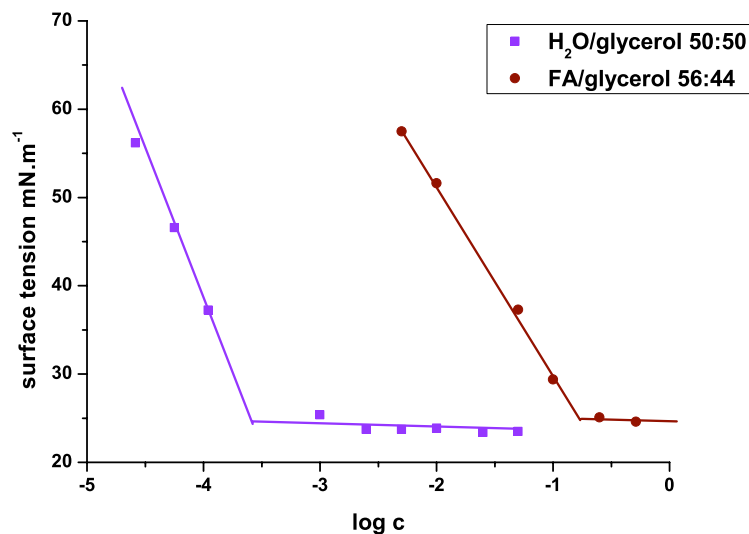


Figure 3.13: Surface tension measurements of the G-Hyd<sub>8</sub><sup>+</sup>/C<sub>12</sub><sup>-</sup> system in a 50:50 H<sub>2</sub>O/glycerol and in a 56:44 FA/glycerol mixture at 45 °C.

The 50:50 H<sub>2</sub>O/glycerol mixture was characterized by a *CAC* close to that of water, whereas the *CAC* of the 56:44 FA/glycerol mixture was determined at 0.16 mol.L<sup>-1</sup> at 45 °C. This latter value is higher than in pure formamide. This can be explained by the fact that a mixture of formamide and glycerol is less structured than pure formamide or pure glycerol. Further studies on the cohesive-energy density value should be performed in order to determine the degree of structuring of FA/glycerol mixtures. DLS measurements detected objects with size between 180 and 250 nm in the case of the FA/glycerol mixture and between 150-200 nm in the H<sub>2</sub>O/glycerol mixture (see table 3.6). In both cases, we assumed the formation of vesicles by G-Hyd<sub>8</sub><sup>+</sup>/C<sub>12</sub><sup>-</sup>, because the typical phase defects of lamellar phases could be observed under the optical microscope using cross polarized light (see fig. 3.14). In the case of the G-Hyd<sub>8</sub><sup>+</sup>/C<sub>12</sub><sup>-</sup> system in a 50:50 H<sub>2</sub>O/glycerol mixture, we could visualize the objects formed by transmission electron microscopy (see fig. 3.15).

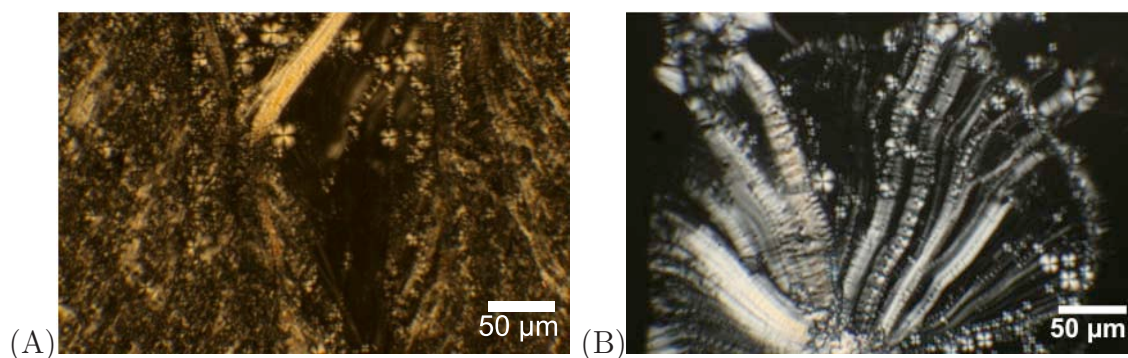


Figure 3.14: Polarized micrographs of **5a** in a 50:50 H<sub>2</sub>O/glycerol (A) and a 56:44 FA/glycerol (B) mixture at 25 °C.

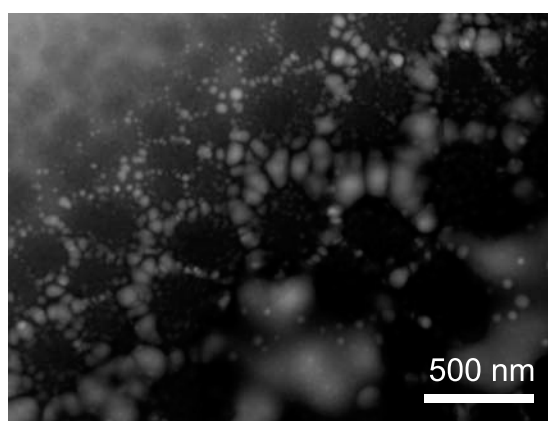


Figure 3.15: Electron micrograph of **5a** in a 50:50 H<sub>2</sub>O/glycerol mixture ( $1.10^{-3}$  mol.L<sup>-1</sup>).

These results were in agreement with our hypothesis of the non-negligible influence of the dielectric constant on the aggregation behavior of cationic surfactants. We could observe that G-Hyd<sub>8</sub><sup>+</sup>/C<sub>12</sub><sup>-</sup> did not form vesicles in pure formamide due to the high dielectric constant. This latter parameter had a dissociative effect on the ion pair and, as a consequence, the geometrical parameter of the cationic association was changed, and the formation of micelles was more likely. Nevertheless, further studies on cationic systems in pure formamide has to be performed by small angle neutron or x-ray scattering (SANS/SAXS) in order to doubtlessly determine the shape and the size of the objects formed.

## Results and Discussion

---

Our hypothesis was based on the fact that the high dielectric constant has an influence on the association of the charged polar headgroups. Therefore, we wanted to study the association degree of the two surfactants in the catanionic ion pair in relation to the different solvents. For this reason, we studied the catanionic system **5a** ( $\text{G-Hyd}_8^+/\text{C}_{12}^-$ ) by infrared spectroscopy. Infrared spectroscopy is based upon the fact that an incident infrared wave length ray can provoke rotation or vibration of molecules and molecule parts. Specific molecule parts (like the carboxylate group) are characterized by specific frequencies and can therefore be easily identified. The wave number  $\nu$ , which is proportional to the energy  $E$  of the incident beam by  $E = h\nu$ , depends on the molecular shape, the molecular mass and its associations to other groups or molecules. The higher wave numbers, the lower the energies of the incident infrared beam. The polar headgroup of the  $\text{G-Hyd}_8^+/\text{C}_{12}^-$  system is composed of the ammonium-1-deoxy-D-glucitol moiety of the cationic part and the carboxylate group of the fatty acid. The electrostatic interactions are mainly due to hydrogen bonds between the ammonium and the carboxylate group. The carboxylate group can be identified by a strong single peak at wave numbers between  $1500\text{-}1600\text{ cm}^{-1}$ . We chose the carboxylate group for our investigations, because the wave number range of the carboxylate group was not superimposed to the absorption bands of water and formamide. We studied equimolar solutions of  $\text{G-Hyd}_8^+/\text{C}_{12}^-$  with concentration over the  $CAC$  ( $1.10^{-1}\text{ mol.L}^{-1}$ ) in pure water, in  $\text{H}_2\text{O}/\text{FA}$  mixtures and in pure formamide by attenuated total reflectance infrared spectroscopy (ATR-IR). ATR-IR is suitable for the characterization of materials that are either too thick or too strongly absorbing to be analyzed by transmission spectroscopy. In our case, we wanted to study the catanionic association in solution. Formamide, as well as water, absorb strongly infrared light. ATR spectroscopy allowed us to study the catanionic surfactant in solution and gave us information about the chemical environment of the polar headgroups. In ad-



dition, the samples could be prepared in the exact same way as for surface tension and DLS measurements, that is to say under the same conditions. The same surfactant concentration was used, as well as the solutions were sonicated in the same way. Hence, the ATR-IR measurements could give comparable results to what has been observed by surface tension and DLS measurements. In fig. 3.16, one can see the absorption spectra of solid G-Hyd<sub>8</sub><sup>+</sup>/C<sub>12</sub><sup>-</sup> and its solutions in different solvents at 55 °C.

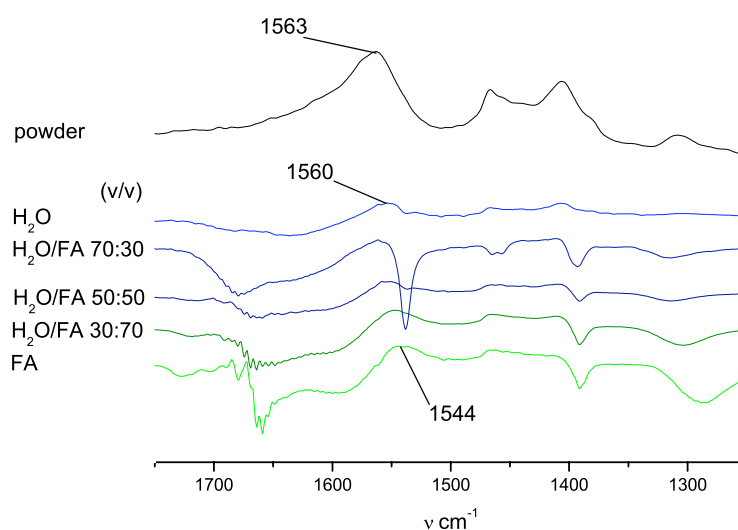


Figure 3.16: ATR-IR spectra of G-Hyd<sub>8</sub><sup>+</sup>/C<sub>12</sub><sup>-</sup> ( $1.10^{-1}$  mol.L<sup>-1</sup>) in the solid state and in different solvent mixtures at 55 °C.

The absorption maxima of the carboxylate group was measured at 1563 cm<sup>-1</sup> in the solid state, at 1560 cm<sup>-1</sup> in water and at 1544 cm<sup>-1</sup> in pure formamide. The difference between the aqueous and the formamide system was calculated at 16 cm<sup>-1</sup>. Assuming that mass and molecular shape of the cationic system were identical in both solvents, the differences could only be explained by the differences of the association degree of the carboxylate group to neighboring groups. The lower wave number corresponding to the formamide system indicated a lower degree of association and a higher freedom. These observations were in agreement with our theory

## Results and Discussion

---

of the dissociative influence of the dielectric constant on the catanionic surfactant. The cohesive-energy density is therefore definitively not the only important parameter in self-aggregation processes of catanionic surfactants in non-aqueous solvents. It is important to note that high cohesive-energy density values are a basic prerequisite to allow self-aggregation phenomena. This is true for aqueous and non-aqueous solutions as well as for the aggregation of ionic, non-ionic and catanionic surfactants. Formamide – this has been demonstrated undoubtedly – possesses a sufficiently high cohesive-energy density value, and therefore micelle and vesicle formation is possible in pure formamide with ionic monocatenar and bicatenar surfactants, respectively. Both micelle and vesicle formation in formamide have been reported numerously in the literature.<sup>62,109,121,122,129,137,138,140,146,147</sup> But in the case of catanionic surfactants, their unique structure has to be considered. Catanionic associations are composed by ion pairs of oppositely charged surfactants. These ion pairs are held together mainly by electrostatic interactions, which can be influenced by the dielectric constant. Hence, the dielectric constant of the medium has become an additional critical parameter as it can have a dissociative effect on the ion pair. The integrity of the catanionic surfactant can be “destroyed” and the geometry (packing parameter  $p$ ) of the association can change from a truncated cone-like form to a cone-like form. As a consequence, catanionic surfactants gave rise to the formation of micelles in pure formamide rather than the expected vesicles. Nevertheless, the aggregate type in pure formamide has to be proved by other methods such as small angle neutron or X-ray scattering studies.

### 3.4 Impact of Ion-Ion Interactions Between the Oppositely Charged Surfactants

As we have seen, the dielectric constant has an influence on the integrity of the cationic association. G-Hyd<sub>8</sub><sup>+</sup>/C<sub>12</sub><sup>-</sup> does form vesicles up to a maximum dielectric constant of about 100. At higher values, the cationic surfactant was more dissociated and were not able to form vesicles anymore. We thought that it is possible to reinforce the attractive interactions between the two ionic surfactants in order to maintain the geometry of the cationic surfactant and obtain vesicles in pure formamide. The attractive forces of cationic surfactants are given by the electrostatic interactions of the charged polar headgroups and by the hydrophobic interactions (van der Waals) between the two alkyl chains of the ionic surfactants (see fig. 3.17).

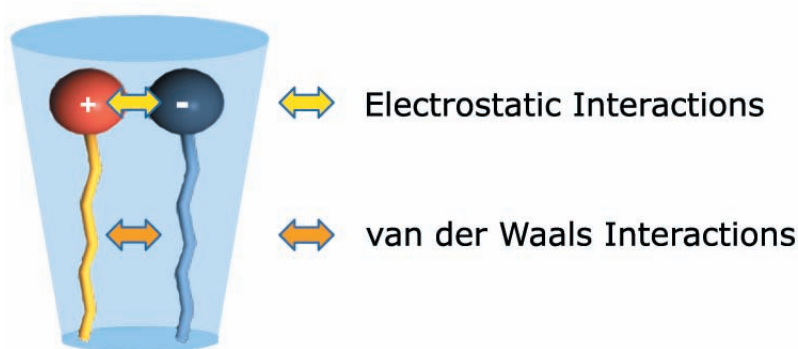


Figure 3.17: Attractive interactions between the two components of a cationic surfactant.

The dielectric constant of the medium has an influence on the electrostatic interactions between the polar headgroups. On the other hand, the solvophobic interactions (e.g. van der Waals) between the alkyl chains can be increased by raising the chain lengths. We studied therefore two cationic surfactants of the type G-Hyd<sub>m</sub><sup>+</sup>/C<sub>n</sub><sup>-</sup> with the same headgroup as G-Hyd<sub>8</sub><sup>+</sup>/C<sub>12</sub><sup>-</sup>, but with longer chains. The aim was to increase

## Results and Discussion

the solvophobia of the system, on the one hand, and to reinforce the hydrophobic interactions between the lipophilic alkyl chains on the other hand. For this issue, we synthesized compounds **5c** (G-Hyd<sub>8</sub><sup>+</sup>/C<sub>16</sub><sup>-</sup>) and **5e** (G-Hyd<sub>16</sub><sup>+</sup>/C<sub>12</sub><sup>-</sup>). These systems were studied in water, in formamide, in glycerol and in some mixtures of these solvents. At first, the Krafft temperatures were measured in order to determine the range of temperature at which we had to work. The  $T_K$  are listed in table 3.7.

Compound	Number of C-atoms	H <sub>2</sub> O	H <sub>2</sub> O:FA (v/v)			FA	Glycerol/H <sub>2</sub> O 50:50 (v/v)
			70:30	50:50	30:70		
<b>5c</b> G-Hyd <sub>8</sub> <sup>+</sup> /C <sub>16</sub> <sup>-</sup>	24	30	35	38	42	45	36
<b>5e</b> G-Hyd <sub>16</sub> <sup>+</sup> /C <sub>12</sub> <sup>-</sup>	28	45	—*	—*	—*	56	51

\*Compound **5e** is not soluble in these solvent mixtures.

Table 3.7: Krafft temperatures in °C of the G-Hyd<sub>8</sub><sup>+</sup>/C<sub>16</sub><sup>-</sup> and G-Hyd<sub>16</sub><sup>+</sup>/C<sub>12</sub><sup>-</sup> systems.

The Krafft points are higher than for the previous G-Hyd<sub>8</sub><sup>+</sup>/C<sub>12</sub><sup>-</sup> system. This is in agreement with the results obtained with the simple model systems. The Krafft points increase with the number of carbon atoms in the lipophilic part. After the determination of the  $T_K$ , we studied the systems by surface tension measurements. As expected, the  $CACs$  of these systems are lower than those of the G-Hyd<sub>8</sub><sup>+</sup>/C<sub>12</sub><sup>-</sup> system due to longer chains and therefore increased solvophobic interactions (see table 3.8 and fig. 3.18).

Compound	Solvent	glycerol/H <sub>2</sub> O	H <sub>2</sub> O	H <sub>2</sub> O/FA (v/v)		FA
		50:50 (v/v)		70:30	30:70	
<b>5c</b>	G-Hyd <sub>8</sub> <sup>+</sup> /C <sub>16</sub> <sup>-</sup>	2.0.10 <sup>-4</sup>	7.9.10 <sup>-5</sup>	3.2.10 <sup>-4</sup>	6.3.10 <sup>-4</sup>	1.6.10 <sup>-2</sup>
<b>5e</b>	G-Hyd <sub>16</sub> <sup>+</sup> /C <sub>12</sub> <sup>-</sup>	7.9.10 <sup>-5</sup>	6.3.10 <sup>-5</sup>	—*	—*	2.5.10 <sup>-3</sup>

\*Compound **5e** is not enough soluble in H<sub>2</sub>O/FA mixtures.

Table 3.8:  $CACs$  (mol.L<sup>-1</sup>) of compound **5c** at 50 °C and compound **5e** at 60 °C.

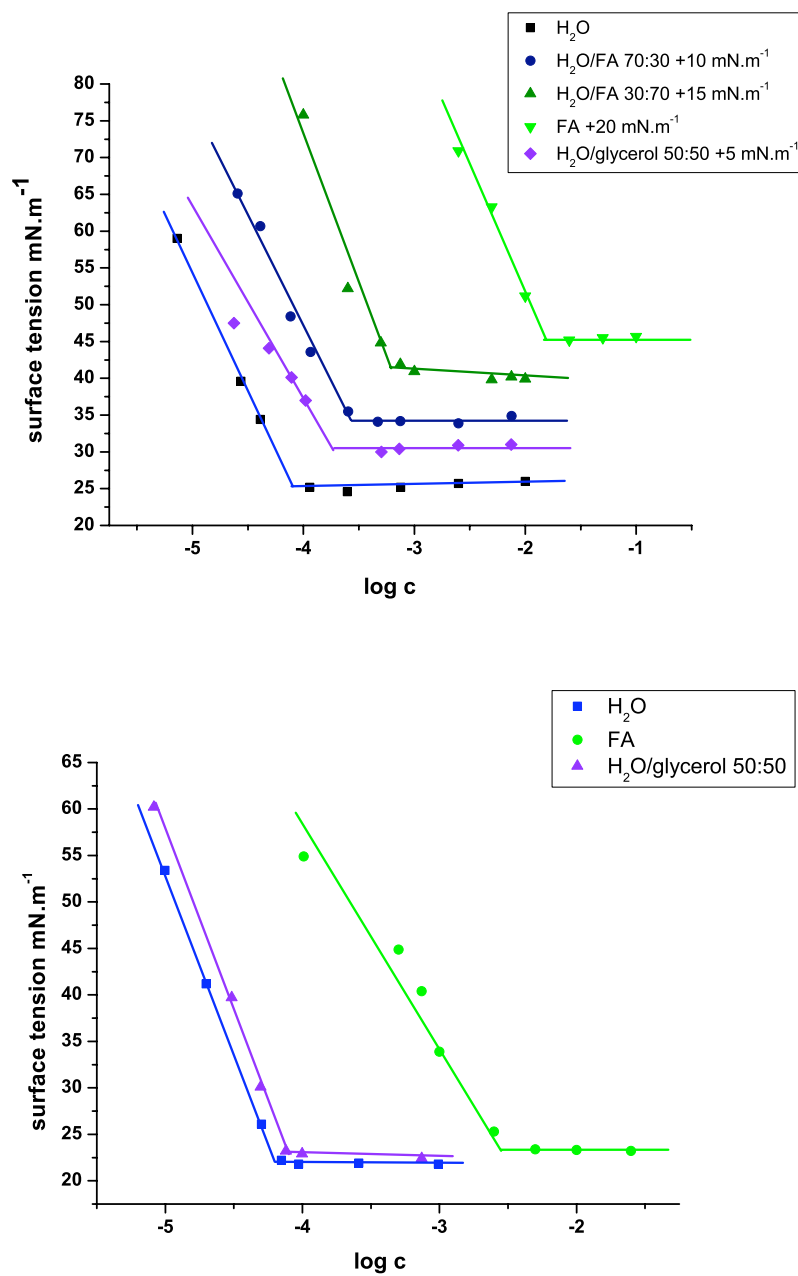


Figure 3.18: Surface tension measurements of compound **5c** (top) at  $50\text{ }^\circ\text{C}$  and compound **5e** (bottom) at  $60\text{ }^\circ\text{C}$ .

## Results and Discussion

---

It has to be noted that surface tension and  $T_K$  of the G-Hyd<sub>16</sub><sup>+</sup>/C<sub>12</sub><sup>-</sup> system could only be determined in pure water, in pure formamide and in H<sub>2</sub>O/glycerol mixtures. It was observed that in the H<sub>2</sub>O/FA mixtures the solubility of the surfactant was significantly reduced and the physico-chemical studies could not be performed. We have not yet been able to completely explain this phenomenon. Nevertheless, the decrease in solubility of the cationic systems in H<sub>2</sub>O/FA mixtures can be linked to the loss of solvent cohesion. Solvent cohesion indicates the degree of structuring of a solvent. For solubility mechanisms – in this case the dissolution of a crystal solid – a highly structured solvent is required. Formamide and water are known to be highly ordered, which is expressed by elevated values of CED. On the other hand, solvent mixtures are less organized than the corresponding pure solvents. Thus, the solubility of the surfactant may be reduced. In addition, the high Krafft points of G-Hyd<sub>16</sub><sup>+</sup>/C<sub>12</sub><sup>-</sup> in the solvent mixtures compelled us to work at high temperatures (> 45 °C). The cohesion of solvents decreases with the temperature. Both temperature and mixing effect have a reducing influence on the solvent cohesion and may lead to the observed solubility difficulties.

Nevertheless, the systems were studied by DLS measurements in order to measure the aggregate size and try to determine the type of objects formed. In the case of G-Hyd<sub>8</sub><sup>+</sup>/C<sub>16</sub><sup>-</sup>, we observed vesicles in a 50:50 H<sub>2</sub>O/glycerol mixture, in pure water and in H<sub>2</sub>O/FA mixtures up to a formamide volume fraction of 70 %. G-Hyd<sub>16</sub><sup>+</sup>/C<sub>12</sub><sup>-</sup> was only tested in H<sub>2</sub>O/glycerol, in pure water and in pure formamide, and formed vesicle in the three studied solvents. Table 3.9 gives the dielectric constants (at 25 °C) and the objects formed for each solvent mixture.

These systems with higher carbon numbers were able to form vesicles in solvent mixtures with higher dielectric constants compared to the previously discussed G-Hyd<sub>8</sub><sup>+</sup>/C<sub>12</sub><sup>-</sup> system. Stronger van der Waals interactions, due to longer chain lengths,

## Results and Discussion

Compound	Solvent	glycerol/H <sub>2</sub> O	H <sub>2</sub> O	H <sub>2</sub> O/FA (v/v)			FA
		50:50 (v/v)		70:30	50:50	30:70	
	$\epsilon_m/\epsilon_0$	64	78.4	92	102	108	109.6
<b>5c</b> G-Hyd <sub>8</sub> <sup>+</sup> /C <sub>16</sub> <sup>-</sup>	object size*	180	120	85	80	85	NO SIGNAL
<b>5e</b> G-Hyd <sub>16</sub> <sup>+</sup> /C <sub>12</sub> <sup>-</sup>	nm	380-400	260	–**	–**	–**	260

\*DLS

\*\*Compound **5e** is not enough soluble in H<sub>2</sub>O/FA mixtures.

Table 3.9: Solvent mixtures dielectric constants at 25 °C and objects obtained with compounds **5c** and **5e**.

might compensate the dissociative effect of the high dielectric constant of formamide. Electron micrographs could confirm the formation of vesicles for these systems. Fig 3.19 shows vesicles formed by G-Hyd<sub>8</sub><sup>+</sup>/C<sub>16</sub><sup>-</sup> in a 70:30 H<sub>2</sub>O/FA. The polydispersity index was determined at 20-50 %. In pure water, the polydispersity decreased to a value of about 15 %.

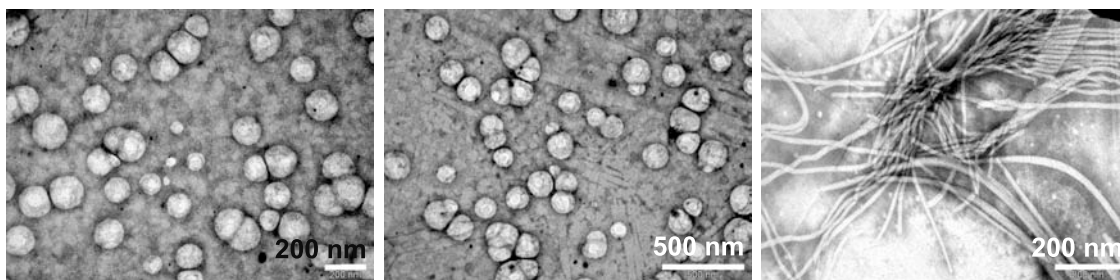


Figure 3.19: TEM micrographs of G-Hyd<sub>8</sub><sup>+</sup>/C<sub>16</sub><sup>-</sup> ( $1.10^{-2}$  mol.L<sup>-1</sup>) in 70:30 H<sub>2</sub>O/FA mixtures.

The first two micrographs in fig. 3.19 typically show the vesicles formed in a 70:30 H<sub>2</sub>O/FA mixture, when the samples were prepared at temperatures above the  $T_K$ . The vesicles had diameters between 50-150 nm. This was in agreement with the diameters measured by DLS (80-120 nm). On the right image, fibers were formed by G-Hyd<sub>8</sub><sup>+</sup>/C<sub>16</sub><sup>-</sup> in a 70:30 H<sub>2</sub>O/FA mixture at room temperatures. As explained above for G-Hyd<sub>8</sub><sup>+</sup>/C<sub>12</sub><sup>-</sup>, G-Hyd<sub>8</sub><sup>+</sup>/C<sub>16</sub><sup>-</sup> also formed gel phase below the Krafft temperature. However, we prove that the G-Hyd<sub>8</sub><sup>+</sup>/C<sub>16</sub><sup>-</sup> system formed vesicles in pure water, in a

## Results and Discussion

---

50:50 H<sub>2</sub>O/glycerol mixture and in H<sub>2</sub>O/FA mixtures with a formamide content up to 70 %. Still, in pure formamide vesicles could not be observed.

At this point, it is interesting to compare the three studied systems. Compound **5a** (G-Hyd<sub>8</sub><sup>+</sup>/C<sub>12</sub><sup>-</sup>) did form vesicles in water, H<sub>2</sub>O/glycerol mixtures and H<sub>2</sub>O/FA mixtures with a formamide content up to 50 % volume, which corresponds to a dielectric constant of ca. 100. In the case of compound **5c** (G-Hyd<sub>8</sub><sup>+</sup>/C<sub>16</sub><sup>-</sup>), we observed the formation of vesicles in water, H<sub>2</sub>O/glycerol and H<sub>2</sub>O/FA mixtures with a formamide content up to 70 % (v/v). This corresponds to a dielectric constant of 108, which is higher than the maximal dielectric constant determined in the case of the G-Hyd<sub>8</sub><sup>+</sup>/C<sub>12</sub><sup>-</sup> system. And finally, in the case of compound **5e** (G-Hyd<sub>16</sub><sup>+</sup>/C<sub>12</sub><sup>-</sup>), vesicle formation could be even observed in pure formamide that possesses a dielectric constant of 109.6. These results were in agreement with our theory of the influence of hydrophobic interactions, such as van der Waals interactions, which would reinforce the ion pair and compensate the dissociative effect of the dielectric constant of the solvent. As a consequence, considering a fixed H<sub>2</sub>O/FA mixture (30:70), the ion pair of the G-Hyd<sub>8</sub><sup>+</sup>/C<sub>16</sub><sup>-</sup> system should possess a lower dissociation degree than the ion pair formed by G-Hyd<sub>8</sub><sup>+</sup>/C<sub>12</sub><sup>-</sup>. As explained previously, we can study the dissociation degree of the ion pair in solution by ATR infrared experiments. We therefore performed ATR-IR experiments on the G-Hyd<sub>8</sub><sup>+</sup>/C<sub>16</sub><sup>-</sup> system. The formation of vesicles by G-Hyd<sub>8</sub><sup>+</sup>/C<sub>16</sub><sup>-</sup> in a 30:70 H<sub>2</sub>O/FA mixture let us suspect a lower dissociation degree of the ion pair than in the case of the G-Hyd<sub>8</sub><sup>+</sup>/C<sub>12</sub><sup>-</sup> system, which did not form vesicles in this solvent mixture. Fig. 3.20 shows the absorption maxima of the carboxylate group of the solid state and in the different solvent mixtures.



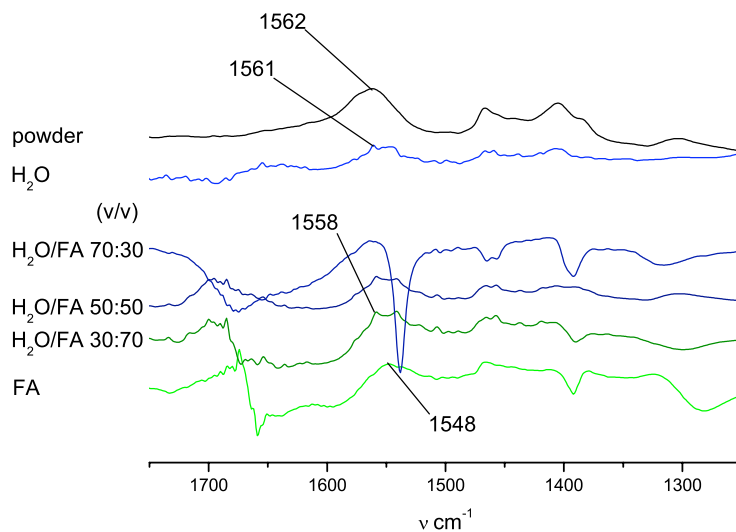


Figure 3.20: ATR-IR spectra of G-Hyd<sub>8</sub><sup>+</sup>/C<sub>16</sub><sup>-</sup> ( $1.10^{-1}$  mol.L<sup>-1</sup>) in different solvent mixtures and of the powder at 55 °C.

The maxima of the carboxylate group in the powder ( $1562\text{ cm}^{-1}$ ), in pure water ( $1561\text{ cm}^{-1}$ ) and in H<sub>2</sub>O/FA mixtures up to 70 % formamide ( $1558\text{ cm}^{-1}$ ) were quite similar and differed only of  $4\text{ cm}^{-1}$ . We could observe vesicle formation in these solvents. Thus, marginal shifts of the peak indicated vesicle formation. On the other hand, in pure formamide, the maximum absorption was significantly shifted and was measured at  $1548\text{ cm}^{-1}$ . This indicated that the carboxylate group was far less associated in pure formamide than in the other solvent/solvent mixtures. In pure formamide, we could not observe vesicle formation by DLS measurements. These results therefore sustain our hypothesis on the non-negligible influence of the dielectric constant that can dissociate the ion pair of the catanionic surfactant.

These results can be compared to the results obtained by surface tension measurements of the compounds **3a**, **5a** and **5c**. In section 3.1.2 of chapter 3, we studied the influence of the non-aqueous solvents on the *CAC* of catanionic surfactants. We

## Results and Discussion

---

observed that the  $CACs$  of compound **3a** ( $C_8^+/C_8^-$ ) increased almost linearly while increasing the FA content (see fig. 3.21).

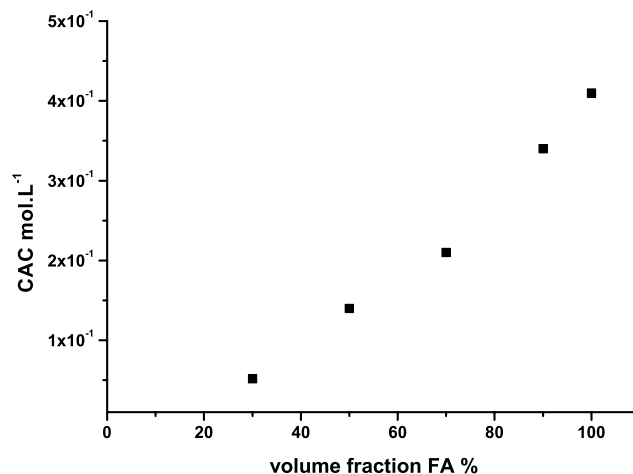
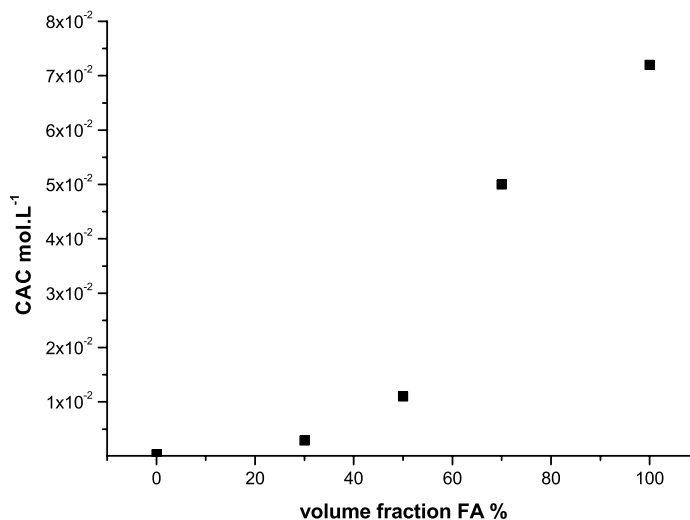


Figure 3.21:  $CAC$  evolution of compound **3a** at 25 °C.

On the other hand, the  $CACs$  of compound **5a** ( $G\text{-Hyd}_8^+/C_{12}^-$ ) increased only slightly while the FA content was low. But when the FA content exceeded 50 % (v/v), the obtained  $CACs$  increased significantly. It is interesting to note that when the evolution of the  $CACs$  increased slowly, the formation of vesicles could be observed. When compound **5a** formed micelles (at dielectric constant higher than 100, 25 °C) the  $CACs$  were much more elevated (see. fig. 3.22)

$G\text{-Hyd}_8^+/C_{16}^-$  shows a similar behavior. Fig. 3.23 shows the  $CAC$  evolution of compound **5c** as a function of the FA volume fraction. The  $CACs$  increased slightly up to a FA content of 70 %, but the  $CAC$  in pure formamide differed significantly. In pure formamide, compound **5c** did not form vesicles but gave rise to the formation of micelles. These results indicate that the  $CACs$  change significantly with increasing FA content, when the catanionic associations were separated due to the influence of the medium dielectric constant.

Figure 3.22: *CAC* evolution of compound **5a** at 45 °C.

Solvent (v/v)	Compound		
	<b>3a</b> 25 °C	<b>5a</b> 45 °C	<b>5c</b> 50 °C
H <sub>2</sub> O	—*	3.4.10 <sup>-4</sup>	2.0.10 <sup>-4</sup>
H <sub>2</sub> O/FA 70:30	7.9.10 <sup>-2</sup>	2.9.10 <sup>-3</sup>	7.9.10 <sup>-5</sup>
H <sub>2</sub> O/FA 50:50	1.7.10 <sup>-1</sup>	1.1.10 <sup>-2</sup>	3.2.10 <sup>-4</sup>
H <sub>2</sub> O/FA 30:70	3.2.10 <sup>-1</sup>	5.0.10 <sup>-2</sup>	6.3.10 <sup>-4</sup>
FA	4.1.10 <sup>-1</sup>	7.2.10 <sup>-2</sup>	1.6.10 <sup>-2</sup>
not soluble in H <sub>2</sub> O			

Table 3.10: *CAC* of compound **3a**, **5a** and **5c**.

This is quite reasonable, since the *CAC* depends (amongst other parameters) on the number of C-atoms in the hydrophilic part. In catanionic association, the number of C-atoms is given by the two chains of the oppositely charged surfactants. But if we imagine that the separation of the catanionic association due to the medium dielectric constant leads to a mixture of monocatenar amphiphiles, the number of C-atoms would be diminished to that of the single chains of the ionic surfactants. In our case, the

## Results and Discussion

---

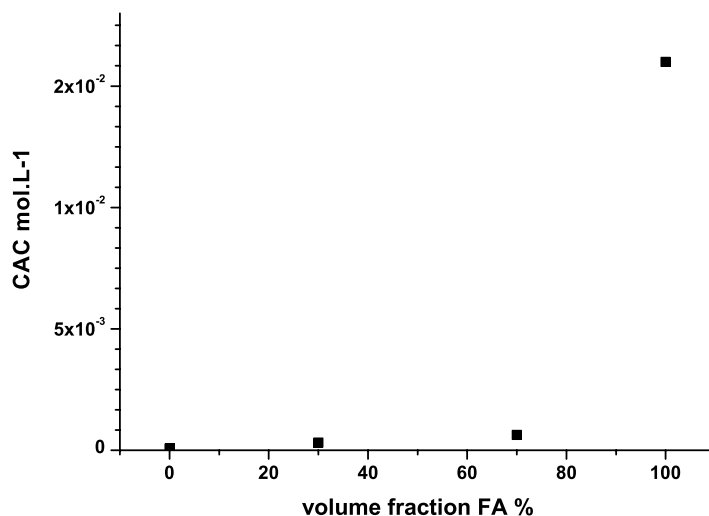


Figure 3.23: *CAC* evolution of compound **5c** at 50 °C.

*CACs* of compounds **5a** and **5c** at low volume fractions of formamide corresponded to the formation of vesicles, which indicated the integrity of the ion pairs and therefore, the low values of *CAC*. At higher FA-content, the *CACs* increased significantly, since the ion pairs are dissociated and the measured *CACs* corresponded to the mixture of monocationic surfactants. In addition, the breaks in the *CAC* evolutions of compounds **5a** and **5c** are in agreement with the results obtained by ATR-IR and DLS measurements, that is to say we obtained the same maximal volume fractions of FA, at which vesicle formation was possible. Therefore, these *CAC* measurements are another point that strengthen our theory of the dissociative influence of the dielectric constant on cationic surfactants.

We could demonstrate that the dielectric constant of the medium has an influence on the aggregation behavior of cationic surfactants. In addition, we could demonstrate that higher numbers of carbon atoms increased both solvophobic and attractive van der Waals interactions, which led to a partial compensation of the dissociative ef-

fect of the dielectric constant. In the case of G-Hyd<sub>16</sub><sup>+</sup>/C<sub>12</sub><sup>-</sup>, which possesses altogether 28 carbon atoms in the lipophilic part, we could observe vesicle formation even in pure formamide. Our studies of the three systems G-Hyd<sub>8</sub><sup>+</sup>/C<sub>12</sub><sup>-</sup>, G-Hyd<sub>8</sub><sup>+</sup>/C<sub>16</sub><sup>-</sup> and G-Hyd<sub>16</sub><sup>+</sup>/C<sub>12</sub><sup>-</sup> allowed us to determine three corresponding maximal dielectric constants, below which vesicle formation was possible, in relation to the total carbon number of the lipophilic tail. With these results we could bring in relation the total carbon number of catanionic G-Hyd<sub>m</sub><sup>+</sup>/C<sub>n</sub><sup>-</sup> systems with the medium dielectric constant. We traced a approximative line in fig. 3.24, which visualized our hypothesis of a maximal dielectric constant as function of the total carbon number in the lipophilic chains. For the following considerations, we indicated the dielectric constant at 25 °. It has to be noted that the dielectric constant is temperature-dependent and decreases with increasing temperature. The dielectric constants of H<sub>2</sub>O/FA mixtures at higher temperatures (> 45 °) were not well-established in the literature.

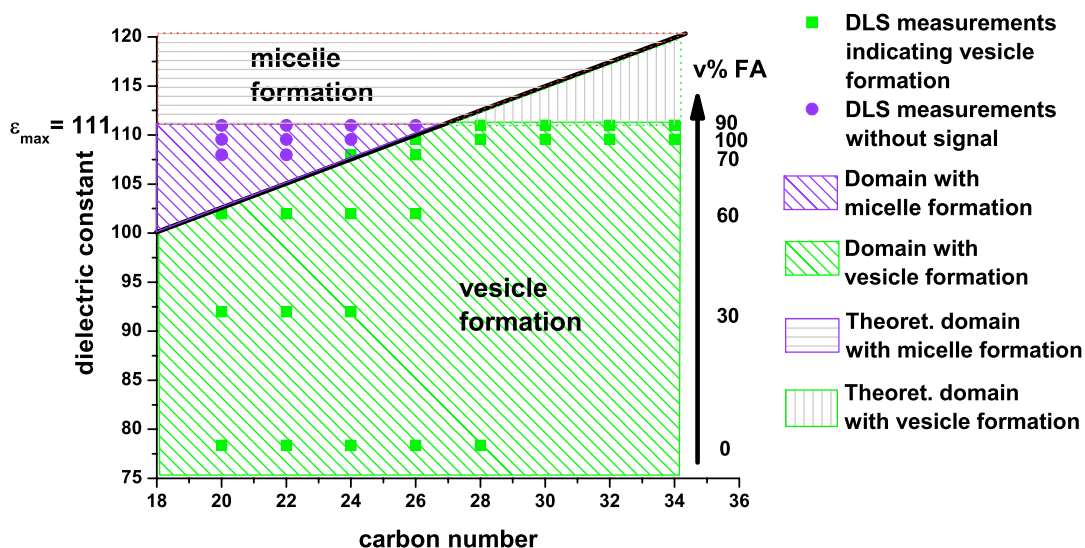


Figure 3.24: Existence domains of vesicles and micelles.

## Results and Discussion

---

Following our hypothesis, surfactants of the G-Hyd<sub>m</sub><sup>+</sup>/C<sub>n</sub><sup>-</sup> type, bearing a definite carbon number, should form vesicles in H<sub>2</sub>O/FA mixtures and in pure formamide below this black line. Above this line, micelle formation was observed. We therefore prepared a series of catanionic systems of the G-Hyd<sub>m</sub><sup>+</sup>/C<sub>n</sub><sup>-</sup> type with various carbon numbers in the lipophilic chains. The surfactants possessed carbon numbers between 20 and 34. DLS measurements were performed in H<sub>2</sub>O/FA mixtures having dielectric constants above and below this theoretical vesicle existence line. Fig. 3.24 shows the results of our study. The points in the green zone indicate vesicle formation observed by DLS measurements (that is to say objects with a size > 50 nm), whereas the points in the violet zone indicate the formation of micelles. As mentioned previously, dielectric constants of H<sub>2</sub>O/FA mixtures differ from the ideal behavior (see fig. 3.10, page 99). The 10:90 H<sub>2</sub>O/FA mixture possesses a higher dielectric constant (111, 25 °C) as pure formamide (109.5, 25 °C). Therefore, we could test the sugar-based catanionic surfactants only up to this dielectric constant. As a consequence, the upper gray zone is a theoretical area, in which, according to our hypothesis, vesicle formation should still be possible below the black line. For example, G-Hyd<sub>16</sub><sup>+</sup>/C<sub>18</sub><sup>-</sup> (carbon number 34) should form vesicles at a dielectric constant of 116 (25 °C). It is not possible to reach a dielectric constant of 116 values with neither water (78.4, 25 °C) nor with formamide (109.5, 25 °C). Further experiments should be performed with other solvents possessing higher dielectric constants, such as *N*-methylsyringone (144, 25 °C) or *N*-methylformamide (182, 25 °C) in order to perform experiments with long-chain surfactants at higher dielectric constants. This would give additional information of the influence of the dielectric constant on the aggregation behavior of catanionic surfactants in non-aqueous solvents. It should also be noted that the G-Hyd<sub>16</sub><sup>+</sup>/C<sub>18</sub><sup>-</sup> system (having the maximal number of carbon of 34) possesses a highly hydrophobic nature. The ratio between headgroup surface area and chain length is very important for the

formation of vesicles. If the active surface area of the headgroup is too small in comparison to the chain lengths, the surfactant systems tend to precipitate in lamellar phases. Similar behavior have already been reported for simple catanionic systems such as our alkylammonium alkanoate model systems ( $C_m^+C_n^-$ ) that were not enough water soluble and precipitated in pure water.

However, we could demonstrate that an increase in chain lengths also increased the ion pair integrity. The stabilized ion pair could maintain its geometry, which led to vesicle formation in pure formamide by G-Hyd $_m^+/C_n^-$  systems with carbon numbers higher than 27. The dissociative effect of the high dielectric constant of formamide could be compensated by increased hydrophobic interactions between the alkyl chains. Moreover, we could obtain a model by the study of three systems with different carbon numbers. With the maximal dielectric constant at which vesicle formation was possible, we could predict the type of aggregate formed in formamide by the catanionic system with a given headgroup (in our case G-Hyd $_m^+/C_n^-$ ). For the moment, our model is true only for the glucose-based systems, but it would be of great interest to study catanionic surfactants with other headgroups, such as pyridinium or phosphate groups. With these studies, it should be possible to confirm the existence of a relationship between vesicle formation by catanionic surfactants on the one hand, and dielectric constant and chain lengths on the other hand. This could help to predict the aggregate type of catanionic surfactants in various solvents with different dielectric constants.

### 3.5 Salt Effect on the Aggregation Behavior of Catanionic Surfactants

As we have seen, the dielectric constant has an influence on the ion pair association. As a consequence, the simple model systems did not form vesicles at all, since the interactions between the oppositely charged ionic surfactants are too weak. The sugar-based G-Hyd<sub>m</sub><sup>+</sup>/C<sub>m</sub><sup>-</sup> systems did not form vesicles in pure formamide when having less than 27 carbon atoms in the hydrophobic chains, whereas vesicles were formed in water. We wanted to know, if we can modify this behavior by addition of salts. Salt addition in surfactant solutions can influence the solvation sphere of the polar headgroups. In some cases, salt addition can decrease the repulsive interactions between objects of the same charge sign. Salt addition might influence the dissociative effect of the dielectric constant on catanionic systems. Former studies on microemulsions in non-aqueous solvents showed that sodium iodide (NaI) is very suitable in formamide systems due to its high solubility (1000 g.L<sup>-1</sup>).<sup>4</sup> It was explained that large anions such as iodide are better soluble in formamide than small ions such as chloride. These studies reported a weak influence of salt addition on nonionic surfactants in formamide. Schubert et al.<sup>99,129</sup> mentioned that the influence of addition of salts to FA solutions is comparable to the one obtained in aqueous solutions. However, we performed four series of experiments with four different catanionic surfactants of the type G-Hyd<sub>m</sub><sup>+</sup>/C<sub>n</sub><sup>-</sup>. Two systems that did not form vesicles in pure formamide (**5a** G-Hyd<sub>8</sub><sup>+</sup>/C<sub>12</sub><sup>-</sup>, **5b** G-Hyd<sub>12</sub><sup>+</sup>/C<sub>8</sub><sup>-</sup>) and two systems that did form vesicles in pure formamide (**5f** G-Hyd<sub>12</sub><sup>+</sup>/C<sub>16</sub><sup>-</sup>, **5g** G-Hyd<sub>12</sub><sup>+</sup>/C<sub>18</sub><sup>-</sup>). We added FA/NaI solutions with different NaI concentrations (10<sup>-5</sup> to 10<sup>-1</sup> mol.L<sup>-1</sup>) to the surfactants. The samples were studied by DLS. We did not observe any difference at low NaI concentrations. The surfactants, which did not form vesicles in pure FA, did not show any vesicle forma-



tion in a NaI concentration range between  $10^{-5}$  and  $10^{-3}$  mol.L $^{-1}$ . On the other hand, the long-chain surfactants that had formed vesicles in pure formamide, also formed vesicles in FA/NaI solutions up to a NaI concentration of  $10^{-3}$  mol.L $^{-1}$ . At high salt concentrations ( $10^{-2}$  to  $10^{-1}$  mol.L $^{-1}$ ), a salting out effect was observed. Salting out is usually observed in aqueous solutions, in which the added salts compete with the surfactant for water molecules. As a consequence, water molecules are removed from the polar headgroups. Water solubility decreases and solute-solute interactions (such as van der Waals interactions) get more important than water-solute interactions. The surfactants coagulate and precipitate. Salts inducing the salting out effect are water structuring, that is to say they influence the water structure in the bulk phase and at the object-solvent interface. Our experiments in formamide showed that high NaI concentrations led to precipitation of the surfactants. The salting-out effect was observed at NaI concentrations higher than  $10^{-2}$  mol.L $^{-1}$ . As a conclusion, NaI did not influence the formation or non-formation of vesicles by cationic surfactants in pure formamide at low NaI concentrations. Nevertheless, high salt concentrations can lead to precipitation of the cationic surfactant.

### 3.6 Influence of Sample Preparation

In order to study the aggregation behavior of cationic surfactants in polar solvents, we performed our experiments in water, formamide and glycerol, as well as in some mixtures of these solvents. For the above presented results we have chosen to prepare our samples with the pure solvent or with the solvent mixture that was mixed beforehand. In this case, the solvent (pure solvent or mixture) is pre-orientated with its own unique structure and properties. The surfactant is directly dissolved by this “new” solvent. But the experiments could also be performed in another way. The surfactant could be dissolved in one of the solvents at a given concentration and the other sol-

## Results and Discussion

---

vent added consecutively in order to obtain the desired surfactant concentration and solvent proportions. In this case, the surfactant is already solubilized and solvated by one of the solvent. After addition of the second solvent, several options are possible. The solvents mix themselves in a homogeneous way similar to the first case, that is to say in the bulk solution and at the solvation layer of the objects. But one can also imagine that the polar headgroups have a preference for one of the solvents. For example, sugar-based headgroups are known to interact strongly with water. If the glucose-based surfactant (previously dissolved in water) is already solvated by water, it might be difficult for formamide molecules to interact with the surfactant headgroups. For example, Huang et *al.*<sup>15,16</sup> tested the influence of several organic additives on vesicles of cationic surfactants pre-formed in water. They observed that even small amounts of formamide can destroy the vesicles in the aqueous systems. As we have seen, this destructing effect of formamide is due to the dissociation of the ion pair resulting from the high dielectric constant of formamide. The consequential change of the geometric parameter gave rise to the formation of micelles rather than vesicles. This also proved that formamide could interact with the polar headgroups that were formerly solvated by water.

We, on the other way round, wanted to test the influence of water addition on highly concentrated surfactant/FA solutions. We therefore studied highly concentrated solutions of G-Hyd<sub>8</sub><sup>+</sup>/C<sub>12</sub><sup>-</sup> and G-Hyd<sub>8</sub><sup>+</sup>/C<sub>16</sub><sup>-</sup> in formamide and added water step-wise. We obtained 10 samples of each series with increasing water content. We tested the samples by DLS measurements. We did not detect any measurable signals in the case of the pure formamide samples as it has already been shown before (absence of vesicles). The dielectric constant of pure formamide is too high to get vesicle formation. In both cases, the samples with 90:10 and 80:20 FA/H<sub>2</sub>O content did not give any evidence of vesicle formation. In the case of G-Hyd<sub>8</sub><sup>+</sup>/C<sub>16</sub><sup>-</sup>, we could observe vesicle formation in

## Results and Discussion

Solvent (v/v)	Concentration <i>mol.L</i> <sup>-1</sup>	Compound			
		<b>5a</b>		<b>5c</b>	
		Preparation		Preparation	
		A	B	A	B
FA	1.10 <sup>-1</sup>	no vesicles	no vesicles	no vesicles	no vesicles
FA/H <sub>2</sub> O 90:10	9.10 <sup>-2</sup>	no vesicles	no vesicles	no vesicles	no vesicles
FA/H <sub>2</sub> O 80:20	8.10 <sup>-2</sup>	no vesicles	no vesicles	no vesicles	no vesicles
FA/H <sub>2</sub> O 70:30	7.10 <sup>-2</sup>	no vesicles	no vesicles	vesicles	vesicles
FA/H <sub>2</sub> O 60:40	6.10 <sup>-2</sup>	no vesicles	no vesicles	vesicles	vesicles
FA/H <sub>2</sub> O 50:50	5.10 <sup>-2</sup>	vesicles	vesicles	vesicles	vesicles
FA/H <sub>2</sub> O 40:60	4.10 <sup>-2</sup>	vesicles	vesicles	vesicles	vesicles
FA/H <sub>2</sub> O 30:70	3.10 <sup>-2</sup>	vesicles	vesicles	vesicles	vesicles
FA/H <sub>2</sub> O 20:80	2.10 <sup>-2</sup>	vesicles	vesicles	vesicles	vesicles
FA/H <sub>2</sub> O 10:90	1.10 <sup>-2</sup>	vesicles	vesicles	vesicles	vesicles

(A) – Preparation of isolated compounds in beforehand mixed solvent mixtures.

(B) – Solvation of the compound in one solvent and admixing the second solvent.

Table 3.11: Results of the DLS measurements on compound **5a** and **5c** using different preparation methods for the solvent mixtures at 50 °C.

the 70:30 FA/H<sub>2</sub>O mixture. This was the same ratio of formamide and water that we had found in our previous experiments with beforehand mixed solvents. The size of the object formed was 50-100 nm, comparable to former measurements. In the case of G-Hyd<sub>8</sub><sup>+</sup>/C<sub>12</sub><sup>-</sup>, objects were observed in a 50:50 FA/H<sub>2</sub>O mixture, with a size of 120-200 nm. The diameters of both systems are in the same order of magnitude as with the other preparation method. We can therefore conclude that the way of preparation affected neither the size nor the type of aggregate formed.

We have seen that the different ways of preparing the solvent mixtures did not affect the aggregation behavior of our catanionic surfactants. But the catanionic systems themselves can be prepared differently in order to study them in non-aqueous solvents. Firstly, the catanionic associations were formed through an acid-base reaction in water and isolated by freeze-drying. The catanionic association was then dissolved in the desired solvent. Secondly, the catanionic surfactant can be synthe-

## Results and Discussion

---

sized directly in a polar protic solvent (such as formamide). We studied the influence of the two preparation methods on the  $\text{G-Hyd}_{12}^+/\text{C}_8^-$  system. In a first experiment, we prepared a catanionic association between  $\text{G-Hyd}_{12}$  and octanoic acid through an acid-base reaction in water, then the mixture was freeze-dried and the resulting powder was dissolved in formamide. In a second experiment, we performed the acid-base reaction between the two components directly in formamide and tested both resulting solutions by surface tension measurements. The *CACs* curves obtained in both cases were superimposable (see fig. 3.25). Moreover, DLS measurements of both solutions showed that the size of the objects were comparable (80-200 nm). We could therefore demonstrate that the preparation method of  $\text{G-Hyd}_{12}^+/\text{C}_8^-$  did not influence the formation of the ion pair and that we obtained objects of the same type and size.

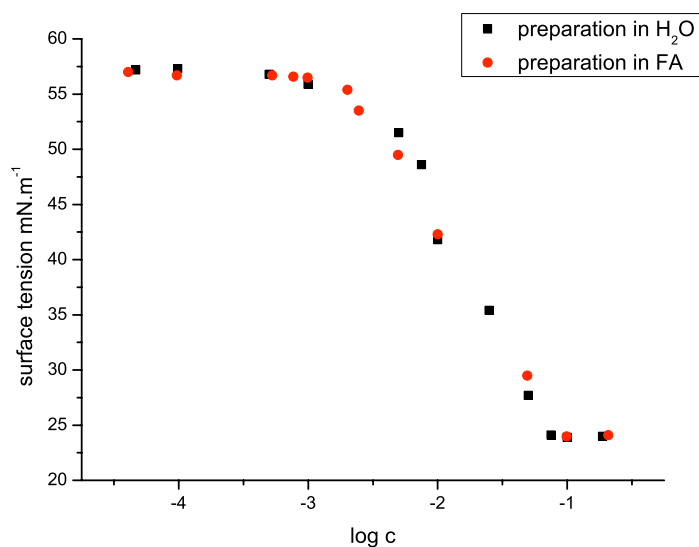


Figure 3.25: Surface tension measurements at 50 °C of the  $\text{G-Hyd}_{12}^+/\text{C}_8^-$  system in FA, prepared in H<sub>2</sub>O or in FA.

### 3.7 Conclusion

The aim of our work was to study the behavior of cationic surfactants in non-aqueous solvents. In a first part of our study, we have demonstrated that cationic surfactants behave similarly to formerly studied ionic surfactants in formamide. With the help of simple model systems, we could demonstrate that the Krafft temperatures  $T_K$  of cationic surfactants are higher in formamide than in water. This can be explained by the ionic nature of liquid formamide. Solvated surfactants in formamide can be compared to mixed salts that possess a more rigid structure and the resulting  $T_K$  are higher than in the analogous aqueous systems. In addition, we showed that the critical aggregation concentrations  $CAC$  of cationic surfactants are higher in non-aqueous solvents than in water. This can be explained by the fact that these polar solvents possess a less cohesive nature, which reduces the solvophobic interactions. These solvophobic interactions are the main driving force of self-aggregation. As a consequence, higher surfactant concentrations are necessary to obtain objects.

The most important result of our experiments was the fact that the dielectric constant of the medium and the number of carbon atoms in the lipophilic part have become additional critical parameters in the aggregation phenomena of cationic surfactants, along with the CED. In systems with less than 28 carbon atoms in the chains, the cationic systems can be dissociated due to a high solvent dielectric constant. As a consequence, the packing parameter  $p$  of cationic surfactants was modified. Cationic surfactants usually form spontaneously vesicles in water, since the particular ion pair structure favors this type of aggregates. However, the dissociating influence of the dielectric constant changed the geometric parameters of the ion pair. Our results let us suspect the formation of micelles rather than vesicles. On the other hand, cationic surfactants with long alkyl chains (e.g. G-Hyd<sub>16</sub><sup>+</sup>/C<sub>12</sub><sup>-</sup>) did form vesicles in water and formamide. The higher number of carbon atoms increased the hydrophobic van

## Results and Discussion

---

der Waals interactions. The ion pair was stabilized and the dissociative effect of the solvent dielectric constant was compensated. We could demonstrate that the cohesive-energy density was therefore not the only important parameter in the aggregation of catanionic surfactants.

# 4

## Surfactants Based upon Large Counterions

### 4.1 General Information

Catanionic surfactants that usually form spontaneously vesicles in water thanks to the favorable geometric form of the cationic association, were studied in non-aqueous solvents. Our experiments have shown that cationic systems did not necessarily form vesicles in non-aqueous solvents. We demonstrated that vesicle formation depended on the dielectric constant of the solvent. High dielectric constants led to the dissociation of the ion pair, of which the cationic association is composed. The separation of the

## Results and Discussion

---

ion pair led to a modification of the packing parameter  $p$ . As a consequence, catanionic surfactants did not form vesicles and gave rise to the formation of micelles. On the other hand, we could show that high numbers of carbon atoms in the lipophilic part can strengthen the ion pair through hydrophobic interactions. This reinforcing effect can compensate the dissociative effect of the dielectric constant. The aggregation of catanionic surfactants therefore depends on the balance between the dielectric constant of the solvent and the degree of association of the ion pair. The effect of the dielectric constant can be visualized with the G-Hyd<sub>8</sub><sup>+</sup>/C<sub>12</sub><sup>-</sup> systems that formed vesicles in water and H<sub>2</sub>O/formamide mixtures with a maximal formamide content of 50 %. At higher formamide concentrations, only micelles could be observed. This modification of the aggregate type of catanionic surfactants with varying dielectric constant can also be viewed as a vesicles-micelle transition depending on the solvent dielectric constant. In the fundamental part, surfactants with large counterions – norbornene methyleneammonium tetradecanoate and hexadecanoate (NbC14 and NbC16) – were presented. Fig. 4.1 shows the structure of NbC14. Both systems were studied in our laboratory by Bordes et al.<sup>47,48,148</sup> It was shown that both systems underwent a micelle-vesicle transition that depended on the concentration of the catanionic association. At low concentrations, micelles were formed, and an increase in surfactant concentration led to the formation of vesicles.

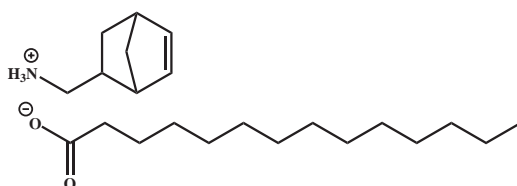


Figure 4.1: Norbornene methyleneammonium tetradecanoate NbC14.



The authors reported two reasons that induced this micelle-vesicle transition. Firstly, NbC14 and NbC16 possessed a favorable ratio of headgroup volume to surfactant chain length which allowed micelle formation at low concentrations.<sup>47,48</sup> It was shown that a bulky headgroup, that is to say a cyclic or branched counterion, was necessary, as well as a sufficiently long anionic surfactant. Secondly, the hydrophobic interactions between the large counterions and the hydrophobic part of the anionic surfactant changed with surfactant concentration. At low concentrations, the interactions were weak and the counterion was less associated. The counterions behaved comparable to classic counterions such as sodium ions. As a consequence, NbC14 and NbC16 were characterized by a cone-like geometry (see fig. 4.2), which favored micelle formation at low concentrations.

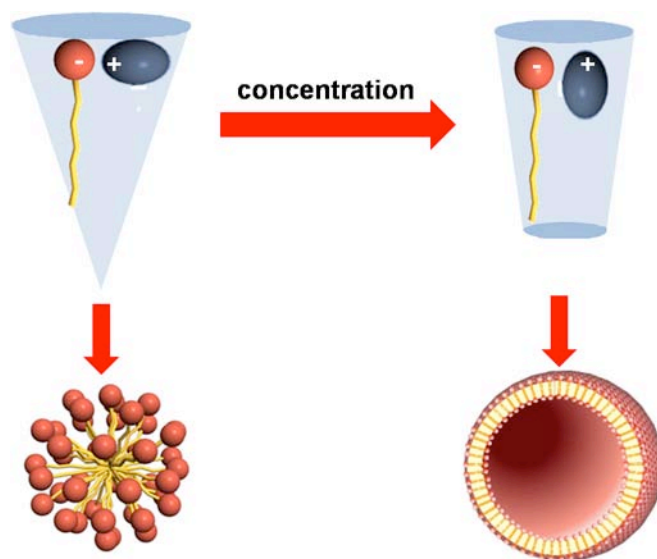


Figure 4.2: Model of the micelle-vesicle transition mechanism.

At higher concentration, the interactions increased and the large counterions intercalated themselves side-by-side between the anionic surfactants. This conformation conferred the catanionic association the truncated cone-like geometry, and vesicle formation was possible at higher concentrations. The micelle-vesicle transition was

## Results and Discussion

---

therefore the consequence of the changing interactions between the counterion and the anionic surfactant and the resulting modification of the counterion positioning. The positioning of the counterion in a side-by-side position between the ionic surfactant or at the outer solvation layer of the micelle depended on the degree of interaction between the counterion and the anionic surfactant. It was shown that a large bulky counterion let less possibilities for hydrophobic interactions than two long chain surfactants such as G-Hyd<sub>m</sub><sup>+</sup>/C<sub>n</sub><sup>-</sup>.

We have seen that the interaction between the two components of a catanionic surfactant depended also on the dielectric constant of the solvent. We wanted therefore to study comparatively NbC14 in water and in pure formamide in order to study the influence of the dielectric constant on the behavior of this kind of catanionic associations. In addition, the behavior of these surfactants with large counterions was compared with what was previously observed with glucose-based surfactants. Following our model of the influence of the dielectric constant and the carbon number on the aggregation behavior of catanionic associations, we expected that the interactions between the counterion and the surfactant should be weaker in formamide than in water. As we explained, the weaker interactions would lead to a positioning of the counterion at the outer solvation layer similar to classic counterions. As a consequence, NbC14 should only form micelles in pure formamide, because of the dissociating effect of formamide. This would also mean that we would not observe micelle-vesicle transition.

## 4.2 Physico-Chemical Studies on NbC14 in Water and in Formamide

We wanted to compare the behavior of NbC14 in pure formamide with that in water. As we explained in the introduction to surfactants in non-aqueous solvents, critical aggregation concentrations and Krafft temperatures are higher in formamide than in water. Therefore, we determined in a first step the Krafft point  $T_K$  of NbC14 in pure formamide, which is 42 °C. NbC14 is then soluble up to a concentration of  $10^{-1}$  mol.L $^{-1}$  in pure formamide at 45 °C. It is interesting to note that NbC14 did not have any  $T_K$  in pure water.<sup>47,48</sup> However, we performed our experiments in water, formamide and H<sub>2</sub>O/FA mixtures at 45 °C, which corresponds to a temperature above the  $T_K$ . Fig. 4.3 shows the surface tension measurements of NbC14 in water, formamide and their mixtures. In water, two plateaus could be observed. As Bordes *et al.* explained, the first plateau corresponded to the formation of micelles at a concentration range between  $6 \cdot 10^{-6}$  and  $6 \cdot 10^{-5}$  mol.L $^{-1}$ . The second plateau, which began at a concentration of  $2 \cdot 10^{-4}$  mol.L $^{-1}$  indicated vesicle formation.<sup>47</sup>

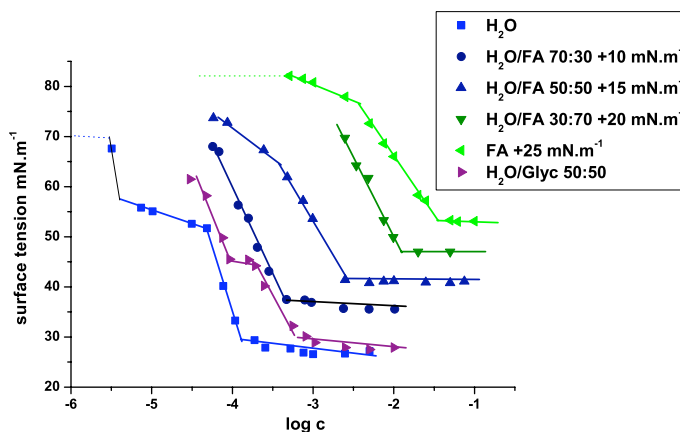


Figure 4.3: Surface tension measurements of NbC14 in different solvents and solvent mixtures at 45 °C.

## Results and Discussion

---

However, two interesting observations could be done. Firstly, the intermediate plateau was not horizontal but characterized by a small slope. This tendency has already been observed by Bordes *et al.* at 30 °C. It can be explained by the fact that at higher temperatures the aggregation number  $N_A$  is less sharply defined than at lower temperatures. As a consequence, the break in the surface tension evolution, which corresponds to the *CMC*, is less pronounced. Hence, the intermediate plateau was not horizontal in the case of NbC14. We could also observe that the existing area of micelles is bigger than at lower temperatures. This has already been observed by Bordes *et al.* in the temperature range between 5 and 30 °C.<sup>47,48</sup> The intermediate plateau increased as well with increasing temperature, which is due to the decreased electrostatic and hydrophobic interactions between the counterion and the ionic surfactant<sup>2</sup> (see fig. 4.4).

Solvent	H <sub>2</sub> O	H <sub>2</sub> O/FA (v/v)			FA	H <sub>2</sub> O/glycerol 50:50 (v/v)
		70:30	50:50	30:70		
<i>CMC</i>	$3.9 \cdot 10^{-6}$	—*	—*	—*	$3.0 \cdot 10^{-3}$	$1.0 \cdot 10^{-4}$
<i>CAC</i> <sub>vesicles</sub>	$1.3 \cdot 10^{-4}$	$4.0 \cdot 10^{-4}$	$2.5 \cdot 10^{-3}$	$1.6 \cdot 10^{-2}$	$4.0 \cdot 10^{-2}$	$5.6 \cdot 10^{-4}$

\* No micelle formation

Table 4.1: *CMC* and *CAC* (mol.L<sup>-1</sup>) of NbC14 at 45 °C.

At concentrations in the range of the second plateau, vesicle formation was observed by DLS. The objects were characterized by diameters between 70 and 80 nm. Electron micrographs confirmed the formation of vesicles of about 100 nm in water (see fig. 4.5). Altogether, we could observe a similar behavior of NbC14 in water at 45 °C in comparison to the behavior at 25 °C.

On the other hand, NbC14 has not yet been studied in formamide. Therefore, we studied the evolution of the surface tension with increasing concentration. In fig. 4.3, the surface tension measurements of NbC14 in water and in formamide can be com-

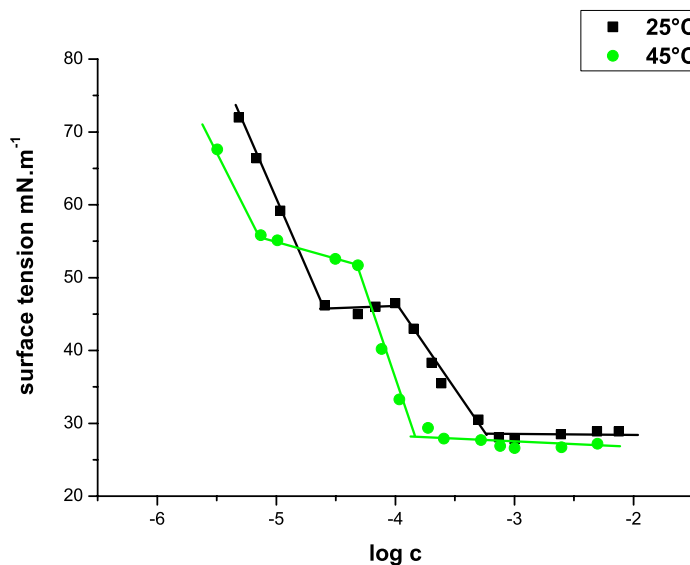


Figure 4.4: Surface tension measurements of NbC14 in H<sub>2</sub>O at 25 and 45 °C.

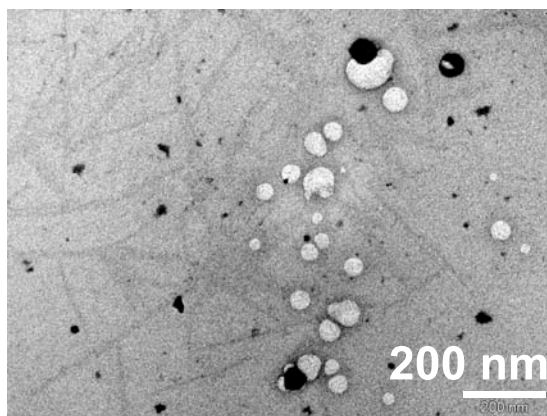


Figure 4.5: Electron micrograph of NbC14 in H<sub>2</sub>O ( $1.10^{-3}$  mol.L<sup>-1</sup>).

pared. We observed a comparable behavior to that in pure water, but it has to be noted that the concentrations were shifted to higher values. As it was explained previously, formamide possesses a less cohesive nature, which leads to a higher surfactant solubility and reduced solvophobic interactions. Higher concentrations are therefore needed in order to obtain the same aggregation behavior than in water. However, in

## Results and Discussion

---

a first concentration range (from  $6 \cdot 10^{-4}$  to  $6 \cdot 10^{-3}$  mol.L<sup>-1</sup>) the surface tension decreases slightly with a slope in the same order of magnitude than in water. In the case of water, we could observe micelle formation in this plateau-like region. Therefore, we assumed that this plateau-like region in the formamide system corresponded to the formation of micelles. We could not detect any signals by DLS, which substantiated our suspicion. Nevertheless, SAXS/WAXS experiments should be performed to prove the formation of micelles and to determine the size of the objects. After this plateau-like region, a break in the surface tension evolution can be observed. The surface tension decreased significantly while increasing surfactant concentration. After another break, we could detect a second plateau at a concentration of about  $4 \cdot 10^{-2}$  mol.L<sup>-1</sup>. The fact that the surfactant measurements of NbC14 in formamide exhibit two plateaus was surprising, since it was not in agreement with our previously presented theory on catanionic surfactants in formamide. As explained before, we expected that only micelles should be formed by NbC14 in pure formamide. The dissociative effect of the dielectric constant would tend to separate the ion pair. As a consequence, the association would behave like classic ionic surfactants, with the counterion weakly associated in the outer solvation sphere. We studied solutions of NbC14 in pure formamide with concentrations in the range of the second plateau by dynamic light scattering in order to determine the size of the aggregates. We could detect objects in the size of 100-120 nm, which would correspond to the formation of vesicles. The formation of vesicles in pure formamide with diameters between 50 and 100 nm could be visualized on electron micrographs (see fig. 4.6). The results showed that NbC14 form two types of aggregates in pure formamide. Similar to the aqueous system, micelles could be formed at lower concentrations and vesicles were formed at higher concentrations.

The formation of vesicles is interesting, since it means that the structural integrity of the ion pair was maintained in pure formamide, that is to say the geometrical

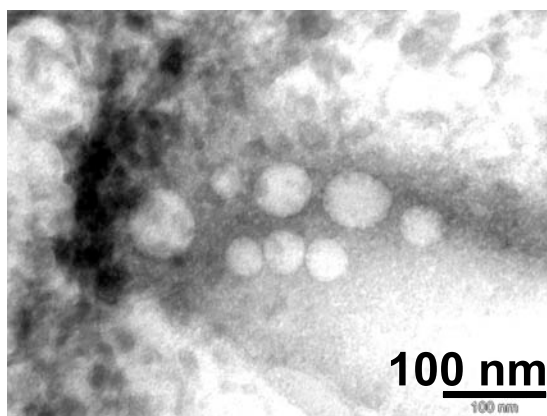


Figure 4.6: Electron micrograph of NbC14 in formamide ( $5.10^{-2}$  mol.L $^{-1}$ ).

features that allow vesicle formation in pure water seem to be the same in pure formamide. This did not fit with our proposed model on cationic surfactants. It has to be noted that our model, describing the influence of the dielectric constant on cationic systems, was based on alkylammonium alkanoate ( $C_m^+/C_n^-$ ) and *N*-alkylammonium-1-deoxy-D-glucitol alkanoate ( $G\text{-Hyd}_m^+/C_n^-$ ) systems. It can be imagined that other cationic systems with different headgroups would behave differently. Moreover, it was also shown that headgroup-solvent interactions played an essential role in formamide.<sup>83,111</sup> Hydrophobic interactions like van der Waals or  $\pi$ -stacking phenomena are more important in non-aqueous solvents than hydrogen bondings and electrostatic interactions.<sup>83,111</sup> Pyridinium-based surfactants, for example, were able to form hexagonal liquid crystalline phases in pure formamide and in *N*-methylsyrnone, whereas alkyltrimethylammonium surfactants could not form this kind of phases.<sup>83,111</sup> Formamide<sup>93</sup> and NMS possess a double bond character, and headgroup-solvent interactions are not only due to electrostatic interactions, but also to hydrophobic interactions. These hydrophobic interactions could compensate the lower cohesive-energy densities of non-aqueous solvents. This additional headgroup-headgroup and headgroup-solvent interactions could also explain the formation of vesicles in the case

## Results and Discussion

---

of NbC14. It was demonstrated that norbornane derivatives can undergo a stacking of the bicycle as shown in fig. 4.7.<sup>149</sup> The stacking of our norbornene-based surfactants might stabilize and maintain the integrity of the ion pair, even if the high dielectric constant exerted a dissociative force on the ion pair.

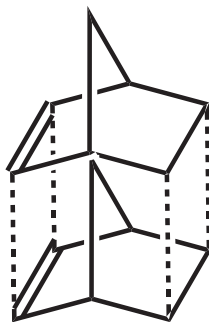


Figure 4.7: Model of the stacking phenomenon of norbornene cycles.

It is interesting to note that NbC14 did not show any micelle-vesicle transition in H<sub>2</sub>O/FA mixtures at 45 °C. Moreover, we could only observe the formation of vesicles in 30, 50 and 70 % formamide mixtures. Micelle formation could not be detected. Surface tension measurements were not characterized by an intermediate plateau. This behavior could be due to a different solubilization behavior of H<sub>2</sub>O/FA mixtures in comparison to the pure solvents. We have already reported that the solubilities of long-chain catanionic surfactants (e.g. G-Hyd<sub>16</sub><sup>+</sup>/C<sub>12</sub><sup>-</sup>) were different in mixed solvents in comparison to the pure solvents. The surfactants were enough soluble in water and formamide to perform surface tension measurements, but not in their mixtures (see chapter 3.4). In the case of NbC14, the surfactant was enough soluble in the solvent mixtures, but showed a different aggregation behavior in comparison to the pure solvents. However, DLS measurements of the mixed H<sub>2</sub>O/FA solutions showed that NbC14 formed vesicles with diameters between 50 and 200 nm. This was also proved by electron micrographs which showed vesicles with diameters in the same order of magnitude (see fig. 4.8).



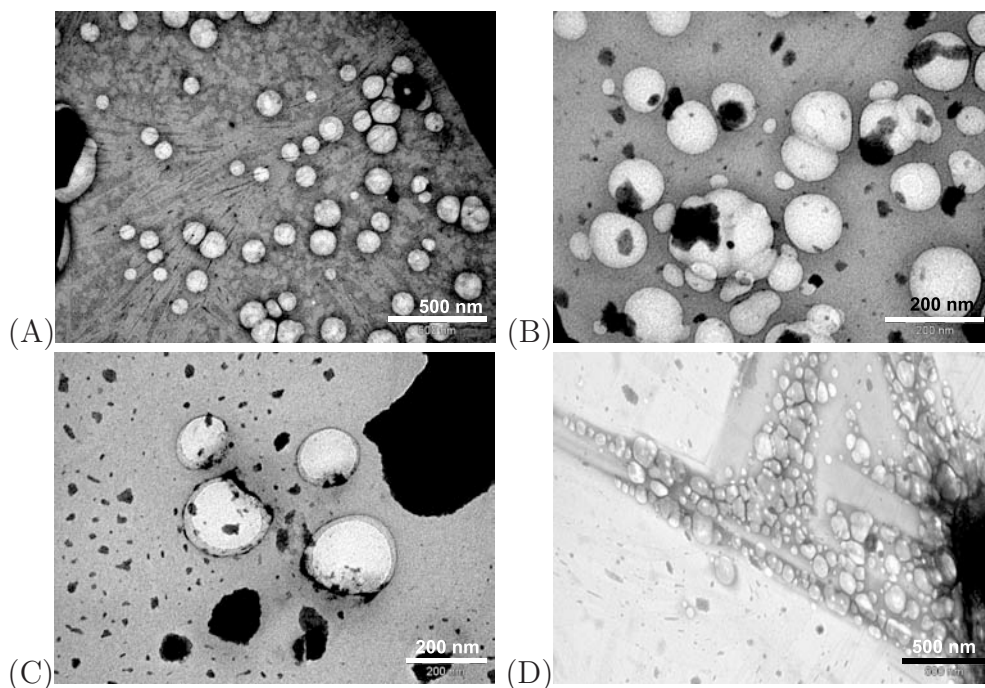


Figure 4.8: Electron micrographs of NbC14; (A) H<sub>2</sub>O/FA 70:30 ( $5.10^{-3}$  mol.L<sup>-1</sup>), (B) H<sub>2</sub>O/FA 50:50 ( $1.10^{-2}$  mol.L<sup>-1</sup>), (C) H<sub>2</sub>O/FA 30:70 ( $5.10^{-2}$  mol.L<sup>-1</sup>), (D) H<sub>2</sub>O/glycerol 50:50 ( $5.10^{-3}$  mol.L<sup>-1</sup>).

Optical micrographs showed also the typical defects that indicated the formation of lamellar phases in these solvents. The formation of lamellar phases is a prerequisite for vesicle formation, since vesicles are composed of bilayers. Fig. 4.9 shows these defects for NbC14 in a 50:50 H<sub>2</sub>O/FA mixture.

We studied also NbC14 in a 50:50 H<sub>2</sub>O/glycerol mixture. In this case, we could observe an intermediate plateau at 45 °C, which could correspond to the formation of micelles. We could detect a population of small objects with diameters of about 10 nm by DLS measurements. This would correspond to the formation of micelles in this concentration range. A second plateau indicated the formation of vesicles. The size of the vesicles was determined by DLS at 100-200 nm. The diameters observed by TEM were in the same order of magnitude, that is to say about 50-200 nm (see fig. 4.8 (D)). NbC14 behaved in a comparable way in the H<sub>2</sub>O/glycerol mixture and in pure

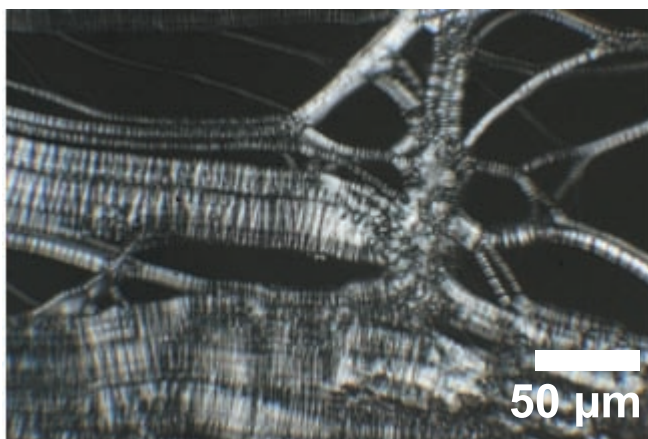


Figure 4.9: Optical micrograph of NbC14 in a 50:50 H<sub>2</sub>O/FA mixture.

water. It seemed that the non-aqueous solvent glycerol did not influence the behavior of surfactants as much as formamide did. We have already been able to observe this with our previously discussed cationic systems. The *CAC* values of sugar-based cationic surfactants in H<sub>2</sub>O/glycerol mixtures were only slightly higher than the ones in water, whereas the *CAC*s of H<sub>2</sub>O/FA mixtures were always significantly shifted to higher concentrations. Similar observations on the weak influence of glycerol on ionic surfactants in H<sub>2</sub>O/glycerol mixtures were done by Carnero Ruiz *et al.*<sup>116</sup>

### 4.3 Insights on Headgroup-Headgroup Interactions

As we have seen, NbC14 showed micelle-vesicle transition in water, in a 50:50 H<sub>2</sub>O/glycerol mixture and in pure formamide. The formation of vesicles in formamide was unexpected since it was not in agreement with our previously proposed model of the influence of dielectric constant on the aggregation behavior of cationic surfactants. We wanted to study this particular behavior of NbC14. Bordes *et al.* studied several systems based upon tetradecanoic acid and large organic counterions.<sup>47,48</sup> They wanted to study the origins and the mechanisms of the micelle-vesicle transitions.

## Results and Discussion

---

They could determine two parameters. Firstly, the ratio between counterion volume and surfactant chain length and secondly, the freedom of positioning, which changed with the surfactant concentration. As we have already mentioned, the formation of vesicles of NbC14 in pure formamide can be due to the particular structure of its large counterion. In order to determine the influence of the counterion structure, we chose one of the counterions Bordes *et al.* studied in their work.<sup>47,48</sup> Cyclohexylamine possesses a cyclic structure and, in the cationic form, a  $\log p$  of about -1.15. Among the tested counterions, this is the closest value of  $\log p$  to that of norbornene methyleneammonium. Therefore, we studied the cyclohexylammonium tetradecanoate (CxC14) in water and formamide at 45 °C in order to compare it with the norbornene-based system.

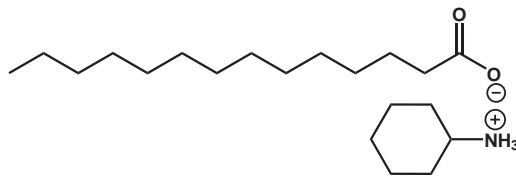


Figure 4.10: Cyclohexylammonium tetradecanoate (CxC14).

In previous studies it was shown that a cyclic structure of the counterion, that is to say a bulky headgroup, favored the micelle-vesicle transition. Surface tension measurements in water at 45 °C showed that CxC14 was characterized by two plateaus. This has already been demonstrated by Bordes *et al.* at lower temperatures.<sup>47,48</sup> Cyclohexylammonium interacted more weakly at lower concentrations with the anionic surfactant and the counterion placed itself at the outer solvation layer. This conformation conferred the ion pair a cone-like geometry and micelles were formed. This behavior is comparable to that of NbC14. At higher concentrations, stronger interactions between counterion and surfactant occurred and the association possessed a more truncated cone-like geometry, which conferred it the possibility to form vesicles.

## Results and Discussion

---

In fig. 4.11, the surface tension measurements of CxC14 in water and formamide are visible. The two plateaus appear at a concentration of  $4.5 \cdot 10^{-5} \text{ mol.L}^{-1}$ , corresponding to micelle formation and  $3.5 \cdot 10^{-4} \text{ mol.L}^{-1}$ , corresponding to vesicle formation. The size of the vesicles could be determined at 200 nm by DLS measurements.

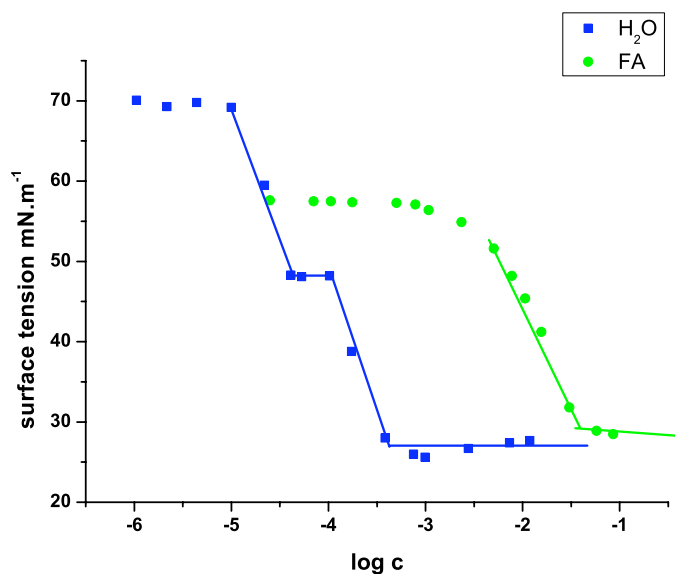


Figure 4.11: Surface tension measurements of the CxC14 system in water and in formamide at 45 °C.

As in the case of NbC14, we performed surface tension measurements of CxC14 in pure formamide. Contrary to the NbC14 system, we obtained only one plateau with a corresponding *CAC* at  $4 \cdot 10^{-2} \text{ mol.L}^{-1}$ . This is about three orders of magnitude higher than the *CMC* obtained in water, and about two orders of magnitude higher than the *CAC*, which indicated vesicle formation in water. However, the existence of a *CAC* should indicate the formation of aggregates. In order to determine the size of the possibly formed objects at concentrations above the *CAC*, we performed DLS measurements. We could not detect any signals, which could be explained that CxC14 did not form vesicles in pure formamide, but gave rise to the formation of micelles.

Solvent	H <sub>2</sub> O	FA
<i>CMC</i>	$4.5 \cdot 10^{-5}$	$4.0 \cdot 10^{-2}$
<i>CAC<sub>vesicle</sub></i>	$3.5 \cdot 10^{-4}$	—*

\* No vesicle formation

Table 4.2: *CMC* and *CAC* (mol.L<sup>-1</sup>) of CxC14 at 45 °C.

Micelle formation would be in agreement with our above presented model of catanionic associations in formamide. CxC14, being an ion pair composed of an anionic surfactant and a large organic counterion, would then be hold together by electrostatic and weak hydrophobic interactions. These interactions would be weaker than in the case of two long chain surfactants (like G-Hyd<sub>m</sub><sup>+</sup>/C<sub>m</sub><sup>-</sup>) due to the fact that the side-by-side position of the cyclohexylammonium and the tetradecanoate lets less possibility for hydrophobic interactions than in the case of two long chain alkyl. According to our model, the dissociative forces in formamide, due to the high dielectric constant, should separate the CxC14 ion pair and increase the freedom of positioning. The resulting geometry of the association would therefore correspond to a cone-like structure leading to the formation of micelles, which could not be detected by DLS. Nevertheless, further SAXS/WAXS experiments should be performed in order to characterize the type and the size of the objects formed.

However, the fact that CxC14 forms only micelles in pure formamide gave rise to some hypotheses concerning the influence of hydrophobic interactions in non-aqueous solvents. As we have described above, we were able to demonstrate that the aggregation of G-Hyd<sub>m</sub><sup>+</sup>/C<sub>n</sub><sup>-</sup> surfactant type depended on the dielectric constant of the solvent and on the number of carbon atoms in the lipophilic part of the surfactant. On the one hand, a too high dielectric constant can dissociate the ion pair, leading to a simple mixture of monocatener surfactants, which are known to form micelles. On the other hand, increasing the number of carbon atoms in the hydrophobic part of the surfac-

## Results and Discussion

---

tants can increase the solvophobic effect and reinforce the ion pair and compensate the dissociative effect of the dielectric constant.

It was shown that G-Hyd<sub>m</sub><sup>+</sup>/C<sub>n</sub><sup>-</sup> surfactants form vesicles in pure formamide when possessing more than 26 C-atoms. As a consequence, only the balance between medium dielectric constant and number of C-atoms lead to the formation of vesicles with catanionic surfactants in non-aqueous solution. In a second part, we studied a catanionic association based upon an anionic surfactant (tetradecanoate) and a large cationic organic counterion (norbornene methyleneammonium). It was shown that this type of surfactant underwent a micelle-vesicle transition in water. The micelle-vesicle transition was due to the modification of the interactions between the two oppositely charged moieties with increasing concentration. Catanionic associations with large counterions are usually characterized by weaker hydrophobic interactions than two ionic surfactants with long alkyl chains. Therefore, it was surprising that NbC14 formed vesicles in formamide and in H<sub>2</sub>O/FA mixtures. We could also observe a micelle-vesicle transition in pure formamide. Contrary to all expectations, our model did not fit on this type of catanionic association. In a third part, we studied a similar system based upon cyclohexylamine. The cyclohexylammonium counterion does not possess any stacking possibilities. In water, we could observe a micelle-vesicle transition similar to the one which occurred with NbC14. However, only the formation of micelles could be observed in formamide. Cyclohexylammonium tetradecanoate did not behave in the same way as norbornene methyleneammonium tetradecanoate did. The differences between the norbornene methyleneammonium and the cyclohexylammonium counterions is that the norbornene residue possesses a bicyclic structure with a double bond, whereas the cyclohexyl residue possesses only a monocyclic structure. It was shown that with the help of the bicyclic structure, norbornane derivatives can undergo a stacking phenomenon.<sup>149</sup> Norbornane derivatives were observed in highly ordered

stacked formations in polar solvents.<sup>149</sup> We have already mentioned the possibility that these additional interactions could explain the formation of vesicles by NbC14 even in pure formamide. Headgroup-headgroup interactions based on hydrophobic interactions are not influenced by the dielectric constant, whereas electrostatic interactions, namely the interactions between two ions, are strongly influenced.<sup>83,110</sup> In the case of NbC14, an additional stabilization of the headgroups can be achieved thanks to the stacking phenomenon of the bicyclic molecule, whereas CxC14 is only held together by electrostatic and weak van der Waals interactions. CxC14 was therefore more influenced by the dissociative effect of the dielectric constant of formamide and the ion pair was separated. As a consequence, the large counterion behaved more like a classic counterion, which resulted in micelle formation in pure formamide. This was in agreement with our previous results on catanionic surfactants. Nevertheless, these results also showed that hydrophobic headgroup-headgroup and headgroup-solvent interactions became an additional parameter, which can favor the formation of vesicles in non-aqueous solution.

### 4.4 Conclusion

NbC14 was previously characterized in water by Bordes *et al.* They observed a new kind of micelle-vesicle transition that was dependent on surfactant concentration. At low concentrations, micelles were formed, whereas at higher concentrations, vesicles could be observed. In formamide, we could observe the same type of micelle-vesicle transition. The formation of vesicles was interesting, since it was not expected. According to our theory, introduced for catanionic alkylammonium alkanoate and G-Hyd<sub>m</sub><sup>+</sup>/C<sub>m</sub><sup>-</sup> systems, we thought that only micelles would form. The formation of vesicles in pure formamide was therefore attributed to different headgroup-solvent interactions, since hydrophobic interactions can be predominant in non-aqueous sol-

## Results and Discussion

---

vents.<sup>83,110</sup> NbC14 possesses a bicyclic structure, which allows stacking.<sup>149</sup> A first indication of the importance of hydrophobic interactions was given by a comparative study between NbC14 and CxC14. The latter product did not possess a bicyclic structure similar to the one of norbornane. Therefore, solvent-solute interactions were weaker than in the case of NbC14, and CxC14 did not show the micelle-vesicle transition. It is also interesting to note that NbC14 did not undergo the micelle-vesicle transition in H<sub>2</sub>O/FA mixtures. Different solubilization behaviors could be responsible for the absence of the transition. However, this particular behavior of NbC14 has to be studied in the future. As a conclusion, the micelle-vesicle transition is a phenomenon which is due to the modification of the counterion position relatively to the anionic surfactant. For the NbC14 system, the transition could be observed in pure water, in pure formamide and in a 50:50 H<sub>2</sub>O/glycerol mixture. On the other hand, CxC14 only showed the transition in pure water, whereas in pure formamide only micelles were observed. This was in agreement with our previous studies on catanionic surfactants and the influence of the dielectric constant on the ion pair integrity. The formation of vesicle by NbC14 in pure formamide, which also indicated the preserved integrity of the ion pair, seemed to be the result of the particular structure of NbC14, which allowed additional headgroup-headgroup and headgroup-solvent interactions.



**Part IV**

**General Conclusion and  
Perspectives**



## General Conclusion and Perspectives

---

Catanionic associations have been extensively studied in water. Their aggregation behavior, namely the formation of vesicles in water, is of great interest for pharmaceutical research. Vesicles are versatile vehicles for drug delivery. Moreover, cationic surfactants are easily synthesized in comparison to covalently linked bicationic surfactants. Cationic assemblies with large counterions, such as norbornene derivatives or caffeic acid can “functionalize” the surfactant and lead to polymerizable or antioxidant systems. In the frame of this work, we have studied cationic associations in polar cohesive solvents. Three different cationic systems were synthesized, characterized and then studied in physico-chemical experiments to compare the aggregation behavior of these associations in aqueous and non-aqueous solution.

In the fundamental part, we explained that surfactant aggregation can also be observed in non-aqueous solvents such as formamide, glycerol or hydrazine. This can be explained by the fact that these solvents possess parameters close to those of water. Among these parameters, the cohesive-energy density is one of the most important. It indicates the degree of structuring of a solvent, which is a prerequisite for aggregation. Both formamide and glycerol are polar and cohesive solvents, in which aggregation of ionic and nonionic surfactants has already been demonstrated. Therefore, and because of their chemical stability, we chose these solvents for our research on the aggregation behavior of cationic surfactants in non-aqueous solvents.

Our first simple cationic model systems were synthesized by a simple acid-base reactions between a fatty acid and an amine, which allowed us to synthesize in an easy way a wide series of cationic associations with a various number of carbon atoms in the hydrophobic part. These simple model systems of the alkylammonium alkanoate type, obtained from commercial reagents, allowed us to study general parameters such as Krafft temperature and  $CAC$  of cationic surfactants in formamide. We were able to confirm that these parameters are higher in this non-aqueous solvent than in water.

## General Conclusion and Perspectives

---

These studies were helpful in determining the working conditions for physico-chemical studies on catanionic systems in non-aqueous solvents. Moreover, we observed an influence of the surfactant chain length on the  $T_K$  and the  $CAC$ . The  $T_K$  increased with increasing number of carbon atoms in the hydrophobic part of the surfactant, whereas the  $CAC$  decreased. Catanionic systems with asymmetric chains behaved differently to those that possess the same total number of carbon atoms but with two identical chains. We observed that the  $T_K$  of asymmetric systems are higher, whereas the  $CACs$  are even lower. This behavior might be attributed to a different crystallization lattice of asymmetric and symmetric catanionic surfactants, since the formation of aggregate and the Krafft temperature are related to the packing of the solid.<sup>133,134</sup> Different packing of the solid led to a different solvation behavior of the asymmetric and the symmetric systems and therefore to different Krafft temperatures and  $CACs$ .

The most striking results of this PhD work have been obtained by studying the catanionic systems comparatively in pure water, in pure formamide, in H<sub>2</sub>O/FA mixtures with various formamide content and in a 50:50 H<sub>2</sub>O/glycerol mixtures. We could not observe vesicle formation in pure formamide with the alkylammonium alkanoates model systems. In the case of *N*-alkylammonium-1-deoxy-D-glucitol alkanoates (G-Hyd<sub>*m*</sub><sup>+</sup>/C<sub>*n*</sub><sup>-</sup>), that have the advantage of being soluble in all solvent systems, we observed vesicle formation in pure water and in a H<sub>2</sub>O/glycerol mixture. Vesicle formation in H<sub>2</sub>O/FA mixtures was observed up to a certain formamide content, depending on the carbon number. The G-Hyd<sub>8</sub><sup>+</sup>/C<sub>12</sub><sup>-</sup> system formed vesicles when the formamide content did not exceed 50 %, whereas the G-Hyd<sub>8</sub><sup>+</sup>/C<sub>16</sub><sup>-</sup> system formed vesicles up to a formamide content of 70 %. Finally, the G-Hyd<sub>16</sub><sup>+</sup>/C<sub>12</sub><sup>-</sup> system underwent vesicle formation even in pure formamide. The fact that all G-Hyd<sub>*m*</sub><sup>+</sup>/C<sub>*n*</sub><sup>-</sup> formed vesicles in water and in H<sub>2</sub>O/glycerol mixtures, but not necessarily in water/formamide mixtures

## General Conclusion and Perspectives

---

can be explained by the unique structure of catanionic surfactants. Effectively, catanionic surfactants are composed of two oppositely charged ionic surfactants that form a globally neutral entity. The ion pair is held together by electrostatic interactions between the polar headgroups and by hydrophobic (namely van der Waals) interactions between the alkyl chains. Especially in the case of the sugar-based catanionic associations, this unique structure, described as truncated cone, usually favors the formation of vesicles in water ( $p$  between 0.5 and 1). In non-aqueous solution on the other hand, two parameters have become crucial. Firstly, the dielectric constant of the solvent: In formamide, which possesses a higher dielectric constant than water, the positive electrostatic interactions between the polar headgroups were reduced. This led to a dissociation of the ion pair, which changed the geometrical feature of the ion pair ( $p$  below 1/2). Thus, catanionic surfactants more likely formed micelles rather than vesicles in pure formamide. Secondly, the hydrophobic effect due to longer chains in the hydrophobic part of the surfactant, increased the interactions between the alkyl chains. It was shown that this effect could partially compensate the dissociative effect of the dielectric constant. In our case, we demonstrated that G-Hyd<sub>*m*</sub><sup>+</sup>/C<sub>*n*</sub><sup>-</sup> with numbers of carbon atoms lower than 26 in the hydrophobic part did not form vesicles in pure formamide, whereas those with higher numbers of carbon atoms did (form vesicles in pure formamide).

The influence of the dielectric constant on the one hand and the stabilizing effect of the hydrophobic interactions on the other hand were also demonstrated by the use of attenuated total reflectance infrared (ATR-IR) on catanionic surfactant solutions. The electrostatic interactions of catanionic surfactants are principally given by the interactions between the carboxylate and the ammonium group. Infrared measurements could give us direct information of the association degree as a function of modifications of the wave numbers of the carboxylate group. The weaker associated the carboxylate

## General Conclusion and Perspectives

---

groups, the lower the values of the carboxylate peak. We observed that the peaks were shifted to lower wave numbers in water/formamide and in formamide solutions compared to water, which indicated the lower association degree. There are other ways to elucidate the influence of the dielectric constant. For example, NMR experiments could be performed using deuterated formamide in the DOSY mode. This mode consists in the measurement of the lateral diffusion coefficients of molecules in a solution. The diffusion coefficient depends on the mass and shape of the molecules. In our case, the diffusion coefficients of the ion pair and of the two dissociated components of the ion pair should be different and give information of the ion pair association degree. Another possibility would be to analyze a catanionic surfactant containing a fluorescent marker such as 12-(1-pyrenyl)dodecanoic acid (PDA). It was already shown in the literature that the fluorescent spectrum of pyrene depends on the polarity of the medium.<sup>150–152</sup> The *CAC* of some surfactants has been determined using the pyrene method.<sup>153</sup> In our case, a certain amount of PDA in the catanionic surfactant mixture would elucidate the degree of penetration of formamide into the objects formed, since the fluorescence signal of PDA, incorporated in the inner part of the objects, depends on the micropolarity of the environment. Formamide that penetrates in the aggregate would increase the polarity and therefore change the fluorescence of PDA.

It has to be noted that all our experiments were limited by the maximal dielectric constant of formamide, that is to say 109 (in a 10:90 H<sub>2</sub>O/FA mixture 111, 25 °C). It would be of great interest to perform these experiments in other polar and cohesive solvents such as *N*-methylformamide or *N*-methylsydnone. It can also be envisaged to use ionic liquids that usually possess high dielectric constants. The formation of aggregates in ionic liquids has already been observed.<sup>82,83,110,154–156</sup> Moreover, the number of C-atoms in the hydrophobic tails can be increased in order to increase the solvophobic effect. This would reinforce the ion pair and therefore aggregates would

## General Conclusion and Perspectives

---

be formed more readily. Nevertheless, it has to be noted that the ratio of surfactant chain length and headgroup surface will become unfavorable for vesicle formation and the catanionic surfactants would precipitate.

In addition to the alkylammonium alkanoates and the *N*-alkylammonium-1-deoxy-D-glucitol alkanoates, we studied catanionic associations based upon large organic counterions. Large organic counterions strongly influence the aggregation behavior of surfactants. The position of the counterion, that is to say on the outer solvation layer or in the inner part of the aggregates, can modify the type of aggregates formed. In our laboratory, norbornene methyleneammonium tetradecanoate (NbC14) and cyclohexylammonium tetradecanoate (CxC14) were studied in water, and underwent a micelle-vesicle transition, depending on the surfactant concentration.<sup>47,48</sup> At low concentrations, the interactions between the surfactant and the counterion were weak and the counterion placed at the outer solvation sphere. At higher concentrations, the solvophobic interactions increased and the counterion intercalated itself between the ionic surfactant, which favored the formation of vesicles.

We comparatively studied NbC14 and CxC14 in water and in formamide at 45 °C, which was above the higher Krafft temperature in formamide. In water, we observed a comparable behavior of NbC14 and CxC14 at 45 °C to what has already been shown at 25 °C, that is to say we detected a micelle-vesicle transition.

In formamide, we expected that the weak hydrophobic interactions and the dissociative effect of the dielectric constant would only lead to micelle formation. Surprisingly, we could observe a micelle-vesicle transition and vesicle formation in the NbC14 system in pure formamide. Moreover, NbC14 formed only vesicles in H<sub>2</sub>O/FA mixtures, but did not undergo a micelle-vesicle transition. On the other hand, CxC14 was characterized only by micelle formation in pure formamide. This different behavior between the two catanionic associations was explained by the fact that the

## General Conclusion and Perspectives

---

norbornene-derived system possesses a bicyclic structure, which may allow a stacking of the bicycles similar to that observed in norbornane systems.<sup>149</sup> It was also shown that hydrophobic interactions (solute-solute and solute-solvent) became more important in non-aqueous solvents such as formamide or *N*-methylsydnone than in water.<sup>83,110</sup> The increased headgroup-headgroup interactions between the cycles could stabilize the ion pair and vesicle formation could be observed even in pure formamide. The monocyclic cyclohexylammonium tetradecanoate system did not possess any possibility of stacking. Thus, the dissociative effect of the dielectric constant of formamide could not be compensated by hydrophobic interactions. Therefore, CxC14 behaved in agreement with our theory, since the dissociative force of the dielectric constant separated the ion pair and led to the formation of micelles rather than vesicles. These results demonstrated that our theory of the influence of the dielectric constant on the aggregation behavior was verified for all the studied systems except NbC14. In the case of NbC14, additional headgroup-headgroup effects have to be considered. Therefore, studies should be envisaged with cationic surfactants with different types of headgroups, such as pyridinium or phosphate headgroups in order to elucidate the influence of the polar headgroups on the aggregation behavior of cationic surfactants.

In summary, our results demonstrated that the aggregation behavior of cationic surfactants in non-aqueous solvents is a complicated phenomenon. We determined several physical solvent parameters that have to be taken into account in order to obtain vesicles. In addition to the cohesive-energy density, which is beyond all doubt a prerequisite for aggregation, the dielectric constant has become a crucial parameter, as it can dissociate the ion pair. Moreover, the ion pair integrity can be increased by increasing the number of carbon atoms in the hydrophobic part of the surfactant. The increased hydrophobic interactions can compensate the dissociative effect of the dielectric constant. In addition, we observed another parameter that influence the



## General Conclusion and Perspectives

---

aggregation behavior of cationic surfactants. Hydrophobic headgroup-headgroup interactions such as  $\pi$ -stacking of norbornene derivatives can favor vesicle formation in non-aqueous solvents. These more fundamental study on cationic surfactants in non-aqueous solution gave a more detailed insight on the complicated interactions and parameters that can influence the aggregation behavior. In the future, we could profit of this work for the application of cationic surfactants in non-aqueous solutions. Several pharmaceutical preparations, for example, are based upon water/glycerol mixtures.<sup>39,40</sup>

Altogether, our results showed that the aggregation mechanisms of cationic surfactants are not yet fully understood. Thus, it is worthwhile to intensify the research on cationic associations in non-aqueous solutions. For this issue, cationic surfactants based on other polar headgroups and additional non-aqueous solvents, such as ionic liquids, should be taken into account in order to rationalize the interesting aggregation behavior of cationic assemblies.



# Part V

## Experimental Part



# 1

## Commercial Reagents

All reagents are analytical grade and were purchased from Fluka or Sigma-Aldrich and used as received, unless otherwise stated. Deionized ultrapure MilliQ water was used for all experiments. Water for physico-chemical analyses was filtered and deionized by a **Purité/Select Analyst HP** apparatus with a final resistivity of about 18 M $\Omega$ . In addition, it was filtered with hydrophilic cellulose membrane filters with pores of 1.2  $\mu\text{m}$  in order to prevent dust contamination. In the case of organic solvents, such as formamide, filters with PTFE-solvent resistant membranes were used with pore diameters of 0.45  $\mu\text{m}$ .

## Experimental Part

### 1.1 Reagents

Substance	CAS	Purity	Provider
$\alpha$ -D-Glucose	492-62-2	99 %	Sigma
5-Norbornene-2-carboxylic-acid	120-74-1	98 % endo-/exo-mixture	Aldrich
Bicyclo[2,2,1]hept-5-ene-2-carbonitrile	95-11-4	98 %	Aldrich
Octanoic acid	124-07-2	$\geq 99.5$ %	Aldrich
Octylamine	111-86-4	99 %	Aldrich
Decanoic acid	334-4-5	98 %	Fluka
Dodecanoic acid	143-07-1	99 %	Sigma
Dodecanoic acid	143-07-1	99.5 %	Acros
Dodecylamine	124-22-1	98 %	Aldrich
Dodecylamine	124-22-1	98 %	Fluka
Tetradecanoic acid	544-63-8	$\geq 98$ %	Aldrich
Hexadecylamine	149-27-1	99 %	Fluka
Hexadecanoic acid	57-10-3	99 %	Sigma
Octadecanoic acid	57-11-4	98.5 %	Fluka
Hexadecyltrimethyl ammonium hydroxide 25 % in MeOH	505-86-2		Acros
Lithium aluminium hydride	16835-85-3	95 %	Aldrich
Sodium borohydride	16940-66-2	99 %	Acros
Sodium chloride	7647-14-5	$\geq 99.5$ %	Sigma-Aldrich
Sodium hydroxide	1310-73-2	98 %	SDS
Sodium phosphotungstate	12501-23-4	99.995 %	Sigma-Aldrich
Sodium sulfate	7754-82-6	99.0 %	Fluka

---

## 1.2 Solvents

<b>Solvent</b>	<b>CAS</b>	<b>Purity</b>	<b>Provider</b>
Formamide	75-12-7	≥ 99.5 %	Fluka
Formamide	75-12-7	≥ 99.5 %	Sigma
Methanol	67-56-1	99.8 %	SDS
Absolute ethanol	64-17-5	99.8 %	VWR international
Glycerol	56-81-5	98 %	Prolabo
Diethyl ether	60-29-7	99.7 %	SDS
<i>n</i> -Hexane	110-54-3	HPLC grade	SDS
Cyclohexane	110-82-7	99.8 %	SDS
Conc. Hydrochloric acid 37 %	7647-01-0		VWR international





# 2

## Characterization and Physico-Chemical Techniques

### **2.1 NMR – Nuclear Magnetic Resonance Spectroscopy**

Nuclear magnetic resonance spectra were recorded on a **Bruker Avance 300** spectrometer with proton and carbon precession frequencies of 300.18 MHz and 75.48 MHz, respectively. The chemical shifts  $\delta$  are given in parts per million (ppm) downfield from

## Experimental Part

---

tetramethylsilane (TMS). Calibration was done on the chemical shift of the solvent (peak of the residual non-deuterated solvent). In order to indicate the multiplicities of the NMR peaks of the  $^1\text{H}$  spectra, following shortenings were used: s (singlet), d (doublet), dd (double doublet), t (triplet) and m (multiplet). The sample concentration ranged from 30-50  $\text{mg}\cdot\text{mL}^{-1}$ .

## 2.2 FT-IR – Fourier-Transform Infrared Spectroscopy

Infrared spectra were performed with a **PERKIN-ELMER IR FT 1760-X** apparatus. For the characterization of the synthesized products, KBr discs with a concentration of 0.5 w/w % were examined.

In order to evaluate the influence of the solvent on the association degree of the ion pair, we studied solutions of two catanionic systems by FT-IR using the ATR (attenuated total reflectance) method. The ATR method can be used to study films or materials that absorb too much the infrared light. In our case, we studied solutions of catanionic surfactants in water, formamide or in the mixture of these two solvents. Both solvents highly absorb the IR light. The above mentioned FT-IR apparatus was used with an adapted ZnSe cylinder-shaped cell for liquids. A MCT (mercury cadmium telluride) detector was used, which was cooled down by liquid nitrogen. We studied equimolar solutions of compounds **5a** ( $\text{G-Hyd}_8^+/\text{C}_{12}^-$ ) and **5c** ( $\text{G-Hyd}_8^+/\text{C}_{16}^-$ ) with a concentration of  $1\cdot 10^{-1} \text{ mol}\cdot\text{L}^{-1}$ , which was above the *CAC* of both catanionic systems. Experiments were performed at  $55\text{ }^\circ\text{C}$ , which was above the Krafft temperature  $T_K$  of both systems. We determined the wave number of the carboxylate group peak ( $-\text{COO}^-$ ) in the different solvents ( $1580\text{-}1540 \text{ cm}^{-1}$ ).

## 2.3 HRMS – High Resolution Mass Spectrometry

Mass spectra were recorded on a **TSQ 7000 Finnigan Mat** apparatus in positive and negative mode. The samples were introduced to triple quadrupole spectrometer by electrospray ionization (ESI) or chemical ionization (CI).

The formation of the ion pairs of the catanionic surfactants were proved using a **Waters Qtof Ultima API**. 50  $\mu\text{L}$  of a 1  $\text{mg}\cdot\text{mL}^{-1}$  ion pair water solution (when it was necessary, up to 20 % chloroform was added to improve solubility) and 50  $\mu\text{L}$  of a 1  $\text{mg}\cdot\text{mL}^{-1}$  NaI solution were added to 900  $\mu\text{L}$  water. The sample was injected into the apparatus with a flow rate of 10  $\mu\text{L}\cdot\text{min}^{-1}$ . The capillary voltage, the cone tension and the collision energy were 3 kV, 100 V and 10 eV, respectively.

## 2.4 Elementary Analysis

The elemental analyses were performed by the analysis service of the “Laboratoire de Chimie de Coordination” (LCC) in Toulouse for carbon, hydrogen and nitrogen. Elemental analyses for boron, sodium and chlorine were sent to the “Service Central d’Analyse” (SCA) in Solaize.

## 2.5 Krafft Temperature $T_K$

Krafft points were determined by a visual method. As indicated in fig. 2.1, the  $T_K$  is the point of intersection between the solubility curve and the *CMC* curve. The solubility of an ionic surfactant increases exponentially above the  $T_K$ . Krafft temperatures can be determined with the help of two highly concentrated solutions (e.g.  $1\cdot 10^{-1}$  and  $5\cdot 10^{-1}$   $\text{mol}\cdot\text{L}^{-1}$ ). Solutions were heated slowly until the solid was completely dissolved. Then the solutions were cooled down slowly under stirring and

## Experimental Part

---

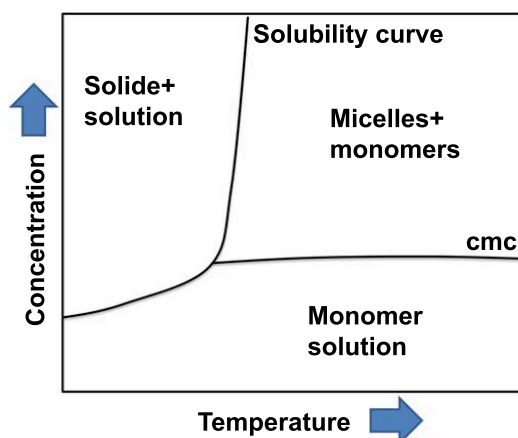


Figure 2.1: Typical phase diagram of a ionic surfactant.

the temperature at which precipitation is occurred is taken as the Krafft temperature  $T_K$ . Very concentrated solutions have to be used in order to obtain comparable  $T_K$  in both cases.

## 2.6 Surface Tension Measurements

Surface tension measurements were performed with a **Krüss EasyDyne** tensiometer using the Wilhelmy plate method. Solutions with different concentrations were prepared by weighting the solid cationic surfactant in glass vials with screwed caps and adding 20 mL of the desired solvent. Surface tension measurements were performed in pure water, pure formamide, water/formamide mixtures with 30%, 50%, 70% and 90% formamide, as well as in 50:50 water/glycerol mixtures. The solvents were mixed beforehand and added to the cationic surfactant. The samples were heated over the Krafft point and stirred/sonicated until a transparent and homogeneous solution was obtained. For systems with a  $T_K$  above room temperature, the samples were stored in a thermostatted bath for equilibration until used. The crystallizer in which the measurements were performed was also thermostatted.

The surface tension measurement using the Wilhelmy plate consists in measuring the force that is exerted on the plate due to wetting. Effectively, the Wilhelmy plate is a thin plate made of platinum with a wetting length of 40.20 mm. It is placed perpendicular to the liquid interface and attached to a microbalance via a thin metal wire. The plate was approached automatically to detect the surface contact (zero position), at which the measurement is performed. Two menisci are formed on both sides of the plate by capillary forces. The formed film exerts a force  $F$  on the plate, which is measured by a microbalance and used to calculate the surface tension  $\gamma$  using the Wilhelmy equation:

$$\gamma = \frac{F}{2l \cdot \cos\theta} \quad (2.1)$$

where  $l$  is the length of the plate and  $\theta$  is the wetting angle. The wetting angle of the Wilhelmy plate is usually considered to be  $0^\circ$ , since complete wetting is assumed. This is ensured by dipping the plate 3 mm into the solution and returning it to the zero position (surface contact) before performing the measurement. Three values were measured of each sample. As described previously, surface tension decreases with increasing surfactant concentration. At a certain concentration, called  $CAC$ , surfactant molecules start to aggregate and form micelles or other types of aggregates. The surface tension usually does not decrease anymore above this concentration and a plateau is formed. As value for the  $CAC$  is therefore taken the point of intersection between the initial slope and the plateau.

### 2.7 DLS – Dynamic Light Scattering

Light can interact with particles with diameters between 0.6 nm a 6  $\mu\text{m}$ . This phenomenon is called light scattering. The light, after interaction with moving particles (due to Brownian motion) is normally scattered in all directions. A maximum scattering for spherical objects can be detected at an angle of 90 °C with respect to the incident light. The scattered light possesses a modified light frequency due to the Doppler effect and therefore dependent on the particles diffusion speed. Following the Stokes-Einstein equation, the diffusion coefficients  $D_T$  and the hydrodynamic radii of the particles are related as followed:

$$R_H = \frac{kT}{3\pi\eta D_T} \quad (2.2)$$

where  $k$  is the Boltzmann constant,  $T$  the absolute temperature and  $\eta$  the bulk viscosity in  $Pa \cdot s$ . The diffusion intensity depends on the number of particles in solution. Taking this fact into account, a statistic model can be applied and a size distribution of the particles can be determined.

Dynamic light scattering (DLS) was performed with a **Malvern Instrument Zetasizer Nano-ZS**, with a measurement range of 0.5 nm to 10  $\mu\text{m}$ . The source of light was a He-Ne laser with a wavelength of 633 nm. The temperature was regulated with a Peltier element with a precision of  $\pm 0.1$  °C. The measuring angle was 173°. The statistic model, that was applied to analyze the measured data, was the NNLS model (non-negative least square). This model allows to distinguish between different size populations. It has to be noted that light scattered by big objects are more intensive than the one scattered by small particles. Small particles are therefore more difficult to be detected. We chose the NNLS model for our experiments and applied it on all measurements in order to obtain comparable results.

Solvent (v/v)	Temperature in °C	Viscosity $\eta$ in cP	Refractive index $n_D$
FA	25	3.36	1.44
	30	2.94	1.44
	40	2.36	1.44
	50	1.97	1.44
	60	1.70	1.44
	70	1.60	1.44
	80	1.40	1.44
FA/H <sub>2</sub> O 90:10	50	1.76	1.43
	60	1.4	1.43
	70	1.2	1.43
FA/H <sub>2</sub> O 70:30	25	2.17	1.42
	30	1.93	1.42
	40	1.60	1.42
	45	1.46	1.42
	50	1.34	1.42
	60	1.2	1.42
FA/H <sub>2</sub> O 60:40	30	1.63	1.41
	40	1.35	1.41
	50	1.21	1.41
FA/H <sub>2</sub> O 50:50	25	1.60	1.40
	30	1.48	1.40
	40	1.23	1.40
	45	1.14	1.40
	50	1.05	1.40
FA/H <sub>2</sub> O 40:60	50	0.93	1.40
FA/H <sub>2</sub> O 30:70	25	1.28	1.39
	30	1.18	1.39
	40	0.98	1.38
	50	0.84	1.38
Glycerol/H <sub>2</sub> O 50:50	25	6.5	1.44
	30	5.6	1.44
	40	4.8	1.44
	45	3.0	1.44
	50	2.5	1.44

Table 2.1: Technical parameters applied for DLS measurements.<sup>144,145,157,158</sup>

## Experimental Part

---

The solutions were prepared in the same way as the samples for surface tension measurements but the solvents were carefully filtered beforehand to prevent dust contamination of the solutions. Samples that had to be heated were placed in quartz cells since it could not be excluded that the formamide might attack plastic cells. Measurements were performed at the same temperatures as for surface tension measurements. The technical parameter applied for the DLS measurements in non-aqueous solvents are listed in table 2.1.

### 2.8 TEM – Transmission Electron Microscopy

The transmission electron microscope (TEM) was a **JEOL JEM 1011** type operating at 100 kV. For the preparation of the samples, a carbon-film covered copper grid (Formvar<sup>®</sup>) was immersed in the sample solution at temperatures above the Krafft point and then in a contrast agent solution containing 2 wt% of sodium phosphotungstate and dried at temperatures between 25 and 30 °C before observation.

### 2.9 Optical Microscopy

The samples for optical microscopy were prepared on glass object holders and examined under polarized and non-polarized light. The microscope was an **Olympus BX 50**. In some cases the samples were heated with a small oven (type **Mettler Fp 82 HT “hot stage”**), enclosing the object holder. Pictures were taken with a **Canon EOS 20** digital camera. For preliminary examinations the contact method was applied. The compound was placed flatly on a glass slide and covered by a small cover slide. On one side of the slide was carefully added a small amount of the solvent (e.g. formamide, water, glycerol or a mixture), which penetrated the sample by capillarity forces. Using this method it was possible to produce a concentration gradient that would allow the



different mesophases of a lyotropic surfactant to form. In some cases the powdery product was placed on the glass holder and then melted by heating up on a heating plate in order to form a thin film which was immediately covered by a glass slide. The sample was then examined under the optical microscope.

### 2.10 Calculation of Partition coefficient $\log p$

Partition coefficients of the molecules were calculated with the software **AlogP** (VC-CLAB v2.1). This software uses a network of neurones in order to correlate structure and value of the partition coefficient. The calculation of  $\log p$  of ions in the absence of their counterion is also possible.



# 3

## Syntheses of the Catanionic Surfactants

### **3.1 Model Systems of the Alkylammonium Alkanoate Type**

Separate diethyl ether solutions of octanoic acid and octylamine were prepared and cooled down to 0 °C in an ice bath. Both solutions were mixed in equimolar amounts and stirred for a few minutes under cooling until precipitation occurred, depending on the chain lengths. The precipitate was filtered off and washed three times with a small quantity of ice-cold diethyl ether.<sup>26,27</sup>

## Experimental Part

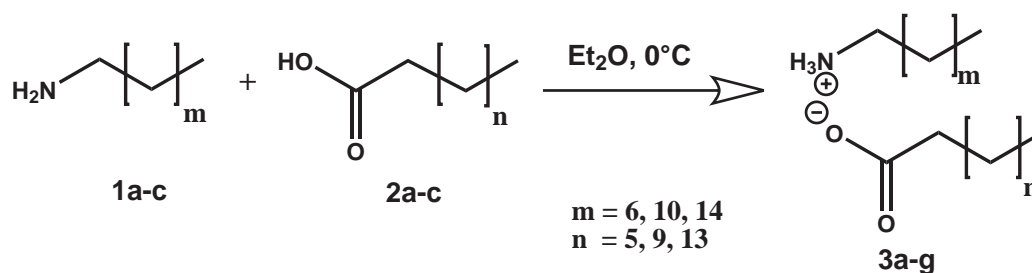
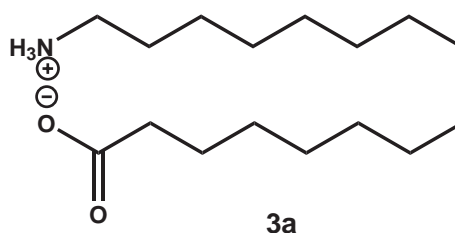


Figure 3.1: Scheme of the synthesis of the alkylammonium alcanoate model systems.

The colorless powder was dried under high vacuum to yield the cationic surfactants. In this way, seven different cationic surfactants with various number of carbon atoms in the hydrophilic chains were synthesized. The products were analyzed by NMR and FT-IR spectroscopy, as well as mass spectrometry. The values of the carboxylate peak and the exact mass of the cationic associations are listed together with the yields of the reactions in table 3.1.

Compound	HRMS (g.mol <sup>-1</sup> ) Na adduct found	HRMS (g.mol <sup>-1</sup> ) Na adduct calculated	Yield	FT-IR (KBr, cm <sup>-1</sup> ) COO <sup>-</sup>	Number of C
<b>3a</b> C <sub>8</sub> <sup>+</sup> /C <sub>8</sub> <sup>-</sup>	296.2943	296.2565	90 %	1548	16
<b>3b</b> C <sub>8</sub> <sup>+</sup> /C <sub>12</sub> <sup>-</sup>	352.2923	352.3191	92 %	1537	20
<b>3c</b> C <sub>12</sub> <sup>+</sup> /C <sub>8</sub> <sup>-</sup>	352.3765	352.3191	91 %	1503	20
<b>3d</b> C <sub>12</sub> <sup>+</sup> /C <sub>12</sub> <sup>-</sup>	408.3835	408.3818	79 %	1511	24
<b>3e</b> C <sub>8</sub> <sup>+</sup> /C <sub>16</sub> <sup>-</sup>	408.3610	408.3818	89 %	1514	24
<b>3f</b> C <sub>16</sub> <sup>+</sup> /C <sub>8</sub> <sup>-</sup>	408.3370	408.3818	84 %	1513	24
<b>3g</b> C <sub>16</sub> <sup>+</sup> /C <sub>16</sub> <sup>-</sup>	520.5148	520.5070	89 %	1511	32

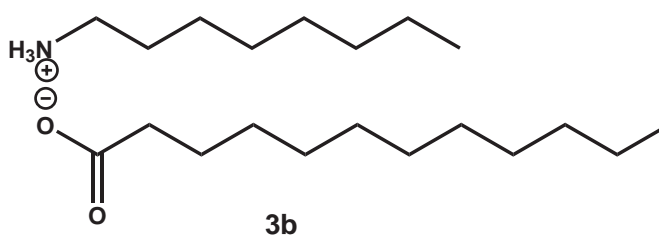
Table 3.1: Characterization of simple model systems.

$C_8^+/C_8^-$ 

 Figure 3.2:  $C_8^+/C_8^-$ 

$^1\text{H NMR}$  (300 MHz,  $\text{CDCl}_3$ ),  $\delta$  ppm: 8.19 (s, 3H,  $\text{NH}_3^+$ ), 2.73 (t, 2H,  $\text{CH}_2\text{NH}_3^+$ ,  $^3J_{\text{HH}}=7.5$ ), 2.09 (t, 2H,  $\text{CH}_2\text{COO}^-$ ,  $^3J_{\text{HH}}=7.5$ ), 1.59 (m, 2H,  $\text{CH}_2\text{CH}_2\text{NH}_3^+$ ), 1.50 (m, 2H,  $\text{CH}_2\text{CH}_2\text{COO}^-$ ), 1.24 (s, 18H, 9 $\text{CH}_2$ ), 0.84 (t, 6H, 2 $\text{CH}_3$ ,  $^3J_{\text{HH}}=7.5$ ).

$^{13}\text{C NMR}$  (75 MHz,  $\text{CDCl}_3$ ),  $\delta$  ppm: 181.4 ( $\text{COO}^-$ ), 39.5 (1C,  $\text{CH}_2\text{NH}_3^+$ ), 38.3 (1C,  $\text{CH}_2\text{COO}^-$ ), 31.8-22.6 (11C, 11 $\text{CH}_2$ ), 14.1 (2C, 2 $\text{CH}_3$ ).

**Elemental Analysis for  $\text{C}_{16}\text{H}_{35}\text{NO}_2$ :** Anal. calc.: C, 70.22; H, 12.90; N, 5.12; O, 11.78; Anal. found: C, 70.44; H, 13.15; N, 5.02; O, 11.39.

 $C_8^+/C_{12}^-$ 

 Figure 3.3:  $C_8^+/C_{12}^-$ 

$^1\text{H NMR}$  (300 MHz,  $\text{CDCl}_3$ ),  $\delta$  ppm: 8.19 (s, 3H,  $\text{NH}_3^+$ ), 2.74 (t, 2H,  $\text{CH}_2\text{NH}_3^+$ ,  $^3J_{\text{HH}}=7.5$ ), 2.10 (t, 2H,  $\text{CH}_2\text{COO}^-$ ,  $^3J_{\text{HH}}=7.5$ ), 1.60 (m, 2H,  $\text{CH}_2\text{CH}_2\text{NH}_3^+$ ), 1.50 (m, 2H,  $\text{CH}_2\text{CH}_2\text{COO}^-$ ), 1.23 (s, 26H, 13 $\text{CH}_2$ ), 0.85 (t, 6H, 2 $\text{CH}_3$ ,  $^3J_{\text{HH}}=6.0$ ).

## Experimental Part

---

$^{13}\text{C}$  NMR (75 MHz,  $\text{CDCl}_3$ ),  $\delta$  ppm: 181.7 ( $\text{COO}^-$ ), 39.8 (1C,  $\underline{\text{C}}\text{H}_2\text{NH}_3^+$ ), 38.6 (1C,  $\underline{\text{C}}\text{H}_2\text{COO}^-$ ), 32.1-23.0 (15C, 11 $\text{CH}_2$ ), 14.4 (2C, 2 $\text{CH}_3$ ).

**Elemental Analysis for  $\text{C}_{20}\text{H}_{43}\text{NO}_2$ :** Anal. calc.: C, 72.89; H, 13.15; N, 4.25; O, 9.71; Anal. found: C, 73.53; H, 12.88; N, 4.25; O, 9.29.

$\text{C}_{12}^+/\text{C}_8^-$

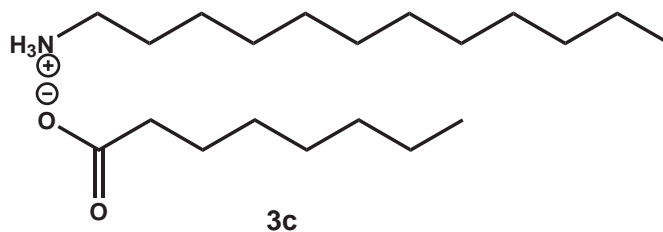
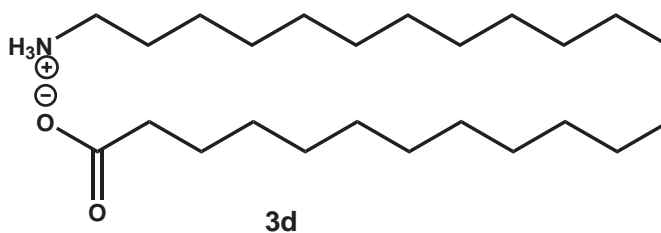


Figure 3.4:  $\text{C}_{12}^+/\text{C}_8^-$

$^1\text{H}$  NMR (300 MHz,  $\text{CDCl}_3$ ),  $\delta$  ppm: 7.34 (s, 3H,  $\text{NH}_3^+$ ), 2.75 (t, 2H,  $\underline{\text{C}}\text{H}_2\text{NH}_3^+$ ,  $^3J_{\text{HH}}=7.5$ ), 2.12 (t, 2H,  $\underline{\text{C}}\text{H}_2\text{COO}^-$ ,  $^3J_{\text{HH}}=7.5$ ), 1.57 (m, 4H,  $\underline{\text{C}}\text{H}_2\text{CH}_2\text{NH}_3^+$  and  $\underline{\text{C}}\text{H}_2\text{CH}_2\text{COO}^-$ ), 1.24 (s, 26H, 13 $\text{CH}_2$ ), 0.87 (t, 6H, 2 $\text{CH}_3$ ).

$^{13}\text{C}$  NMR (75 MHz,  $\text{CDCl}_3$ ),  $\delta$  ppm: 181.6 ( $\text{COO}^-$ ), 40.0 (1C,  $\underline{\text{C}}\text{H}_2\text{NH}_3^+$ ), 38.4 (1C,  $\underline{\text{C}}\text{H}_2\text{COO}^-$ ), 32.3-23.0 (15C, 15 $\text{CH}_2$ ), 14.6 (2C, 2 $\text{CH}_3$ ).

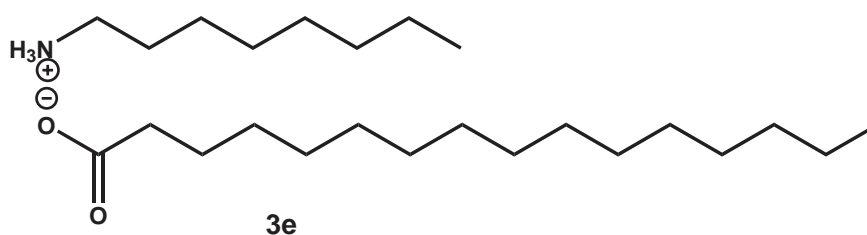
**Elemental Analysis for  $\text{C}_{20}\text{H}_{43}\text{NO}_2$ :** Anal. calc.: C, 72.89; H, 13.15; N, 4.25; O, 9.71; Anal. found: C, 73.38; H, 13.37; N, 4.06; O, 9.19.

$C_{12}^+/C_{12}^-$ Figure 3.5:  $C_{12}^+/C_{12}^-$ 

$^1\text{H NMR}$  (300 MHz,  $\text{CDCl}_3$ ),  $\delta$  ppm: 8.18 (s, 3H,  $\text{NH}_3^+$ ), 2.74 (t, 2H,  $\text{CH}_2\text{NH}_3^+$ ,  $^3J_{\text{HH}}=7.5$ ), 2.10 (t, 2H,  $\text{CH}_2\text{COO}^-$ ,  $^3J_{\text{HH}}=7.5$ ), 1.60 (m, 2H,  $\text{CH}_2\text{CH}_2\text{NH}_3^+$ ), 1.51 (m, 2H,  $\text{CH}_2\text{CH}_2\text{COO}^-$ ), 1.23 (s, 34H, 17 $\text{CH}_2$ ), 0.86 (t, 6H, 2 $\text{CH}_3$ ,  $^3J_{\text{HH}}=6.0$ ).

$^{13}\text{C NMR}$  (75 MHz,  $\text{CDCl}_3$ ),  $\delta$  ppm: 181.3 ( $\text{COO}^-$ ), 39.5 (1C,  $\text{CH}_2\text{NH}_3^+$ ), 38.2 (1C,  $\text{CH}_2\text{COO}^-$ ), 32.0-22.7 (19C, 19 $\text{CH}_2$ ), 14.1 (2C, 2 $\text{CH}_3$ ).

**Elemental Analysis for  $\text{C}_{24}\text{H}_{51}\text{NO}_2$ :** Anal. calc.: C, 74.68; H, 13.33; N, 3.63; O, 8.36; Anal. found: C, 74.83; H, 13.16; N, 3.64; O, 8.37.

 $C_8^+/C_{16}^-$ Figure 3.6:  $C_8^+/C_{16}^-$ 

$^1\text{H NMR}$  (300 MHz,  $\text{CDCl}_3$ ),  $\delta$  ppm: 7.70 (s, 3H,  $\text{NH}_3^+$ ), 2.75 (t, 2H,  $\text{CH}_2\text{NH}_3^+$ ,  $^3J_{\text{HH}}=7.5$ ), 2.12 (t, 2H,  $\text{CH}_2\text{COO}^-$ ,  $^3J_{\text{HH}}=7.5$ ), 1.60 (m, 2H,  $\text{CH}_2\text{CH}_2\text{NH}_3^+$ ), 1.52 (m, 2H,  $\text{CH}_2\text{CH}_2\text{COO}^-$ ), 1.24 (s, 34H, 17 $\text{CH}_2$ ), 0.87 (t, 6H, 2 $\text{CH}_3$ ,  $^3J_{\text{HH}}=7.5$ ).

## Experimental Part

---

$^{13}\text{C}$  NMR (75 MHz,  $\text{CDCl}_3$ ),  $\delta$  ppm: 181.6 ( $\text{COO}^-$ ), 39.9 (1C,  $\underline{\text{C}}\text{H}_2\text{NH}_3^+$ ), 38.4 (1C,  $\underline{\text{C}}\text{H}_2\text{COO}^-$ ), 32.3-23.0 (19C, 19 $\text{CH}_2$ ), 14.4 (2C, 2 $\text{CH}_3$ ).

**Elemental Analysis for  $\text{C}_{24}\text{H}_{51}\text{NO}_2$ :** Anal. calc.: C, 74.74; H, 13.39; N, 3.63; O, 8.51; Anal. found: C, 74.81; H, 13.25; N, 3.53; O, 8.41.

$\text{C}_{16}^+/\text{C}_8^-$

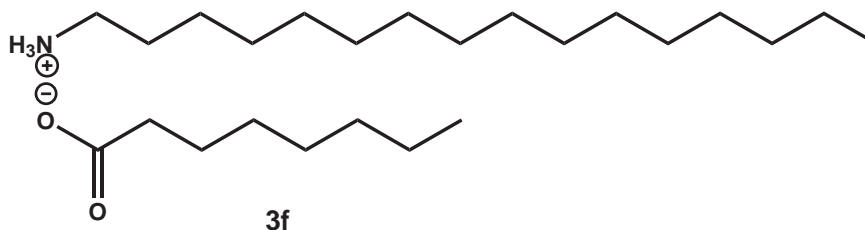


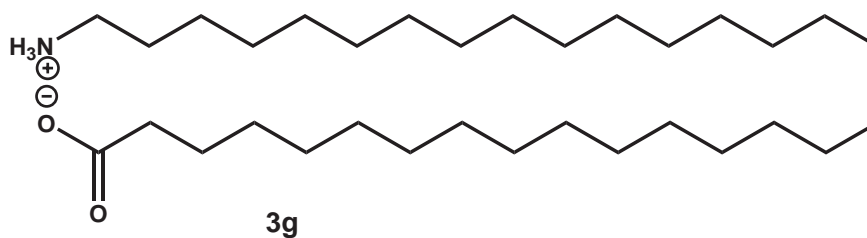
Figure 3.7:  $\text{C}_{16}^+/\text{C}_8^-$

$^1\text{H}$  NMR (300 MHz,  $\text{CD}_3\text{OD}/\text{CDCl}_3$  50:50 v/v, locked on  $\text{CD}_3\text{OD}$ ),  $\delta$  ppm: 2.85 (t, 2H,  $\underline{\text{C}}\text{H}_2\text{NH}_3^+$ ,  $^3J_{\text{HH}}=7.5$ ), 2.17 (t, 2H,  $\underline{\text{C}}\text{H}_2\text{COO}^-$ ,  $^3J_{\text{HH}}=7.5$ ), 1.61 (m, 4H,  $\underline{\text{C}}\text{H}_2\text{CH}_2\text{NH}_3^+$  and  $\underline{\text{C}}\text{H}_2\text{CH}_2\text{COO}^-$ ), 1.30 (m, 34H, 17 $\text{CH}_2$ ), 0.91 (t, 6H, 2 $\text{CH}_3$ ).

$^{13}\text{C}$  NMR (75 MHz,  $\text{CD}_3\text{OD}/\text{CDCl}_3$  50:50 v/v, locked on  $\text{CD}_3\text{OD}$ ),  $\delta$  ppm: 181.6 ( $\text{COO}^-$ ), 39.3 (1C,  $\underline{\text{C}}\text{H}_2\text{NH}_3^+$ ), 37.7 (1C,  $\underline{\text{C}}\text{H}_2\text{COO}^-$ ), 31.6-22.3 (19C, 19 $\text{CH}_2$ ), 14.5-14.4 (2C, 2 $\text{CH}_3$ ).

**Elemental Analysis for  $\text{C}_{24}\text{H}_{51}\text{NO}_2$ :** Anal. calc.: C, 74.74; H, 13.39; N, 3.63; O, 8.51; Anal. found: C, 74.93; H, 13.63; N, 3.43; O, 8.01.



$C_{16}^+/C_{16}^-$ Figure 3.8:  $C_{16}^+/C_{16}^-$ 

**$^1\text{H}$  NMR** (300 MHz,  $\text{CDCl}_3/\text{CD}_3\text{OD}$  70:30 v/v, locked on  $\text{CD}_3\text{CD}$ ),  $\delta$  ppm: 2.97 (t, 2H,  $\underline{\text{C}}\text{H}_2\text{NH}_3^+$ ,  $^3J_{\text{HH}}=7.5$ ), 2.32 (t, 2H,  $\underline{\text{C}}\text{H}_2\text{COO}^-$ ,  $^3J_{\text{HH}}=7.5$ ), 1.75 (m, 4H,  $\underline{\text{C}}\text{H}_2\text{CH}_2\text{NH}_3^+$  and  $\underline{\text{C}}\text{H}_2\text{CH}_2\text{COO}^-$ ), 1.40 (s, 50H, 25 $\text{CH}_2$ ), 1.02 (t, 6H, 2 $\text{CH}_3$ ,  $^3J_{\text{HH}}=6.0$ ).

**$^{13}\text{C}$  NMR** (75 MHz,  $\text{CDCl}_3/\text{CD}_3\text{OD}$  70:30 v/v, locked on  $\text{CD}_3\text{CD}$ ),  $\delta$  ppm: 181.7 ( $\text{COO}^-$ ), 39.6 (1C,  $\underline{\text{C}}\text{H}_2\text{NH}_3^+$ ), 37.7 (1C,  $\underline{\text{C}}\text{H}_2\text{COO}^-$ ), 31.9-22.6 (27C, 27 $\text{CH}_2$ ), 14.0 (2C, 2 $\text{CH}_3$ ).

**Elemental Analysis for  $\text{C}_{32}\text{H}_{67}\text{NO}_2$ :** Anal. calc.: C, 77.13; H, 13.56; N, 2.81; O, 6.50; Anal. found: C, 77.63; H, 13.84; N, 2.76; O, 5.77.

### 3.2 Synthesis of *N*-amino-1-deoxy-D-glucitol G-Hyd<sub>m</sub>

#### G-Hyd<sub>8</sub>

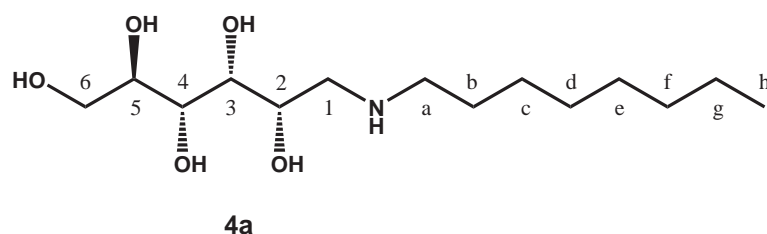


Figure 3.9: G-Hyd<sub>8</sub>

Glucose (5.0 g, 27.8 mmol) was placed in a round bottom flask and dissolved in 50 mL methanol. Octylamine (3.60 g, 27.8 mmol, 1.0 equiv.) was added and the solution was stirred for 24 h at room temperature and then heated for 30 min at 60 °C. 1.07 g sodium borohydride (30 mmol, 1.2 equiv.) were added in portions at 0 °C to the previously formed imine.

After the addition, the solution was stirred for another 24 h at room temperature and then heated for 30 min at 60 °C. The mixture was then cooled down in an ice-bath, and a concentrated HCl solution was added dropwise until a pH of 2-3 was reached and a white precipitate appeared. A bit of the solvent was evaporated carefully in order to eliminate the highly volatile methyl borates formed. Then the white solid was filtered and washed with a small amount of ice-cold ethanol and icy-water. The dried product was taken up into a round bottom flask and stirred overnight with a slight excess (compared to the weighed crude product) of sodium hydroxide in 25 mL methanol. The vacuum dried free amine was then washed with a small amount of ice-cold ethanol and ice-cold water. The white product was dried under high vacuum. Two recrystallizations from ethanol were performed in order to eliminate the remaining

glucose, amine and imine, and gave the pure *N*-octylamino-1-deoxy-D-glucitol as a white powder.<sup>131</sup>

**Yield: 40%**

<sup>1</sup>H NMR (300 MHz, CD<sub>3</sub>OD),  $\delta$  ppm: 3.90-3.60 (m, 6H, H-2, H-3, H-4, H-5, H-6a, H-6b), 2.74 (m, 2H, H-1), 2.60 (m, 2H, H-a), 1.52 (t, 2H, H-b, <sup>3</sup>J<sub>HH</sub>=6.0), 1.31 (s, 10H, H-c to H-g), 0.90 (t, 3H, H-h, <sup>3</sup>J<sub>HH</sub>=7.5).

<sup>13</sup>C NMR (75 MHz, CD<sub>3</sub>OD),  $\delta$  ppm: 71.4-71.2 (4C, C-2 to C-5), 63.5 (1C, C-6), 51.0 (1C, C-1), 49.5 (1C, C-a), 31.7-22.4 (6C, C-b to C-g), 13.6 (1C, C-h).

**Mass spectrometry** (ESI/positive mode): m/z 294.4 [M+H]<sup>+</sup>

**Elemental Analysis for C<sub>14</sub>H<sub>31</sub>NO<sub>5</sub>:** Anal. calc.: C, 57.31; H, 10.65; N, 4.77; O, 27.27; Anal. found: C, 57.17; H, 10.51; N, 4.86; O, 27.35, B < 50 ppm, Na < 100 ppm.

### G-Hyd<sub>12</sub>

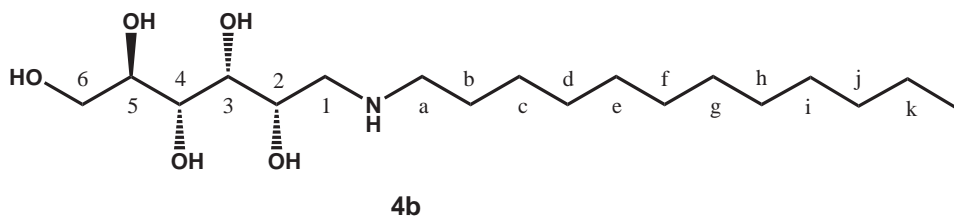


Figure 3.10: G-Hyd<sub>12</sub>

A protocol identical to the one used for the synthesis of G-Hyd<sub>8</sub> was performed. 5.00 g (27.8 mmol) of glucose and 5.14 g (27.8 mmol) of dodecylamine were weighed for this synthesis. The product was a very hydrophobic white solid.

**Yield: 50%**

<sup>1</sup>H NMR (300 MHz, CD<sub>3</sub>OD),  $\delta$  ppm: 3.90-3.62 (m, 6H, H-2, H-3, H-4, H-5, H-6a,

## Experimental Part

---

H-6b), 2.76 (m, 2H, H-1), 2.62 (m, 2H, H-a), 1.53 (t, 2H, H-b), 1.30 (s, 18H, H-c to H-k), 0.91 (t, 3H, H-l,  $^3J_{\text{HH}}=7.5$ ).

$^{13}\text{C}$  NMR (75 MHz,  $\text{CD}_3\text{OD}$ ),  $\delta$  ppm: 71.4-71.2 (4C, C-2 to C-5), 63.5 (1C, C-6), 51.0 (1C, C-1), 49.5 (1C, C-a), 31.7-22.4 (10C, C-b to C-k), 13.6 (1C, C-l).

**Mass spectroscopy** (ESI/positive mode):  $m/z$  350.4  $[\text{M}+\text{H}]^+$

**Elemental Analysis for  $\text{C}_{18}\text{H}_{39}\text{NO}_5$** : Anal. calc.: C, 61.86; H, 11.25; N, 4.01; O, 22.89; Anal. found: C, 61.64; H, 11.42; N, 3.87; O, 22.79.

### G-Hyd<sub>16</sub>

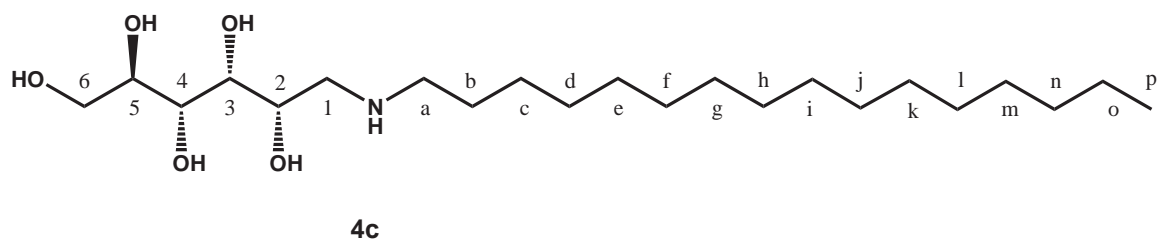


Figure 3.11: G-Hyd<sub>16</sub>

A protocol identical to the one used for the synthesis of G-Hyd<sub>8</sub> was performed. 5.00 g (27.8 mmol) of glucose and 6.70 g (27.8 mmol) of hexadecylamine were weighed for this synthesis. The product was a very hydrophobic white solid.

**Yield: 50%**

$^1\text{H}$  NMR (300 MHz,  $\text{CD}_3\text{OD}$ ),  $\delta$  ppm: 3.93-3.62 (m, 6H, H-2, H-3, H-4, H-5, H-6a, H-6b), 2.79 (m, 2H, H-1), 2.70-2.60 (m, 2H, H-a), 1.56 (t, 2H, H-b), 1.30 (s, 26H, H-c to H-o), 0.92 (t, 3H, H-p).

$^{13}\text{C}$  NMR (75 MHz,  $\text{CD}_3\text{OD}$ ),  $\delta$  ppm: 71.5-71.2 (4C, C-2 to C-5), 63.5 (1C, C-6), 51.2 (1C, C-1), 49.5 (1C, C-a), 31.9-22.4 (14C, C-b to C-o), 13.2 (1C, C-p).

**Mass spectroscopy** (ESI/positive mode): 406.6  $[\text{M}+\text{H}]^+$ .

**Elemental Analysis for C<sub>22</sub>H<sub>47</sub>NO<sub>5</sub>:** Anal. calc.: C, 65.14; H, 11.68; N, 3.45; O, 19.72; Anal. found: C, 65.21; H, 11.45; N, 3.42; O, 19.53; B, 0.16; Na, 0.15.

### 3.3 Synthesis of Catanionic Associations of the G-Hyd<sub>m</sub><sup>+</sup>/C<sub>n</sub><sup>-</sup> Type

The catanionic associations of the G-Hyd<sub>m</sub><sup>+</sup>/C<sub>n</sub><sup>-</sup> type were synthesized by a simple acid-base reaction. Equimolar quantities of the glucitol derivative (G-Hyd<sub>8</sub>, G-Hyd<sub>12</sub> or G-Hyd<sub>16</sub>) and of the fatty acid (C8, C12, C16, C18) were stirred in adequate volumes of water at room temperature for two days. The final compound was isolated by freeze-drying to give a colorless powder in quantitative yield.

#### G-Hyd<sub>8</sub><sup>+</sup>/C<sub>12</sub><sup>-</sup>

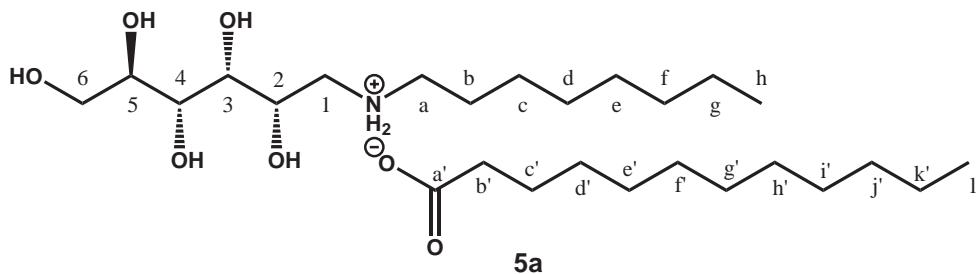


Figure 3.12: G-Hyd<sub>8</sub><sup>+</sup>/C<sub>12</sub><sup>-</sup>

1.00 g (3.4 mmol) of G-Hyd<sub>8</sub> and 0.68 g (3.4 mmol) of dodecanoic acid were stirred in 50 mL water. The white powdery product was obtained after freeze-drying in quantitative yield.

<sup>1</sup>H NMR (300 MHz, CD<sub>3</sub>OD),  $\delta$  ppm: 4.07 (m, 1H, H-2), 3.85-3.63 (m, 5H, H-3, H-4, H-5, H-6a, H-6b), 3.18 (m, 2H, H-1), 3.02 (m, 2H, H-a), 2.20 (t, 2H, H-b'), 1.71 (t, 2H, H-c'), 1.59 (t, 2H, H-b), 1.29 (s, 26H, H-c to H-g, H-d' to H-k'), 0.89 (t, 6H, H-h, H-l').

## Experimental Part

---

$^{13}\text{C}$  NMR (75 MHz,  $\text{CD}_3\text{OD}$ ),  $\delta$  ppm: 181.4 (1C, C-a'), 71.5 (1C, C-2), 70.9 (1C, C-5), 70.7 (1C, C-4), 68.6 (1C, C-3), 63.3 (1-C, C-6), 49.7 (1C, C-1), 37.5 (2C, C-a, C-b'), 31.7-31.5 (2C, C-b, C-c'), 29.5-22.4 (13C, C-c to C-g, C-d' to C-k'), 13.0 (2C, C-h, C-l').

**FT-IR** (KBr):  $1561\text{ cm}^{-1}$  ( $\text{COO}^-$ ).

**Elemental Analysis for  $\text{C}_{26}\text{H}_{55}\text{NO}_7$** : Anal. calc.: C, 63.25; H, 11.23; N, 2.84; O, 22.68; Anal. found: C, 62.34; H, 11.34; N, 2.76; O, 23.63.

### G-Hyd $_{12}^+$ /C $_8^-$

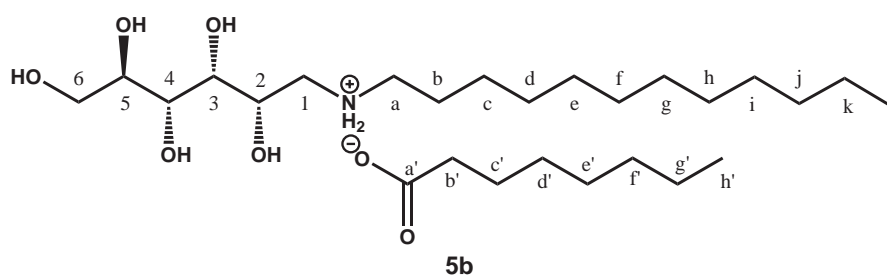


Figure 3.13: G-Hyd $_{12}^+$ /C $_8^-$

1.00 g (2.9 mmol) of G-Hyd $_{12}$  and 0.41 g (2.9 mmol) of octanoic acid were stirred in 50 mL of water. The white powdery product was obtained after freeze-drying in quantitative yield.

$^1\text{H}$  NMR (300 MHz,  $\text{CD}_3\text{OD}$ ),  $\delta$  ppm: 4.12-4.06 (m, 1H, H-2), 3.88-3.66 (m, 5H, H-3, H-4, H-5, H-6a, H-6b), 3.19 (m, 2H, H-1), 3.01 (m, 2H, H-a), 2.20 (t, 2H, H-b',  $^3J_{\text{HH}}=7.5$ ), 1.73 (m, 2H, H-b), 1.63 (m, 2H, H-c'), 1.33 (s, 26H, H-c to H-k, H-d' to H-g'), 0.94 (t, 6H, H-l, H-h',  $^3J_{\text{HH}}=6.0$ ).

$^{13}\text{C}$  NMR (75 MHz,  $\text{CD}_3\text{OD}$ ),  $\delta$  ppm: 181.1 (1C, C-a'), 71.5 (1C, C-2), 70.8-70.7 (2C, C-4, C-5), 68.5 (1C, C-3), 63.3 (1-C, C-6), 49.6 (1C, C-1), 37.3 (2C, C-a, C-b'),

31.7-31.6 (2C, C-b, C-c'), 29.4-22.4 (13C, C-c to C-k, C-d' to C-g'), 13.1 (2C, C-l, C-h').

**FT-IR** (KBr): 1564  $\text{cm}^{-1}$  ( $\text{COO}^-$ ).

**Elemental Analysis for  $\text{C}_{26}\text{H}_{55}\text{NO}_7$** : Anal. calc.: C, 63.25; H, 11.23; N, 2.84; O, 22.68; Anal. found: C, 61.97; H, 11.51; N, 2.86; O, 22.26.

## Experimental Part

---

### G-Hyd<sub>8</sub><sup>+</sup>/C<sub>16</sub><sup>-</sup>

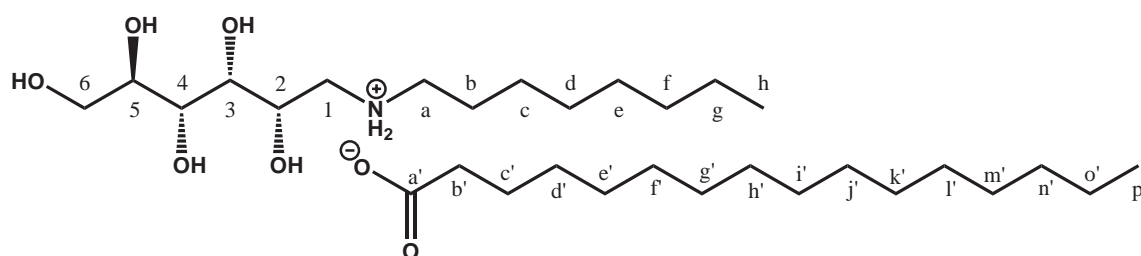


Figure 3.14: G-Hyd<sub>8</sub><sup>+</sup>/C<sub>16</sub><sup>-</sup>

1.00 g (3.4 mmol) of G-Hyd<sub>8</sub> and 0.87 g (3.4 mmol) of hexadecanoic acid were stirred in 50 mL of water. The white powdery product was obtained after freeze-drying in quantitative yield.

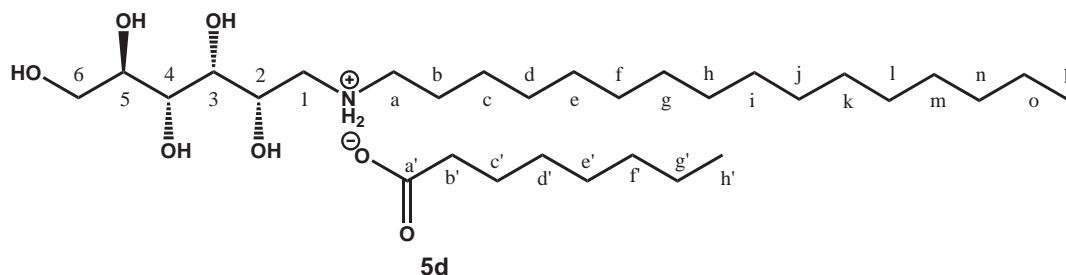
<sup>1</sup>H NMR (300 MHz, CD<sub>3</sub>OD),  $\delta$  ppm: 4.11-4.05 (m, 1H, H-2), 3.86-3.64 (m, 5H, H-3, H-4, H-5, H-6a, H-6b), 3.14 (m, 2H, H-1), 3.00 (m, 2H, H-a), 2.18 (t, 2H, H-b'), 1.72 (m, 2H, H-c'), 1.61 (t, 2H, H-b), 1.31 (s, 34H, H-c to H-g, H-d' to H-o'), 0.92 (t, 6H, H-h, H-p').

<sup>13</sup>C NMR (75 MHz, CD<sub>3</sub>OD),  $\delta$  ppm: 181.3 (1C, C-a'), 71.4 (1C, C-2), 70.8 (1C, C-5), 70.6 (1C, C-4), 68.5 (1C, C-3), 63.2 (1C, C-6), 49.6 (1C, C-1), 37.5 (2C, C-a, C-b'), 31.6-31.5 (2C, C-b, C-c'), 29.3-22.3 (17C, C-c to C-g, C-d' to C-o'), 13.0 (2C, C-h, C-p').

**FT-IR** (KBr): 1561 cm<sup>-1</sup> (COO<sup>-</sup>).

**Elemental Analysis for C<sub>30</sub>H<sub>63</sub>NO<sub>7</sub>**: not done



G-Hyd<sub>16</sub><sup>+</sup>/C<sub>8</sub><sup>-</sup>Figure 3.15: G-Hyd<sub>16</sub><sup>+</sup>/C<sub>8</sub><sup>-</sup>

1.00 g (2.5 mmol) of G-Hyd<sub>16</sub> and 0.35 g (2.5 mmol) of octanoic acid were stirred in 100 mL of water. The white powdery product was obtained after freeze-drying in quantitative yield.

<sup>1</sup>H NMR (300 MHz, CD<sub>3</sub>OD),  $\delta$  ppm: 4.09-4.04 (m, 1H, H-2), 3.87-3.65 (m, 5H, H-3, H-4, H-5, H-6a, H-6b), 3.17 (m, 2H, H-1), 2.99 (m, 2H, H-a), 2.20 (t, 2H, H-b', <sup>3</sup>J<sub>HH</sub>=7.5), 1.71 (m, 2H, H-b), 1.63 (m, 2H, H-c'), 1.32 (s, 34H, H-c to H-o, H-d' to H-g'), 0.93 (t, 6H, H-p and H-h', <sup>3</sup>J<sub>HH</sub>=6.0).

<sup>13</sup>C NMR (75 MHz, CD<sub>3</sub>OD),  $\delta$  ppm: 181.3 (1C, C-a'), 71.4 (1C, C-2), 70.6-70.6 (2C, C-4, C-5), 68.4 (1C, C-3), 63.0 (1C, C-6), 49.1 (1C, C-1), 37.1 (2C, C-a, C-b'), 31.5-31.4 (2C, C-b, C-c'), 29.3-22.3 (17C, C-c to C-o, C-d' to C-g'), 12.9 (2C, C-p, C-h').

FT-IR (KBr): 1563 cm<sup>-1</sup> (COO<sup>-</sup>).

Elemental Analysis for C<sub>30</sub>H<sub>63</sub>NO<sub>7</sub>: Anal. calc.: C, 65.53; H, 11.55; N, 2.55; O, 20.37; Anal. found: C, 63.33; H, 11.44; N, 2.53; O, 20.85.

## Experimental Part

---

### G-Hyd<sub>16</sub><sup>+</sup>/C<sub>12</sub><sup>-</sup>

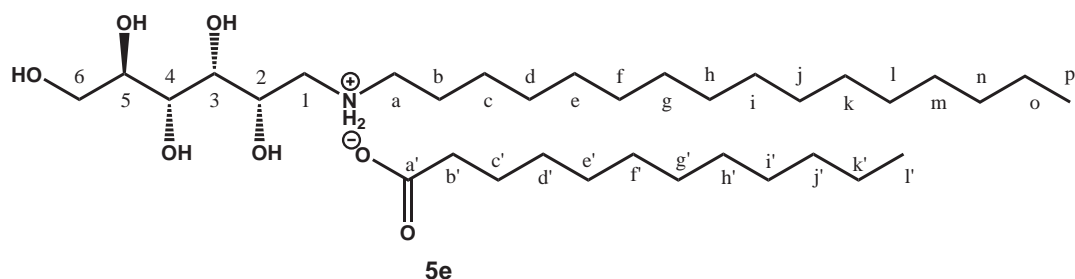


Figure 3.16: G-Hyd<sub>16</sub><sup>+</sup>/C<sub>12</sub><sup>-</sup>

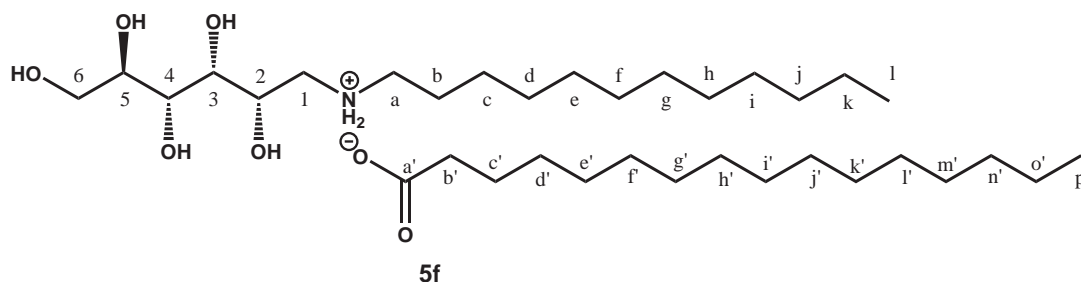
1.00 g (2.5 mmol) of G-Hyd<sub>16</sub> and 0.49 g (2.5 mmol) of dodecanoic acid were stirred in 100 mL of water. The white powdery product was obtained after freeze-drying in quantitative yield.

<sup>1</sup>H NMR (300 MHz, CDCl<sub>3</sub>/(CD<sub>3</sub>)<sub>2</sub>CO 50:50 v/v, locked on (CD<sub>3</sub>)<sub>2</sub>CO),  $\delta$  ppm: 4.02 (m, 1H, H-2), 3.81-3.66 (m, 5H, H-3, H-4, H-5, H-6a, H-6b), 3.02 (d, 2H, H-1), 2.84 (m, 2H, H-a), 2.22 (t, 2H, H-b'), 1.62 (m, 4H, H-b and H-c'), 1.27 (s, 42H, H-c to H-o, H-d' to H-k'), 0.88 (t, 6H, H-p, H-l').

<sup>13</sup>C NMR (300 MHz, CDCl<sub>3</sub>/(CD<sub>3</sub>)<sub>2</sub>CO 50:50 v/v, locked on (CD<sub>3</sub>)<sub>2</sub>CO),  $\delta$  ppm: 181.3 (1C, C-a'), 71.4 (1C, C-2), 70.6-70.6 (2C, C-4, C-5), 68.4 (1C, C-3), 63.0 (1C, C-6), 49.1 (1C, C-1), 37.1 (2C, C-a, C-b'), 31.5-31.4 (2C, C-b, C-c'), 29.3-22.3 (21C, C-c to C-o, C-d' to C-k'), 12.9 (2C, C-p, C-l').

**FT-IR** (KBr): 1526 cm<sup>-1</sup> (COO<sup>-</sup>).

**Elemental Analysis for C<sub>34</sub>H<sub>71</sub>NO<sub>7</sub>**: Anal. calc.: C, 67.39; H, 11.81; N, 2.31; O, 18.48; Anal. found: C, 66.99; H, 11.95; N, 2.25; O, 18.88.

G-Hyd<sub>12</sub><sup>+</sup>/C<sub>16</sub><sup>-</sup>Figure 3.17: G-Hyd<sub>12</sub><sup>+</sup>/C<sub>16</sub><sup>-</sup>

1.00 g (2.9 mmol) of G-Hyd<sub>12</sub> and 0.73 g (2.9 mmol) of hexadecanoic acid were stirred in 100 mL of water. The white powdery product was obtained after freeze-drying in quantitative yield.

<sup>1</sup>H NMR (300 MHz, CD<sub>3</sub>OD/CDCl<sub>3</sub> 50:50 v/v, locked on CD<sub>3</sub>OD),  $\delta$  ppm: 4.05 (m, 1H, H-2), 3.82-3.67 (m, 5H, H-3, H-4, H-5, H-6a, H-6b), 3.06 (m, 2H, H-1), 2.81-2.75 (t, 2H, H-a), 2.20 (t, 2H, H-b', <sup>3</sup>J<sub>HH</sub>=7.5), 1.66-1.57 (m, 4H, H-b, H-c'), 1.27 (s, 42H, H-c to H-k, H-d' to H-o'), 0.89 (t, 6H, H-l, H-p').

<sup>13</sup>C NMR (75 MHz, CD<sub>3</sub>OD/CDCl<sub>3</sub> 50:50 v/v, locked on CD<sub>3</sub>OD),  $\delta$  ppm: 181.2 (1C, C-a'), 77.3 (1C, C-5), 72.0-69.0 (3C, C-2, C-3, C-4), 63.6 (1C, C-6), 50.3 (1C, C-1), 37.2 (1C, C-a, C-b'), 31.8 (1C, C-b, C-c'), 29.5-22.5 (21C, C-c to C-k, C-d' to C-o'), 14.2 (2C, C-l, C-p').

**FT-IR** (KBr): 1555 cm<sup>-1</sup> (COO<sup>-</sup>).

**Elemental Analysis for C<sub>34</sub>H<sub>71</sub>NO<sub>7</sub>**: Anal. calc.: C, 67.39; H, 11.81; N, 2.31; O, 18.48; Anal. found: C, 67.56; H, 12.02; N, 2.06; O, 18.36.

## Experimental Part

---

### G-Hyd<sub>12</sub><sup>+</sup>/C<sub>18</sub><sup>-</sup>

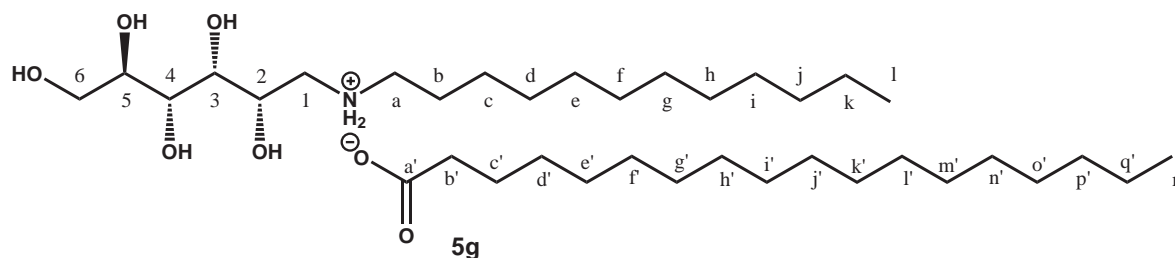


Figure 3.18: G-Hyd<sub>12</sub><sup>+</sup>/C<sub>18</sub><sup>-</sup>

1.00 g (2.9 mmol) of G-Hyd<sub>12</sub> and 0.81 g (2.9 mmol) of octadecanoic acid were stirred in 150 mL of water. The white powdery product was obtained after freeze-drying in quantitative yield.

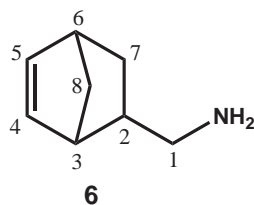
<sup>1</sup>H NMR (300 MHz, CDCl<sub>3</sub>),  $\delta$  ppm: 3.96 (m, 1H, H-2), 3.73-3.58 (m, 5H, H-3, H-4, H-5, H-6a, H-6b), 2.97-2.95 (m, 2H, H-1), 2.81-2.75 (t, 2H, H-a), 2.14-2.09 (t, 2H, H-b'), 1.57-1.48 (m, 4H, H-b, H-c'), 1.18 (s, 46H, H-c to H-k, H-d' to H-o'), 0.80 (t, 6H, H-l and H-r').

<sup>13</sup>C NMR (75 MHz, CDCl<sub>3</sub>),  $\delta$  ppm: 182.6 (1C, C-a'), 78.8 (1C, C-5), 73.0-70.5 (3C, C-2, C-3, C-4), 65.0 (1C, C-6), 51.7 (1C, C-1), 38.6 (2C, C-a, C-b'), 33.2 (2C, C-b, C-c'), 30.9-23.9 (23C, C-c to C-k, C-d' to C-q'), 15.0 (2C, C-l, C-r').

**FT-IR** (KBr): 1561 cm<sup>-1</sup> (COO<sup>-</sup>).

**Elemental Analysis for C<sub>26</sub>H<sub>55</sub>NO<sub>7</sub>**: Anal. calc.: C, 68.20; H, 11.92; N, 2.21; O, 17.67; Anal. found: C, 67.78; H, 12.09; N, 2.01; O, 18.12.

### 3.4 Synthesis of Bicyclo[2,2,1]hept-5-ene-2-methyleneamine (NbNH<sub>2</sub>)

Figure 3.19: NbNH<sub>2</sub>

A solution of 12 g (100 mmol) of bicyclo[2,2,1]hept-5-ene-2-carbonitrile (endo/exo ratio 60/40) in 80 mL sodium dried diethyl ether was added dropwise under stirring and under a gentle argon stream to a suspension of 6 g LiAlH<sub>4</sub> (160 mmol, 1.6 eq) in 50 mL dried diethyl ether. During the addition the temperature was kept below 15 °C with an ice-bath. After the addition, when the reaction mixture reached room temperature, the solution was stirred for 1.5 h under reflux. After cooling down to room temperature, 20 mL diethyl ether and 30 mL water were carefully added in order to hydrolyze the excess of LiAlH<sub>4</sub>. The temperature was maintained under 25 °C. A white precipitate appeared, which was filtered off. The ether solution was extracted three times with water. The organic phases were gathered and washed with brine and then dried over Na<sub>2</sub>SO<sub>4</sub>. After filtration, the solvent was evaporated under reduced pressure to give a yellowish oil. The crude oil was distilled under reduced pressure (13 mmHg, 55 °C) to yield the bicyclo[2,2,1]hept-5-ene-2-methyleneamine as a colorless oil without modifying the endo/exo ratio.

**Yield: 70%**

<sup>1</sup>H NMR (300 MHz, CDCl<sub>3</sub>)  $\delta$  ppm (n=endo, x=exo) : 6.09-5.86 (m, 2H, H<sub>n</sub>-4, H<sub>x</sub>-4, H<sub>n</sub>-5, H<sub>x</sub>-5), 2.83-2.28 (m, 3H, H<sub>x</sub>-1, H<sub>n</sub>-3, H<sub>x</sub>-3, H<sub>n</sub>-6, H<sub>x</sub>-6), 2.07-2.02 (t, 1H,

## Experimental Part

---

$H_n$ -1), 1.85-1.77 (m, 1H,  $H_n$ -7), 1.38-1.04 (m, 3H,  $H_x$ -2,  $H_x$ -7,  $H_n$ -8,  $H_x$ -8, H), 0.49-0.46 (ddd, 2H,  $H_n$ -2).

$^{13}\text{C}$  NMR (300 MHz,  $\text{CDCl}_3$ )  $\delta$  ppm: 137.6-136.56 ( $C_n$ -4,  $C_x$ -4), 131.9 ( $C_n$ -5,  $C_x$ -5), 49.5 ( $C_x$ -8), 47.8 ( $C_n$ -8), 46.4 ( $C_x$ -1), 45.0 ( $C_n$ -1), 44.0 ( $C_x$ -6), 43.5 ( $C_n$ -6), 43.0 ( $C_x$ -7), 42.5 ( $C_n$ -7), 42.3 ( $C_x$ -3), 41.6 ( $C_x$ -3), 31.1 ( $C_x$ -2), ( $C_n$ -2).

HRMS (CI ( $\text{NH}_3$ )/positive mode):  $m/z$  124.0  $[\text{M}+\text{H}]^+$ , 141.1  $[\text{M}+\text{NH}_3]^+$

### 3.5 Preparation of the Ion Pair NbC14 – Norbornene Methyleneammonium Tetradecanoate

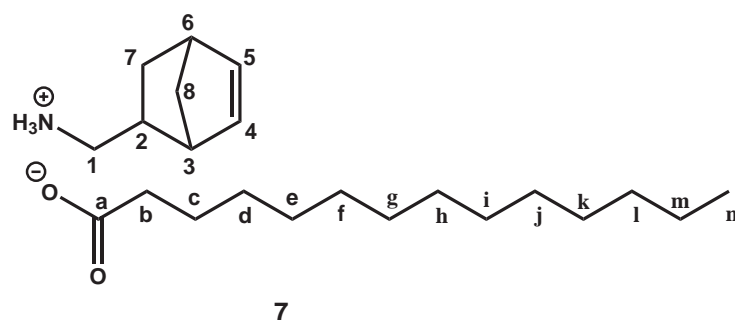


Figure 3.20: NbC14

At room temperature and under stirring, 742 mg (3.25 mmol) tetradecanoic acid solubilized in a minimum of hexane was added dropwise to a solution of 400 mg (3.25 mmol) bicyclo[2.2.1]hept-5-ene-2-methyleneamine (compound **6**) in 25 mL hexane. After 2 hours of stirring, the reaction mixture was placed for 12 hours at  $-18\text{ }^\circ\text{C}$  (freezer). The obtained precipitate was filtered over a n° 4 frit. The product was a colorless powder.

**Yield: 80%**

## Experimental Part

---

**$^1\text{H}$  NMR** (300 MHz,  $\text{CDCl}_3$ )  $\delta$  ppm ( $n=endo$ ,  $x=exo$ ): 7.94 (s, 3H,  $\text{NH}_3$ ), 6.18-6.15 (m, 1H,  $\text{H}_{n-5}$ ), 6.06 (m, 2H,  $\text{H}_{x-4}$  and  $\text{H}_{x-5}$ ), 5.99-5.97 (m, 1H,  $\text{H}_{n-4}$ ), 2.94 (m, 1H,  $\text{H}_{x-1}$ ), 2.90-2.82 (m, 1H,  $\text{H}_{n-1}$ ), 2.59-2.56 (m, 1H,  $\text{H}_{n-1}$ ), 2.40-2.37 (m, 1H,  $\text{H}_{n-3}$ ,  $\text{H}_{x-3}$ ), 2.21-2.16 (t, 3H, H-b), 2.00-1.91 (m, 1H,  $\text{H}_{x-2}$ ), 1.71-1.50 (m, 4H, H-c,  $\text{H}_{n-7}$ ,  $\text{H}_{n-8}$ ,  $\text{H}_{x-8}$ ), 1.30 (s, 22H, H-d to H-m), 0.93 (t, 3H, H-n), 0.62-0.60 (ddd, 2H,  $\text{H}_{n-2}$ ).

**$^{13}\text{C}$  NMR** (300 MHz,  $\text{CDCl}_3$ )  $\delta$  ppm ( $n=endo$ ,  $x=exo$ ): 181.1 (1C, C-a), 138.1 (1C,  $\text{C}_n-5$ ), 136.9 (1C,  $\text{C}_x-5$ ), 136.1 (1C,  $\text{C}_x-4$ ), 131.9 (1C,  $\text{C}_n-4$ ), 49.6 (1C,  $\text{C}_n-1$ ), 45.0 (1C,  $\text{C}_n-8$ ), 44.9 (1C,  $\text{C}_x-8$ ), 44.1 (2C,  $\text{C}_n-3$ ,  $\text{C}_n-3$ ), 43.6 ( $\text{C}_x-1$ ), 42.5 (1C,  $\text{C}_n-2$ ), 41.8 (1C,  $\text{C}_x-2$ ), 38.5 (1C,  $\text{C}_x-2$ ), 38.1 (1C,  $\text{C}_n-6$ ), 38.1 (1C, C-b), 31.9 (1C,  $\text{C}_x-7$ ), 31.1 (1C,  $\text{C}_n-7$ ), 30.4-22.7 (11C, C-c to C-m), 14.1 (1C, C-n)

**FT-IR** (KBr): 1521  $\text{cm}^{-1}$  ( $\text{COO}^-$ ).

**Elemental Analysis for  $\text{C}_{22}\text{H}_{41}\text{NO}_2$** : Anal. calc.: C, 75.16; H, 11.75; N, 3.98; Anal. found: C, 75.14; H, 11.80; N, 3.88.

### 3.6 Ion Pair CxC14 – Cyclohexylammonium Tetradecanoate

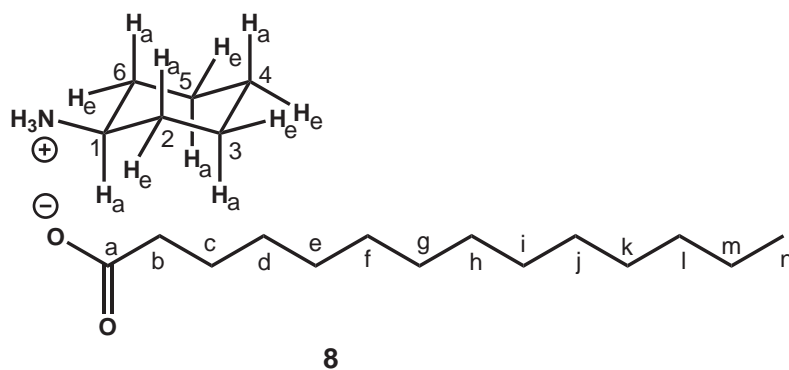


Figure 3.21: CxC14

CxC14 was synthesized by Bordes *et al.* following an optimized protocol. The product was stored in the freezer. For our experiments, the stored powder was freeze-dried before using. NMR spectrometry was performed in order to verify that no degradation has occurred.



# 4

## Additional Experiments

### 4.1 Influence of Sample Preparation

#### 4.1.1 Preparation of the Catanionic Associations

All physico-chemical experiments were performed with beforehand prepared catanionic associations, that is to say the catanionic surfactant was synthesized in water by an acid-base reaction and then isolated in pure form by freeze-drying (see chapter 3). The catanionic association was then dissolved in the desired solvent or solvent mixture in order to perform the physico-chemical studies, such as surface tension or

## Experimental Part

---

DLS measurements. It is also possible to directly prepare the catanionic association in a protic solvent such as formamide. For example, Friberg *et al.* performed their studies on catanionic associations directly in formamide.<sup>14</sup> We studied therefore the behavior of a catanionic system based upon glucose, which was formed in situ in formamide in order to compare it with our previous results.

Equimolar quantities of G-Hyd<sub>12</sub> and octanoic acid were weighed in vials with screwed caps and 20 mL of formamide were added. The samples were thermostatted at 50 °C. Friberg *et al.*<sup>14</sup> mentioned that non-aqueous systems needed longer times to equilibrate than aqueous systems. In our case, we obtained a homogeneous solution after one week. Surface tension measurements were performed using the Wilhelmy plate method at 50 °C. At the same temperature surface tension measurements of G-Hyd<sub>12</sub><sup>+</sup>/C<sub>8</sub><sup>-</sup> were performed, which was prepared in water and then isolated. Sample concentrations ranged from 10<sup>-5</sup> to 5.10<sup>-1</sup> mol.L<sup>-1</sup>, which were the identical concentrations used for the surface tension measurements of the beforehand isolated G-Hyd<sub>12</sub><sup>+</sup>/C<sub>8</sub><sup>-</sup> system.

### 4.1.2 Influence of the Solvent

For our physico-chemical studies in solvent mixtures, we mixed the solvents in the desired ratio prior to the preparation of the samples. This preparation method (A) provides a solvation of the surfactant by an already structured solvent/solvent mixture, in which molecules of both solvents can participate on the solvation process. Another possible preparation method (B) is to dissolve the catanionic association in a certain amount of one of the solvents and, to add the second solvent in order to obtain the desired ratio of solvents and concentration of surfactant. In this case, the surfactant is solvated by the first solvent. After addition of the second solvent, the bulk solution is mixed easily, whereas solvent molecules in the solvation sphere may be stronger

associated with the surfactant. The second solvent may not be able to interfere directly with the surfactant, that is to say the second solvent may not be able to replace some solvent molecules of the first solvent in the solvation sphere. In order to study the differences between the two preparation methods, we performed DLS measurements comparatively on surfactant solutions in water/FA mixtures that were prepared in two different ways. For this issue, we studied two G-Hyd<sub>m</sub><sup>+</sup>/C<sub>n</sub><sup>-</sup> type surfactants, which did not form vesicles in pure formamide. We dissolved G-Hyd<sub>8</sub><sup>+</sup>/C<sub>12</sub><sup>-</sup> and G-Hyd<sub>8</sub><sup>+</sup>/C<sub>16</sub><sup>-</sup> in pure formamide (1.0.10<sup>-1</sup> mol.L<sup>-1</sup>). By diluting this mother solutions with water, we prepared water/FA mixtures with 10, 20, 30, 40, 50, 60, 70, 80, 90 % water. It was ensured that the samples had concentrations above the *CMCs* determined beforehand by surface tension measurements. The mixtures were stirred for 30 minutes and then thermostatted for 1 day at 45 °C. The samples were analyzed by DLS in order to determine the formation of objects. Following table 4.1 shows the results obtained.

Solvent (v/v)	Concentration <i>mol.L</i> <sup>-1</sup>	Compound			
		<b>5a</b>		<b>5c</b>	
		Preparation		Preparation	
		A	B	A	B
FA	1.10 <sup>-1</sup>	no vesicles	no vesicles	no vesicles	no vesicles
FA/H <sub>2</sub> O 90:10	9.10 <sup>-2</sup>	no vesicles	no vesicles	no vesicles	no vesicles
FA/H <sub>2</sub> O 80:20	8.10 <sup>-2</sup>	no vesicles	no vesicles	no vesicles	no vesicles
FA/H <sub>2</sub> O 70:30	7.10 <sup>-2</sup>	no vesicles	no vesicles	vesicles	vesicles
FA/H <sub>2</sub> O 60:40	6.10 <sup>-2</sup>	no vesicles	no vesicles	vesicles	vesicles
FA/H <sub>2</sub> O 50:50	5.10 <sup>-2</sup>	vesicles	vesicles	vesicles	vesicles
FA/H <sub>2</sub> O 40:60	4.10 <sup>-2</sup>	vesicles	vesicles	vesicles	vesicles
FA/H <sub>2</sub> O 30:70	3.10 <sup>-2</sup>	vesicles	vesicles	vesicles	vesicles
FA/H <sub>2</sub> O 20:80	2.10 <sup>-2</sup>	vesicles	vesicles	vesicles	vesicles
FA/H <sub>2</sub> O 10:90	1.10 <sup>-2</sup>	vesicles	vesicles	vesicles	vesicles

(A) – Preparation of isolated compounds in beforehand mixed solvent mixtures.

(B) – Solvation of the compound in one solvent and admixing the second solvent.

Table 4.1: Results of the DLS measurements on compound **5a** and **5c** using different preparation methods for the solvent mixtures.

### 4.2 Salt Effect

Aqueous surfactant solutions can be influenced by electrolyte addition. Salt effects depend on the type of surfactant, but also of the type of salt.<sup>2</sup> It can be observed that the *CMC* of ionic surfactants (anionic and cationic) is influenced more significantly by electrolyte addition than the *CMC* of zwitterionic and nonionic surfactants. The *CMC* decrease with increasing salt concentration due to the decrease of the effective head-group area, which also decreases the electrostatic repulsion between the headgroups.<sup>2</sup> It was shown that salts with big anions ( $\text{PO}_4^{3-}$ ,  $\text{CO}_3^{2-}$ ) exerted higher influence on the *CMC* of SDS than small anions ( $\text{Cl}^-$ ).<sup>159</sup> In the case of nonionic surfactants, two major salt effects are known – salting-in and salting-out. These effects depend on the capacity of making or breaking the water structure.<sup>2</sup> Small ions that possess a large ionic charge/radius ratio such as  $\text{F}^-$  are highly hydrated and compete with the surfactant molecule for hydration water. As a consequence, the polar headgroups and the alkyl chains are less hydrated and electrostatic and hydrophobic interactions increase, leading to the precipitation of the surfactant. Moreover, the *CMC* of nonionic surfactants decrease.<sup>2</sup> The contrary behavior – salting-in – is induced by salts with structure breaking properties. In this case, the added salt liberates water molecules for surfactant hydration. Surfactant solubility and *CMC* increase. In surfactant/FA solutions, it was observed that salt additions lead to similar behaviors of nonionic surfactants in comparison to aqueous systems.<sup>99,129</sup> In our case, we wanted to test the influence of salt addition on the aggregation behavior of cationic surfactant in formamide. The experiments were performed with sodium iodide (NaI), since previous studies by Gautier et al.<sup>4</sup> on the salt effect on microemulsions in formamide showed that NaI is soluble up to  $1000 \text{ g.L}^{-1}$  in this solvent. We tested the effect of the formation or non-formation of vesicles in formamide with increasing NaI concentration. Four cationic systems of the type  $\text{G-Hyd}_m^+/C_n^-$  were tested, among which the two associations **5a**

(G-Hyd<sub>8</sub><sup>+</sup>/C<sub>12</sub><sup>-</sup>) and **5b** (G-Hyd<sub>12</sub><sup>+</sup>/C<sub>8</sub><sup>-</sup>) do not form vesicles in pure formamide, and the two associations **5f** (G-Hyd<sub>12</sub><sup>+</sup>/C<sub>16</sub><sup>-</sup>) and **5g** (G-Hyd<sub>12</sub><sup>+</sup>/C<sub>18</sub><sup>-</sup>) do form vesicles in pure formamide. Six equimolar samples of each series were prepared, among which one solution in pure formamide and five with NaI concentrations between  $1.10^{-5}$  mol.L<sup>-1</sup> and  $1.10^{-1}$  mol.L<sup>-1</sup>. The samples were tested by DLS in order to verify the formation or non-formation of objects in relation to the salt addition. The surfactant concentrations were depending on the chain lengths. The *CACs* of compounds **5a** and **5b** were measured at  $7.2.10^{-2}$  and  $8.0.10^{-2}$  mol.L<sup>-1</sup>, respectively. The sample concentrations were therefore fixed at  $1.10^{-1}$  mol.L<sup>-1</sup> for both compounds. For the compounds **5f** and **5g** a concentration of  $1.10^{-3}$  mol.L<sup>-1</sup> was chosen, which was above the estimated *CAC*. The solutions were prepared in the same way as solutions for surface tension or DLS measurements. Then they were thermostatted above the Krafft temperatures before analyzing by DLS at temperatures above the  $T_K$ .



---

## References

1. Evans, D. F.; Wennerstroem, H. *The Colloidal Domain: Where Physics, Chemistry, Biology, and Technology Meet*; Wiley-VCH: 2nd ed.; 1999.
2. Rosen, M. J. *Surfactants and Interfacial Phenomena*; Wiley and sons: New York: 3rd ed.; 2004.
3. Israelachvilli, J. N.; Mitchell, D. J.; Ninham, B. W. *J. Chem. Soc., Faraday Trans. 2* **1976**, *72*, 1525-1568.
4. Gautier, M.; Rico, I.; Ahmad-Zadeh Samii, A.; De Savignac, A.; Lattes, A. *J. Colloid Interface Sci.* **1986**, *112*, 484-487.
5. Gautier, M.; Rico, I.; Lattes, A. *J. Org. Chem.* **1990**, *55*, 1500-1503.
6. Lattes, A.; Rico, I. *Colloids Surf.* **1989**, *35*, 221-235.
7. Rico, I.; Lattes, A. *Nouv. J. Chim.* **1984**, *8*, 429-31.
8. Smith, G. D.; Donelan, C. E.; Barden, R. E. *J. Colloid Interface Sci.* **1997**, *60*, 488-496.
9. Angel, L. R.; Evans, D. F.; Ninham, B. W. *J. Phys. Chem.* **1983**, *87*, 538-540.
10. Daniellson, I.; Lindmann, B. *Colloids Surf.* **1981**, *3*, 381.
11. Friberg, S. E. *Colloids Surf.* **1982**, *4*, 201-201.
12. Santanna, V. C.; Curbelo, F. D. S.; Castro Dantas, T. N.; Dantas Neto, A. A.; Albuquerque, H. S.; Garnica, A. I. C. *J. Pet. Sci. Eng.* **2009**, *66*, 117-120.
13. Shah, D. O.; Schechter, R. S. *Improved Oil Recovery by Surfactant and Polymer Flooding*; Academic Press, New York: 1977.

## References

---

14. Friberg, S. E.; Sun, W. M.; Yang, Y.; Ward, A. J. I. *J. Colloid Interface Sci.* **1990**, *139*, 160-168.
15. Huang, J. B.; Zhu, B. Y.; Zhao, G. X.; Zhang, Z. Y. *Langmuir* **1997**, *13*, 5759-5761.
16. Huang, J. B.; Zhu, B. Y.; Mao, M.; He, P.; Wang, J.; He, X. *Colloid Polym. Sci.* **1999**, *277*, 354-360.
17. Blanzat, M.; Massip, S.; Speziale, V.; Perez, E.; Rico-Lattes, I. *Langmuir* **2001**, *17*, 3512-3514.
18. Douliez, J.-P.; Pontoire, B.; Gaillard, C. *ChemPhysChem* **2006**, *7*, 2071-2073.
19. Douliez, J.-P.; Gaillard, C.; Navailles, L.; Nallet, F. *Langmuir* **2006**, *22*, 2942-2945.
20. Douliez, J.-P. *J. Am. Chem. Soc.* **2005**, *127*, 15694-15695.
21. Douliez, J.-P.; Navailles, L.; Nallet, F. *Langmuir* **2006**, *22*, 622-627.
22. Zemb, T.; Dubois, M.; Deme, B.; Gulik-Krzywicki, T. *Science* **1999**, *283*, 816-819.
23. Dubois, M.; Deme, B.; Gulik-Krzywicki, T.; Dedieu, J. C.; Vautrin, C.; Desert, S.; Perez, E.; Zemb, T. *Nature* **2001**, *411*, 672-675.
24. Dubois, M.; Lizunov, V.; Meister, A.; Gulik-Krzywicki, T.; Verbavatz, J. M.; Perez, E.; Zimmerberg, J.; Zemb, T. *Proceedings of the National Academy of Sciences of the United States of America* **2004**, *101*, 15082-15087.
25. Khan, A.; Marques, E. *Specialist Surfactants*; London, 1997.
26. Jokela, P.; Joensson, B.; Khan, A. *J. Phys. Chem.* **1987**, *91*, 3291-3298.



- 
27. Jokela, P.; Joensson, B.; Eichmueller, B.; Fontell, K. *Langmuir* **1988**, *4*, 187-192.
28. Blanzat, M.; Perez, E.; Rico-Lattes, I.; Prome, D.; Prome, J.-C.; Lattes, A. *Langmuir* **1999**, *15*, 6163-6169.
29. Blanzat, M.; Perez, E.; Rico-Lattes, I.; Lattes, A. *New J. Chem.* **1999**, *23*, 1063-1065.
30. Bramer, T.; Dew, N.; Edsman, K. *J. Pharm. Pharmacol.* **2007**, *59*, 1319-1334.
31. Kaler, E. W.; Murthy, A. K.; Rodriguez, B. E.; Zasadzinski, J. A. N. *Science* **1989**, *245*, 1371-1374.
32. Menger, F. M.; Binder, W. H.; Keiper, J. S. *Langmuir* **1997**, *13*, 3247-3250.
33. Blanzat, M.; Turrin, C.-O.; Perez, E.; Rico-Lattes, I.; Caminade, A.-M.; Majoral, J.-P. *Chem. Commun.* **2002**, 1864-1865.
34. Blanzat, M.; Perez, E.; Rico-Lattes, I.; Lattes, A.; Gulik, A. *Chem. Commun.* **2003**, 244-245.
35. Rico-Lattes, I.; Blanzat, M.; Franceschi-Messant, S.; Perez, E.; Lattes, A. *C. R. Chim.* **2005**, *8*, 807-814.
36. Brun, A.; Brezesinski, G.; Mohwald, H.; Blanzat, M.; Perez, E.; Rico-Lattes, I. *Colloids Surf. A* **2003**, *228*, 3-16.
37. Bramer, T.; Paulsson, K.; Edwards, K.; Edsman, K. *Pharm. Res.* **2003**, *20*, 1661-1667.
38. Bramer, T.; Dew, N.; Edsman, K. *J. Pharm. Sci.* **2006**, *95*, 769-780.

## References

---

39. Consola, S.; Blanzat, M.; Perez, E.; Garrigues, J. C.; Bordat, P.; Rico-Lattes, I. *Chem. Eur. J.* **2007**, *13*, 3039-3047.
40. Consola, S.; Blanzat, M.; Rico-Lattes, I.; Perez, E.; Bordat, P. **2007**, *EP2006/064502*, 2006; *WO2007039561*, 2007,.
41. Soussan, E.; Blanzat, M.; Rico-Lattes, I.; Brun, A.; Teixeira, C. V.; Brezesinski, G.; Al-Ali, F.; Banu, A.; Tanaka, M. *Colloids Surf. A* **2007**, *303*, 55-72.
42. Soussan, E.; Mille, C.; Blanzat, M.; Bordat, P.; Rico-Lattes, I. *Langmuir* **2008**, *24*, 2326-2330.
43. Bhattacharya, S.; De, S.; Subramanian, M. *J. Org. Chem.* **1998**, *63*, 7640-7651.
44. Fischer, A.; Hebrant, M.; Tondre, C. *J. Colloid Interface Sci.* **2002**, *248*, 163-168.
45. Kondo, Y.; Uchiyama, H.; Yoshino, N.; Nishiyama, K.; Abe, M. *Langmuir* **1995**, *11*, 2380-2384.
46. Soussan, E.; Cassel, S.; Blanzat, M.; Rico-Lattes, I. *Angew. Chem., Int. Ed. Engl.* **2009**, *48*, 274-288.
47. Bordes, R.; Rbii, K.; Gonzalez-Perez, A.; Franceschi-Messant, S.; Perez, E.; Rico-Lattes, I. *Langmuir* **2007**, *23*, 7526-7530.
48. Bordes, R. *SYNTHESE, PHYSICOCHIMIE ET POLYMERISATION DE TENSIOACTIFS PAIRES D'IONS DERIVES DU NORBORNENE*, Thesis, Université Toulouse III - Paul Sabatier, 2007.
49. Rudiuk, S.; Franceschi-Messant, S.; Chouini-Lalanne, N.; Perez, E.; Rico-Lattes, I. *Langmuir* **2008**, *24*, 8452-8457.

## References

---

50. Rudiuk, S.; Delample, M.; Franceschi-Messant, S.; Chouini-Lalanne, N.; Perez, E.; Garrigues, J. C.; Rico-Lattes, I. **2009**, *in press*.
51. Underwood, A. L.; Anacker, E. W. *J. Phys. Chem.* **1984**, *88*, 2390-2393.
52. Bales, B. L.; Tiguida, K.; Zana, R. *J. Phys Chem. B* **2004**, *107*, 8661-8668.
53. Bonilha, J. B. S.; Geogretto, R. M. Z.; Abuin, E.; Lissi, E.; Quina, F. J. *J. Colloid Interface Sci.* **1990**, *135*, 238-245.
54. Bostrom, G.; Backlund, S.; Blokhuis, A. M.; Hoiland, H. *J. Colloid Interface Sci.* **1989**, *128*, 169-175.
55. Jansson, M.; Stilbs, P. *J. Phys. Chem.* **1987**, *91*, 113-116.
56. ud Din, K.; David, S. L.; Kumar, S. *J. Mol. Liq.* **1998**, *75*, 25-32.
57. Sugihara, G.; Arakawa, Y.; Tanaka, K.; Lee, S.; Moroi, Y. *J. Colloid Interface Sci.* **1995**, *170*, 399-406.
58. Hassan, P. A.; Raghaven, S. R.; Kaler, E. W. *Langmuir* **2002**, *18*, 2543-2548.
59. Kawasaki, H.; Imahayashi, R.; Tanaka, S.; Almgren, M.; Karlsson, G.; Maeda, H. *J. Phys Chem. B* **2003**, *107*, 8661-8668.
60. Gonzalez, Y. I.; Nakanishi, H.; Stjerndahl, M.; Kaler, E. W. *J. Phys Chem. B* **2005**, *109*, 11675-11682.
61. Yin, H.; Lei, S.; Zhu, S.; Huang, J.; Ye, J. *Chem. Eur. J.* **2006**, *12*, 2825-2835.
62. Lattes, A.; Rico, I.; de Savignac, A.; Samii, A. A.-Z. *Tetrahedron* **1987**, *43*, 1725-1735.
63. Lowery, T.; Richardson, K. *Mechanism and Theory in Organic Chemistry*; Harper Collins Publishers: 3rd ed.; 1987.

## References

---

64. Reichardt, C. *Solvents and Solvents Effects in Organic Chemistry*; Wiley-VCH: 2004.
65. Grunwald, E.; Winstein, S. *J. Am. Chem. Soc.* **1948**, *70*, 846-854.
66. Kosower, E. M. *J. Am. Chem. Soc.* **1958**, *80*, 3267-3270.
67. Kosower, E. M. *J. Am. Chem. Soc.* **1958**, *80*, 3253-3260.
68. Kosower, E. M. *J. Am. Chem. Soc.* **1958**, *80*, 3261-3267.
69. Gutmann, V. *Int. Symp. Specific Interact. Mol. Ions, Proceeding* **1976**, *1*, 182-187.
70. Geiser, L.; Cherkaoui, S.; Veuthey, J.-L. *J. Chromatogr.* **2002**, *979*, 389-398.
71. Peters, D.; Miethchen, R. *Colloid Polym. Sci.* **1993**, *271*, 91-94.
72. Beesley, A. H.; Evans, D. F.; Laughlin, R. G. *J. Phys. Chem.* **1988**, *92*, 791-793.
73. Hildebrand, J.; Scott, R. L. *Solubility of non electrolytes*; Reinhold: 3rd ed.; 1950.
74. Lewis, W. C. H. *Trans. Frod. Soc.* **1911**, *7*, 94-115.
75. Gordon, J. E. *J. Am. Chem. Soc.* **1965**, *7*, 4343.
76. Root, L. J.; Stillinger, F. H. *J. Chem. Phys.* **1989**, *90*, 1200-1208.
77. Ohtaki, H.; Funaki, A.; Rode, B. M.; Reibnegger, G. J. *Bull. Chem. Soc. Jpn.* **1983**, *56*, 2116-2121.
78. Radnai, T.; Megyes, T.; Bako, I.; Kosztolanyi, T.; Palinkas, G.; Ohtaki, H. *J. Mol. Liq.* **2004**, *110*, 123-132.
79. Nagy, J. B. *Solutions Behavior of Surfactants*; volume 2 Plenum Press: 1982.

- 
80. Christenson, H.; Friberg, S. E.; Larsen, D. W. *J. Phys. Chem.* **1980**, *84*, 3633-3638.
81. Ramadan, M. S.; Evans, D. F.; Lumry, R. *J. Phys. Chem.* **1983**, *87*, 4538-4543.
82. Evans, D. F.; Yamauchi, A.; Roman, R.; Casassa, E. Z. *J. Colloid Interface Sci.* **1982**, *88*, 89-96.
83. Rico, I.; Lattes, A. *Surfactant Science Series* **1992**, *44*, 115-124.
84. Akhter, M. S.; Alawi, S. M.; Bose, A. N. *Colloids Surf. A* **1995**, *94*, 173-176.
85. Akhter, M. S. *Colloids Surf., A* **1995**, *99*, 255-258.
86. Akhter, M. S. *Colloids Surf., A* **1997**, *121*, 103-109.
87. Rico, I.; Lattes, A. *J. Phys. Chem.* **1986**, *90*, 5870-5872.
88. Costain, C. . C.; Dowling, J. M. *J. Chem. Phys.* **1960**, *32*, 158-165.
89. Gardiner, D. J.; Lees, A. J.; Straughan, B. P. *J. Mol. Struct.* **1979**, *53*, 15-24.
90. Hirota, E.; Sugisaki, R.; Nielsen, C. J.; Sorerensen, G. O. *J. Mol. Spectrosc.* **1974**, *49*, 251-267.
91. Kurland, R. J.; Wilson, E. B. *J. Chem. Phys.* **1957**, *27*, 585-590.
92. Lees, A. J.; Straughan, B. P.; Gardiner, D. J. *J. Mol. Struct.* **1981**, *71*, 61-70.
93. Drakenberg, T.; Forsen, S. *J. Phys. Chem.* **1970**, *74*, 1-7.
94. Kamei, H. *Bull. Chem. Soc. Jpn.* **1968**, *41*, 2269-&.
95. Lees, A. J.; Straughan, B. P.; Gardiner, D. J. *J. Mol. Struct.* **1979**, *54*, 37-47.
96. Couper, A.; Gladden, G. P.; Ingram, T. *Far. Disc. Chem. Soc.* **1975**, *59*, 63-75.

## References

---

97. Ray, A. *J. Am. Chem. Soc.* **1969**, *91*, 6511-6512.
98. Ray, A. *Nature* **1971**, *231*, 313-314.
99. Schubert, K. V.; Busse, G.; Strey, R.; Kahlweit, M. *J. Phys. Chem.* **1993**, *97*, 248-254.
100. Mukerjee, P. *J. Phys. Chem.* **1962**, *66*, 1375-1376.
101. Shinoda, K.; Hutchinson, E. *J. Phys. Chem.* **1962**, *66*, 577-582.
102. Desnoyers, J. E.; Caron, G.; De Lisi, R.; Roberts, D.; Roux, A. H.; Perron, G. *J. Phys. Chem.* **1983**, *87*, 1397-1406.
103. Roux, A. H.; Hetu, D.; Perron, G.; Desnoyers, J. E. *J. Soln. Chem.* **1984**, *13*, 1-25.
104. Blandamer, M. J.; Cullis, P. M.; Soldi, L. G.; Engberts, J. B. F. N.; Kacper-ska, A.; Van Os, N. M.; Subha, M. C. S. *Adv. Colloid Interface Sci.* **1995**, *58*, 171-209.
105. Auvray, X.; Petipas, C.; Lattes, A.; Rico-Lattes, I. *Colloids Surf., A* **1997**, *123-124*, 247-251.
106. Thomason, M. A.; Bloor, D. M.; Wyn-Jones, E. *J. Phys. Chem.* **1991**, *95*, 6017-6020.
107. Almgren, M.; Swarup, S.; Loeffroth, J. E. *J. Phys. Chem.* **1985**, *89*, 4621-4626.
108. Belmajdoub, A.; Marchal, J.; Canet, D.; Rico, I.; Lattes, A. *New J. Chem.* **1987**, *11*, 415-418.
109. Perche, T.; Auvray, X.; Petipas, C.; Anthore, R.; Rico-Lattes, I.; Lattes, A. *Langmuir* **1997**, *13*, 1475-1480.

- 
110. Auvray, X.; Petipas, C.; Perche, T.; Anthore, R.; Marti, M. J.; Rico, I.; Lattes, A. *J. Phys. Chem.* **1990**, *94*, 8604-8607.
111. Auvray, X.; Perche, T.; Petipas, C.; Anthore, R.; Marti, M. J.; Rico, I.; Lattes, A. *Langmuir* **1992**, *8*, 2671-2679.
112. Auvray, X.; Petipas, C.; Anthore, R.; Rico, I.; Lattes, A.; Ahmah-Zadeh Samii, A.; de Savignac, A. *Colloid Polym. Sci.* **1987**, *265*, 925-932.
113. Greaves, T. L.; Drummond, C. J. *Chem. Soc. Rev.* **2008**, *37*, 1709-1726.
114. Lattes, A.; Perez, E.; Rico-Lattes, I. *C. R. Chimie* **2009**, *12*, 45-53.
115. Belmajdoub, A.; ElBayed, K.; Brondeau, J.; Canet, D.; Rico, I.; Lattes, A. *J. Phys. Chem.* **1988**, *92*, 3569-3573.
116. Carnero Ruiz, C.; Diaz-Lopez, L.; Aguiar, J. *J. Colloid Interface Sci.* **2007**, *305*, 293-300.
117. Lin, Z.; Davis, H. T.; Scriven, L. E. *Langmuir* **1996**, *12*, 5489-5493.
118. Auvray, X.; Perche, T.; Anthore, R.; Petipas, C.; Rico, I.; Lattes, A. *Langmuir* **1991**, *7*, 2385-2393.
119. Wårnheim, T.; Jånsson, A. *J. Colloid Interface Sci.* **1988**, *125*, 627-633.
120. Johansson, L. B.-A.; Kalman, B.; Wiklander, G.; Fransson, A.; Fontell, K.; Bergenstahl, B.; Lindblom, G. *Biochim. Biophys. Acta* **1993**, *1149*, 285-291.
121. Meliani, A.; Perez, E.; Rico, I.; Lattes, A.; Petipas, C.; Auvray, X. *Prog. Colloid Polym. Sci.* **1992**, *88*, 140-145.
122. Meliani, A.; Perez, E.; Rico, I.; Lattes, A.; Moisand, A. *New J. Chem.* **1991**, *15*, 871-872.

## References

---

123. Casyias, J. L.; Schechter, R. S.; Wade, W. H. *J. Colloid Interface Sci.* **1977**, *59*, 31-38.
124. Fletcher, P. D. I.; Galal, M. F.; Robinson, B. H. *J. Chem. Soc., Faraday Trans. 1* **1984**, *80*, 3307-3314.
125. Rico, I.; Lattes, A. *J. Colloid Interface Sci.* **1984**, *102*, 285-287.
126. Rico, I.; Couderc, F.; Perez, E.; Laval, J. P.; Lattes, A. *J. Chem. Soc., Chem. Commun.* **1987**, 1205-1206.
127. Rico, I.; Lattes, A.; Das, K. P.; Lindman, B. *J. Am. Chem. Soc.* **1989**, *111*, 7266-7267.
128. Hisao, V. K. S.; Yong, K.-T.; Cartwright, A. N.; Swihart, M. T.; Prasad, P. N.; Lloyd, P. F.; Bunning, T. J. *J. Mater. Chem.* **2009**, *19*, 3998-4003.
129. Schubert, K. V.; Strey, R.; Kahlweit, M. *Progr. Colloid Polym. Sci.* **1992**, *89*, 263-267.
130. Karlsson, S.; Backlund, S.; Friman, R. *Colloid Polym. Sci.* **2000**, *278*, 8-14.
131. van Doren, H. A.; Terpstra, K. R. *J. Mater. Chem.* **1995**, *5*, 2513-2560.
132. Viseu, M. I.; Goncalves da Silva, A. M.; Costa, S. M. B. *Langmuir* **2001**, *17*, 1529-1537.
133. Vlachy, N.; Arteaga, A. F.; Klaus, A.; Touraud, D.; Dreclisler, M.; Kunz, W. *Colloids Surf. A* **2009**, *338*, 135-141.
134. Tomašić, V.; Popović, S.; Filipović-Vinceković, N. *J. Colloid Interface Sci.* **1999**, *215*, 280-289.
135. Almgren, M.; Swarup, S.; Loeffroth, J. E. *J. Phys. Chem.* **1985**, *89*, 4621-4626.



- 
136. Bakshi, M. S.; Singh, K.; Singh, J. *J. Colloid Interface Sci.* **2006**, *297*, 284-291.
137. Molina-Bolívar, J. A.; Aguiar, J.; Peula-Garcia, J. M.; Ruiz, C. C. *Mol. Phys.* **2002**, *100*, 3259 - 3269.
138. Perche, T.; Auvray, X.; Petipas, C.; Anthore, R.; Perez, E.; Rico-Lattes, I.; Lattes, A. *Langmuir* **1996**, *12*, 863-871.
139. Smits, E.; Engberts, J. B. F. N.; Kellogg, R. M.; Van Doren, H. A. *Liq. Cryst.* **1997**, *23*, 481-488.
140. Meliani, A.; Perez, E.; Rico-Lattes, I.; Lattes, A. *Comun. Jorn. Com. Esp. Deterg.* **2006**, *36*, 335-341.
141. Moore, W. E. *J. Am. Pharm. Assoc. (1912-1977)* **1958**, *47*, 855-857.
142. Hernandez-Luis, F.; Galleguillos-Castro, H.; Estesó, M. A. *Fluid Phase Equilib.* **2005**, *227*, 245-253.
143. Rohdewald, P.; Moldner, M. *J. Phys. Chem.* **1973**, *77*, 373-377.
144. Kinart, C. M.; Kinart, W. *J. Phys. Chem. Liq.* **1996**, *33*, 159-170.
145. Saleh, J. M.; Khalil, M.; Hikmat, N. A. *J. Iraqi Chem. Soc.* **1986**, *11*, 89-104.
146. Das, J.; K., I. *J. Colloid Interface Sci.* **2009**, *337*, 227-233.
147. Gamboa, C.; Rios, H.; Sanchez, V. *Langmuir* **1994**, *10*, 2025-2027.
148. Bordes, R.; Vedrenne, M.; Coppel, Y.; Franceschi-Messant, S.; Perez, E.; Rico-Lattes, I. *ChemPhysChem* **2007**, *8*, 2013-2018.
149. Haselwander, T. F. A.; Heitz, W.; Krügel, S. A.; Wendorff, J. H. *Macromol. Chem. Phys.* **1996**, *197*, 3435-3453.

## References

---

150. L'Heureux, G. P.; Fragata, M. *J. Colloid Interface Sci.* **1987**, *117*, 513-522.
151. L'Heureux, G. P.; Fragata, M. *Biophys. Chem.* **1988**, *30*, 293-301.
152. Nucci, N.; Zelent, B.; Vanderkooi, J. *Journal of Fluorescence* **2008**, *18*, 41-49.
153. Basu Ray, G.; Chakraborty, I.; Moulik, S. P. *J. Colloid Interface Sci.* **2006**, *294*, 248-254.
154. Evans, D. F.; Yamauchi, A.; Wei, G. J.; Bloomfield, V. A. *J. Phys. Chem.* **1983**, *87*, 3537-3541.
155. Tamura-Lis, W.; Lis, L. J.; Quinn, P. J. *J. Colloid Interface Sci.* **1992**, *150*, 200-207.
156. Thomaier, S.; Kunz, W. *J. Mol. Liq.* **2007**, *130*, 104-107.
157. Akhtar, S.; Faruk, A. N. M. O.; Saleh, M. A. *Phys. Chem. Liq.* **2001**, *39*, 383-399.
158. Gomez Marigliano, A. C.; Solimo, H. N. *J. Chem. Eng. Data* **2002**, *47*, 796-800.
159. Demchenko, P. A. *Microbiology (Moscow, Russ. Fed.)* **1961**, *23*, 528-&.

# List of Tables

<b>Fundamentals</b>	<b>11</b>
2.1 Physical parameters of common solvents at 25 °C. <sup>64,70-72</sup> . . . . .	34
2.2 Free energy, free enthalpy and entropy of micellization in H <sub>2</sub> O and hydrazine. . . . .	46
<b>Results and Discussion</b>	<b>65</b>
2.1 Model systems <b>3a-g</b> . . . . .	71
2.2 Sugar-based surfactants <b>4a-c</b> and catanionic systems <b>5a-g</b> . . . . .	73
3.1 Krafft temperatures $T_K$ (°C) of different catanionic surfactants in polar solvents. . . . .	81
3.2 $CACs$ (mol.L <sup>-1</sup> ) of compounds <b>3a</b> (25 °C) and <b>5a</b> (45 °C) in H <sub>2</sub> O, in formamide and in H <sub>2</sub> O/FA mixtures. . . . .	89
3.3 $CACs$ of the simple model systems ( $C_m^+C_n^-$ , 70 °C) and the sugar-based systems (G-Hyd <sub>m</sub> <sup>+</sup> /C <sub>n</sub> <sup>-</sup> , 60 °C) in pure formamide. . . . .	94

## Appendix

---

3.4	Dielectric constants of H <sub>2</sub> O/FA mixtures at 25 °C and objects obtained with G-Hyd <sub>8</sub> <sup>+</sup> /C <sub>12</sub> <sup>-</sup> . . . . .	99
3.5	Cohesive-energy densities of water, formamide and glycerol at 25 °C. . . . .	102
3.6	Dielectric constants of different polar solvent mixtures at 25 °C and objects obtained with compound <b>5a</b> at 45 °C. . . . .	103
3.7	Krafft temperatures in °C of the G-Hyd <sub>8</sub> <sup>+</sup> /C <sub>16</sub> <sup>-</sup> and G-Hyd <sub>16</sub> <sup>+</sup> /C <sub>12</sub> <sup>-</sup> systems. . . . .	110
3.8	<i>CACs</i> (mol.L <sup>-1</sup> ) of compound <b>5c</b> at 50 °C and compound <b>5e</b> at 60 °C. . . . .	110
3.9	Solvent mixtures dielectric constants at 25 °C and objects obtained with compounds <b>5c</b> and <b>5e</b> . . . . .	113
3.10	<i>CAC</i> of compound <b>3a</b> , <b>5a</b> and <b>5c</b> . . . . .	117
3.11	Results of the DLS measurements on compound <b>5a</b> and <b>5c</b> using different preparation methods for the solvent mixtures at 50 °C. . . . .	125
4.1	<i>CMC</i> and <i>CAC</i> (mol.L <sup>-1</sup> ) of NbC14 at 45 °C. . . . .	134
4.2	<i>CMC</i> and <i>CAC</i> (mol.L <sup>-1</sup> ) of CxC14 at 45 °C. . . . .	143

## Experimental Part 159

2.1	Technical parameters applied for DLS measurements. <sup>144,145,157,158</sup> . . . . .	169
3.1	Characterization of simple model systems. . . . .	174
4.1	Results of the DLS measurements on compound <b>5a</b> and <b>5c</b> using different preparation methods for the solvent mixtures. . . . .	197

---

**Résumé****225**

- 1 Température de Krafft  $T_K$  ( $^{\circ}\text{C}$ ) de différents tensioactifs cationiques dans des solvants polaires. . . . . 237
- 2 Constantes diélectriques de différents mélanges  $\text{H}_2\text{O}/\text{FA}$  à  $25\text{ }^{\circ}\text{C}$  et les objets obtenus avec  $\text{G-Hyd}_8^+/\text{C}_{12}^-$ . . . . . 241
- 3 Constantes diélectriques de différents mélanges de  $\text{H}_2\text{O}$ , de  $\text{FA}$  et de glycérol à  $25\text{ }^{\circ}\text{C}$  et les objets obtenus avec  $\text{G-Hyd}_8^+/\text{C}_{12}^-$  à  $45\text{ }^{\circ}\text{C}$ . . . . . 242



# List of Figures

<b>General Introduction</b>	<b>3</b>
1 Schematic representation of a monocatener surfactant. . . . .	3
2 Positioning of surfactant molecules at the water-air interface. . . . .	4
<b>Fundamentals</b>	<b>11</b>
1.1 Micelle (A), cylindrical micelle (B), hexagonal phase $H_\alpha$ (C), cubic phase I (D), cubic phase II (E), bilayer (lamellar phase $L_\alpha$ ) (F). . . . .	13
1.2 Aggregation type according to the packing parameter $p$ . . . . .	15
1.3 Typical phase diagram of a four-component system. (O/W) microemulsion (A), (W/O) microemulsion (B), bicontinuous microemulsion (C), lamellar phase (D). . . . .	17
1.4 Schematic representations of catanionic (A) and bicatener (B) surfactants.	19
1.5 Schematic representation of a vesicle. . . . .	21
1.6 Structure of the first water soluble catanionic surfactant at equimolarity.	22
1.7 Catanionic systems synthesized in our laboratory with a bicatener (A) and a gemini (B) structure. . . . .	23

## Appendix

---

1.8	Structure of a catanionic surfactant resulting from the association of an anti-inflammatory drug (indometacin) with a sugar-derived surfactant.	23
1.9	Tricatenar catanionic surfactant.	24
1.10	Counterions influencing the aggregation behavior.	27
1.11	Norbornene methyleneammonium tetradecanoate NbC14.	28
1.12	Surface tension measurements of NbC14 in H <sub>2</sub> O at 25 °C.	29
1.13	Schematic representation of the micelle-vesicle transition mechanism.	29
2.1	3D model of a water molecule.	32
2.2	Representation of the 3D structure of liquid water.	34
2.3	3D models of glycerol (A) and formamide (B).	36
2.4	Structures of the glycerol dimer (A) and the condensed glycerol phase (B).	37
2.5	Possible arrangements of FA molecules in the liquid state. Linear dimer (A); ring structure (B). <sup>78</sup>	38
2.6	Proposed structure for liquid formamide. <sup>78</sup>	38
2.7	Schematic representation of a simple phase diagram indicating the $T_K$ .	40
2.8	Mesomeric structure of liquid formamide.	41
2.9	Mesomeric structure of <i>N</i> -methylnone.	49
2.10	Optical micrograph under polarizing light: lyotropic hexagonal phase of SDS in FA. <sup>114</sup>	56
2.11	Phase diagram of formamide, octylamine and octanoic acid. I <sub>α</sub> : liquid isotropic phase; A: crystalline salt formed by octanoic acid and octylamine at equimolar ratio.	61



<b>Results and Discussion</b>	<b>65</b>
2.1 Synthesis of simple model systems $C_m^+/C_n^-$ . . . . .	70
2.2 Reaction scheme for compounds of the type G-Hyd $_m^+/C_n^-$ . . . . .	72
2.3 $^{13}\text{C}$ NMR spectra of the hexadecanoic acid <b>2c</b> and the catanionic surfactant <b>5f</b> (G-Hyd $_{12}^+/C_{16}^-$ ) in $\text{CD}_3\text{OD}$ . . . . .	75
2.4 FT-IR spectra of the hexadecanoic acid <b>2c</b> and the catanionic surfactant <b>5f</b> (G-Hyd $_{12}^+/C_{16}^-$ ). . . . .	76
2.5 Mass spectrum of compound <b>3a</b> ( $C_8^+/C_8^-$ ). . . . .	77
3.1 Evolution of the surface tension as a function of the surfactant concentration. . . . .	86
3.2 Surface tension measurements of compound <b>3a</b> at 25 °C in different $\text{H}_2\text{O}/\text{FA}$ mixtures. . . . .	88
3.3 Surface tension measurements of compound <b>5a</b> at 45 °C in different $\text{H}_2\text{O}/\text{FA}$ mixtures. . . . .	89
3.4 Evolution of the $CAC$ as a function of the FA volume fraction for compounds <b>3a</b> (top, 25 °C) and <b>5a</b> (bottom, 45 °C). . . . .	90
3.5 Surface tension measurements of the $C_m^+C_n^-$ systems at 70 °C in pure FA. . . . .	92
3.6 Surface tension measurements of the G-Hyd $_m^+/C_n^-$ systems at 60 °C in pure FA. . . . .	93
3.7 Electron micrographs of compound <b>5a</b> (G-Hyd $_8^+/C_{12}^-$ ) in $\text{H}_2\text{O}$ ( $1.10^{-3}$ mol.L $^{-1}$ ). . . . .	95
3.8 Micrograph of G-Hyd $_8^+/C_{12}^-$ in $\text{H}_2\text{O}$ at 25 °C. . . . .	96
3.9 Model of the influence of the medium dielectric constant on the aggregation behavior of catanionic surfactants. . . . .	98
3.10 Evolution of the dielectric constant of $\text{H}_2\text{O}/\text{FA}$ mixtures at 25 °C. . . . .	99

## Appendix

---

3.11	Electron micrographs of G-Hyd <sub>8</sub> <sup>+</sup> /C <sub>12</sub> <sup>-</sup> in a 70:30 H <sub>2</sub> O/FA mixture (1.10 <sup>-2</sup> mol.L <sup>-1</sup> ). . . . .	100
3.12	Proposed complexes for the structure of FA/glycerol mixtures. . . . .	103
3.13	Surface tension measurements of the G-Hyd <sub>8</sub> <sup>+</sup> /C <sub>12</sub> <sup>-</sup> system in a 50:50 H <sub>2</sub> O/glycerol and in a 56:44 FA/glycerol mixture at 45 °C. . . . .	104
3.14	Polarized micrographs of <b>5a</b> in a 50:50 H <sub>2</sub> O/glycerol (A) and a 56:44 FA/glycerol (B) mixture at 25 °C. . . . .	105
3.15	Electron micrograph of <b>5a</b> in a 50:50 H <sub>2</sub> O/glycerol mixture (1.10 <sup>-3</sup> mol.L <sup>-1</sup> ). . . . .	105
3.16	ATR-IR spectra of G-Hyd <sub>8</sub> <sup>+</sup> /C <sub>12</sub> <sup>-</sup> (1.10 <sup>-1</sup> mol.L <sup>-1</sup> ) in the solid state and in different solvent mixtures at 55 °C. . . . .	107
3.17	Attractive interactions between the two components of a catanionic surfactant. . . . .	109
3.18	Surface tension measurements of compound <b>5c</b> (top) at 50 °C and compound <b>5e</b> (bottom) at 60 °C. . . . .	111
3.19	TEM micrographs of G-Hyd <sub>8</sub> <sup>+</sup> /C <sub>16</sub> <sup>-</sup> (1.10 <sup>-2</sup> mol.L <sup>-1</sup> ) in 70:30 H <sub>2</sub> O/FA mixtures. . . . .	113
3.20	ATR-IR spectra of G-Hyd <sub>8</sub> <sup>+</sup> /C <sub>16</sub> <sup>-</sup> (1.10 <sup>-1</sup> mol.L <sup>-1</sup> ) in different solvent mixtures and of the powder at 55 °C. . . . .	115
3.21	<i>CAC</i> evolution of compound <b>3a</b> at 25 °C. . . . .	116
3.22	<i>CAC</i> evolution of compound <b>5a</b> at 45 °C. . . . .	117
3.23	<i>CAC</i> evolution of compound <b>5c</b> at 50 °C. . . . .	118
3.24	Existence domains of vesicles and micelles. . . . .	119
3.25	Surface tension measurements at 50 °C of the G-Hyd <sub>12</sub> <sup>+</sup> /C <sub>8</sub> <sup>-</sup> system in FA, prepared in H <sub>2</sub> O or in FA. . . . .	126
4.1	Norbornene methyleneammonium tetradecanoate NbC14. . . . .	130

4.2	Model of the micelle-vesicle transition mechanism. . . . .	131
4.3	Surface tension measurements of NbC14 in different solvents and solvent mixtures at 45 °C. . . . .	133
4.4	Surface tension measurements of NbC14 in H <sub>2</sub> O at 25 and 45 °C. . . . .	135
4.5	Electron micrograph of NbC14 in H <sub>2</sub> O (1.10 <sup>-3</sup> mol.L <sup>-1</sup> ). . . . .	135
4.6	Electron micrograph of NbC14 in formamide (5.10 <sup>-2</sup> mol.L <sup>-1</sup> ). . . . .	137
4.7	Model of the stacking phenomenon of norbornene cycles. . . . .	138
4.8	Electron micrographs of NbC14; (A) H <sub>2</sub> O/FA 70:30 (5.10 <sup>-3</sup> mol.L <sup>-1</sup> ), (B) H <sub>2</sub> O/FA 50:50 (1.10 <sup>-2</sup> mol.L <sup>-1</sup> ), (C) H <sub>2</sub> O/FA 30:70 (5.10 <sup>-2</sup> mol.L <sup>-1</sup> ), (D) H <sub>2</sub> O/glycerol 50:50 (5.10 <sup>-3</sup> mol.L <sup>-1</sup> ). . . . .	139
4.9	Optical micrograph of NbC14 in a 50:50 H <sub>2</sub> O/FA mixture. . . . .	140
4.10	Cyclohexylammonium tetradecanoate (CxC14). . . . .	141
4.11	Surface tension measurements of the CxC14 system in water and in formamide at 45 °C. . . . .	142

## Experimental Part

159

2.1	Typical phase diagram of a ionic surfactant. . . . .	166
3.1	Scheme of the synthesis of the alkylammonium alkanoate model systems.	174
3.2	C <sub>8</sub> <sup>+</sup> /C <sub>8</sub> <sup>-</sup> . . . . .	175
3.3	C <sub>8</sub> <sup>+</sup> /C <sub>12</sub> <sup>-</sup> . . . . .	175
3.4	C <sub>12</sub> <sup>+</sup> /C <sub>8</sub> <sup>-</sup> . . . . .	176
3.5	C <sub>12</sub> <sup>+</sup> /C <sub>12</sub> <sup>-</sup> . . . . .	177
3.6	C <sub>8</sub> <sup>+</sup> /C <sub>16</sub> <sup>-</sup> . . . . .	177
3.7	C <sub>16</sub> <sup>+</sup> /C <sub>8</sub> <sup>-</sup> . . . . .	178
3.8	C <sub>16</sub> <sup>+</sup> /C <sub>16</sub> <sup>-</sup> . . . . .	179

## Appendix

---

3.9	G-Hyd <sub>8</sub>	180
3.10	G-Hyd <sub>12</sub>	181
3.11	G-Hyd <sub>16</sub>	182
3.12	G-Hyd <sub>8</sub> <sup>+</sup> /C <sub>12</sub> <sup>-</sup>	183
3.13	G-Hyd <sub>12</sub> <sup>+</sup> /C <sub>8</sub> <sup>-</sup>	184
3.14	G-Hyd <sub>8</sub> <sup>+</sup> /C <sub>16</sub> <sup>-</sup>	186
3.15	G-Hyd <sub>16</sub> <sup>+</sup> /C <sub>8</sub> <sup>-</sup>	187
3.16	G-Hyd <sub>16</sub> <sup>+</sup> /C <sub>12</sub> <sup>-</sup>	188
3.17	G-Hyd <sub>12</sub> <sup>+</sup> /C <sub>16</sub> <sup>-</sup>	189
3.18	G-Hyd <sub>12</sub> <sup>+</sup> /C <sub>18</sub> <sup>-</sup>	190
3.19	NbNH <sub>2</sub>	191
3.20	NbC14	192
3.21	CxC14	194

## Résumé

**225**

1	Représentation schématique d'un tensioactif.	227
2	Micelle (A), micelle allongée (B), phase hexagonale $H_\alpha$ (C), phase cubique I (D), phase cubique II (E), bicouche (phase lamellaire $L_\alpha$ ) (F).	230
3	Représentation schématique d'un tensioactif catanionique (A) et bicaténaire (B).	231
4	Représentations schématique d'une vésicule.	232
5	Représentation schématique du mécanisme de la transition micelle-vésicule.	233
6	Évolution de la $CAC$ des systèmes <b>3a</b> (gauche) et <b>5a</b> (droite) en fonction de la fraction volumique du FA.	239
7	Cliché de MET du système <b>5a</b> (G-Hyd <sub>8</sub> <sup>+</sup> /C <sub>12</sub> <sup>-</sup> ) dans H <sub>2</sub> O ( $1.10^{-3}$ mol.L <sup>-1</sup> ).	240

---

8	Cliché de MET du système <b>5a</b> dans H <sub>2</sub> O (1.10 <sup>-2</sup> mol.L <sup>-1</sup> ) dans un mélange H <sub>2</sub> O/FA de 70 :30. . . . .	242
9	Représentation schématique de l'influence de la constante diélectrique. .	243
10	Domaine d'existence des vésicules et des micelles. . . . .	245
11	Mesures de tension superficielle du NbC14 dans différents solvants et dans les mélanges de solvants à 45°C. . . . .	249
12	Représentation schématique de l'empilement du contre-ion du dérivé du norbornène. . . . .	250



## Résumé





# Part I – Introduction

De nos jours, les tensioactifs font partie de nombreux processus biologiques. Ils sont également des composants des membranes de cellules physiologiques. On peut aussi les trouver dans plusieurs formulations industrielles et pharmaceutiques. Les tensioactifs sont des molécules amphiphiles, caractérisées par une tête polaire et une queue hydrophobe (cf fig. 1). Ce caractère amphiphile leur confère deux propriétés principales. Premièrement, les tensioactifs peuvent se placer à l'interface entre l'eau et l'huile ou bien entre l'eau et l'air, le tout accompagné par une baisse de la tension superficielle. Deuxièmement, les tensioactifs sont capables de s'agréger en systèmes organisés comme par exemple des micelles, des vésicules ou des phases lamellaires.

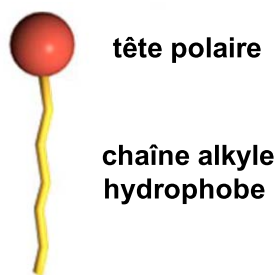


Figure 1 – Représentation schématique d'un tensioactif.

## Appendix

---

Les tensioactifs peuvent être classés selon leur tête polaire. Il existe des tensioactifs avec une tête chargée (anioniques, cationiques), avec une tête neutre ou avec une tête zwitterionique (charge positive et négative sur la même tête polaire). La nature variée des tensioactifs permet de multiples applications dans tout type d'industrie. Les tensioactifs catanioniques constituent un type particulier de tensioactifs. Ils sont composés d'une paire d'ions entre un tensioactif cationique et un tensioactif anionique. Ils peuvent ainsi être décrits comme des tensioactifs bicaténaires avec deux chaînes hydrophobes. Dans la littérature on trouve peu de choses sur le comportement d'agrégation des tensioactifs catanioniques dans des solvants polaires et cohésifs. C'est pourquoi nous avons réalisé une étude comparative des tensioactifs catanioniques dans l'eau ainsi que dans des solvants polaires et cohésifs.

## Part II – Rappel bibliographique

### Chapitre 1 – Solutions aqueuses

Une des caractéristiques les plus importantes des tensioactifs est de pouvoir former des agrégats dans l'eau. Pour des systèmes binaires, c.-à-d. des solutions aqueuses de tensioactifs, la formation d'agrégats a lieu au-dessus d'une certaine concentration, la concentration d'agrégation critique (CAC). En effet, le contact entre les chaînes hydrophobes et l'eau n'est pas favorable à l'énergie du système. Par contre, si la concentration de l'amphiphile augmente, l'énergie du système augmente elle aussi. À partir de la CAC des micelles peuvent se former. Les chaînes hydrophobes sont rassemblées à l'intérieur de l'agrégat, tandis que les têtes polaires se placent à la surface de l'agrégat. De cette manière, le contact entre l'eau et les chaînes hydrophobes est réduit à un minimum, tandis que le contact entre l'eau et les têtes polaires est augmenté. Les tensioactifs peuvent former différents types d'agrégats selon leur concentration. Ces phases lyotropes sont données dans la figure 2.

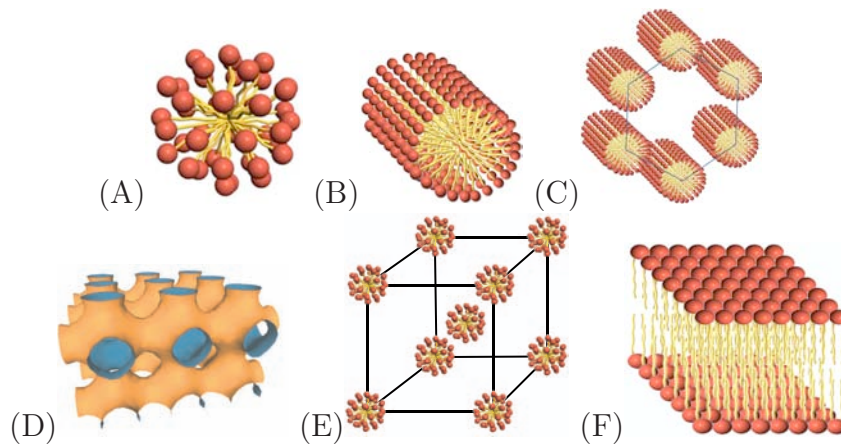


Figure 2 – Micelle (A), micelle allongée (B), phase hexagonale  $H_\alpha$  (C), phase cubique I (D), phase cubique II (E), bicouche (phase lamellaire  $L_\alpha$ ) (F).

Outre des phases lyotropes, on peut trouver des phases thermotropes, où le type d'agrégat change avec la température pour une concentration donnée.

En 1976, Israelachvili a introduit le paramètre d'empilement  $p$ , qui permet de prédire le type d'agrégation à partir de la forme géométrique du tensioactif en solution aqueuse diluée. Ce paramètre est défini comme :

$$p = \frac{v}{a_0 \cdot l_c} \quad (1)$$

Où  $v$  et  $l_c$  sont respectivement le volume et la longueur moyenne de la chaîne hydrophobe, et  $a_0$  est la surface effective de la tête polaire.  $V$ ,  $l_c$  et  $a_0$  peuvent être calculés ou mesurés. La relation selon Israelachvili entre la forme géométrique et le type d'agrégat formé est donnée dans la figure 1.2 (Part II, p. 15). Mises à part les solutions binaires, on peut trouver des systèmes ternaires ou quaternaires. Ces systèmes peuvent former des émulsions. Une émulsion est une dispersion de deux liquides non miscibles qui est stabilisée par des molécules amphiphiles. Il existe des émulsions huile dans l'eau (H/E), avec des gouttelettes d'huile dispersées dans l'eau, ou bien des émulsions eau dans l'huile (E/H), où l'eau est dispersée dans une huile. Les émulsions ne sont

pas stables thermodynamiquement et ont tendance à se séparer. Une microémulsion est un type spécial d'émulsion, puisqu'il s'agit d'un système thermodynamiquement stable, mais avec une concentration en tensioactif plus élevée que pour les émulsions « normales ».

Les tensioactifs catanioniques constituent un type spécial de molécule amphiphile. Leur structure particulière composée d'un tensioactif cationique et d'un tensioactif anionique peut être décrite comme bicaténaire, ce qui leur confère une forme géométrique qui favorise la formation de vésicules dans l'eau (cf fig. 3).

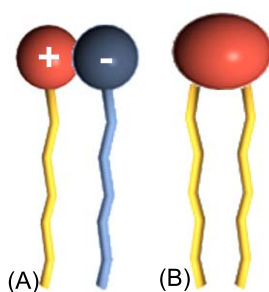


Figure 3 – Représentation schématique d'un tensioactif catanionique (A) et bicaténaire (B).

Les vésicules possèdent une structure de bicouche autour d'une cavité aqueuse. Les vésicules permettent donc d'incorporer des principes actifs hydrophiles (dans la cavité aqueuse) et hydrophobes (dans la bicouche) (cf fig. 4). La formation de vésicules par des tensioactifs catanioniques a été mise au point dans notre laboratoire pour des applications pharmaceutiques.

Un type particulier de tensioactif catanionique est le tensioactif ionique à gros contre-ion organique. La taille du contre-ion est suffisante pour permettre les interactions hydrophobes entre la chaîne alkyle du tensioactif et le contre-ion. Ceci peut, selon le degré d'hydrophobie, influencer le comportement d'auto-agrégation, car le contre-ion peut soit se placer à la sphère de solvatation – comme le ferait un contre-ion

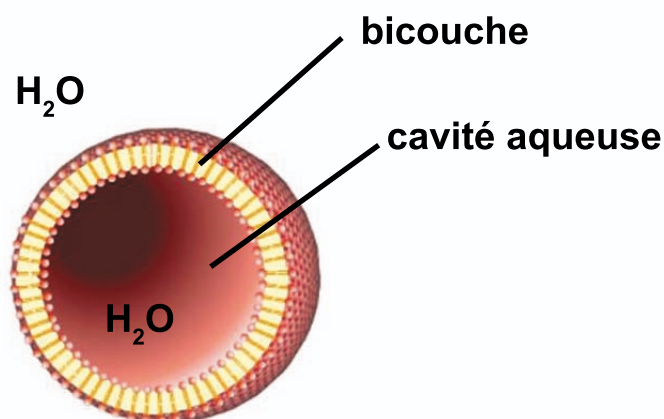


Figure 4 – Représentations schématique d'une vésicule.

classique – soit s'intercaler entre les tensioactifs ioniques. Dans notre laboratoire, une association entre un acide gras et le norbornène méthylèneammonium a été étudiée dans l'eau. Ce système montre un comportement particulier, car il forme des micelles à des concentrations faibles, tandis qu'il forme des vésicules à des concentrations plus élevées. Cette transition micelle-vésicule peut être visualisée par la mesure de la tension superficielle. L'évolution de la tension superficielle en fonction du logarithme de concentration montre deux paliers indiquant la formation de micelles et de vésicules.

En effet, le contre-ion se comporte de la même manière qu'un contre-ion classique à de faibles concentrations, et se place ainsi à la sphère de solvation du tensioactif ionique. Si la concentration augmente, les interactions hydrophobes augmentent également. Le contre-ion s'intercale donc entre les tensioactifs ioniques pour premièrement réduire les interactions peu favorables entre le contre-ion et l'eau, et deuxièmement augmenter les interactions hydrophobes entre la chaîne alkyle du tensioactif et le contre-ion. La figure 5 est une représentation schématique du mécanisme de la transition micelle-vésicule. Suite à l'intercalation du contre-ion, le paramètre d'empilement change et la formation de vésicules est favorisée.

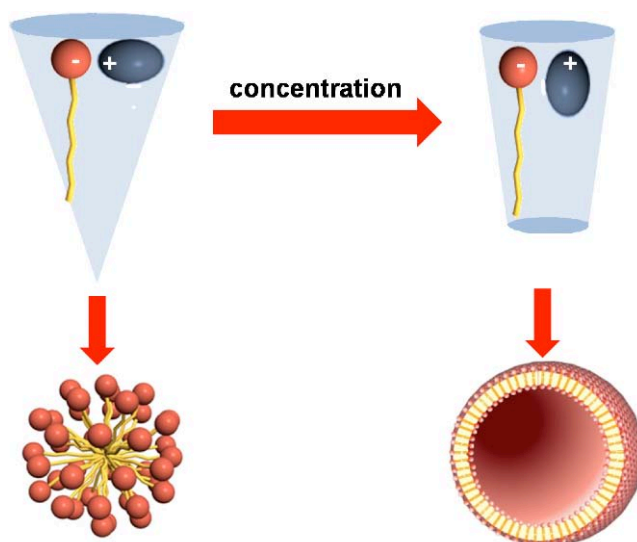


Figure 5 – Représentation schématique du mécanisme de la transition micelle-vésicule.

## Chapitre 2 – Solutions non aqueuses

L'auto-agrégation est souvent décrite dans l'eau, puisque ce solvant possède les paramètres physico-chimiques les plus adéquats pour la formation de systèmes organisés. En effet, l'eau est un solvant très polaire possédant un caractère structuré. La polarité peut être indiquée par le moment dipolaire, ainsi que par la constante diélectrique. Ces paramètres ne permettent cependant pas de décrire entièrement la polarité d'un solvant, car ils regardent souvent le solvant comme un continuum isotrope et non structuré, dans lequel les interactions solvant-solvant et solvant-soluté sont négligées. Il n'existe pas de théorie simple pour décrire la polarité d'un solvant. Une approche alternative est donc l'utilisation des échelles empiriques basées sur des valeurs bien connues, comme par exemple l'absorbance d'un colorant solvochromique (échelle de Kosower, Reichardt et Dimroth). Le caractère structuré du solvant est important, outre pour sa polarité, pour la formation d'objets. Ceci peut être décrit par la tension superficielle, la pression interne ( $\Pi$ ) et la densité d'énergie de cohésion (DEC).

## Appendix

---

Ce dernier paramètre est censé être le plus important, car, par définition, il représente la force totale de la structure intermoléculaire du solvant.

$$CED = \frac{\Delta U_v}{V_m} = \frac{\Delta H_v - R \cdot T}{V_m} \quad (2)$$

Où  $V_m$  est le volume molaire du solvant,  $\Delta U_v$  et  $\Delta H_v$  sont respectivement l'énergie et l'enthalpie (chaleur) de vaporisation d'un solvant en une vapeur dans laquelle toutes les interactions de type solvant-solvant ont été cassées. Parmi les solvants les plus polaires, le glycérol et le formamide possèdent une DEC élevée, ce qui indique le caractère structuré de ces solvants et pourrait permettre l'auto-agrégation de tensioactifs. L'auto-agrégation de tensioactifs monocaténares et bicaténares dans le formamide et dans le glycérol a déjà été étudiée dans notre laboratoire. Ces expériences nous ont montré que des phases lyotropes, similaires à celles qui se forment dans l'eau, peuvent se former dans les solvants non aqueux. Il a été montré que les tensioactifs forment des micelles sphériques, ainsi que des phases hexagonales et lamellaires. La formation de vésicules a été observée pour des tensioactifs bicaténares dans le FA et dans le glycérol. De plus, des microémulsions composées de formamide, d'un tensioactif et d'un cotensioactif, ainsi que d'une huile, ont été étudiées comme milieu réactif. Leur structure est comparable à celle des systèmes aqueux. Certaines réactions, comme par exemple la photo-amidation, ont été effectuées plus efficacement dans les microémulsions bi-continues et non aqueuses que dans les mêmes systèmes aqueux.



## Part III – Résultats et discussion

### Chapitre 1 – Conception du problème

Nous avons voulu étudier comparativement les tensioactifs catanioniques dans l'eau ainsi que dans des solvants polaires et cohésifs, notamment dans le formamide et le glycérol. Dans un premier temps nous avons synthétisé des systèmes modèles à base d'acides gras et d'amines grasses. Avec ces associations catanioniques, nous avons étudié la température de Krafft et l'influence des solvants polaires sur la CAC.

Ces systèmes modèles ne sont que peu solubles dans l'eau. C'est pourquoi nous avons introduit dans un deuxième temps un système catanionique à base de glucose (G-Hydm<sup>+</sup>/Cn<sup>-</sup>) qui est soluble dans l'eau, dans le formamide, dans le glycérol ainsi que dans les mélanges de ces solvants. Nous avons donc effectué une étude comparative de ce système pour déterminer l'influence de certains paramètres physico-chimiques sur le comportement d'agrégation des tensioactifs catanioniques. Nous avons aussi étudié l'effet hydrophobe, en modifiant la longueur des chaînes. Enfin, deux tensioactifs à gros contre-ion organique ont été également étudiés comparativement dans l'eau et dans des solvants polaires et cohésifs. Cette étude a montré l'importance des interactions hydrophobes au niveau des têtes polaires.

### Chapitre 2 – Synthèse et caractérisation

Les systèmes modèles ont été synthétisés par une réaction acido-basique dans l'éther diéthylique entre un acide gras et une amine grasse à 0°C. L'association catanionique a précipité de manière équimolaire. Le précipité a été filtré et lavé trois fois avec de l'éther diéthylique, puis le produit final a été séché sous vide. Les systèmes à base de glucose ont été synthétisés dans notre laboratoire. La partie cationique a été obtenue en suivant le protocole décrit en référence [131]. Il s'agit d'une amination réductrice du glucose à l'aide du NaBH<sub>4</sub>. Puis l'association catanionique a été obtenue via une réaction acido-basique dans l'eau pendant 3 jours à température ambiante. Le produit final a été isolé par lyophilisation en rendement quantitatif. Nous avons caractérisé les systèmes catanioniques par des méthodes spectroscopiques (IR, RMN) pour confirmer indirectement la formation de la paire d'ions. En effet, les systèmes catanioniques sont composés d'un carboxylate et d'un ammonium. Le pic de carboxylate diffère significativement de celui de l'acide gras n'ayant pas réagi. L'absence de pic pour l'acide carboxylique et la présence du signal du carboxylate confirme la formation de la paire d'ions. La spectrométrie de masse permet de visualiser l'entité catanionique directement sous forme d'une association de sodium. La pureté de la paire d'ions a été confirmée par l'analyse élémentaire. Cette méthode permet également de vérifier l'équimolarité de l'association catanionique.

## Chapitre 3 – Tensioactifs catanioniques en solution non aqueuse

### Étude physico-chimique générale

#### Température de Krafft

La température de Krafft des systèmes ioniques est très importante puisqu'un tensioactif chargé peut former des agrégats seulement au-dessus de cette température. Dans la littérature on trouve que la température de Krafft des tensioactifs ioniques est plus élevée dans le FA que dans l'eau. Ceci peut être expliqué par le caractère ionique du formamide liquide, ce qui augmente les interactions entre le solvant et la tête polaire du tensioactif par rapport au même système dans l'eau. Nous nous sommes donc attendu à trouver des températures de Krafft plus élevées dans le FA que dans l'eau pour les tensioactifs catanioniques. En effet, nous avons observé, dans le cas des tensioactifs catanioniques à base de glucose, que les températures de Krafft sont plus élevées dans le FA que dans l'eau (cf tableau 1).

	Composé	Nombre de carbone	H <sub>2</sub> O	FA	H <sub>2</sub> O/Glycérol 50 :50 (v/v)
<b>5a</b>	G-Hyd <sub>8</sub> <sup>+</sup> /C <sub>12</sub> <sup>-</sup>	20	<25	40	33
<b>5b</b>	G-Hyd <sub>12</sub> <sup>+</sup> /C <sub>8</sub> <sup>-</sup>	20	<25	44	35
<b>5c</b>	G-Hyd <sub>8</sub> <sup>+</sup> /C <sub>16</sub> <sup>-</sup>	24	30	45	36
<b>5d</b>	G-Hyd <sub>16</sub> <sup>+</sup> /C <sub>8</sub> <sup>-</sup>	24	32	47	34
<b>5e</b>	G-Hyd <sub>16</sub> <sup>+</sup> /C <sub>12</sub> <sup>-</sup>	28	45	56	51
<b>5f</b>	G-Hyd <sub>12</sub> <sup>+</sup> /C <sub>16</sub> <sup>-</sup>	28	47	58	49
<b>5g</b>	G-Hyd <sub>12</sub> <sup>+</sup> /C <sub>18</sub> <sup>-</sup>	30	47	66	60

Tableau 1 – Température de Krafft  $T_K$  (°C) de différents tensioactifs catanioniques dans des solvants polaires.

## Appendix

---

### Concentration d'agrégation critique

Après avoir déterminé les températures de Krafft des systèmes catanioniques, nous avons continué notre étude avec la détermination de la concentration d'agrégation critique ( $CAC$ ). Pour nos expériences nous avons choisi la méthode de Wilhelmy. Nous avons étudié comparativement les systèmes modèles et les systèmes à base de glucose, dans l'eau, dans le FA, dans le glycérol, ainsi que dans les mélanges de ces solvants. Dans le cas du système modèle **3a** ( $C_m^+/C_n^-$ ) nous avons observé que la  $CAC$  augmente avec une concentration croissante de FA (cf fig. 6). Comme expliqué précédemment, la concentration d'agrégation critique est plus élevée dans les solvants non aqueux que dans les solvants aqueux. Ceci est dû à la nature moins cohésive de ces solvants, ce qui réduit la solvophobie qui est une des forces motrices de l'auto-agrégation. Il faut préciser que la  $CAC$  du système **3a** dans l'eau pure n'a pas pu être déterminée, car ce système n'est pas assez soluble dans l'eau. Ce phénomène est probablement dû à des difficultés de solvation de la tête polaire. Dans tous les cas, la  $CAC$  augmente de manière linéaire comme nous pouvons le voir dans la figure 6. Ce comportement a pu être confirmé pour les systèmes à base de glucose. La figure 6 montre l'évolution de la  $CAC$  du système **5a** ( $G\text{-Hyd}_8^+/C_{12}^-$ ). Mais dans le cas des tensioactifs catanioniques à base de glucose, la  $CAC$  augmente de manière non linéaire.

Nous avons également étudié l'influence de la longueur des chaînes sur la  $CAC$  des tensioactifs catanioniques. Nous avons observé que la  $CAC$  diminue avec un nombre de carbone croissant. Ceci a déjà été décrit pour les tensioactifs ioniques dans l'eau ainsi que dans les solvants non aqueux. La  $CAC$  diminue avec une solvophobie croissante du système.

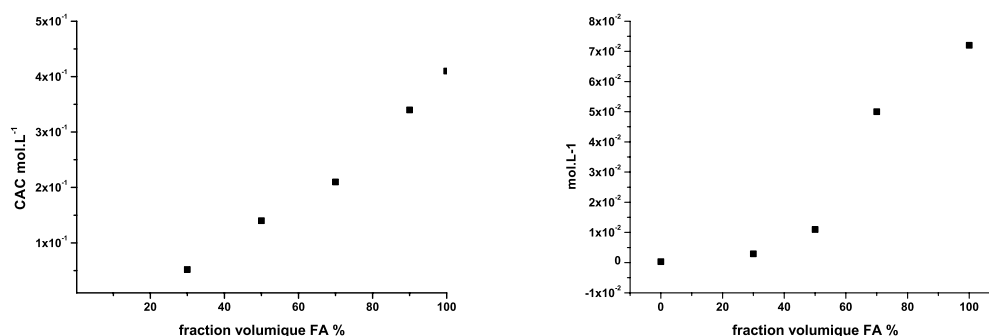


Figure 6 – Évolution de la  $CAC$  des systèmes **3a** (gauche) et **5a** (droite) en fonction de la fraction volumique du FA.

## Caractérisation des agrégats formés par les systèmes catanioniques

Après avoir déterminé la température de Krafft et la  $CAC$ , nous nous sommes intéressés aux types d'agrégats formés. Pour ce faire, nous avons étudié les systèmes par diffusion quasi élastique de la lumière. Les mesures de DLS ont montré que le système  $G\text{-Hyd}_8^+/C_{12}^-$  forme des vésicules dans l'eau, comme attendu, car les tensioactifs catanioniques ont tendance à former ce type d'agrégats. La formation de vésicules est visible sur la figure 7 qui montre un cliché de MET (microscopie électronique à transmission) du composé **5a** dans l'eau pure. Les vésicules formées ont un diamètre entre 50-200 nm. Nous avons également observé la formation de fibres. En effet, le système  $G\text{-Hyd}_8^+/C_{12}^-$  forme une phase de gel à des concentrations élevées. Les fibres se forment probablement pendant la préparation de l'échantillon qui consiste à déshydrater celui-ci pour former un film. La concentration peut également augmenter.

Les tensioactifs catanioniques forment donc des vésicules dans l'eau pure. Nous nous sommes alors attendu à la formation de vésicules dans le FA pur pour le système **5a**. Toutefois, nous n'avons pas obtenu un signal par les mesures de DLS. Deux explications sont possibles. Premièrement, les systèmes catanioniques étudiés ne forment

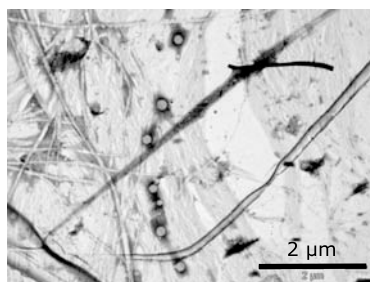


Figure 7 – Cliché de MET du système **5a** ( $\text{G-Hyd}_8^+/\text{C}_{12}^-$ ) dans  $\text{H}_2\text{O}$  ( $1.10^{-3} \text{ mol.L}^{-1}$ ).

pas d'agrégats du tout ; cela est contradictoire avec l'existence des *CAC*s obtenues. Deuxièmement, les objets formés sont trop petits pour être détectés par l'appareil de DLS utilisé ( $d_H < 5 \text{ nm}$ ). L'examen par microscopie optique n'a pas donné d'indices pour la formation de vésicules dans le formamide pur.

### **Influence de la constante diélectrique du solvant**

La non-formation de vésicules dans le formamide pur était étonnante, vu que nous nous attendions à la formation de ce type d'agrégats. La formation de vésicules dans le formamide pour les tensioactifs bicaténaires a été décrite dans notre laboratoire. La nature moins cohésive du formamide indiquée par une densité d'énergie de cohésion plus faible est donc suffisante pour la formation d'agrégats. Le fait que les systèmes catanioniques ne forment pas de vésicules dans le formamide pur est donc lié à un autre paramètre. Huang *et al.* ont mentionné que la constante diélectrique du solvant peut avoir une influence sur le comportement d'agrégation des tensioactifs catanioniques. Ils ont étudié des systèmes catanioniques à base d'un mélange entre un acide gras et une amine grasse. Les contre-ions restent en solution. Les systèmes forment des vésicules dans l'eau, mais un ajout de formamide détruit les vésicules, montrant une influence cruciale de ce solvant. Ils ont suggéré que la constante diélectrique plus élevée du formamide pourrait avoir une influence sur les interactions électrostatiques de la

paire d'ions. En effet, la relation entre la constante diélectrique et les interactions électrostatiques est approximativement décrite par la loi de Coulomb :

$$F = \frac{1}{4\pi\epsilon_0} \frac{q_1 q_2}{r^2} \quad (3)$$

Où  $F$  est la force électrostatique entre deux charges sphériques  $q_1$  et  $q_2$ ,  $\epsilon_r$  et  $\epsilon_0$  sont respectivement la constante diélectrique du solvant et la constante du vide, et  $r$  et la distance entre les charges. Nous avons alors étudié nos résultats en relation avec la constante diélectrique. Le tableau 2 montre les mesures de DLS du système G-Hyd<sub>8</sub><sup>+</sup>/C<sub>12</sub><sup>-</sup> dans l'eau, dans le formamide, ainsi que dans les mélanges de ces solvants par ordre de constante diélectrique croissante.

Solvant	H <sub>2</sub> O	H <sub>2</sub> O/FA (v/v)			FA
		70 :30	50 :50	30 :70	
$\epsilon_{id}/\epsilon_0$	78.4	87.8	94.0	100.2	109.6
$\epsilon_m/\epsilon_0$	78.4	92	102	108	109.6
Taille d'objet* nm	90-180	100-150	150-200	PAS DE SIGNAL	

\*DLS

Tableau 2 – Constantes diélectriques de différents mélanges H<sub>2</sub>O/FA à 25 °C et les objets obtenus avec G-Hyd<sub>8</sub><sup>+</sup>/C<sub>12</sub><sup>-</sup>.

Nous pouvons remarquer que des objets d'un diamètre d'environ 40-200 nm sont formés dans l'eau pure et dans les mélanges H<sub>2</sub>O/FA jusqu'à une fraction volumique de formamide de 50%. Ce mélange possède une constante diélectrique d'environ 100. Au-dessus de cette valeur, nous n'avons pas pu observer la formation de gros objets. Nous avons d'abord vérifié s'il s'agissait de vésicules dans les mélanges H<sub>2</sub>O/FA, où de gros objets ont été observés. La figure 8 montre un cliché de MET du système **5a** dans un mélange H<sub>2</sub>O/FA de 70 :30. La taille et la forme des objets correspondent à celles mesurées par DLS.

## Appendix

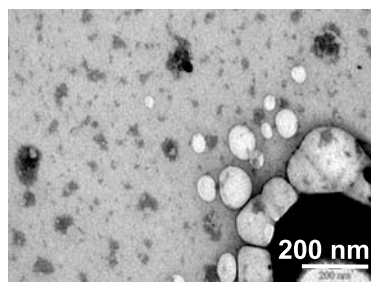


Figure 8 – Cliché de MET du système **5a** dans H<sub>2</sub>O ( $1.10^{-2}$  mol.L<sup>-1</sup>) dans un mélange H<sub>2</sub>O/FA de 70 :30.

Pour vérifier qu'une constante diélectrique trop élevée empêche la formation de vésicules contrairement à la faible DEC du formamide (par rapport à l'eau), nous avons étudié le système **5a** dans un mélange H<sub>2</sub>O/glycérol et FA/glycérol. Ces deux mélanges possèdent *a priori* une DEC plus faible que celle de l'eau. Les différentes valeurs de la constante diélectrique et les mesures de DLS sont listées dans le tableau 3. Nous pouvons observer la formation de vésicules dans les deux cas. La formation de vésicules par des tensioactifs catanioniques est donc possible dans des solvants avec une DEC et une constante diélectrique faibles.

Solvant	glycérol	H <sub>2</sub> O/glycérol (v/v) 50 :50	FA/glycérol (v/v) 56 :44	H <sub>2</sub> O	FA
$\varepsilon_{id}/\varepsilon_0$	42.9	60.7	78	78.4	109.6
$\varepsilon_m/\varepsilon_0$	42.9	64	72	78.4	109.6
Taille des objets* nm	trop visqueux	80-130	150-200	90-180	PAS DE SIGNAL

\*DLS

Tableau 3 – Constantes diélectriques de différents mélanges de H<sub>2</sub>O, de FA et de glycérol à 25 °C et les objets obtenus avec G-Hyd<sub>8</sub><sup>+</sup>/C<sub>12</sub><sup>-</sup> à 45 °C.

Nous avons donc établi avec ces résultats le modèle suivant (cf fig. 9) pour le comportement des tensioactifs catanioniques dans le formamide pur. Les tensioactifs catanioniques possèdent lors de leur synthèse une forme géométrique décrite comme



un cône tronqué qui favorise la formation de vésicules dans l'eau. Si la constante diélectrique augmente, les interactions électrostatiques entre les têtes peuvent diminuer et la paire d'ions peut être dissociée. Or l'intégrité de la paire d'ions est nécessaire pour obtenir des vésicules ; une constante diélectrique élevée peut donc empêcher la formation de vésicules.

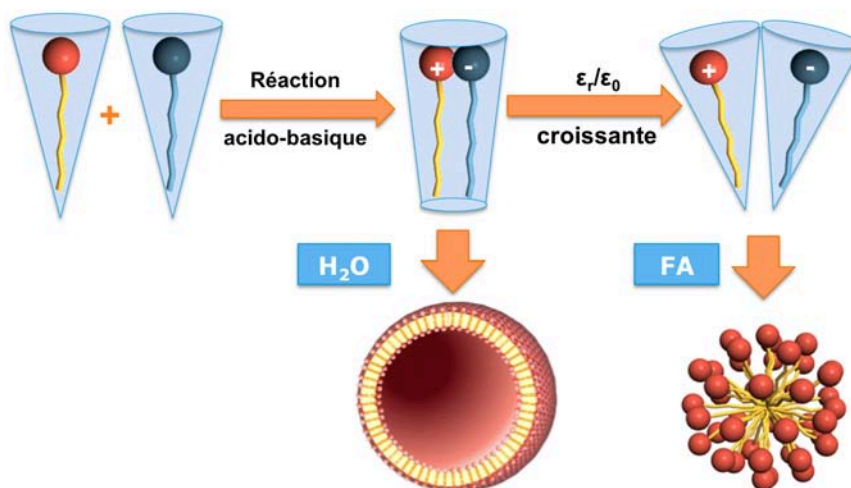


Figure 9 – Représentation schématique de l'influence de la constante diélectrique.

Notre modèle indique donc que la paire d'ions est moins associée dans le FA que dans l'eau. Nous avons étudié le système  $G\text{-Hyd}_8^+/C_{12}^-$  par réflexion totale atténuée (*Attenuated total reflectance* - ATR) infrarouge. Cette méthode particulière de spectroscopie infrarouge permet d'étudier des solutions et des films de matériaux très absorbants. Les interactions électrostatiques entre les têtes polaires sont surtout localisées entre le groupe ammonium et le groupe carboxylate. Le carboxylate est caractérisé par un seul pic net qui n'est pas superposé au pic du solvant. Nous nous sommes donc particulièrement intéressés au signal du groupe carboxylate qui se trouve vers  $1540\text{ cm}^{-1}$ . La figure 3.16 (Part III, p. 107) montre les mesures du composé **5a** solide, ainsi qu'en solution ( $\text{H}_2\text{O}$ , FA et mélanges de ces solvants) à  $55^\circ\text{C}$ , ce qui est au-dessus de la température de Krafft. Nous pouvons remarquer que le pic du carboxylate dans le

## Appendix

---

solide est situé à  $1563\text{ cm}^{-1}$ ,  $1560\text{ cm}^{-1}$  dans l'eau et à  $1544\text{ cm}^{-1}$  dans le FA pur. Le signal est décalé de  $16\text{ cm}^{-1}$  vers des longueurs d'onde plus petites. Or les longueurs d'onde sont directement reliées à l'énergie par  $E = h\nu$ ; le décalage indique donc une association moins forte du groupe carboxylate dans le FA pur. Ces résultats renforcent notre théorie de l'influence de la constante diélectrique qui est un nouveau paramètre déterminant pour la formation de vésicules par des tensioactifs catanioniques.

### **Impact des interactions ion-ion entre deux charges différentes**

L'influence de la constante diélectrique joue un rôle sur l'intégrité de la paire d'ions. Les forces attractives de la paire d'ions sont, entre autres, les interactions électrostatiques entre les têtes polaires d'un côté, et les interactions hydrophobes (van der Waals) entre les chaînes hydrophobes de l'autre. Ces dernières peuvent être augmentées par des chaînes plus longues. Pour ce faire nous avons synthétisé deux systèmes du type G-Hyd<sub>m</sub><sup>+</sup>/C<sub>n</sub><sup>-</sup>, notamment les systèmes G-Hyd<sub>8</sub><sup>+</sup>/C<sub>16</sub><sup>-</sup> et G-Hyd<sub>16</sub><sup>+</sup>/C<sub>12</sub><sup>-</sup>. Les températures de Krafft de ces systèmes sont plus élevées que pour le système précédemment décrit. Les *CAC* sont plus basses, ce qui est dû à la solvophobie élevée de ces deux systèmes. Il faut noter que le système G-Hyd<sub>16</sub><sup>+</sup>/C<sub>12</sub><sup>-</sup> n'a pu être étudié que dans l'eau pure, dans le FA pur et dans le mélange H<sub>2</sub>O/glycérol. Ce système n'était pas assez soluble dans les mélanges H<sub>2</sub>O/FA. Ce phénomène n'est pas encore tout à fait expliqué, mais pourrait être attribué à une diminution de la cohésion résultant du mélange des deux solvants. Néanmoins ces deux systèmes ont pu être étudiés comparativement dans l'eau, dans le FA et dans un mélange H<sub>2</sub>O/glycérol 50 :50. Dans le cas du système G-Hyd<sub>8</sub><sup>+</sup>/C<sub>16</sub><sup>-</sup>, nous avons pu observer la formation de vésicules dans l'eau pure et dans des mélanges H<sub>2</sub>O/FA jusqu'à une concentration de FA de 70 %. Ceci est plus élevé que dans le cas du système G-Hyd<sub>8</sub><sup>+</sup>/C<sub>12</sub><sup>-</sup> et correspond à une constante diélectrique d'environ 108 (25°C). Sur le cliché (fig. 3.19, Part III, p. 113), nous pouvons voir des vésicules

formées par le G-Hyd<sub>8</sub><sup>+</sup>/C<sub>16</sub><sup>-</sup> dans un mélange H<sub>2</sub>O/FA 30 :70. Le système G-Hyd<sub>16</sub><sup>+</sup>/C<sub>12</sub><sup>-</sup> forme des vésicules même dans le FA pur avec une constante diélectrique de 109 (25°C). Des mesures de l'IR en mode ATR montrent aussi que le degré d'association, indiqué par le décalage du signal du groupe carboxylate vers des longueurs d'onde moins importantes, est plus élevé pour le système G-Hyd<sub>8</sub><sup>+</sup>/C<sub>16</sub><sup>-</sup> que pour le système G-Hyd<sub>8</sub><sup>+</sup>/C<sub>12</sub><sup>-</sup>, qui possède des chaînes plus courtes. Des expériences avec une série de tensioactifs catanioniques du type G-Hyd<sub>m</sub><sup>+</sup>/C<sub>n</sub><sup>-</sup> nous ont donné le diagramme de phase suivant (cf fig. 10) avec des domaines d'existence de vésicules et de micelles en fonction de constantes diélectriques des mélanges croissantes.

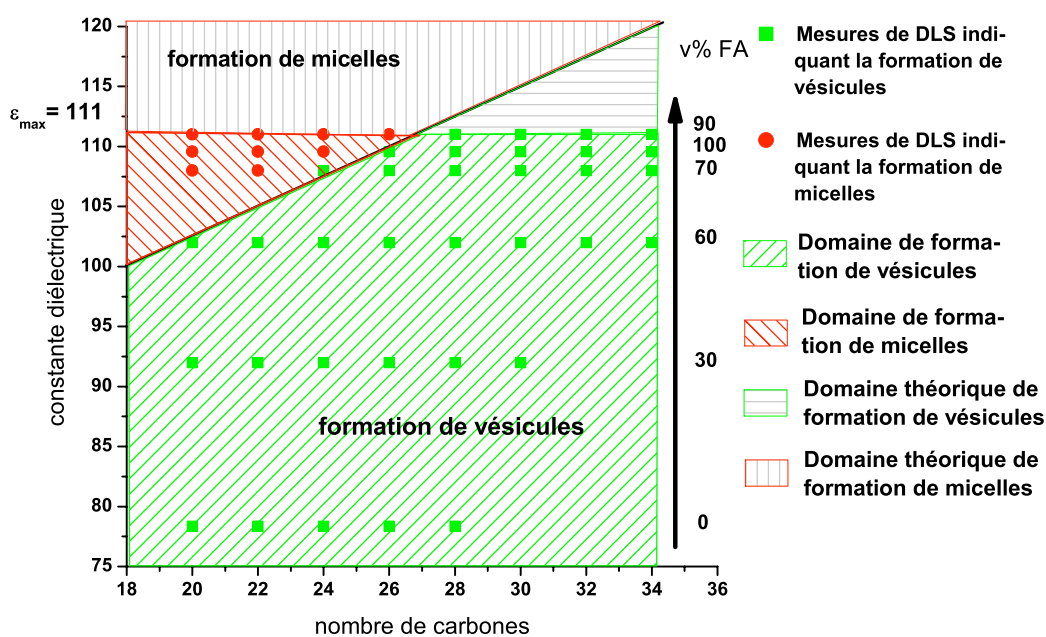


Figure 10 – Domaine d'existence des vésicules et des micelles.

Nous pouvons observer dans la zone verte la formation de vésicules (mesures obtenues par DLS). La zone rouge représente la formation de micelles, c.-à-d. des mesures de DLS où aucun signal n'a été détecté. La ligne noire indique donc, pour un nombre

## Appendix

---

de carbone donné, la constante diélectrique maximale avec laquelle la formation de vésicules est possible. Ce modèle n'est cependant valable que pour les tensioactifs catanioniques du type  $G\text{-Hyd}_m^+/C_n^-$ . Néanmoins nous avons pu montrer qu'il existe une relation entre la longueur des chaînes et la constante diélectrique : des chaînes plus longues apportent une intégrité plus élevée à la paire d'ions, ce qui permet la formation de vésicules, même dans le formamide pur.

### Effet sel sur le comportement d'agrégation

L'influence de l'ajout de sel sur le comportement des tensioactifs catanioniques en milieu non-aqueux a été testée avec l'iodure de sodium, car ce sel est suffisamment soluble dans le FA. Quatre tensioactifs catanioniques du type  $G\text{-Hyd}_m^+/C_n^-$  (dont deux formaient des vésicules dans le FA pur, et deux n'en formaient pas), ont été solubilisés dans le FA pur avec différentes concentrations de NaI (de  $10^{-5}$  à  $10^{-1}$  mol.L $^{-1}$ ). Les mesures de DLS ont montré qu'il n'y a pas d'influence à des concentrations faibles en NaI ( $10^{-5}$  à  $10^{-3}$  mol.L $^{-1}$ ), c.-à-d. que ces systèmes, qui ne formaient pas de vésicules dans le FA, n'en formaient pas après ajout du sel. De la même manière, les systèmes qui ont formé des vésicules dans le FA avant ajout du sel en formaient aussi après. À des concentrations plus élevées ( $10^{-2}$  et  $10^{-1}$  mol.L $^{-1}$ ), nous avons pu observer un effet salting-out, c.-à-d. que les tensioactifs catanioniques n'étaient plus solubles dans le formamide.

### Influence de la préparation des échantillons

Les résultats présentés ci-dessus ont été obtenus dans des mélanges de solvants préalablement préparés. Dans ce cas, les tensioactifs catanioniques ont été solubilisés dans un nouveau solvant pré-orienté (méthode A). Mais il est également possible de disperser le tensioactif dans un solvant et de diluer avec le deuxième (méthode B). Cette

dernière méthode peut conduire à plusieurs résultats; les solvants se mélangent de manière homogène ou bien le premier solvant possède une affinité élevée pour le tensioactif et ne se fait pas remplacer par le deuxième. Nous avons donc étudié quatre séries d'expériences avec deux types de tensioactifs catanioniques dispersés selon la méthode A et B. Nous n'avons trouvé aucune différence, c.-à-d. que les tensioactifs sont solubilisés pareillement dans le FA et dans l'eau et ne possèdent pas d'affinité pour un des deux solvants. Nous avons également vérifié que la façon de préparer les tensioactifs catanioniques n'influence pas le comportement d'agrégation. En effet, un tensioactif catanionique peut être préalablement synthétisé dans l'eau, puis lyophilisé et re-dispersé dans le solvant ou le mélange des solvants souhaités. Mais il est aussi possible qu'un tensioactif catanionique puisse se former in situ dans un solvant polaire et protique, comme par exemple l'eau et le formamide. Nous avons comparé ces deux différentes méthodes de préparation et nous n'avons observé aucune différence. Les courbes de mesure de tension superficielle (fig. 3.25, Part III, p. 126) sont quasiment identiques et montrent que la manière de préparer a une influence négligeable.

## Chapitre 4 – Tensioactifs à gros contre-ion organique

### Information générale

Dans une dernière partie nous avons comparé le comportement du système NbC14 dans l'eau et dans le FA. Comme écrit plus haut, ce type de paire d'ions subit une transition micelle-vésicule dans l'eau. à faible concentration se forment des micelles; en effet les interactions entre le contre-ion et le tensioactif ionique sont faibles, et le contre-ion se comporte comme un contre-ion classique. Lorsque la concentration de la paire d'ions augmente, les interactions hydrophobes augmentent également et le contre-ion se place

## Appendix

---

côte-à-côte avec les tensioactifs ioniques. Ceci a pour effet le changement de la forme géométrique de la paire d'ions ainsi que la formation de vésicules.

Comme nous l'avons vu, certains tensioactifs catanioniques ne forment plus de vésicules dans le formamide à cause des interactions électrostatiques, qui sont réduites dans ce solvant. étant donné que les interactions hydrophobiques sont moins élevées dans le cas du système NbC14 que dans celui des tensioactifs catanioniques avec deux chaînes hydrophobes, nous avons pensé que la paire d'ions NbC14 devrait seulement s'agréger en micelles dans le formamide pur.

### **Étude physico-chimique du système NbC14 dans l'eau et dans le formamide**

Nous avons comparé le comportement du système NbC14 dans l'eau et dans le formamide. La température de Krafft de ce système est plus élevée dans le FA que dans l'eau. Les expériences ont donc été effectuées à 45°C. La figure 11 montre les mesures de tension superficielle. Les courbes dans l'eau pure et dans le mélange H<sub>2</sub>O/glycérol sont caractérisées par un palier intermédiaire qui indique clairement une transition micelle-vésicule dans l'eau pure et dans le mélange H<sub>2</sub>O/glycérol.

La formation de vésicules dans tous les solvants utilisés peut être mise en évidence par des mesures de DLS et des clichés de microscopie électronique à transmission (fig. 4.5, 4.6 et 4.8, Part III, p. 135-139). Bien que les courbes de la tension superficielle du NbC14 dans les mélanges eau-formamide et dans le formamide pur soient caractérisées par un changement de la pente avec une concentration croissante, nous n'avons pas pu déterminer une transition micelle-vésicule. La formation de vésicules dans le formamide pur est intéressante. En effet, nous avons supposé que les forces hydrophobiques entre le contre-ion et le tensioactif ionique étaient moins élevées que

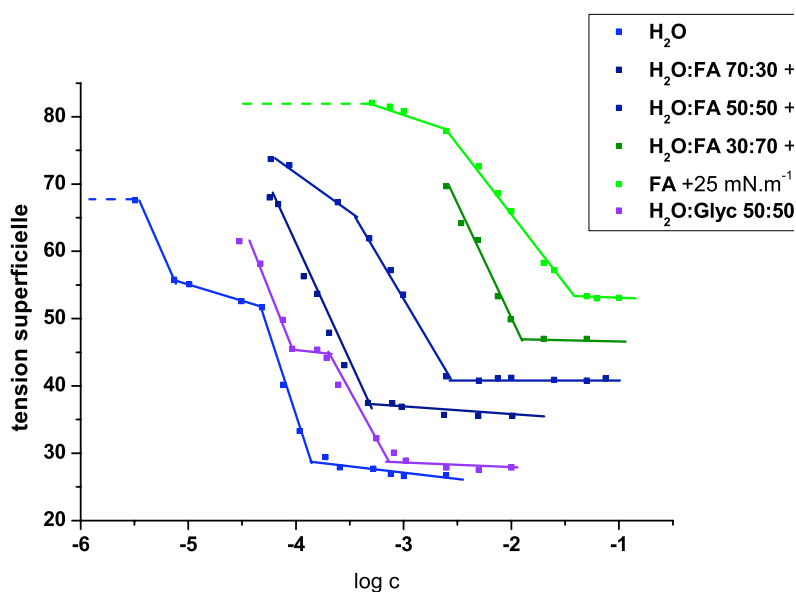


Figure 11 – Mesures de tension superficielle du NbC14 dans différents solvants et dans les mélanges de solvants à 45°C.

celles entre deux tensioactifs à longue chaîne ; l'influence de la constante diélectrique, comme nous l'avons vu, aurait donc dû empêcher la formation de vésicules.

## Interactions entre les têtes polaires

Nous avons donc étudié ce comportement particulier du NbC14. La formation de vésicules peut être expliquée par la structure particulière du contre-ion. Le bicycle dérivé du norbornène permet l'empilement du contre-ion comme montré dans le schéma suivant (cf fig. 12).

Cet empilement pourrait augmenter la stabilité de l'objet formé et donc permettre la formation de vésicules dans le formamide pur. Nous avons alors étudié le tétradécanoate de cyclohexylammonium (CxC14). Ce tensioactif possède un contre-ion volumineux, qui permet une transition micelle-vésicule dans l'eau à 25°C. Contrairement au NbC14, ce contre-ion n'est pas constitué d'un bicycle. Nos mesures de tension

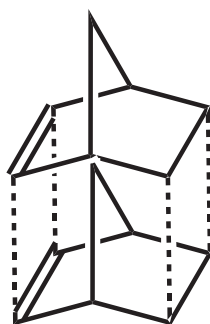


Figure 12 – Représentation schématique de l'empilement du contre-ion du dérivé du norbornène.

superficielle à 45°C (au-dessus de la température de Krafft) ont montré dans l'eau un palier intermédiaire, ce qui indique une transition micelle-vésicule. Dans le formamide, la courbe de tension superficielle n'a montré qu'un palier à des concentrations très élevées. Nous n'avons pas observé de palier intermédiaire, ce qui nous a fait supposer la formation de micelles. En effet, nous n'avons obtenu aucun signal par les mesures de DLS du système CxC14 dans le formamide pur. Ces expériences ont montré l'influence de la structure du contre-ion sur le comportement d'agrégation des tensioactifs cationiques. Le système NbC14 est capable de former des vésicules dans le formamide pur grâce à un effet stabilisant de l'empilement des contre-ions, alors que le système CxC14, qui ne possède pas cette structure bicyclique, n'est pas capable de former des vésicules dans le formamide pur.



## Part IV – Conclusion et perspectives

Nous avons étudié comparativement des tensioactifs catanioniques dans l'eau, dans le formamide et dans le glycérol, ainsi que dans les mélanges de ces solvants. Nous avons synthétisé trois différents systèmes catanioniques, parmi une série d'alcanoates d'alkylammonium, qui nous servait de système modèle. Ces derniers tensioactifs catanioniques étaient caractérisés par une température de Krafft très élevée. La *CAC* augmentait avec une concentration croissante du FA. Ce système n'était cependant pas suffisamment soluble dans l'eau pour permettre une étude comparative. C'est pourquoi nous avons synthétisé un deuxième système à base de glucose. Ce tensioactif catanionique du type alcanoate de N-alkylammonium-1-déoxy-D-glucitol est soluble dans l'eau, dans le formamide et dans le glycérol. Avec ce système nous avons pu montrer une influence de la constante diélectrique sur le comportement d'agrégation des tensioactifs catanioniques dans les solvants polaires. En effet, une constante diélectrique élevée peut conduire à la réduction des interactions électrostatiques entre les têtes polaires, ce qui conduit à la séparation des tensioactifs. Ceci peut changer la forme géométrique de la paire d'ions et la formation de vésicules n'est plus possible. Cet effet dissociatif de la constante diélectrique a pu être compensé par l'utilisation des chaînes hydrophobes plus longues. Les interactions hydrophobes entre les chaînes alkyle des tensioactifs ca-

## Appendix

---

tanioniques ont augmenté la stabilité de la paire d'ions et la formation de vésicules était possible dans le formamide pur. Finalement, nous avons montré que la structure de la tête polaire pouvait également influencer le comportement d'agrégation des tensioactifs catanioniques. En effet, le système NbC14, un tensioactif à gros contre-ion organique (tétradécanoate de norbornène méthylèneammonium) est capable de former des vésicules dans le formamide pur ; pourtant, les interactions hydrophobes entre la partie lipophile du contre-ion et la chaîne du tensioactif ionique sont moins élevées que celles dans le système à base de sucre avec deux chaînes alkyle. La formation peut s'expliquer par les interactions hydrophobes entre les contre-ions. La structure bicyclique du dérivé du norbornène permet l'empilement. Cet empilement peut stabiliser l'agrégat formé et permettre la formation de vésicules dans le formamide pur. Un système similaire, le tétradécanoate de cyclohexylammonium (CxC14) a également été étudié. Ce système nous a permis de montrer l'influence des interactions hydrophobes entre les têtes polaires sur le comportement des tensioactifs catanioniques. En effet, ce système ne forme pas de vésicules dans le formamide pur, car l'influence dissociative de la constante diélectrique ne peut pas être compensée par les faibles interactions hydrophobes entre les contre-ions du type cyclohexylammonium, contrairement aux dérivés du norbornène.

**Author: Roland Ramsch**

## **Catanionic Surfactants in Polar Cohesive Solvents**

### **Impact of Physical Solvent Parameters on their Aggregation Behavior**

**Director of the thesis:** Isabelle Rico-Lattes

**Place and date of the PhD defense:** Université Paul Sabatier, Toulouse, 22<sup>nd</sup> January 2010

**Abstract:**

In the literature, little work has been done on **catanionic surfactants** in non-aqueous solution. Catanionic surfactants are ion pairs composed of an anionic and a cationic surfactant. In the frame of this work, we wanted to rationalize the aggregation behavior of this surfactant type by studying them in **water**, in **formamide**, in **glycerol** and in some **mixtures of these polar and cohesive solvents**. For this issue, we synthesized three different types of catanionic surfactants (**alkylammonium alkanolate**, **norbornene methyleneammonium tetradecanoate**, ***N*-alkylammonium-1-deoxy-D-glucitol alkanolate**).

Catanionic surfactants usually form **vesicles** in water. In the case of non-aqueous solvents and mixtures of solvents, we could observe that the type of aggregates formed with catanionic surfactants depends on two major factors: the **dielectric constant** of the solvent and the **degree of interaction between the two surfactants**. Effectively, formamide having a higher dielectric constant than water exerts a **dissociative force** on the ion pair. The ion pair can be separated leading to a mixture of monocatener ionic surfactants, which then forms micelles. On the other hand, **hydrophobic effects** can be increased using longer hydrophobic chains, which reinforce the ion pair and lead to the formation of vesicles in pure formamide. Moreover, the study on the norbornene methyleneammonium tetradecanoate showed the importance of **hydrophobic headgroup-headgroup interactions**, an additional parameter which can favor vesicle formation in pure formamide.

**Keywords:** catanionic surfactants, polar cohesive solvents, formamide, glycerol, dielectric constant, cohesive-energy density (CED), vesicle

**Discipline:** Supramolecular and macromolecular chemistry

Laboratoire des Interactions Moléculaire Réactivité Chimique et Photochimique  
Université Paul Sabatier, 118, route de Narbonne, 31062 Toulouse

**Auteur : Roland Ramsch**

**Catanionic Surfactants in Polar Cohesive Solvents**

**Impact of Physical Solvent Parameters on their Aggregation Behavior**

**Directeur de thèse :** Isabelle Rico-Lattes

**Lieu et date de soutenance :** Université Paul Sabatier, Toulouse, le 22 janvier 2010

**Résumé :**

On trouve peu d'études, dans la littérature, sur les **tensioactifs (TA) catanioniques** – formés d'une paire d'ions entre un TA anionique et un TA cationique – en milieu non-aqueux. Nous avons voulu rationaliser, dans ce travail, le comportement d'agrégation de ce type de tensioactifs en les étudiant comparativement dans **l'eau**, dans **le formamide**, dans **le glycérol** et dans des mélanges de ces solvants polaires et cohésifs. Nous avons pour ce faire synthétisé trois différents types de TA catanioniques (**alcanoate d'alkylammonium**, **tétradécanoate de norbornène méthylène ammonium**, **alcanoate de N-alkylammonium-1-déoxy-D-glucitol**).

Les TA catanioniques ont la propriété de s'agréger en **vésicules** dans l'eau. Dans le cas des autres solvants ou mélanges des solvants, nous avons constaté que le type d'agrégat que forment les TA catanioniques dépend de deux principaux facteurs : **la constante diélectrique** du solvant et **le degré d'interaction entre les deux TA**. En effet, le formamide ayant une constante diélectrique plus élevée que l'eau, il exerce une **force dissociative** sur la paire d'ions qui peut ainsi être séparée pour conduire à un mélange de TA ioniques monocaténaires formant alors des micelles. D'autre part, une augmentation de l'effet hydrophobe, obtenu en utilisant des chaînes hydrophobes plus longues, renforce la paire d'ions et conduit à la formation de vésicules dans le formamide pur. Par ailleurs, l'étude du système tétradécanoate de norbornène méthylène ammonium a également montré l'importance des **interactions hydrophobes entre les têtes polaires**, un autre facteur pouvant favoriser la formation de vésicules dans le formamide pur.

**Mots clés :** tensioactifs catanioniques, solvants polaires et cohésifs, formamide, glycérol, constante diélectrique, densité d'énergie de cohésion (DEC), vésicule

**Discipline :** Chimie supramoléculaire et macromoléculaire

Laboratoire des Interactions Moléculaire Réactivité Chimique et Photochimique  
Université Paul Sabatier, 118, route de Narbonne, 31062 Toulouse